STRUCTURE-FUNCTION ANALYSIS OF MULTI-COPPER OXIDASES

Catarina Isabel Simões Pires da Silva

Dissertation presented to obtain the PhD degree in Biochemistry
at the Instituto de Tecnologia Química e Biológica,
Universidade Nova de Lisboa

Supervisor

Isabel Maria Travassos de Almeida de Jesus Bento

FCT Fundação para a Ciência e a Tecnologia
MINISTÉRIO DA EDUCAÇÃO E CIÊNCIA

Instituto de Tecnologia Química e Biológica
Universidade Nova de Lisboa

Oeiras, June 2013

27th June 2013

From left to right: Dr. Shabir Najmudin, Professor Dr. Peter F. Lindley, Dr. Marta Ferraroni, Dr. Isabel Bento, Catarina S. Silva, Professor Dr. Mª Arménia Carrondo, Professor Dr. Luís Gales

ITQB-UNL – Instituto de Tecnologia Química e Biológica, UNL

Macromolecular Crystallography Unit – Structural Genomics Laboratory

Av. da República (EAN), 2785-572 Oeiras, Portugal

ACKNOWLEDGEMENTS

First, I would like to thank to Professor Mª Arménia Carrondo, head of the Macromolecular Crystallography Unit, for her support and high standards that instils in the lab; and to Dr. Isabel Bento, my supervisor, for her sympathy, support and teaching. To both I thank the opportunity to have worked at the Macromolecular Crystallography Unit.

To all my lab colleagues for providing a great environment at work, in particular Ana Teresa and David Marçal for their true endless friendship throughout these years, constant availability and great conversations; Daniele de Sanctis for his simplicity, good character, friendship and amazing Italian night outs; Joana Rocha, Susana Gonçalves and Mário Correia for their sympathy. To all I thank the great moments spent together, the laughts and camaraderie. Also, to Miguel Pessanha, a good friend, for his sympathy and integrity; and to Przemek Nogly for his friendship and interest in discussing Science.

I would also like to thank to all the collaborators involved in my project in particular João M. Damas (long lasting friend from the University) and Cláudio M. Soares from the Protein Modeling Group; and Paulo Durão, Zhenjia Chen, André T. Fernandes and Lígia O. Martins from the Microbial & Enzyme Technology laboratory. To all I thank their input into the project and the helpful discussions. A particular thanks goes to Peter F. Linley, a former researcher at the Macromolecular Crystallography Unit, not only for his helpful insights into the project but also for his inspiring enthusiasm towards Science.

Also, a special thanks to Pedro Matias for sharing his experience and expertise during synchrotron trips and to Colin E. McVey for help in troubleshooting software setup issues.

To all my colleagues from InTeraQB, for making possible the concretization of this 'project'.

To ITQB, for its good environment and multi-disciplinary background, an asset for carrying out this project and for what is yet to come.

To all my friends in Portugal, who always supported and encouraged me, and to my new friends and colleagues at the EMBL, especially Taiana, Ottilie and Karine for their dedicated friendship.

Philippe for all his support, incentive, belief and understanding; for making me smile every day, lifting my spirit even at the toughest moments. Thanks for being there for me.

Above all, I thank all my family, for their care, support, understanding and for always believing in me; in particular a big thank you to my parents and sister, for their love.

Lastly, Fundação para a Ciência e Tecnologia (FCT) and Fundo Social Europeu (FSE) are also acknowledged for financial support in the frame of the Quadro Comunitário de apoio through the PhD grant SFRH/BD/40586/2007.

To all, my most sincere thanks!

THESIS PUBLICATIONS

1. P. Durão, Z. Chen, **C.S. Silva**, C.M. Soares, M.M. Pereira, S. Todorovic, P. Hildebrandt, I. Bento, P.F. Lindley, and L.O. Martins, "Proximal mutations at the type 1 copper site of CotA laccase: spectroscopic, redox, kinetic and structural characterization of I494A and L386A mutants", **Biochem. J.** (2008) **412**(2): 339-46.

2. Z. Chen, P. Durão, **C.S. Silva**, M.M. Pereira, S. Todorovic, P. Hildebrandt, I. Bento, P.F. Lindley and L.O. Martins, "The role of Glu^{498} in the dioxygen reactivity of CotA-laccase from *Bacillus subtilis*", **Dalton Trans.** (2010) **39**(11): 2875-2882.

3. I. Bento, **C.S. Silva**, Z. Chen, L.O. Martins, P.F. Lindley and C.M. Soares, "Mechanisms underlying dioxygen reduction in laccases. Structural and modelling studies focusing on proton transfer.", **BMC Structural Biology** (2010) **10**(28): 1-14.

4. A.T. Fernandes, M.M. Pereira, **C.S. Silva**, P.F. Lindley, I. Bento, E.P. Melo and L.O. Martins, "The removal of a disulfide bridge in CotA-laccase changes the slower motion dynamics involved in copper binding but has no effect on the thermodynamic stability", **J. Biol. Inorg. Chem.** (2011), **16**(4): 641-651.

5. C.S. Silva, P. Durão, A. Fillat, P.F. Lindley, L.O. Martins, I. Bento, "Crystal structure of the multicopper oxidase from the pathogenic bacterium *Campylobacter jejuni* CGUG11284: characterization of a metallo-oxidase", **Metallomics** (2012), **4**(1), 37-47 (Front cover).

6. C.S. Silva*, J.M. Damas*, Z. Chen, V. Brissos, L.O.Martins, C.M. Soares, P.F. Lindley, I. Bento, "The role of Asp116 in the reductive cleavage of dioxygen to water in CotA laccase: assistance during the proton-transfer mechanism", **Acta Cryst. D (Biol Crystallogr.)** (2012) **68**(2), 186-193.
(* authors contributed equally to this work)

Other publications not included in this thesis:

7. A.M.D. Gonçalves, **C.S. Silva**, T.I. Madeira, R. Coelho, D. de Sanctis, M.V. San Romão, I. Bento, "Endo-β-D-1,4-mannanase from *Chrysonilia sitophilla* displays a novel loop arrangement for substrate selectivity", **Acta Cryst. D (Biol Crystallogr.)** (2012) **68**(11), 1468-1478**.**

Dioxygen is a ubiquitous electron acceptor in aerobic biological systems, playing a vital role in many biological processes upon its activation and reduction. However, the precise routes through which such mechanisms occur are still poorly understood for many enzyme families. The work presented in this dissertation focuses on Multi-copper oxidases (MCOs), a family of enzymes able to couple the one-electron oxidation of a vast array of substrate molecules with the four-electron reduction of dioxygen to water. In MCOs such reactions are mediated between two distinct copper centres; a mononuclear type 1 blue copper centre (T1), and a trinuclear cluster consisting of two type 3 (T3) and one type 2 (T2) copper atoms.

Studies have focused on two distinct bacterial MCOs; the CotA laccase from *Bacillus subtilis* and the MCO from the pathogenic bacterium *Campylobacter jejuni* (McoC). CotA laccase is the first bacterial laccase whose structure has been determined. Isolated from the outer layer of the spore coat and with well known thermostability and thermoactivity properties, this *sensu stricto* laccase (oxidase activity towards aromatic compounds) has been used as a model system for structure-function studies. In order to address the role of specific residues and their effect on the activity and stability of the enzyme, several CotA laccase mutants have been produced by both structure-based site-directed mutagenesis and site-saturation mutagenesis. These mutants have been crystallised and their three-dimensional structures determined by X-ray crystallography, followed by correlation of the structural results with biochemical data.

Substrate oxidation at the T1 Cu centre is considered to be the catalytic rate-limiting step for laccases. One of the major factors that dictate the electron transfer rate is the difference in redox potential between the T1 Cu and the substrate molecule, which in turn can be influenced by several factors including the solvent accessibility of the site. In the present work the modulation of the redox potential at the T1 Cu site was investigated by mutating the hydrophobic residues Ile494 and Leu386 into alanines. The crystal structures of both mutants show an increase in solvent accessibility at the T1 Cu site and, as a consequence, a decrease of the redox potential of the metal centre was observed for both mutants.

The role of the single disulfide bridge of CotA laccase, as a possible molecular determinant of the enzyme's stability, was also investigated. CotA laccase possesses an intra-domain disulfide bridge, Cys229-Cys322, located in domain II at one of the edges of the enzyme's substrate binding site. The disulfide bridge was disrupted by mutation of residue Cys322 into an alanine, using site-directed mutagenesis. The crystal structure shows that the overall structure remains the same, but that there is a slight change of the substrate binding pocket configuration with a concomitant decrease of the T1 Cu site redox potential. The available biochemical data show that although the disulfide bond is not involved in the enzyme's stability, it contributes to the enzyme's conformational dynamics with implications on the rates of copper incorporation or loss.

Other aspects investigated in this thesis concern the mechanism of dioxygen reduction to water by MCOs. In order to investigate the nature of the native state in CotA laccase, the crystal structures of the holo-protein and of the oxidised form of the apo-protein, which had previously

been reconstituted *in vitro* with Cu(I), have been determined and the spectroscopic analysis of both crystals (before and after data collection) and protein solutions undertaken. The results reveal that the shoulder usually observed at 330nm in the UV/Vis spectrum is not exclusive for a hydroxyl bridging moiety at the T3 Cu site, but is also present when the T3 Cu ions are bridged with a dioxygen species, suggesting that different resting states may exist for different MCOs.

Another key question arising from the process of reductive cleavage of dioxygen to water is the nature of the protonation events taking place during this catalytic step. In addition to four electrons this reduction process also requires four protons. Mutagenesis studies have proposed these protons to be facilitated by acidic residues located within the entrance and exit channels of MCOs. In CotA laccase these are the structurally conserved Glu498 placed at the dioxygen entrance channel and the sequentially conserved Asp116 sited within the exit channel. Equilibrium protonation simulations performed on CotA laccase indicate that Glu498 is the only proton-active group in the neighbourhood of the trinuclear centre, whereas Asp116 is fully ionized. In order to access the role of each of these residues during the protonation process, different mutants were produced and their crystal structures determined. Site-directed mutagenesis was used to produce the E498 mutants (E498D, E498T and E498L) and site-saturation mutagenesis to produce the D116 mutants (D116E, D116N and D116A). Overall, the results clearly indicate that Glu498 plays a decisive role in the protonation mechanisms, channelling protons during the reduction process and possibly stabilizing the site as a whole. D116 also has a key role as it modulates the protonation events occurring during catalysis, and is also important for

maintaining the local geometry and water connectivity at the trinuclear site.

Lastly, the crystal structure of the recombinant bacterial MCO from *Campylobacter jejuni* (McoC) CGUG11284 was solved at 1.95Å resolution. The three-dimensional structure shows that this enzyme has a typical laccase fold as well as the characteristic spectral features of MCOs. Furthermore, in the McoC structure, the presence of secondary structure elements near the T1 Cu site (substrate binding site), namely a Met-rich region, have been shown to function as a barrier for the access of bulkier substrates to this site. Indeed, biochemical and functional studies show that this enzyme has a higher efficiency towards metal ions, such as Cu(I) and Fe (II), than for bulky aromatic substrates. Moreover, a fifth putative Cu binding site was identified near the Met-rich region, which has been implicated in Cu homeostasis in other MCOs. Altogether, these results indicate that McoC is essentially a metallo-oxidase, mainly showing specificity as a cuprous oxidase.

The knowledge gained by the above studies not only clarifies the mechanisms of dioxygen reduction, but may also be further rationalised and used in protein engineering, for biotechnological purposes.

O oxigénio molecular é um aceitador de electrões universal nos sistemas biológicos aeróbios, desempenhando um papel vital em muitos destes processos após a sua activação e redução. Contudo, para muitas famílias de enzimas, as vias exactas através das quais estes mecanismos ocorrem estão ainda pouco compreendidas. O trabalho apresentado nesta dissertação foca-se nas oxidases de Multi-cobre (MCOs), uma família de enzimas capaz de conjugar a oxidação de uma vasta gama de substratos com a redução do oxigénio molecular a água. Trata-se de um processo de oxidação monoelectrónico, sendo necessários quatro electrões e quatro protões para a completa redução do oxigénio molecular. Nas MCOs, estas reacções ocorrem entre dois centros de cobre distintos; um centro de Cu (azul) mononuclear tipo 1 (T1) e um centro trinuclear composto por dois cobres tipo 3 (T3) e um cobre tipo 2 (T2).

O presente estudo focou-se em duas MCOs bacterianas; a enzima CotA lacase de *Bacillus subtilis* e a MCO da bactéria patogénica *Campylobacter jejuni* (McoC). A CotA lacase é parte constituinte da camada exterior da capa do esporo e possui reconhecidas propriedades de termoestabilidade e termoactividade. Esta *sensu stricto* lacase (actividade de oxidase relativamente a compostos aromáticos), foi a primeira de origem bacteriana a ter a estrutura tridimensional determinada e, desde então, tem sido usada como sistema modelo para estudos de estrutura-função. Com o objectivo de elucidar a função de determinados resíduos e esclarecer o seu efeito na actividade e estabilidade da enzima, foram produzidas diversas enzimas mutantes da CotA lacase. Estas enzimas, resultantes de mutagénese dirigida, baseada em estruturas já determinadas, e/ou

mutagénese de base evolutiva, foram cristalizadas e a sua estrutura tridimensional determinada por cristalografia de Raios-X, e posteriormente usada para a realização de estudos de estrutura-função através da correlação com dados bioquímicos disponíveis.

A oxidação do substrato no centro T1 é considerada ser o passo limitante da velocidade catalítica nas lacases. Um dos principais factores que dita a velocidade de transferência electrónica nestas enzimas é a diferença de potencial redox criada entre o centro T1 e a molécula de substrato, que por sua vez pode ser afectada por diversos factores incluindo a acessibilidade do centro ao solvente. No presente trabalho, investigou-se a modulação do potencial redox do centro T1 através da mutação dos resíduos hidrofóbicos Ile494 e Leu386, para alaninas. Para ambos os mutantes, a caracterização estrutural e bioquímica obtida evidencia um aumento da acessibilidade do centro T1 ao solvente e uma diminuição do potencial redox deste centro.

Foi também investigado o papel da única ponte persulfureto presente na enzima CotA lacase, como possível determinante molecular da estabilidade da enzima. Esta ponte persulfureto, Cys229-Cys322, localiza-se no domínio II (é intra-domínio) numa das extremidades do local de ligação ao substrato. A quebra da ponte persulfureto foi produzida por mutagénese dirigida, tendo-se mutado o resíduo Cys322 para alanina. A estrutura cristalográfica obtida revela que o enrolamento global da enzima permanece igual, existindo apenas uma pequena alteração na configuração do local de ligação ao substrato. Os dados bioquímicos disponíveis revelaram que, para além de uma diminuição do potencial redox do centro T1, a ponte persulfureto contribui para a dinâmica conformacional da

enzima, com implicações na velocidade de incorporação ou perda do átomo de cobre no centro T1.

Outros aspectos igualmente investigados na presente tese dizem respeito ao mecanismo de redução do oxigénio molecular a água pelas MCOs. Com o objectivo de averiguar a natureza do estado nativo da enzima CotA lacase, determinaram-se as estruturas cristalográficas da holo-enzima e de uma forma re-oxidada da mesma, e procedeu-se à análise espectroscópica dos cristais (antes e depois da recolha de dados) e das soluções de proteína. Os resultados obtidos mostram que o ombro usualmente observado a 330nm no espectro de UV/Vis não é exclusivo da presença de uma espécie hidroxilo coordenada entre os dois cobres T3, podendo também ocorrer quando estes estão coordenados com uma espécie diatómica de oxigénio, sugerindo a existência de diferentes estados nativos para diferentes MCOs.

Outra questão importante que deriva do processo de redução do oxigénio molecular a água é a natureza dos eventos de protonação que ocorrem durante este passo catalítico. Para além de quatro electrões, este processo de redução requer igualmente quatro protões. Estudos de mutagénese realizados propuseram que estes protões poderiam ser providenciados por resíduos acídicos localizados nos canais de entrada e saída das MCOs. Na enzima CotA lacase, estes resíduos correspondem ao Glu498, estruturalmente conservado e localizado no canal de entrada do oxigénio molecular, e o Asp116 posicionado no canal de saída do solvente. Simulações de equilíbrio de protonação realizadas para a CotA lacase indicam que o Glu498 é o único resíduo protonável presente nas imediações do centro trinuclear, enquanto, por seu lado, o Asp116 se

encontra totalmente ionizado. De modo a determinar o papel de cada um desses resíduos durante o processo de protonação, diferentes mutantes foram produzidos e as suas estruturas cristalográficas determinadas. O método de mutagénese dirigida foi usado para produzir os mutantes do E498 (E498D, E498T e E498L) enquanto que mutagénese de natureza evolutiva foi usada para originar os mutantes do D116 (D116E, D116N e D116A). De um modo geral, os resultados indicam claramente que o Glu498 desempenha um papel decisivo nos mecanismos de protonação, canalizando os protões para o centro trinuclear durante o processo de redução do oxigénio molecular e, possivelmente, estabilizando o local como um todo. Por seu lado, o D116 também desempenha um papel relevante na medida em que modula os eventos de protonação que ocorrem durante a catálise, sendo também importante para a manutenção da geometria local e da rede de águas presentes no centro trinuclear.

Por fim, a estrutura cristalográfica da forma recombinante da MCO bacteriana de *Campylobacter jejuni* (McoC) CGUG11284 foi resolvida a 1.95Å de resolução. A sua estrutura tridimensional mostra que esta enzima possui o enrolamento típico das lacases bem como os traços espectroscópicos característicos das MCOs. Além disso, foi demonstrado que a presença de elementos de estrutura secundária próximo do centro T1 (local de ligação do substrato), nomeadamente uma região rica em metioninas, funciona como barreira ao acesso de substratos mais volumosos a este centro. De facto, estudos bioquímicos e funcionais mostram que esta enzima possui uma maior eficiência catalítica para iões metálicos, tais como Cu(I) and Fe(II), que possuem outro local de ligação, do que para substratos aromáticos volumosos. Adicionalmente, foi ainda identificado um putativo quinto local de ligação de cobre, próximo da

região rica em metioninas, equivalente ao que tem sido associado em outras MCOs ao processo de homeostase de cobre. Os resultados obtidos neste estudo indicam que a McoC é essencialmente uma metalo-oxidase, detendo principalmente especificidade como oxidase de cobre (Cu(I)).

O conhecimento adquirido com a presente dissertação permite não só clarificar os mecanismos de redução do oxigénio molecular nestas enzimas, mas também entender outros determinantes moleculares da actividade e estabilidade da enzima CotA lacase que, racionalizados, poderão ser utilizados na engenharia de proteínas com vista à produção de biocatalisadores para aplicações biotecnológicas.

TABLE OF CONTENTS

Chapter 1: General Introduction

Chapter 2: Proximal mutations at the type1 copper site of CotA laccase: characterization of I494A and L386A mutants

CHAPTER 1

GENERAL INTRODUCTION

1.1 The Multi-copper Oxidase family of enzymes

1.1.1 Molecular evolution

Multi-copper Oxidases (MCOs) are part of the multi-domain protein family of Multi-Copper Blue Proteins (MCBPs), together with Nitrite Reductases (NIRs) (Nakamura and Go, 2005; Nersissian and Shipp, 2002). The MCBPs family members present themselves as single polypeptide chains of variable length (from 100 to more than 1000 amino acid residues) and are characterized by repeats of a homologous sequence domain, the cupredoxin-fold domain. This comprises of an eight-stranded Greek-key β-barrel topology and carries a copper binding site responsible for these enzymes' typical blue colour (Hoegger *et al.*, 2006; Messerschmidt, 1997; Nersissian and Shipp, 2002; Murphy *et al.*, 1997) (Figure 1).

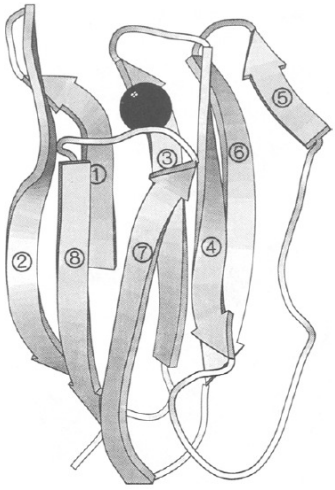

Figure 1 – The cupredoxin-fold domain formed by an eight-stranded Greek-key β-barrel, comprising two β-sheets composed by four strands each, arranged in a sandwich conformation. A type 1 blue copper is shown as sphere. (adapted from Rydén and Hunt, 1993).

Division between MCOs and NIRs, within MCBPs, is based not only on their function but also on their domain organization, with NIRs-type

proteins being composed of two cupredoxin-fold domains (forming functional homotrimers), whereas MCOs usually comprise three or six domains (Nakamura and Go, 2005; Lindley, 2001; Solomon *et al.*, 1996). These are considered to originate from a common ancestor, a single-domain cupredoxin protein (such as azurin, pseudoazurin, plastocyanin, rusticyanin, amicyanin and phytocyanins), by domain multiplication and modifications. Such modifications include domain enlargement, the formation of substrate and inter-domain copper-binding sites, the regression of the intra (blue copper) or inter-domain copper-binding sites formed, or even the insertion of new domains (Rydén and Hunt, 1993; Nakamura and Go, 2005).

The growing number of genomic, phylogenetic, structural and functional information available on these proteins over the last decades has allowed for the investigation of their evolutionary relationships (Rydén and Hunt, 1993; Murphy *et al.*, 1997; Nakamura *et al.*, 2003; Nakamura and Go, 2005; Hoegger *et al.*, 2006). Mainly focused on the phylogenetic relationships derived from sequence analysis, Rydén and Hunt (Rydén and Hunt, 1993) have proposed that a structure closest to the contemporary C-terminal copper-binding domain evolved first, with subsequent duplication, originating a double domain protein. Addition of ligands to both domains led to the formation of the trinuclear inter-domain copper-binding site, yielding a functional enzyme. Further addition of a single domain (the middle domain, the most divergent of the three) originated the three-domain MCBPs, whereas the six-domain MCBPs derived from a double duplication of the original double domain (Rydén and Hunt, 1993). In all the cases, however, loss of copper-binding sites after domain duplication beyond the two-domain stage had to occur. At the same time, considering the evident similarities in structure and function of the inter-domain

copper-binding sites within the MCO members laccases, ascorbate oxidase and ceruloplasmin, Murphy *et al.* (Murphy *et al.*, 1997) proposed a dependent evolution, with either the 6 domain ceruloplasmin losing the three middle domains, originating a laccase-type protein (3 domains), or with the former one building after domain addition or duplication from the latter. Taking into account both threads of evolution, Nakamura *et al.* (Nakamura *et al.*, 2003; Nakamura and Go, 2005) suggested the existence of two-domain MCBPs (TdMCBPs) containing trinuclear inter-domain copper-binding sites, which would constitute the evolutionary intermediates of this multi-domain protein family. According to this hypothesis (Nakamura and Go, 2005) (Figure 2), three types of two-domain proteins are proposed, based on the location of their blue copper-binding site; type A, comprising a blue copper binding-site in both domains; and types B and C, containing a blue copper-binding site only in the second and first domain, respectively, as a result of regression during evolution. Type C TdMCBPs are considered to be the direct predecessors of NIRs, which present a mononuclear inter-domain copper-binding site resulting from further loss of coppers, and type B TdMCBPs would be the predecessors of MCOs, which maintain a trinuclear inter-domain copper-binding site.

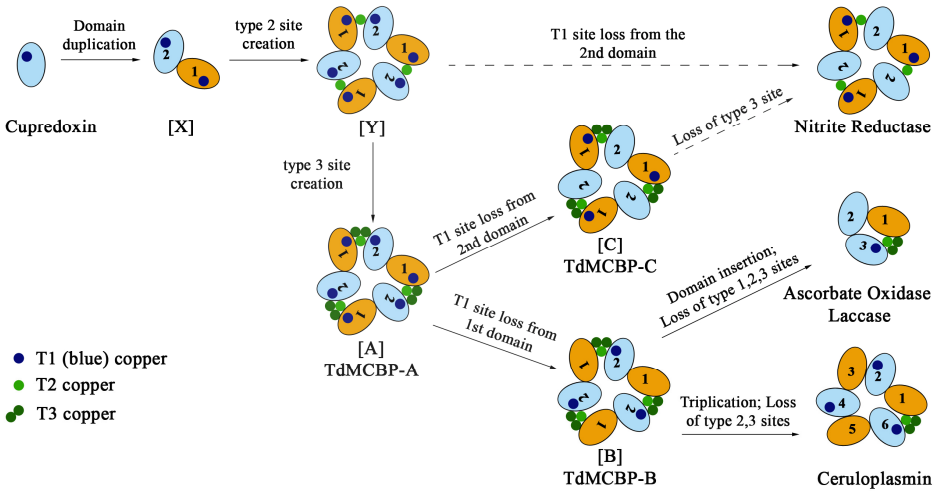

Figure 2 - Schematic representation of the molecular evolution of MCBPs. An oval shape indicates a cupredoxin domain. Blue and green dots indicate type 1 (intra-domain) and type 2/3 (inter-domain) copper atoms, respectively. Solid arrows indicate the postulated evolutionary pathways and dotted arrows indicate alternative evolutionary pathways. Conventional MCBPs are shown on the right. Five hypothetical proteins are shown with bracketed labels. Three of them ([**X**], [**Y**], and [**A**]) have blue copper (type 1) binding sites in both domains, whereas [**B**] and [**C**] have one of such sites only in the second and first domain, respectively. The hypothetical proteins [**A**], [**B**] and [**C**] have trinuclear inter-domain sites, whereas [**Y**] has a mononuclear inter-domain copper binding site. (adapted from Nakamura and Go, 2005).

The existence of such proteins has been confirmed (Nakamura and Go, 2005; Skálová *et al.*, 2009; Lawton *et al.*, 2009), further supporting this theory for the molecular evolution of MCBPs. However, further analysis will be needed as new structures become available, since certain details are not totally certain, as is the case of the possibility that three- and six-domain blue proteins may have acquired first the trinuclear copper-binding site with the other MCBPs having evolved from this common ancestor.

1.1.2 Overall architecture and function

Multi-copper oxidases are enzymes that exploit the distinctive redox properties of copper ions, catalyzing the oxidation of a vast array of substrates molecules with subsequent reduction of dioxygen to water.

Despite broad sequence similarities and different inter-domain copper and substrate-binding sites, the overall structural fold of these enzymes is generally conserved, consisting of cupredoxin-type domains, usually comprising two four-stranded β-sheets, arranged in a sandwich-like manner (Nakamura and Go, 2005; Murphy *et al.*, 1997). In MCOs, the resulting Greek-key β-barrel motif differs from the typical Greek-key β-barrel (containing only anti-parallel β-strands) in that the first and third strands form parallel connections to their respective β-sheets. Within this fold, the eight conserved β-strands, constituting the core structure, are connected by structurally non-conserved regions of polypeptide chain and a discontinuity is observed as strand two crosses to strand three from one sheet to the other as shown in Figure 1 (Murphy *et al.*, 1997).

Combined spectroscopic studies and X-ray crystallography have revealed that all members of the MCO family contain at least two distinct copper centres as their minimal functional unit, comprising a total of four copper atoms; a mononuclear type 1 blue copper centre (T1) and a hybrid trinuclear cluster consisting of two type 3 (T3) and one type 2 (T2) copper atoms (see the following section for the classification of the Cu centres). Such copper binding sites are easily recognized at the level of these enzymes' primary amino acid sequences, through the presence of signature patterns of conserved ligands, accounting for a total of ten histidine residues (eight of which arranged in four highly conserved His-X-His motifs) and a cysteine residue (Solomon *et al.*, 1996) (Figure 3).

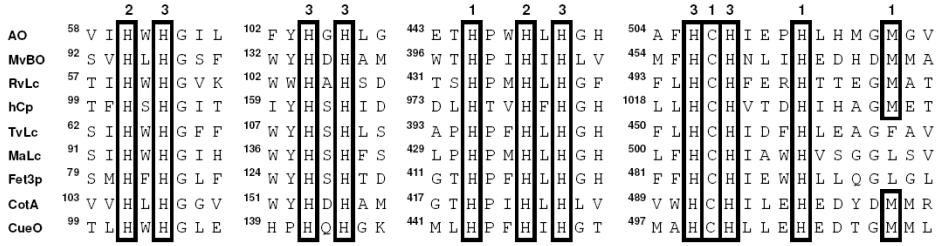

Figure 3 - Sequence alignment of amino acid sequences around the copper-binding sites of different MCOs. Encased inside boxes are the conserved residues that coordinate the three different copper centres of MCOs; numbers above the sequences indicate the type of copper centre to which the ligand coordinates (type 1, 2 and 3). Zuchini squash ascorbate oxidase (AO), *Myrothecium verrucaria* bilirubin oxidase (MvBO), *Rhus vernificera* laccase (RvLc), human Ceruloplasmin (hCp), basidiomycete *Trametes versicolor* laccase (TvLc), ascomycete *Melanocarpus albomyces* laccase (MaLc), yeast Fet3 protein (Fet3p), *Bacillus subtilis* CotA laccase (CotA), *Escherichia coli* CueO (CueO).

Based on their domain organization and function, ascorbate oxidase, ceruloplasmin, laccases and a few other metallo-oxidases are the most commonly recognized members within the MCO family of enzymes (Messerschmidt, 1997; Lindley, 2001; Solomon *et al.*, 1996; Giardina *et al.*, 2010; Kosman, 2010). Ascorbate oxidase (AO) (L-ascorbate: dioxygen oxidoreductase, EC 1.10.3.3) is known to catalyze the oxidation of L-ascorbate to dehydroascorbate, via the semidehydroascorbate radical disproportionation. This MCO has been identified in fungi and bacteria, but is mostly spread among higher plants where it has been associated with the cell wall, participating in plant growth via cell elongation. In plants, AOs occur as homodimeric proteins, whilst for instance the bacterial AO from *Acremonium sp.* HI-25 is a monomer with a higher degree of glycosylation (Solomon *et al.*, 1996 and references therein). The fully oxidised form of AO from the green zucchini squash (*Cucurbita pepo medulosa*) was the first MCO whose crystallographic structure was determined (PDB id: 1AOZ, 1.9Å resolution), revealing the three-domain architecture and the nature and spatial arrangement of the copper centres

typical of this family of enzymes (Messerschmidt *et al.*, 1989 and 1992) (Figure 4a)).

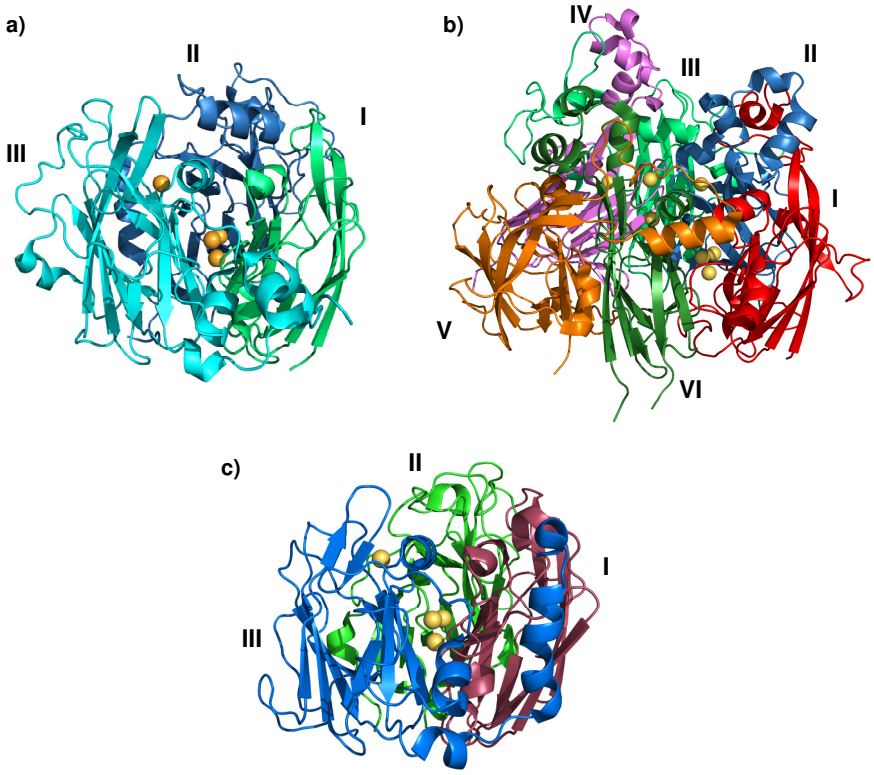

Figure 4 – Overall view of the three-dimensional structure of three different MCOs, consisting of cupredoxin-type domains and showing the disposition of the copper centres. Copper ions are represented as spheres and each domain is identified by a number. **Ascorbate oxidase (a)** presents the typical three-domain organization with the T1 Cu centre located in domain 3 (cyan) and the trinuclear cluster embedded in between domains 1 (green) and 3. **Human ceruloplasmin (hCp) (b)** in turn, is formed by six cupredoxin-type domains, possessing three T1 Cu centres placed in domains 2 (blue), 4 (violet) and 6 (dark green), whereas the trinuclear cluster is placed between domains 1 (red) and 6. **Laccases (c)**; their three-dimensional architecture resembles that of Ascorbate oxidase (represented is the structure of the fungal *Cerrena maxima* laccase).

In its functional homodimeric structure, each monomer of AO contains three sequentially arranged cupredoxin-type domains (plus an additional four-stranded β-sheet constituting an N-terminal extension of this

domain). In this tripartite organization, the T1 Cu is located in domain 3 and the trinuclear cluster is located between domains 1 and 3, bound to the canonical eight His residues symmetrically supplied by both domains. In such a unique subdomain structure, both copper centres are positioned approximately 12-13Å apart from each other (Solomon *et al.*, 1996; Messerschmidt *et al.*, 1989 and 1992). Moreover, two solvent channels were identified, giving clear access to the trinuclear centre: a broader channel directed towards the T3 Cu pair on one side of the trinuclear cluster, and a narrower channel connecting the T2 Cu ion to the protein surface, on the other side of the cluster.

Ceruloplasmin (Fe(II): dioxygen oxidoreductase, EC 1.16.3.1) is a MCO found mainly in the blood serum of vertebrates. It may well be multi-functional, but its precise functions are still a matter of debate. Thus, it may play a vital role in iron homeostasis by oxidising Fe(II) to Fe(III) for subsequent uptake by transferrin. However, it has also been associated with antioxidant functions and the oxidation of organic (e.g. epinephrine, norepinephrine, serotonin) and other inorganic compounds (e.g. Ca^{2+}, Co^{2+}) (Zaitzeva *et al.*, 1996; Zaitzev *et al.*, 1999; Bento *et al.*, 2007). A role in copper transport has also been proposed, although this seems unlikely as a specific function from a consideration of its structure. The determination of the human Ceruloplasmin (hCp) three-dimensional structure by X-ray crystallography (PDB id: 1KCW and 2J5W, at 3.1 and 2.8Å resolution, respectively) revealed this enzyme to be composed of a rather unusual number of six consecutive cupredoxin-type domains arranged in a triangular array and comprising six integral copper ions: three occupying mononuclear Cu centres (domains 2, 4 and 6), whereas the remaining three form a trinuclear cluster placed at the interface between domains 1 and 6 (Figure 4b)). In hCp structure, the trinuclear

centre, together with the nearest mononuclear Cu centre (that of domain 6), form a cluster very similar to that seen in AO and other three-domain MCOs (Zaitzeva *et al.*, 1996; Bento *et al.*, 2007), as is the case of laccases and other metallo-oxidases. Laccases (p-diphenol: dioxygen oxidoreductase, EC 1.10.3.2) constitute the simplest members of the MCO family of enzymes (Figure 4c)). These are present in all domains of life (Eukarya, Bacteria and Archaea) (Hoegger *et al.*, 2006; Giardina *et al.*, 2010; Sharma *et al.*, 2007; Claus, 2003) exerting a vast diversity of functions by oxidising a broad range of substrates (mainly aromatic but also inorganic compounds) using dioxygen as an acceptor (Solomon *et al.*, 1996; Nakamura and Go, 2005; Kosman, 2010; Mayer and Staples, 2002). In turn, metallo-oxidases are laccase-like MCOs that present higher efficiency towards the oxidation of lower valency, first row transition metal ions as compared with aromatic substrates (Stoj and Kosman, 2005). Examples of these are the hCp homologues, Fet3 protein (Fet3p) from *Saccharomyces cerevisiae* and the CueO protein from *Escherichia coli*; the former participates in the yeast iron metabolism by catalyzing the conversion of ferrous to ferric iron (Taylor *et al.*, 2005) and the latter is involved in the copper efflux system of *E. coli* (Outten *et al.*, 2001).

Functionally, and despite their diverse substrate specificities and consequent biological roles, MCOs are responsible for the coupling of the single-electron oxidation of four substrate molecules with the four-electron reduction of dioxygen to water. Such reactions are coordinated between the two canonical copper centres, with the substrate oxidation occurring at the T1 Cu centre, which shuttles electrons to the trinuclear centre where dioxygen binding and reduction occurs with the concomitant production of two water molecules (Lindley, 2001; Solomon *et al.*, 1996 and 2001) (Figure 5).

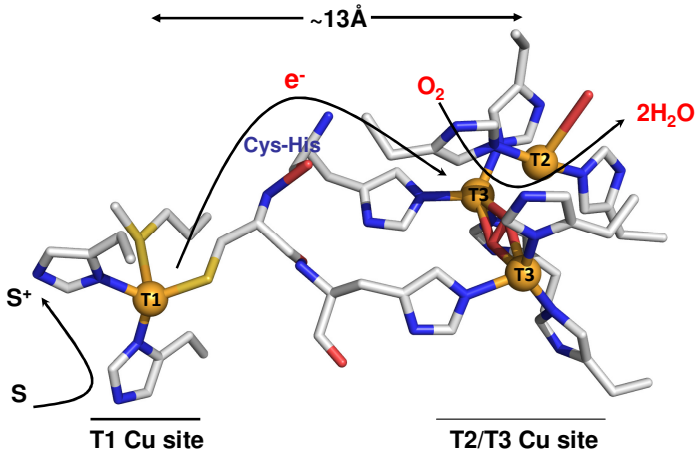

Figure 5 – Structure of the MCOs active site showing the flow of substrates, electrons (e^-) and dioxygen (O_2). Copper ions are represented as spheres. Substrate oxidation occurs at T1 Cu site, whereas dioxygen binding and reduction occurs at the trinuclear cluster. Figure generated from the crystal structure of CotA laccase (PDB id: 1W6L (Bento *et al.*, 2005)).

Within this vast category of enzymes, the present dissertation will focus on the laccases.

1.1.3 The copper-binding centres

Copper classification in the MCO family of enzymes is based on the characteristic spectroscopic properties exhibited by each one of these ions (Solomon *et al.*, 1996; Malmström, 1982), reflecting the geometry and electronic structure of each of the centres. In MCOs, all four copper atoms are coordinated by highly conserved residues. Typically, the T1 Cu (Cu1) is coordinated by two histidine nitrogens and a cysteine thiolate sulphur, forming a tight trigonal coordination where such residues occupy an equatorial position. In addition, a conserved methionine, placed 10 residues apart from the cysteine and approximately 3.2Å from the Cu ion, may also occur as a fourth soft axial ligand (SD atom), conferring the site

a flattened tetrahedral configuration (Giardina *et al.*, 2010; Bento *et al.*, 2006; Solomon *et al.*, 2001; Kosman, 2010) (Figure 5). Although this is the case for the vast majority of MCOs, in some such as the fungal laccases, this axial position is occupied instead by either a leucine or a phenylalanine, sited at approximately 3.5Å or more from the T1 Cu, and hence not taking part in the ligand-metal coordination (Hakulinen *et al.*, 2002; Piontek *et al.*, 2002) (Figure 6). In this Cu centre, the charge transfer transition between the cysteine sulphur and the Cu atom (when fully oxidised) is responsible for the blue colour of these proteins, yielding an intense electronic absorption band at approximately 600nm (ε>3000 M^{-1} cm^{-1}). Moreover, this site is EPR detectable, showing a narrow parallel hyperfine coupling ($A_{||} < 95 \times 10^{-4}$ cm^{-1}) (Bento *et al.*, 2006 and references therein).

At the trinuclear centre, the copper ions are coordinated by eight histidine residues, three for each of the T3 Cu ions (Cu2 and Cu3) and two for the T2 Cu ((Cu4); the T2 centre) that becomes three-coordinated with a water-derived ligand, bound to it on the opposite side of the binuclear centre (T3 site) (Figure 6). The T2 Cu centre does not exhibit absorption bands in the UV/Visible region, being solely characterized by a large parallel hyperfine splitting in the EPR spectrum ($A_{||} > 140 \times 10^{-4}$ cm^{-1}) (Giardina *et al.*, 2010; Bento *et al.*, 2006; Solomon *et al.*, 1996). On the other hand, the T3 Cu's, additionally coordinated by a bridging ligand placed between them (oxygen derived species), exhibit a charge transfer absorption band at around 330nm and are EPR silent as a result of the antiferromagnetic coupling through this type of bridging species (Solomon *et al.*, 1996 and 2001). At the trinuclear centre, both the binuclear and the T2 Cu sites are arranged in a triangular manner, roughly 12Å apart (Figure 6) from the T1 Cu center.

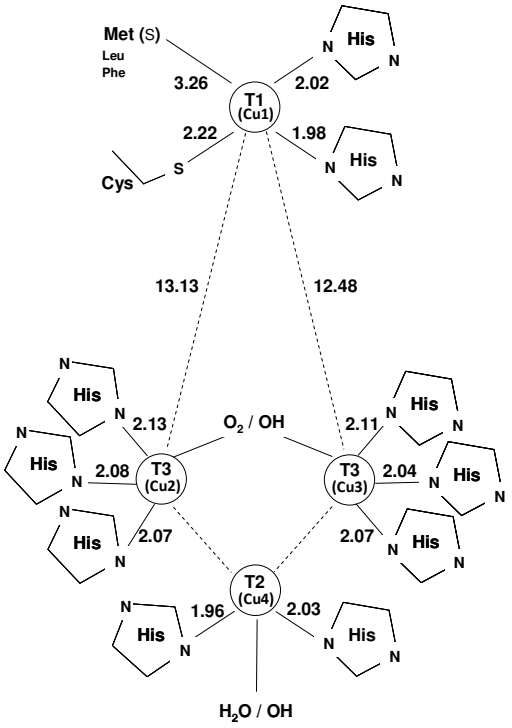

Figure 6 – Schematic representation of the copper centres of MCOs. For better illustration, the inter-atomic distances observed for CotA laccase (PDB id: 1W6L (Bento *et al.*, 2005)), among all the relevant atoms, are shown (distances provided in Angstroms, Å). In the CotA laccase structure an O_2 molecule is bridged in between the T3 Cu's and a water molecule is bound at the T2 Cu.

1.1.4 The substrate binding site and substrate oxidation

In MCOs the T1 Cu site is usually located within a groove at the enzyme's surface that forms the substrate binding site. Such facilitates the role of the T1 copper as the primary centre at which electrons from reducing substrates are accepted. The size and shape of this substrate binding site vary considerably among MCOs, in accordance with the range of substrates that they can accommodate and oxidise. MCOs substrates can generally be divided into two main groups: electron-no-proton donors and electron-proton donors (Shleev *et al.*, 2005). Included in the first group are simple inorganic redox compounds (e.g., $Fe(CN)_6^{4-}$, Cu^{1+}, Fe^{2+}), and organic substrates, which are oxidised by the enzyme through a cation radical mechanism (e.g., ABTS, [2,2'-azinobis-(3-ethylbenzothiazoline-6-

sulfonate)]); the second group includes phenols and aromatic amines for which the formal potentials, determined by the compounds chemical structure and the presence of electron-withdrawing or donating substituents at the phenolic ring, are strongly dependent on the surrounding pH (Shleev *et al.*, 2005; Xu, 1996; Garzillo *et al.*, 1998).

To date, only a few MCO complex structures have been reported. These include the *Trametes versicolor* laccase complexed with 2,5-xylidine (PDB id: 1KYA, 2.4Å resolution) (Bertrand *et al.*, 2002), the *Bacillus subtilis* CotA laccase complexed with ABTS (PDB id: 1OF0, 2.5Å resolution) (Enguita *et al.*, 2004), the *Trametes trogii* laccase complexed with the competitive inhibitor p-methylbenzoate (PDB id: 2HRG, 1.6Å resolution) (Matera *et al.*, 2008) and the *Melanocarpus albomyces* laccase complexed with 2,6-dimethoxyphenol (2,6-DMP) (PDB id: 3FU8, 1.8Å resolution) (Kallio *et al.*, 2009). Despite showing different substrate binding modes and displaying distinct pocket features (e.g. surface loops, amino acid composition), the reported crystal structures share a few traits that enable insights into the initial electron transfer steps, from the substrate to the T1 Cu centre. The most pronounced similarity in all four structures is that the reducing substrates were found to bind near the imidazole ring of a surface-exposed histidine residue, one of the ligands of the T1 Cu (His497 in CotA laccase, His508 in *M. albomyces*, His458 in *T. versicolor* and His455 in *T. trogii*). Such a configuration, where the substrates are hydrogen-bonded to the His ligand (for ABTS the distance is some 3.32Å), and not directly interacting with the T1 Cu ion, suggests that this residue functions as the entrance door for electrons during their transfer from the substrate to the T1 Cu centre. Therefore, placed at a privileged position, this His residue acts as the primary electron acceptor during the catalytic

mechanism (Bertrand *et al.*, 2002; Enguita *et al.*, 2004; Matera *et al.*, 2008; Kallio *et al.*, 2009; Giardina *et al.*, 2010).

Another interesting feature found in the complexed structures of the fungal laccases (*T. versicolor, T. trogii and M. albomyces*) is the presence of a conserved carboxylic acid (Asp/Glu) placed at the rear wall of the substrate binding cavity. This residue (Glu235 in *M. albomyces*, Asp206 in *T. versicolor* and Asp205 in *T. trogii*) constitutes the only hydrophilic residue present in these enzymes' highly hydrophobic pocket and has been reported to play a key role during the oxidation of phenolic substrates, by abstraction of a proton from the substrates' OH group (Bertrand *et al.*, 2002; Matera *et al.*, 2008; Kallio *et al.*, 2009). In the bacterial CotA laccase, however, this carboxylic acid is replaced by Thr260, possibly indicating a slightly different mechanism of this enzyme towards the oxidation of phenolic substrates (Enguita *et al.*, 2004; Kallio *et al.*, 2009).

Other MCOs of known structure, however, do not have the T1 Cu histidine ligands directly exposed to the solvent, hence they are not directly accessible to reducing substrates. Therefore, for these enzymes, additional hydrogen-bond pathways are required for the electrons to be transferred from the substrate to the T1 Cu centre. This seems to be the case of metallo-oxidases. One such example is the yeast ferroxidase Fet3p (PDB id: 1ZPU) (Taylor *et al.*, 2005; Quintanar *et al.*, 2007). Compared to laccase structures, this enzyme contains a more constrained active site, as a result of the longer structural motifs (strands and loops) framing the T1 Cu site at the putative binding pocket. Moreover, within these secondary structure elements resides a set of acidic residues (Glu185, Asp283 and Asp409), immediately adjacent to the T1 Cu site, that confer a negatively charged surface. These residues, implicated in Fe(II) binding and Fe(III) trafficking, are involved in the electronic coupling pathway that supports

the intermolecular electron transfer from the Fe(II) to the T1 Cu ion (Taylor *et al.*, 2005). Indeed, both T1 Cu histidine ligands (His489 and His413) are hydrogen-bonded to two of these acidic residues (Glu185 and Asp409, respectively), which in turn are exposed to the solvent and thereby accessible for interaction with a metallo-substrate. Being conserved among ferroxidases, these two acidic residues are considered to constitute the signature motifs of a MCO ferroxidase (Taylor *et al.*, 2005; Quintanar *et al.*, 2007). Similarly, in the hCp a similar set of carboxylates (e.g. Glu931, Glu932 and Asp230 for domain 6 of hCp) is observed in the neighbourhood of the putative ferroxidase site, providing a "holding site" for Fe(III) (Lindley *et al.*, 1997). One further example is the metallo-oxidase CueO, from *E. coli* (PDB id: 1KV7) (Roberts *et al.*, 2002 and 2003). The three-dimensional structure of this MCO reveals the presence of a methionine-rich large helical region (residues 355-371; seven Met) and loop (residues 372-379; two Met), located at the beginning of domain 3 and in close proximity to the mononuclear T1 Cu site. Another five additional methionines, not resolved in the crystal structure, are located in this region, comprising a total of fourteen methionine residues. In CueO, while obstructing the access of bulky substrates to the T1 Cu site, the Met-rich region has also been suggested to provide additional binding sites for exogenous Cu (Roberts *et al.*, 2003; Kataoka *et al.,* 2007). Indeed, a fifth Cu ion, buried just under the Met-rich region and close to the T1 copper site, was reported for the structure of CueO soaked with $CuCl_2$. This labile Cu ion is sited at 7.5Å from the protein surface and coordinates with two Met and two Asp residues, one of each coming from the Met-rich region (Met355 and Asp360), and the two other placed near the T1 Cu site (Met441 and Asp439). In its turn, one of these carboxylates (Asp439) is hydrogen-bonded to H443, a T1 Cu ligand, connecting this

site to the labile Cu site. Therefore, a regulatory role has been suggested for the labile copper, where the arrangement of D439 seems to be responsible for the mediation of electrons from the substrates to the T1 Cu (Roberts *et al.*, 2003). Such a Met-rich region is also present in other proteins implicated in Cu homeostasis (Arnesano *et al.*, 2002; Huffman *et al.*, 2002), and recent studies by Singh *et al.* have hypothesized that it may in fact be used for copper binding during CueO's response to copper toxicity (Singh *et al.*, 2011).

Substrate oxidation at the T1 Cu site is considered to be the catalytic rate-limiting step in MCOs (Solomon *et al.*, 1996), with the first electron transfer from the substrate (S) to the enzyme (E) being predominantly regulated by the redox potential difference between the substrate and the T1 Cu(II) ($\Delta E^\circ = E^\circ_E - E^\circ_S$). However, evidence of different activities observed for a single MCO towards substrates detaining comparable oxidation potentials (Xu, 1996; Garzillo *et al.*, 1998) suggests that structural features on the enzyme also influence the oxidation rates of substrates.

In laccases, the redox potential of the T1 Cu site spans between the broad range of 430-790mV (Shleev *et al.*, 2005; Zhukhlistova *et al.*, 2008; and references therein), with fungal laccases generally presenting much higher values (mostly above 700mV) than those of plant and bacterial laccases (usually below 550mV) (Solomon *et al.*, 1996). Such a difference has been attributed to the presence, in fungal laccases, of a non-coordinating leucine or phenylalanine residue instead of the usual T1 Cu coordinating axial Met. Indeed, site-directed mutagenesis studies targeting the replacement of the axial Met ligand on the bacterial *Pseudomonas aeruginosa* azurin by a Leu (Karlsson *et al.*, 1989) and on the *Bacillus subtilis* CotA laccase by a Leu and Phe (Durão *et al.*, 2006) led to an increase of

the T1 Cu redox potential by approximately 70mV, 100mV and 60mV, respectively. Similarly, studies performed on the fungal *Trametes villosa* laccase, where the corresponding natural variant Phe was mutated into a Met, yielded a lowering of the T1 site redox potential by 100mV (Xu *et al.*, 1999), further supporting the importance of the T1 Cu axial ligand nature to the redox potential of this site. Nevertheless, significant differences in redox potential also exist among fungal laccases (Xu *et al.*, 1996), which indicates that other protein factors, in the vicinity of the T1 Cu site, contribute as well to affect this site redox potential. Such factors include solvent accessibility, internal hydrogen bonding to the T1 Cu ligands and dielectric anisotropy around the site (Xu *et al.*, 1996; Marshall *et al.*, 2009).

1.2 Laccases

1.2.1 Distribution and Physiological role

Laccases (p-diphenol: dioxygen oxidoreductase, EC 1.10.3.2) are the simplest representative members of the MCO family of enzymes, constituting good model systems for the investigation of structure-function relationships. Such an enzyme was first identified on the Japanese lacquer tree *Rhus vernificera*, from where its name originates ("lacquer") (Hoegger *et al.*, 2006).

Widely distributed in nature, laccases are present in Eukaryotes (animal, plant, fungi), Prokaryotes (bacterial) and Archaea, composing the largest subgroup of MCOs (Giardina *et al.*, 2010; Sharma *et al.*, 2007; Claus, 2004) and exerting wide-ranging functions as well as participating in several processes. Indeed, laccases have been reported to be associated with lignin biosynthesis, wound healing and iron oxidation, in plants; lignin

degradation, fruiting body formation, pigmentation, sporulation, pathogenesis and detoxification processes, in fungi; melanisation, cuticule sclerotization and oxidation of dietary toxic compounds, in insects; morphogenesis, endospore coat protection, Mn oxidation and Cu homeostasis, in bacteria (Dwivedi *et al.*, 2011; Hoegger *et al.,* 2006; Giardina *et al.*, 2010; Nakamura and Go, 2005; Claus, 2003; Sharma *et al.*, 2007; and references therein). Despite the particularities intrinsic to each function (directly dependant on the enzyme's source organism and physiological conditions), overall, laccases are capable of catalyzing the oxidation of a plethora of substrates, varying from aromatic (e.g. phenols, substituted phenols, non-phenols, amines) to inorganic compounds (e.g. $Mo(CN)_8^{4-}$, $Fe(CN)_6^{4-}$ and lower valency metal ions, such as Cu^{1+}, Fe^{2+}, Mn^{2+}), with accompanying reduction of dioxygen to water (Solomon *et al.*,1996; Nakamura and Go, 2005; Kosman, 2010; Alexandre and Zhulin, 2002). In the case of the oxidation of aromatic substrates, the free reactive radicals formed can further undergo non-enzymatic reactions, divided into three main categories; cross-linking of monomers, degradation of polymers and ring cleavage of aromatic compounds (Claus, 2003 and 2004). This wide reaction capability and substrate versatility is the basis for the increasing interest and usefulness of these enzymes from the perspective of biotechnological applications (Rodríguez Couto and Toca Herrera, 2006; Riva, 2006; Dwivedi *et al.*, 2011). Such applications include detoxification and decontamination of soils, waste and industrial effluents (e.g. pulp, paper, textile and petrochemical industries); biobleaching of dyes; organic synthesis; and their function as bioremediation agents.

The vast majority of the so far structurally reported laccases are derived from fungi, whereas bacterial laccases remain far less well characterized. Examples of fungal laccases with known three-dimensional structure are

the ones from the basidiomycetes *Coprinus cinereus* (PDB id: 1A65), *Trametes versicolor* (PDB id: 1GYC), *Cerrena maxima* (PDB id: 2H5U), *Rigidoporus lignosus* (PDB id: 1V10), *Trametes hirsuta* (PDB id: 3FPX), *Coriolus zonatus* (PDB id: 2HZH) and *Lentinus tigrinus* (PDB id: 2QT6), as well as, the laccase from the ascomycete *Melanocarpus albomyces* (PDB id: 1GW0) (Ducros *et al.*, 2001; Piontek *et al.*, 2002; Lyashenko *et al.*, 2006a; Garavaglia *et al.*, 2004; Polyakov *et al.*, 2009*;* Lyashenko *et al.*, 2006b; Ferraroni *et al.*, 2007; Hakulinen *et al.*, 2002; respectively). Nevertheless, recent progress in whole genome analysis, along with databank searches, have provided evidence for novel bacterial laccases or laccase-like proteins, identified in many gram-negative and gram-positive bacteria (Hoegger *et al.*, 2006; Giardina *et al.*, 2010; Alexandre and Zhulin, 2002; Claus, 2003 and 2004). Even in thermophilic organisms, for which such proteins are rarely found, corresponding laccase-like proteins have also been identified, including in Archaea (Sharma *et al.*, 2007; Fernandes *et al.*, 2007 and 2010; Sakuraba *et al.*, 2011; Bello *et al.*, 2012). The first three-dimensional structure of a bacterial laccase was reported for the CotA laccase from *Bacillus subtilis* (PBD id: 1GSK) (Enguita *et al.*, 2003). Another well characterized bacterial MCO, whose structure has been solved, is the CueO protein from *Escherichia coli* (PBD id's: 1KV7, 1N68), which in fact is a metallo-oxidase (Roberts *et al.*, 2002 and 2003).

Crystal structure comparison of these enzymes shows the typical three-dimensional organization of MCOs, evidencing their highly conserved nature.

1.2.2 CotA laccase from *Bacillus subtilis*

The gram-positive soil bacterium *Bacillus subtilis* is capable of producing complex cellular structures, the endospore, when subjected to stress

conditions such as starvation. During the differentiation process, such structures become encased in a proteinaceous multi-layered coat that gives resistance against physical (e.g. heat, desiccation, radiation) and chemical (e.g. oxidising agents, lytic enzymes) agents, at the same time controlling the spore's response to the environment's stimuli and, consequently, its germination (Driks, 1999; Henriques and Moran, 2000). This endospore coat is composed of over 25 different proteins, self-assembled between an amorphous undercoat, a lamellar inner structure and a striated electron-dense outer coat (Driks, 1999; Henriques and Moran, 2000). One of such proteins is CotA laccase, located at the outer layer of the spore coat and reported to be involved in the biosynthesis of the spore brown pigment, contributing to the spore's protection against UV-light and hydrogen peroxide (Hullo *et al.*, 2001; Martins *et al.*, 2002). Furthermore, this monomeric 65 KDa protein (513 residues) is a highly thermoactive and intrinsically thermostable enzyme, exhibiting a maximal activity at 75ºC and a half-life of inactivation ($t_{1/2}$) of approximately 2h, at 80ºC (in both cases using ABTS as substrate) (Martins *et al.*, 2002). With an already determined three-dimensional structure, such assets make CotA laccase a suitable model for structure-function studies, as not many characterized laccases are capable of enduring such conditions. Indeed, in general, bacterial laccases are highly active and withstand higher temperatures and pH values than fungal laccases, in much reflecting the environmental conditions of their source organisms (Dwivedi *et al.*, 2011).

Functionally, CotA is a *sensu stricto* laccase, exhibiting oxidase activity with respect to aromatic compounds (Martins *et al.*, 2002).

The first structure reported for the native CotA laccase (PDB id: 1GSK) showed a severe copper depletion, in particular at the trinuclear Cu centre, likely to result from the purification methods (Enguita *et al.*, 2003, Martins

et al., 2002). At a later stage, efforts were made to minimize copper depletion of the sample by addition of $CuCl_2$ to the protein solution and crystals (PDB id: 1W6L) (Bento *et al.*, 2005), resulting in a nearly fully copper loaded enzyme. More recently, the implementation of a new protein expression protocol by Durão and co-workers (Durão *et al.*, 2008a) has allowed full copper incorporation by the enzyme. This was achieved through supplementation of the media with $CuCl_2$, together with a switch from aerobic to microaerophilic conditions, during cell growth. This method was followed to obtain the samples used for the studies presented in this dissertation. For this reason, only the "as isolated" state soaked with $CuCl_2$ will be considered for comparisons in the present work, as a reference of the oxidised state of the enzyme (Bento *et al.*, 2005).

1.2.2.1 Overall structure and copper centres

The CotA laccase structure, determined by X-ray crystallography (PBD id: 1GSK) (Enguita *et al.*, 2003), shows the characteristic fold of MCOs, with the T1 Cu centre located in domain 3 and the trinuclear cluster located at the interface between domains 1 and 3. In CotA structure, all three cupredoxin-type domains are linked by external inter-domain loops, with domain 2 connecting to domain 1 through a short α-helical segment, and to domain 3 through a larger loop, acting as a bridge between both domains (Figure 7). Such a feature was reported to increase the packing level of the CotA laccase (Enguita *et al.*, 2003) and seems to be characteristic of prokaryotic laccases, as it is also present in the bacterial MCO CueO, but not in fungal laccases (where it corresponds to an internal connection).

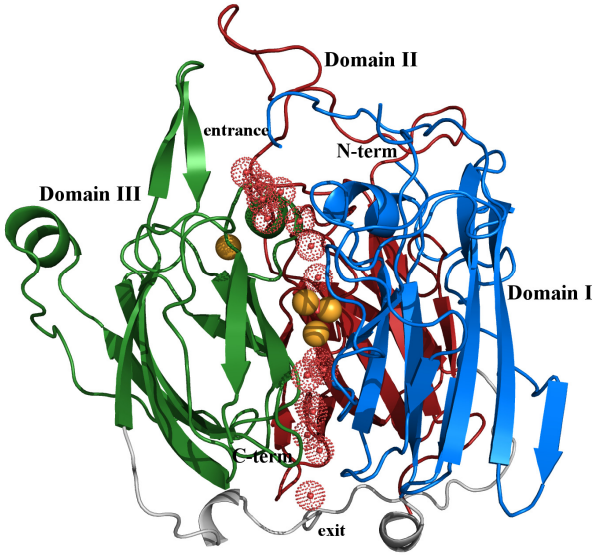

Figure 7 – Overall view of the three-dimensional structure of CotA laccase from *Bacillus subtilis* (PDB id: 1W6L (Bento *et al.*, 2005)) **highlighting the entrance and exit channels of the catalytic mechanism.** Copper atoms are represented as spheres. (adapted from (Bento *et al.*, 2005)).

Another noteworthy structural feature of the CotA laccase is the lid-like structure that protrudes over the enzyme's putative substrate binding site, near the T1 Cu centre (Figure 7). This feature, composed of a loop and short α-helix, has been associated to some degree of flexibility, mediating the access of bulkier substrate molecules to the T1 Cu site. Indeed, CotA laccase presents large molecular and solvent accessible areas at this site, with the putative binding cavity being formed mainly by apolar residues, both in agreement with the lack of substrate specificity reported for this enzyme (Enguita *et al.*, 2003; Martins *et al.*, 2002).

Regarding the Cu centres, in CotA laccase the T1 Cu centre is bound to the protein by two histidines (His497 and His419) and a cysteine (Cys492), with a fourth distant axial methionine residue (Met502) placed

3.26Å apart (Cu-SD distance), functioning as a soft ligand and giving the site a distorted tetrahedral configuration.

The trinuclear cluster is coordinated by the canonical pattern of four His-X-His motifs, two from domain 1 and two from domain 3, with a bridging ligand in between both T3 Cu ions (a dioxygen molecule when in the oxidised state) (Bento *et al.*, 2005). Each T3 Cu binds to three His residues (His107, His153, His493 for Cu2 and His155, His424 and His491 for Cu3), whereas T2 Cu (Cu4) binds to two His residues (His105 and His422). The access of molecular oxygen to the trinuclear site and egress for the water molecules resulting from dioxygen reduction, arise from the presence of two solvent channels placed at opposite sides of this centre; the access channel directed towards the two T3 Cu ions, and the exit channel directed towards the T2 Cu site, both allowing communication with the protein surface (Figure 7). These solvent channels are mainly formed by polar and neutral residues, arranged in a tunnel-like form (Enguita *et al.*, 2003; Bento *et al.*, 2005).

1.2.2.2 Dioxygen reduction in CotA laccase: structural studies

The precise catalytic mechanism of MCOs and, in particular, of the dioxygen reduction process, has been unclear. With this in mind, Bento *et al.* (Bento *et al.*, 2005) performed additional X-ray structure investigations on CotA laccase, which allowed further insights into the principal stages of this process. For that purpose, crystal structures of CotA laccase corresponding to the reduced and oxidised states and in the presence of hydrogen peroxide and the laccase inhibitor azide were obtained. Although the determined structures show the typical architecture of multi-

copper oxidases, both in terms of overall fold and spatial arrangement of the copper centres, some differences were observed at the level of the trinuclear Cu site (Bento *et al.*, 2005). In the oxidised state of CotA laccase (Figure 8a)), corresponding to the "as isolated" state soaked with $CuCl_2$ (PDB id: 1W6L), a molecular oxygen species is placed amid both T3 copper ions (Cu2…Cu3 separation of 4.72Å), almost symmetrically positioned relatively to the Cu2-Cu3 axis and directly interacting with all three coppers (this structure differs from the ABTS complex structure obtained by Enguita and co-workers (Enguita *et al.*, 2004), where a dioxygen molecule was found trapped in the water channel leading towards the trinuclear cluster, but not bound to it). Additionally, this species hydrogen bonds, through its O1 atom, to a water molecule placed 2.40Å away in the access solvent channel that in turn hydrogen bonds to the carboxylate side chain of an acidic residue (Glu498). On the other side of the cluster, the T2 Cu (Cu4), placed 2.42Å distant from the dioxygen O2 atom, is also bound to a water molecule localised 2.98Å away in the outlet channel (Bento *et al.*, 2005). A similar orientation of the dioxygen species was observed for the oxidised state of the fungal laccase from *M. albomyces* (Hakulinen *et al.*, 2002); however, is this structure, the channel providing access to the trinuclear cluster is partially blocked by the C-terminal end of the protein molecule and it is reported that a chlorine atom is bound instead to the T2 Cu ion.

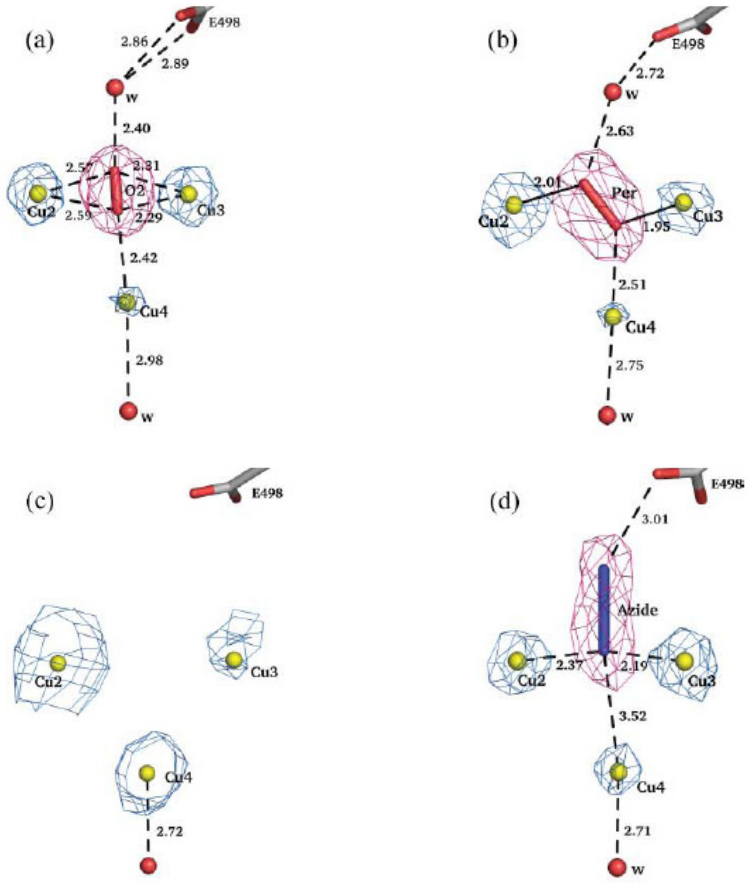

Figure 8 – CotA laccase structures in the a) oxidised ('as isolated') state, b) in complex with hydrogen peroxide (H_2O_2), c) in the reduced state and d) in complex with the inhibitor azide. In each panel the electron density was calculated from SigmaA weighted 2|Fo|-|Fc| Fourier syntheses, for the Cu ions, and from omit Fourier syntheses computed with SigmaA wighted coefficients |Fo|-|Fc|, for the adducts. The relative volumes of the electron density peaks reflect the respective occupancies of the Cu ions. (figure taken from (Bento *et al.*, 2005))

The oxidised state of CotA laccase also differs from structures obtained for the "as isolated" state of other MCOs, in which two hydroxyl moieties are observed, one bridged between both T3 Cu ions, and a second one bound to the T2 Cu ion (Messerschmidt *et al.*, 1989 and 1992).

As for the peroxide adduct (PDB id: 1W8E) (Figure 8b)), crystal soaking with hydrogen peroxide retrieved a peroxide species (O_2^{2-} anion) bridging

in a zigzag mode in between both T3 Cu ions, with each of the coppers binding to only one of the oxygen atoms. In this structure, the diatomic moiety is inclined 51º relatively to the Cu2-Cu3 axis, with Cu2...Cu3 distance shortening to 4.66Å, yet maintaining the hydrogen bond with the solvent molecule located at the entrance channel (placed 2.63Å away). On the opposite side of the cluster, the peroxide species is 2.51Å distant from the T2 Cu (Cu4), which remains bound to the exiting water molecule sited 2.75Å apart (Bento *et al.*, 2005). This structure differs from that observed previously for AO, in which the peroxide species is found to bind terminally to only one of the T3 Cu ions (Cu2) and oriented along the solvent access channel (Messerschmidt *et al.*, 1993).

In its turn, when in the fully reduced state (PDB id: 2BHF) (Figure 8c)), obtained by soaking the crystals with sodium dithionite in anaerobic conditions, there is no bridging ligand bound to the T3 Cu's, which become further apart (Cu2…Cu3 distance of 5.05Å), as well as in relation to the T2 Cu (Cu4). This results from the movement of each copper ion towards their respective coordinating ligands, with the T2 Cu remaining bound to the water molecule placed at the exit channel (2.72Å distant), ending in all Cu ions becoming three-coordinated (preferred stereochemistry for Cu(I) ions) (Bento *et al.*, 2005). For the most part, this structure is similar to that observed for the reduced form of AO, except that a hydroxyl moiety is found to bind to the T2 Cu ion of AO (Messerschmidt *et al.*, 1993).

Finally, for the azide adduct (PDB id: 1W6W) (Figure 8d)), the laccase inhibitor azide prevents binding of dioxygen to the site, occupying its place amid both T3 Cu ions (Cu2…Cu3 distance of 4.52Å), in an almost symmetric position. In this structure, the azide molecule is terminally bound to the T3 Cu's by its N1 atom, resembling the O2 atom from the

$CuCl_2$ soaked structure, while at the other end its N3 atom replaces the water molecule observed at the entrance channel of this same structure, still remaining hydrogen bonded to the Glu498 residue. At the other end of the cluster, the T2 Cu (Cu4) is also bound to the exiting water molecule sited at a distance of 2.71Å (Bento *et al.*, 2005). In the equivalent structure of AO, the position occupied by the azide is different, as two azide moieties were found to bind terminally with only one of the T3 Cu ions (Cu2) (Messerschmidt *et al.*, 1993).

For all the structures, some Cu depletion was observed, in particular for the T2 Cu (Cu4).

1.3 The catalytic mechanism of MCOs: insights into the dioxygen reduction process

In MCOs both copper centres operate in order to steer electrons from the reducing substrate to molecular oxygen, without the release of potential harmful intermediates (e.g. $O_2^{\cdot-}$ or H_2O_2). This is achieved by means of sequential electron transfer steps between both Cu sites and by the ability of the trinuclear cluster to "store" these electrons, made available for the reduction of dioxygen to two water molecules. During the electronic pathway of the catalytic mechanism, the reducing substrate donates electrons to the T1 Cu ion through one of its His ligands (His497 in CotA laccase); in the subsequent steps, the electrons are transferred over approximately 13Å, via the highly conserved His-Cys-His bifurcated intramolecular pathway, where the T1 Cu Cys ligand (Cys492 in CotA) shuttles the electrons to the trinuclear Cu site, via the two adjacent His residues binding to each one of the T3 Cu ions (His493 for Cu2 and

His491 for Cu3, in CotA laccase) (Bento *et al.*, 2005). This process occurs through two electrons at a time. In addition to four electrons, the reduction process of dioxygen to water also requires four protons.

Over the years, the process of dioxygen reduction in MCOs has been the object of many studies and the use of different techniques has led to the proposal of different mechanisms, some of them derived from a more structural background, whereas others are mainly based on biochemical and spectroscopic information.

The first catalytic mechanism proposed for MCOs was that of Ascorbate oxidase (AO). Proposed by Messerschmidt and co-workers (Messerschmidt *et al.*, 1989, 1992 and 1993), this was deduced from the X-ray structures determined for AO in the fully oxidised and reduced forms, and the derivative peroxide adduct, but also considering the available data from kinetic and spectroscopic studies (Messerschmidt *et al.*, 1989, 1992 and 1993). In the proposed mechanism, the catalytic cycle starts from the resting form of the enzyme in which all four copper ions are in the fully oxidised +2 state and a hydroxyl moiety is bridged in between both T3 Cu ions (different from the oxidised form of CotA laccase); a second hydroxide ligand is found to bind to the T2 Cu ion, on the external side of the cluster (Figure 9a)). In a first step, the T1 Cu becomes reduced after receiving one electron from the reducing substrate (Figure 9b)). The electrons are then shuttled sequentially to the trinuclear centre, originating the fully reduced enzyme after four transferred electrons, in which the bridging hydroxyl moiety is released. At this point, a dioxygen molecule is thought to bind terminally to the Cu2 (Figure 9c)).

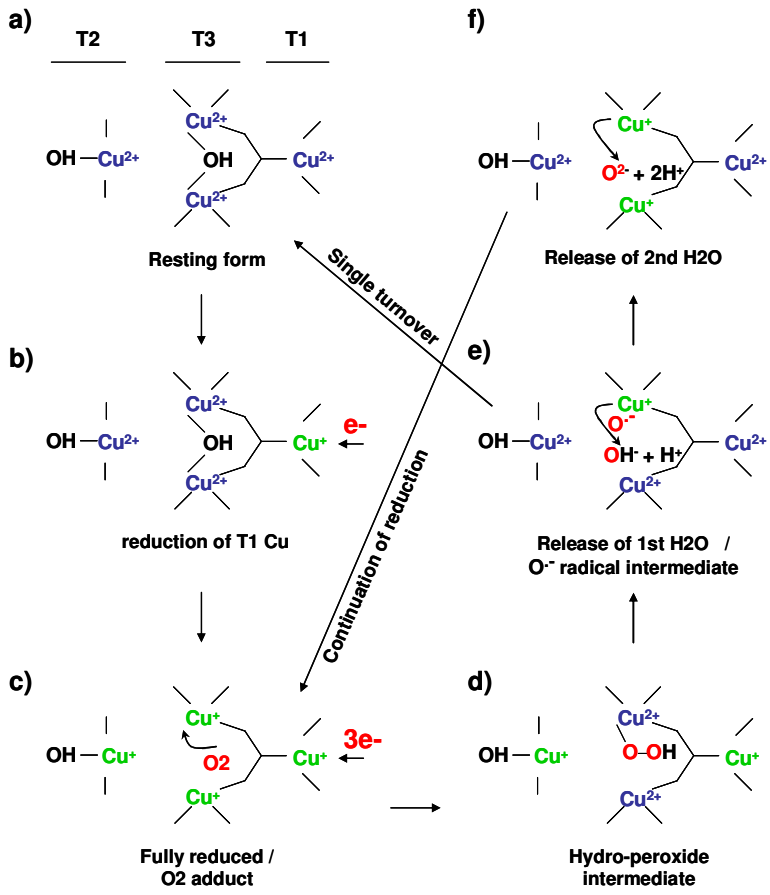

Figure 9 – Proposed catalytic mechanism for dioxygen reduction to water by AO. (adapted from Messerschmidt, 1997)

Two electrons are then transferred from the T3 Cu ion pair to the dioxygen, together with a proton, originating a hydroperoxide intermediate (peroxide derivative) (Figure 9d)). Two further electron transfers (one from the T2 Cu to the hydroperoxide intermediate, leading to the O-O bond breakage; and a fourth one coming from the T1 Cu to the Cu2 ion), together with the supply of a proton, originates the release of the first water molecule and the formation of an oxygen radical bound to the Cu2 ion (transient state), which remains reduced at this stage (Figure 9e)). A further T1 Cu reduction, and subsequent transfer of the

electron to the Cu3 ion, leads the fourth electron to be transferred from the Cu2 to the oxygen radical intermediate, with the release of the second water molecule after the supply of two protons (Figure 9f)) (Messerschmidt *et al.*, 1992 and 1993). According to Messerschmidt *et al.*, if only four electrons are transferred, the catalytic reaction may lead to the resting form of the enzyme with the second water molecule remaining bound as the bridging ligand placed amid the T3 Cu ions (which would require a significant rearrangement within the trinuclear cluster). If, on the other hand, the reduction process progresses, then the trinuclear cluster may retain a structure resembling the fully reduced form (Messerschmidt *et al.*, 1992 and 1993).

Another molecular mechanism has been hypothesised by Solomon and co-workers (Solomon *et al.*, 2008; and references therein), on the basis of spectroscopic and kinetic studies performed on the yeast ferroxidase Fet3p. Although relatively similar to the previous one, differences exist, in particular in what concerns the intermediates states formed. According to this mechanism, once dioxygen binds to the reduced form of the enzyme, the reaction proceeds via two sequential two-electron steps. In a first step, considered to be the rate limiting step, a peroxide intermediate (PI) is formed after the transfer of one electron coming from the T2 Cu and another one coming from one of the T3 Cu ions. This peroxide moiety forms an internal bridge between both T2 and T3 Cu centres and, unlike the case of AO, no proton is involved in this step. In a fast second step, two further electrons, one from the T1 Cu (which results in reduction of the T2 Cu ion and loss of its strong bond to peroxide), and another one from the T3 Cu ion that remained reduced, results on the reductive cleavage of the O-O bond. Together with a proton coming from the

water molecule that is bound to the T2 Cu ion, a native intermediate (NI) state is originated. This is characterized by a fully oxidised all bridged structure, where a μ3-oxo bridge is formed and an hydroxyl moiety is bridged in between the T3 Cu ions. This structure is considered to be consistent with the fast four-electron reduction of the NI into the fully reduced enzyme, as the μ3-oxo bridge would allow electron delocalization over the three Cu centres for easy electron transfer through the cluster. On the other hand, in the absence of reducing substrate, the NI is considered to decay into the resting oxidised form of the enzyme (equivalent to the one of AO). This interconversion between the two fully oxidised forms of the enzyme is though to proceed slowly via successive proton-assisted steps and involving a rearrangement of the μ3-oxo bridge from the inside to the outside of the cluster, with one of the oxygen atoms from the O_2 reduction ending up bound to the T2 Cu ion as a hydroxyl moiety, whereas the other one is released as a water molecule. As such, in this mechanism, the NI state is considered to be the catalytically relevant fully oxidised form of the enzyme, providing superexchange pathways for rapid electron transfer to all Cu's from the trinuclear cluster, through the μ3-oxo bridge (Solomon *et al.*, 2008; and references therein).

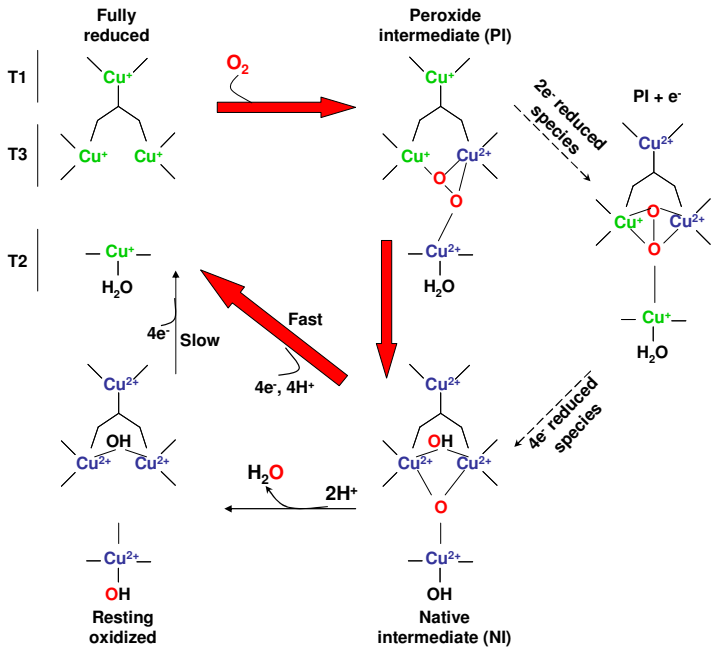

Figure 10 – Mechanism of O_2 reduction to water by the MCOs, proposed by Solomon and co-workers. Red arrows indicate steps that take place in the catalytic cycle; black arrows indicate steps that can be experimentally observed but are not part of the catalytic cycle. (figure adapted from Solomon *et al.*, 2008)

Recent studies by Ferraroni and co-workers (Ferraroni *et al.*, 2012), on the laccase from *Steccherinum ochraceum* allowed to trap and structurally characterize the reaction intermediates proposed by Solomon and co-workers. In these studies, a multi-crystal data collection strategy at progressively higher X-ray radiation doses and basic pH environment (pH 9), has enabled the authors to characterize, in particular, the native and peroxide intermediates (Ferraroni *et al.*, 2012) proposed previously by Solomon and co-workers (Solomon *et al.*, 2008).

More recently, Bento and co-workers have proposed an alternative more straightforward mechanism for the reduction of dioxygen to water in MCOs (Bento *et al.*, 2005). This putative mechanism was suggested on the

basis of the determined X-ray structures of CotA laccase in different redox states (Bento *et al.*, 2005) and with adducts (Bento *et al.*, 2005; Enguita *et al.*, 2004), and by comparison of these with other reported structures from different MCOs, which correspond to potential structural intermediates of the mechanism. In the proposed mechanism, the first stage involves the movement of molecular oxygen into the trinuclear Cu centre, through the access channel, progressing to an almost symmetric binding position in between both T3 Cu ions and interacting with the T2 Cu; at this stage, all Cu ions will be in the oxidised +2 state (resting oxidised state; Figure 11a)). The provision of two electrons, by two successive reducing substrates, originates a peroxide species (O_2^{2-}) (peroxide intermediate; Figure 11b)) that splits into two hydroxide ions, after two further electrons and two protons, with one of the hydroxyl groups remaining in a bridging position amid the T3 Cu ions; the second hydroxyl moiety migrates across the trinuclear cluster, becoming bound to the T2 Cu ion but facing the exit solvent channel (resting oxidised state of AO; Figure 11c)).

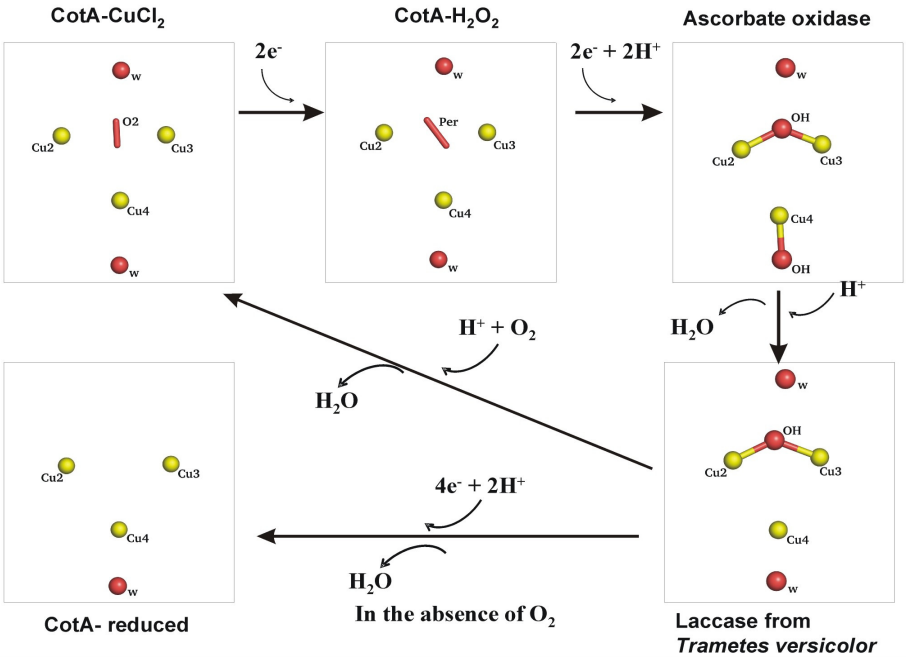

Figure 11 – Putative mechanism proposed by Bento *et al.* for the reductive cleavage of dioxygen to water in MCOs. Crystal structures of potential intermediates: **a) oxidised CotA laccase** (resting state) (1W6L, Bento *et al.*, 2005), **b) CotA-H_2O_2** (1W8E, Bento *et al.*, 2005), **c)** resting state of **Ascorbate oxidase** from Zucchini (1ASO, Messerschmidt *et al.*, 1992), **d) *T. versicolor* laccase** (1GYC, Piontek *et al.*, 2002), **e) reduced CotA laccase** (2BHF, Bento *et al.*, 2005). (figure taken from (Bento *et al.*, 2005))

Although this last step does not appear easy to explain from the X-ray structures alone, it was proposed that it would require a site transient structural reorganization, with the T2 Cu being slightly displaced, using the two coordinating histidines as pivot points. This hypothesis is further supported by the Cu depletion usually observed at this site (Cu4), indicating the T2 Cu as the most labile of the three (Ducros *et al.*, 1998). Following the addition of a proton to the hydroxyl group bound at this site, the first water molecule is released (state observed for *T. versicolor* laccase; Figure 11d)). At a next stage, the second hydroxyl moiety, bridging the two T3 Cu ions, is expected to migrate to the opposite side of the T2 Cu and become protonated, in a similar manner as before,

releasing the second water molecule. At this point, the enzyme is then able to uptake a new dioxygen molecule, re-starting the catalytic cycle. Alternatively, if in anaerobic conditions, four further electrons will take the enzyme into the fully reduced state (Bento *et al.*, 2005), ready to bind dioxygen as soon as it becomes available (Figure 11e)).

In this mechanism, Bento and co-workers suggested that the acidic residues occupying the walls of the access solvent channel were the most likely candidates for donating protons, in particular, Glu498, a structurally conserved residue placed at the dioxygen entrance channel, at a hydrogen-bond distance from a water molecule that interacts with the dioxygen moiety bridged between both T3 Cu ions. The same was proposed by Kataoka and co-workers, as well as, Solomon and co-workers, through site-directed mutagenesis studies conducted on the prokaryotic MCO CueO (Kataoka *et al.*, 2009) and on the eukaryotic MCO Fet3p (Augustine *et al.*, 2007; Solomon *et al.*, 2008). More recently, additional site-directed mutagenesis studies on CueO (Kataoka *et al.*, 2009; Ueki *et al.*, 2006) and Fet3p (Quintanar *et al.*, 2005; Augustine *et al.*, 2007; Solomon *et al.*, 2008) also suggested an aspartate residue (Asp116 in CotA), present in the solvent exit channel, to play an important role in the protonation process. This sequentially conserved residue is sited in close proximity to the T2 Cu ion within the exit channel, participating in a network of hydrogen bonds involving ligands of the trinuclear centre.

Although a more detailed description of the catalytic events taking place during the dioxygen reductive cleavage in MCOs is now available, this subject is still under intense debate. In many ways the proposed mechanisms resemble each other, agreeing on the existence of a peroxide intermediate, as well as of a state where the hydroxyl moiety is placed

amid the T3 Cu ions. However, some controversies still exist, concerning the nature of the resting state of these enzymes, the mechanisms of protonation and the mechanism by which the hydroxyl species or water molecules produced during the catalytic process pass the T2 Cu ion into the exit channel.

In the present dissertation it was aimed to address these and other questions, mainly through a structure-based approach and using CotA laccase as the target. X-ray crystallography was used to determine the three-dimensional structure of several CotA laccase mutants produced by both, site-directed mutagenesis and site-saturation mutagenesis, in order to investigate the role of targeted residues on this enzyme's structure and the catalytic mechanism; ultimately, the effect of the mutants on the activity and stability of the enzyme was also assessed through correlation with available biochemical data. Furthermore, the bacterial MCO from *Campylobacter jejuni*, suggested to be associated to copper homeostasis, was also investigated in order to provide a better understanding of its functional role and, ultimately, to further develop structure-function relationships in the MCOs.

CHAPTER 2

PROXIMAL MUTATIONS AT THE TYPE 1 COPPER SITE OF CotA LACCASE: CHARACTERIZATION OF I494A AND L386A MUTANTS

This chapter was published in the following refereed paper:

P. Durão, Z. Chen, C.S. Silva, C.M. Soares, M.M. Pereira, S. Todorovic, P. Hildebrandt, I. Bento, P.F. Lindley, and L.O. Martins, "Proximal mutations at the type 1 copper site of CotA laccase: spectroscopic, redox, kinetic and structural characterization of I494A and L386A mutants", Biochem. J. (2008) 412(2): 339-46.

The construction of the plasmids, expression, purification and biochemical studies were performed by P. Durão and Z. Chen. The EPR and RR measurements were performed by M.M. Pereira and S. Todorovic, respectively, and the simulation studies carried out by C.M. Soares. Catarina S. Silva performed the crystallisation experiments and has been involved in the X-ray structural characterization.

2.1 Summary

In the present study the CotA laccase from *Bacillus subtilis* has been mutated at two hydrophobic residues in the vicinity of the type 1 copper site. The mutation of Leu386 to an alanine residue appears to cause only very subtle alterations in the properties of the enzyme indicating minimal changes in the structure of the copper centres. However, the replacement of Ile494 by an alanine residue leads to significant changes in the enzyme. Thus the major visible absorption band is upshifted by 16 nm to 625 nm and exhibits an increased intensity, whereas the intensity of the shoulder at approx. 330 nm is decreased by a factor of two. Simulation of the EPR spectrum of the I494A mutant reveals differences in the type 1 as well as in the type 2 copper centre reflecting modifications of the geometry of these centres. The intensity weighted frequencies $<\nu_{Cu-S}>$, calculated from resonance Raman spectra are 410 cm^{-1} for the wild-type enzyme and 396 cm^{-1} for the I494A mutant, indicating an increase of the Cu–S bond length in the type 1 copper site of the mutant. Overall the data clearly indicate that the Ile494 mutation causes a major alteration of the structure near the type 1 copper site and this has been confirmed by X-ray crystallography. The crystal structure shows the presence of a fifth ligand, a solvent molecule, at the type 1 copper site leading to an approximate trigonal bipyramidal geometry. The redox potentials of the L386A and I494A mutants are shifted downwards by approx. 60 and 100 mV respectively. These changes correlate well with decreased catalytic efficiency of both mutants compared with the wild-type.

2.2 Introduction

Laccases are the simplest members of the multi-copper oxidase (MCO) family of enzymes that includes ascorbate oxidase (L-ascorbate: dioxygen

oxidoreductase, EC 1.10.3.3) and ceruloplasmin [Fe(II): dioxygen oxidoreductase, EC 1.16.3.1]. MCOs are characterized by having four copper(II) ions that are classified into three distinct types of copper sites, namely type 1 (T1), type 2 (T2) and type 3 (T3) (Solomon *et al.*, 1996; Messerschmidt, 1997; Lindley, 2001; Stoj *et al.*, 2005). The classical T1 copper site comprises two histidine residues and a cysteine residue arranged in a distorted trigonal geometry around the copper ion with bonding distances of approx. 2.0 Å (1 Å=0.1 nm); a weaker fourth methionine ligand completes the tetrahedral geometry with a Cu–S distance of approx. 3.2 Å. The copper–cysteine linkage is characterized by an intense $S(\pi)\rightarrow Cu(d_{x^2-y^2})$ CT (charge transfer) absorption band at approx. 600 nm, the origin of an intense blue colour of these enzymes, and a narrow parallel hyperfine splitting [$A_{\parallel} = (43–90)\times10^{-4}$ cm^{-1}] in the EPR spectrum. Upon excitation into the CT band, the RR (resonance Raman) spectra of blue copper proteins typically display several bands between 350 and 430 cm^{-1} involving the Cu–S(cysteine) stretching coordinates. The intensity weighted frequency average of these modes allows estimation of the Cu–S bond length and thus provides insight into the T1 site geometry (Blair *et al.*, 1985). The function of the T1 copper site is to shuttle electrons from substrates (via one of the histidine ligands oriented towards the molecular surface) to the trinuclear copper centre where molecular oxygen is reduced to two molecules of water during the complete four-electron catalytic cycle. The trinuclear centre contains a T2 copper coordinated by two histidine residues and one water molecule, lacks strong absorption bands and exhibits a large parallel hyperfine splitting in the EPR spectrum [$A_{\parallel} = (150–201)\times10^{-4}$ cm^{-1}]. The T2 copper site is in close proximity to two T3 copper ions, which are each coordinated by three histidine residues and typically coupled, for example,

through a hydroxide bridge. The T3 or coupled binuclear copper site is characterized by an intense absorption band at 330 nm originating from the bridging ligand and by the absence of an EPR signal due to the antiferromagnetical coupling of the copper ions.

The catalytic rate-limiting step in laccases is considered to be the oxidation of the substrate at the T1 copper site, which switches between the +1 and +2 redox states (Solomon *et al.*, 1996). The reduction potential of the copper(II)/copper(I) couple is thus a crucial physicochemical parameter for the enzyme function. Understanding molecular factors such as the copper ligation pattern, the polarity of the protein environment and the solvent accessibility of the metal site responsible for its modulation is of utmost importance. Several studies have demonstrated that a weak axial bond at the T1 copper site preferentially destabilizes the oxidised state, and is therefore a key factor for the high reduction potentials (400–700 mV) of blue copper sites in MCOs (Solomon *et al.*, 1996). Previously we have shown that the replacement of Met502 (weakly coordinating to the T1 copper) in CotA laccase by the non-coordinating residues leucine and phenylalanine allowed the maintenance of the T1 copper geometry while causing an increase in the redox potential by ~100 mV (Durão *et al.*, 2006). Nevertheless, mutations of the axial ligand have a profound impact on the thermodynamic stability of the enzyme and no direct correlation was found between the redox potentials and the oxidation rates of the enzyme, as lower turnover rates were measured for both mutants. In the present study site-directed mutagenesis has been used to replace the residues Ile494 and Leu386 in the CotA laccase by an alanine residue in order to change the hydrophobic environment of the T1 copper site, namely the hydrophobic patch surrounding its His497 ligand (Figure 12). This latter residue is exposed to the solvent and is presumably involved in

the electron transfer pathway from reducing substrates to T1 copper (Enguita *et al.*, 2004).

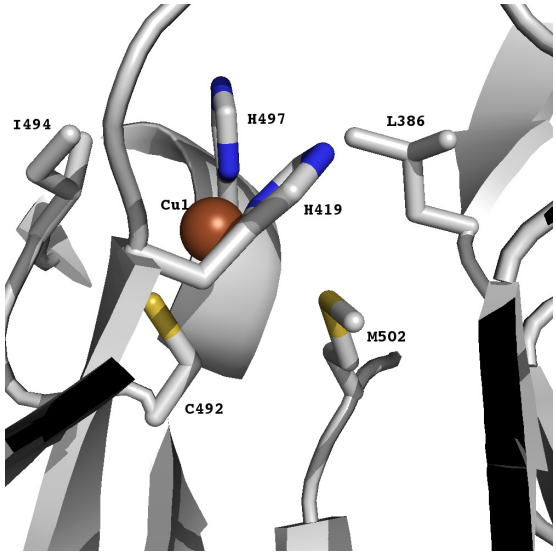

Figure 12 - Structural detail of the T1 copper site in the native CotA laccase structure showing the hydrophobic Ile494 and Leu386 residues (Bento *et al.*, 2005).

The effect of the replacements of hydrophobic Ile494 and Leu386 on the T1 copper of CotA laccase has been examined by various spectroscopic techniques (UV/visible, EPR and RR) and by X-ray crystallography. In the case of the L386A mutant, two crystal structures have been evaluated, one for a 'fully loaded' copper sample at the medium resolution of 2.9 Å and the second for a sample significantly depleted in T2 and T3 copper ions, but at an improved resolution of 2.4 Å. The results obtained from all of these different techniques allowed for elucidation of the impact of the mutations on the redox and kinetic properties of the enzyme.

2.3 Materials and Methods

Construction of CotA mutants

Single amino acid substitutions in the T1 copper centre were created using the QuikChange® site-directed mutagenesis kit (Stratagene). Plasmid pLOM10 (containing the wild-type CotA sequence) was used as a template (Martins *et al.*, 2002). The primers 5'- CGTATGGCATTGCCAT GCTCTAGAGCATGAAGAC-3' (forward) and 5'-GTCTTCATGCTC TAGAAGCATGGCAATGCCATACG-3' (reverse) were used to generate the I494A mutant, whereas the primers 5'-CGGCAGA CCCGTCGCTCTGCTTAATAACAAACGC-3' (forward) and 5'-GCGT TTGTTATTAAGCAGAGCGACGGGTCTGC-3' (reverse) were used to generate the L386A mutation. The presence of the desired mutations in the resulting plasmids, pLOM27 (carrying the I494A point mutation) and pLOM15 (bearing the L386A point mutation) and the absence of unwanted mutations in other regions of the insert were confirmed by DNA sequence analysis. Plasmids pLOM27 and pLOM15 were transformed into *Escherichia coli* Tuner (DE3) strains (Novagen) to obtain strains AH3547 and AH3560 respectively.

Overproduction and purification

Strains AH3517 (containing pLOM10), AH3547 and AH3560 were grown in Luria–Bertani medium supplemented with ampicillin (100 μg/ml) at 30ºC. Growth was followed until the mid-log phase (D_{600} =0.6), at which time 0.1 mM IPTG (isopropyl β-D-thiogalactoside) and 0.25mM $CuCl_2$ were added to the culture medium. The temperature was changed to 25ºC and agitation was maintained for 4 h. The agitation was then interrupted and the cells were maintained overnight at the same

temperature. Such a protocol leads to a maximum occupancy of the copper sites (Durão *et al.*, 2008a). Mutants prepared by this protocol will be referred to as 'fully loaded'. In a previous protocol involving overnight shaking (Martins *et al.*, 2002), significant copper depletion was observed in both the T2 and T3 sites and the sample of L386A mutant prepared in this manner will be referred as 'copper depleted'. Cell harvesting and disruption and protein purification using a two-step protocol procedure were undertaken as previously described (Bento *et al.*, 2005; Martins *et al.*, 2002). Purified enzymes were stored at −20ºC until use.

UV/visible, EPR and RR spectra

UV/visible spectra were acquired using a Nicolet Evolution 300 spectrophotometer from Thermo Industries. EPR spectra were measured with a Bruker EMX spectrometer equipped with an Oxford Instruments ESR-900 continuous-flow helium cryostat. The spectra obtained under non-saturating conditions (160 μM protein content) were theoretically simulated using the Aasa and Väangard approach (Aasa and Väangard, 1975). RR spectra were measured from the frozen sample (−190ºC) using a confocal spectrograph (Jobin Yvon, XY) equipped with grating of 1800 lines/mm and a liquid-nitrogen-cooled back-illuminated CCD (charge-coupled-device) camera. For excitation, the 567.9 nm line of a Kr^+ laser (Coherent, Innova 300K), laser power of 5 mW at the sample, was used. Typical accumulation times were 40s. Approximately 2 *μl* of 1mM 'as purified' oxidised CotA, I494A and L386A mutants (in 20 mM Tris buffer, pH 7.6) were introduced into a liquid-nitrogen-cooled cold finger (Linkam THMS600) mounted on a microscope stage. The RR spectra (350–450 cm^{-1} region) were submitted to band-fitting analysis using Lorentzian bandshapes. The fitted band intensities and frequencies were

used for determination of the intensity weighted frequency $<\nu_{Cu-S}>$ (Blair *et al.*, 1985).

Redox titrations and enzyme assays

Redox titrations were performed at 25ºC and pH 7.6, under an argon atmosphere, and monitored by UV/visible spectroscopy (300-900 nm), using a Shimadzu Multispec-1501 spectrophotometer as described by Durão *et al.* (Durão *et al.*, 2006). The laccase-catalysed oxidation reactions of ABTS [2,2'-azinobis-(3-ethylbenzothiazoline-6-sulfonic acid)], 2,6-DMP (2,6-dimethoxyphenol) and SGZ (syringaldazine) were photometrically monitored, as previously described (Durão *et al.*, 2006). Kinetic data were determined from Lineweaver–Burk plots assuming that simple Michaelis–Menten kinetics was followed. The reaction mixtures contained ABTS (10–240 μM, pH 4), 2,6-DMP (10–1000 μM at pH 7 for wild-type and the L386A mutant, or 100–7500 μM at pH9 for the I494A mutant) or SGZ (1–100 μM at pH 7 for wild-type and the L386A mutant, or at pH 8 for the I494A mutant). All enzymatic assays were performed at least three times.

Crystallisation

Crystals of the I494A mutant were obtained at room temperature (20ºC) from a crystallisation solution containing 0.1 M sodium citrate, 10% PEG (poly(ethylene glycol)) MME 5K and 14% propan-2-ol at pH 5.5. Pale blue hexagonal prisms appeared from a drop containing 10.8 mg of protein/ml. In a similar manner, crystals of the L386A mutants appeared at room temperature from a crystallisation solution containing 20% PEG MME 5K, 0.1 M sodium citrate and 8% propan-2-ol at pH 5.5 and a

protein concentration of 7.9 mg/ml. Cryo conditions were provided by adding 22% ethylene glycol to the crystallization solution or, in the case of the copper-depleted L386A crystals, 25% glycerol was added.

X-ray data collection and refinement

Data collection was performed at 100 K using synchrotron radiation at the European Synchrotron Radiation Facility, Grenoble, France, and the Swiss Light Source at the Paul Scherrer Institut, Villigen, Switzerland. Data collection details are shown in Table 1.

Table 1 - X-ray data collection. Values in parentheses refer to the highest resolution shells as follows: for I494A, 1.69–1.60Å; for L386A (fully copper loaded), 3.06–2.90Å; and for L386A (copper depleted), 2.53–2.40Å. ESRF, European Synchrotron Radiation Facility, Grenoble, France; SLS, Swiss Light Source, Paul Scherrer Institut, Villigen, Switzerland.

	I494A	L386A-fully copper loaded	L386A-copper depleted
Synchrotron beam line	ESRF ID14-3	ESRF ID14-2	SLS X06FA
Wavelength (Å)	0.931	0.933	0.9184
Detector distance (mm)	150.4	275.5	250
Resolution (Å)	1.6	2.9	2.4
Space group	P3121	P3121	P3121
Cell parameters (Å)			
a	101.87	101.78	101.96
c	137.04	137.12	136.14
Mosaicity (°)	0.44	0.55	0.53
Oscillation range (°)	0.3	0.8	1.0
Oscillation angle (°)	90	96	90
No. of unique *hkl*	107969 (15440)	107199 (15756)	180374 (26244)
Completeness (%)	99.4 (98.4)	100.0 (100.0)	100.0 (100.0)
$I/\sigma(I)$	6.9 (2.1)	6.2 (2.3)	5.5 (5.6)
R_{symm}	0.064 (0.346)	0.100 (0.315)	0.076 (0.32)
Multiplicity	5.2 (3.9)	5.7 (5.8)	5.5 (5.6)

Data sets for the I494A and L386A mutant enzymes were processed with MOSFLM (Leslie, 2006) and scaled with SCALA (Evans, 2006) from

the CCP4 program suite (CCP4, 1994). The data set for the copper-depleted L386A mutant extended to a significantly higher resolution, 2.4Å compared with 2.9Å for the fully loaded mutant, and hence was included in the present study. The structures were elucidated by molecular replacement using MOLREP (Vagin and Teplyakov, 1997). The starting model was the CotA native structure (PDB code: 1W6L (Bento *et al.*, 2005)) from which all the copper ions and solvent atoms had been removed. In each case only one solution was evident. Subsequent electron density syntheses enabled the location of the four copper ions in the molecule. Refinement was performed using the maximum likelihood functions implemented in REFMAC5 (Murshudov *et al.*, 1999). Rounds of conjugate-gradient sparse-matrix refinement with bulk-solvent modelling according to the Babinet principle (Tronrud, 1996) were alternated with model building using the Coot program suite (Emsley and Cowtan, 2004) in combination with SigmaA weighted $2|F_o|-|F_c|$ and $|F_o|-|F_c|$ maps (Read, 1986). After the first rounds of refinement, solvent molecules were added to the models based on standard geometrical and chemical restraints; molecules of ethylene glycol, used as a cryoprotectant, were also located. In all cases, in a similar manner to the wild-type structure, the loop region between residues 89 and 97 was very poorly defined. The occupancies of the copper ions were adjusted such that their isotropic thermal vibration parameters refined approximately to the values of their local environment. For the T2 copper centre in particular, including the fully loaded mutants, assignment of full occupancy led to thermal vibration coefficients significantly higher than the local average and significant features in difference Fourier syntheses. Careful use of omit and standard difference Fourier syntheses, as well as monitoring of thermal vibration coefficients during refinement and modelling studies,

enabled the identification of diatomic species in between the T3 copper sites in all cases and this was interpreted as a dioxygen-type species: refinement proceeded constraining the O–O distances to a target value of 1.20Å. Moreover, in both fully loaded mutants, additional electron density was observed in the vicinity of Cys35 and this was modelled as an oxidised cysteine species occupying two distinct configurations. Details of the overall refinement and final quality of the models are shown in Table S1.

Simulation studies

Simulated redox titrations (Baptista *et al.*, 2002; Teixeira *et al.*, 2002) were performed for studying the equilibrium binding of protons and electrons. The methodology is based on CE (continuum electrostatic) methods and MC (Monte-Carlo) sampling of binding states. The CE calculations were performed using the package MEAD (version 2.2.0) (Bashford and Gerwert, 1992; Bashford, 1997). The sets of atomic radii and partial charges were taken from GROMOS96 (Scott *et al.*, 1999; van Gunsteren *et al.*, 1996), except in the case of the metal centres, where quantum chemical calculations (see below) were used to derive charges. Dielectric constants of 80 and 10 were used for the solvent and protein, respectively, which are values within the range where pK_a prediction is optimized (Teixeira *et al.*, 2005). The solvent probe radius was 1.4Å, the ion-exclusion layer was 2.0Å, the ionic strength was 0.1 M and the temperature was 27ºC. The program PETIT (Baptista *et al.*, 2002; Teixeira *et al.*, 2002) was used for the MC sampling of proton and electron binding states. Site pairs were selected for double moves when at least one pairwise term was greater than 2 p*K* units. Averages were computed using 10^5 MC steps. In all simulations, the trinuclear centre was considered to be

in the fully oxidised state, whereas the T1 copper centre was considered as titrable. Redox titrations are usually relative due to the unavailability of an E_{mod}, i.e. the redox potential of an adequate model compound in water; this is the case for the T1 copper centre. Owing to this, the experimental value for the wild-type enzyme was used to fit the redox titrations by adding a constant value to the potential so that the calculated and measured redox potentials for the wild-type enzyme were the same. The values for the mutants were then obtained relative to this. Partial charges for the two metal clusters (T1 copper and the T2 and T3 copper ions) were calculated considering model compounds with the conformation of the oxidised structure obtained previously (Bento *et al.*, 2005). The ligands of the metals were considered up to the C-β carbon (C-α in the case of the cysteine residue of the T1 copper). A dioxygen molecule bound to the T3 copper ions was considered, as well as the water molecule bound to the T2 copper. Single point calculations were performed using Gaussian 98 (Frisch *et al.*, 1998), with the B3LYP and the 6-31G(d) basis set for all atoms, with the exception of copper atoms, for which the 6-31G(2df) basis set was used. These calculations were employed to derive electrostatic potentials, which were then fitted using RESP (Bayly *et al.*, 1993) to calculate the partial charges. For the T1 copper, partial charges were calculated for the oxidised and reduced states, since both were required to simulate the redox titration of this group.

Other methods

Protein copper content was determined through the trichloroacetic acid/bicinchoninic acid method of Brenner and Harris (Brenner and Harris, 1995). The protein concentration was measured using the

absorption band of CotA laccase at 280 nm (ε280 =84739M^{-1} cm^{-1}) or the Bradford assay (Bradford, 1976) using BSA as a standard.

2.4 Results and Discussion

Spectroscopic analysis of mutant enzymes

Site-directed mutagenesis replacing residues Ile494 and Leu386 with an alanine residue in the CotA laccase was undertaken in order to change the hydrophobic environment of the T1 copper centre (Figure 12). The resulting mutant enzymes showed the same chromatographic pattern during purification as the wild-type CotA laccase. Protein samples were judged to be homogeneous by the observation of a single band on Coomassie-Blue-stained SDS/PAGE. Each protein 'as isolated' contained approx. 4 mol of copper per 1 mol of protein (Table 2).

Table 2 - Copper content and spectral properties for the wild-type CotA and the I494A and L386A mutants. Units are: λ, nm; ε, mM^{-1} cm^{-1}

	Copper content (mol of Cu/mol of protein)	T1 λ (ε)	T3 λ (ε)
CotA wild-type	3.7 ± 0.1	609 (4.0)	330 (4.0)
L386A	4.0 ± 0.2	609 (3.3)	330 (3.0)
I494A	4.0 ± 0.2	624 (5.6)	330 (1.5)

Figures 13, 14 and 15 show the visible, RR and EPR spectral characteristics of the wild-type enzyme and the L386A and I494A mutants.

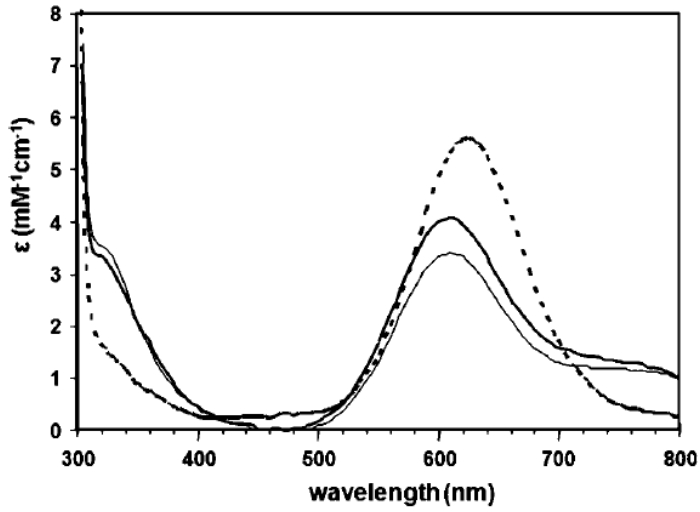

Figure 13 – UV/visible spectra of wild-type CotA (solid thick line), **the L386A mutant** (solid thin line) **and the I494A mutant** (broken line).

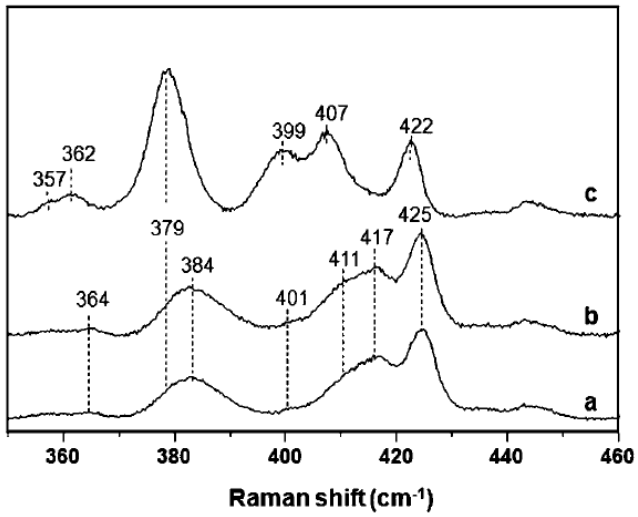

Figure 14 - RR spectra of the wild-type CotA (a), the L386A mutant (b) and the I494A mutant (c), obtained with 567.9 nm excitation and 5 mW laser power at 77 K, with an accumulation time of 40s.

The spectroscopic analysis of the L386A mutant revealed very subtle differences when compared with the wild-type protein, indicating minimal changes in the structure of the copper centres. On the other hand, the I494A mutant showed distinct changes in the absorption spectra such as a

shift of the CT transition (T1 copper site) from 609 nm to 625 nm, a more intense blue colour (ε of 5600 instead of 4000 mM^{-1} cm^{-1}) and a 2-fold decrease of the absorption of the 330 nm band (a transition characteristic of the T3-coupled copper ions) (Figure 13 and Table 2). The RR spectra of the wild-type CotA, and the I494A and L386A mutants, obtained with a 567.9 nm excitation at −190ºC, displayed seven vibrational bands between 350 and 440 cm^{-1} (Figure 14). Overall, the spectra bear strong similarities with those of other copper proteins containing the T1 blue copper site (Blair *et al.*, 1985; Dave *et al.*, 1993; Palmer *et al.*, 1999; Machonkin *et al.*, 2001; Green, 2006; Qiu *et al.*, 1995). However, quite different intensity distribution among the various modes in the spectrum of the I494A mutant, as compared with the wild-type protein and the L386A mutant (Figure 14), indicates a substantial perturbation of the T1 site geometry upon replacing Ile494 with an alanine residue. Since excitation in the resonance with the CT transition predominantly provides enhancement to the modes through the Cu–S stretching coordinate, its contribution to the various modes can be considered to be directly related to the relative RR intensities. Consequently, the intensity-weighted band frequencies allow determination of the intrinsic Cu–S stretching frequency, which is inversely proportional to the Cu–S bond length and thus provides a quantitative basis for description of the structural perturbation of the T1 copper site (Blair *et al.*, 1985; Dave *et al.*, 1993; Palmer *et al.*, 1999; Machonkin *et al.*, 2001; Green, 2006; Qiu *et al.*, 1995). The intensity-weighted band frequencies, obtained by a band-fitting analysis, include only vibrational fundamentals below 500 cm^{-1}. The value for the intrinsic Cu–S stretching frequency $<\nu_{Cu-S}>$ was found to be 410 cm^{-1} for the wild-type protein, whereas for the T1 copper site of I494A it was

substantially lower (396 cm^{-1}), corresponding to a lengthening of the Cu–S(cysteine) bond for the latter. For the L386A mutant, a value very similar to the one determined for the wild-type, $<\nu_{Cu-S}>=408$ cm^{-1}, was obtained. The EPR spectra are shown in Figure 15 and the parameters used in the simulations of these spectra are shown in Table 3.

Table 3 - EPR parameters used in the simulation of wild-type CotA, L386A and I494A mutant spectra.

	Copper centres	g_{min}	g_{med}	g_{max}	A_{max} ($\times 10^{-4}$ cm^{-1})
CotA wild-type	T1	2.044	2.052	2.230	64
	T2	2.025	2.099	2.255	179
L386A	T1	2.046	2.048	2.235	64
	T2	2.025	2.095	2.258	174
I494A	T1	2.038	2.068	2.305	45
	T2	2.055	2.102	2.347	93

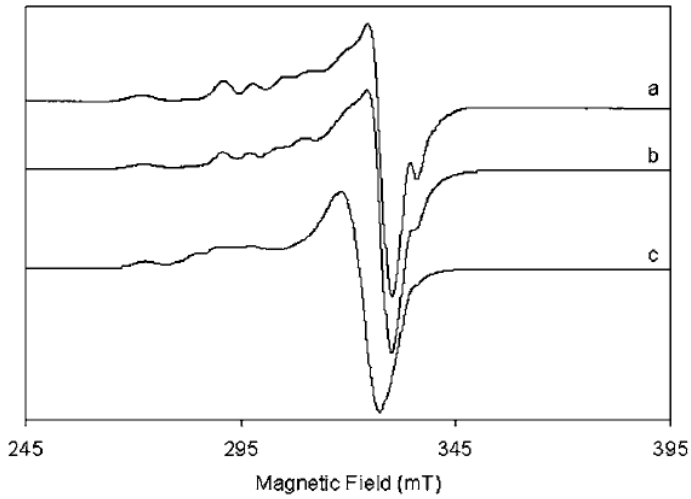

Figure 15 - EPR spectra of the wild-type CotA (a), the L386A mutant (b) and the I494A mutant (c), obtained at 10 K, a microwave frequency of 9.39 GHz, 2.4 mW and a modulation amplitude of 0.9 mT.

The EPR spectrum of the L386A mutant is quite similar to the wild-type, whereas the EPR spectrum and the *g* values, as well as the hyperfine constants of the I494A mutant reveal significant differences in both the T1 and T2 copper centres. For the T1 centre in the I494A mutant, compared with the spectrum of the wild-type, an increase in g_{max} and g_{med} values and a decrease in g_{min} value, as well as a decrease in the hyperfine constant value were observed. These observations are compatible with an increase of the distortion of the tetrahedron, which could further account for an increase in the Cu–S(cysteine) distance, as indicated by the RR results. Interestingly, both EPR and RR data indirectly suggest the existence of an altered moiety in the proximity of T1 copper of the I494A mutant. The former, based on a Vänngard–Peisach–Blumberg plot (g_{max} versus A_{max}), suggests a similarity of the T1 copper centre of the I494A mutant to the T1 copper site present in blue copper proteins having an oxygen atom as a ligand (Andrew *et al.*, 1994; Diederix *et al.*, 2000). The latter results imply, through the weakening of the Cu–S bond, that the T1 copper ion experiences an extra electron-donor interaction from the neighbouring oxygen or possibly an extra polar interaction, which may be sufficient to increase the Cu–S distance substantially (Blair *et al.*, 1985). The changes of the *g* values of T2 copper in the I494A mutant and the decrease of the A_{max} value, approaching values typical for T1 copper centres, reflect an increase in tetrahedral distortion of the T2 site. Thus the mutation of Ile494 in the vicinity of the T1 copper site seems to cause a perturbation in the trinuclear centre as monitored by EPR and absorption (see above). The T1 copper site is approx. 13 Å away from the trinuclear centre and is bridged through the T1 copper–Cys–His–T3 copper backbone, a possible efficient pathway for rapid intramolecular electron transfer (Solomon *et al.*, 1996; Messerschmidt, 1997; Lindley,

1997; Stoj and Kosman, 2005). Therefore taking into consideration the structural and functional closeness, it is reasonable to assume that drastic modifications of the T1 copper site in the I494A mutant, such as a lower covalency of the T1 Cu–S(cysteine) bond, could lead to alterations in the properties of the trinuclear centre.

Structural characterization of CotA mutants

The modifications of the T1 copper site geometry in the I494A and L386A mutants are clearly confirmed by X-ray crystallography as shown in Figures 16(A) and 16(B). In the case of the L386A mutant, the T1 copper ion is barely perturbed, being coordinated by three strong ligands (Cys492, His419 and His497) at distances of approx. 2.1 Å, with a fourth weaker ligand, Met502, at a distance of 3.2 Å. However, in the case of the I494A mutant, the reduction in the size of the 494 residue increases the accessibility of the T1 copper site such that a solvent molecule is able to interact with the copper ion at a distance of approx. 3.0 Å. The coordination geometry thus changes from distorted tetrahedral in the case of the wild-type protein and the L386A mutant, to a distorted trigonal bipyramidal in the I494A mutant. The solvent molecule itself is part of a chain of hydrogen-bonded water molecules leading to the external surface of the molecule.

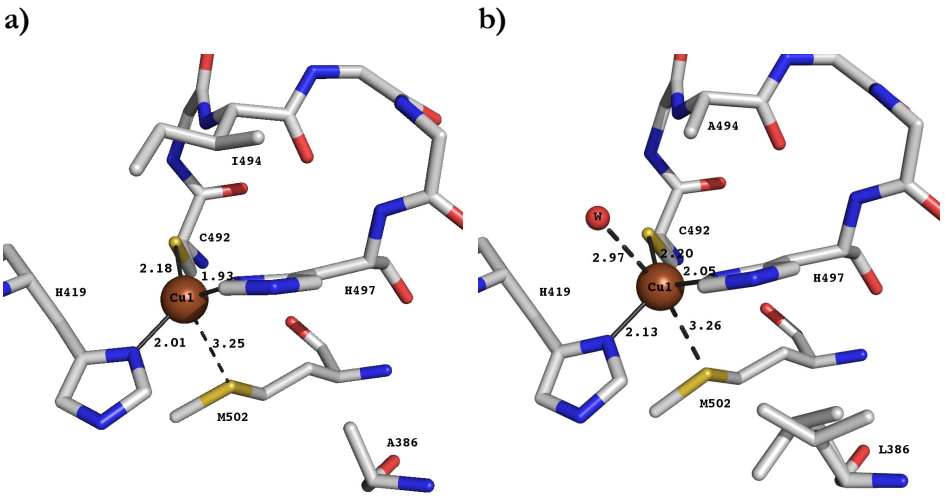

Figure 16 - Structure of the T1 copper centre in the L386A mutant (a) and the I494A mutant (b).

The resolution of the X-ray data does not, however, permit the observation of any significant change in the Cu–S bond length and therefore the strength of the bond. It therefore cannot substantiate the RR and EPR in this context. Quantitatively, the increase in accessibility (Binkowski *et al.*, 2003) of the T1 copper site is approx. 418.8 $Å^2$. Concomitantly, the accessibility of the site to substrate molecules should also be increased, thus affecting the catalytic properties of this mutant. In addition, the X-ray structural data do not indicate any significant changes in the geometry of the T2 copper centre as indicated by the spectroscopic data. However, there has to be some flexibility at this centre in order for the water molecules, resulting from reduction of dioxygen, to access the exit solvent channel, and a concomitant movement of the T2 copper may be reflected by the EPR data. Furthermore, the presence of the dioxygen molecule bisecting the T3 copper ions and with the O2 atom only some 2.5 Å distant from the T2 copper may also have some effect. Changes in its spin state in the I494A mutant may be reflected in the EPR spectra for

the T2 copper ion. In the case of the L386A mutant, two crystal structures have been evaluated, one for a fully loaded copper sample at the medium resolution of 2.9 Å and the second for a sample significantly depleted in T2 and T3 copper ions, but at the improved resolution of 2.4 Å. Despite differences in copper content within the trinuclear cluster, the two L386A mutant structures are remarkably similar. There are differences in the solvent structure, but these are mainly related to the differences in the resolution of the respective data sets and consequently revealed by the respective electron density maps in details. Thus in the fully loaded L386A data set only 44 solvent molecules have been modelled. However, since the structure of the copper-depleted L386A mutant extends to a significantly higher resolution than the copper fully loaded structure and there appear to be no essential differences with respect to the copper centres, this structure can be used to provide a better definition of the T1 copper site. The geometry of the trinuclear copper centre in both the I494A and depleted L386A mutants is essentially the same as that found previously in the native structure (see for example (Bento *et al.*, 2005)) with the optimum model incorporating a dioxygen species in between the two T3 copper atoms and almost perpendicular to their connecting vector. The presence of an oxidised cysteine residue at position 35 in the fully loaded structures is surprising and is likely to arise from the production protocol, since intense efforts have been made to minimize and to monitor radiation damage during the data collection procedures. Apart from the T1 copper centre and residue 35, the mutant enzymes show no significant structural changes with respect to the wild-type enzyme.

Redox properties of the mutants

The reduction of the T1 copper ion was measured by the disappearance of the CT absorption band in the 500–800 nm regions. The redox potentials of the T1 copper site were determined to be 525, 429 and 466 mV for the wild-type protein and the I494A and L386A mutants respectively (Table 4).

These results indicate that the geometry changes at the active site have led to a stabilization of the copper(II) form of both mutants. The Cu–S(cysteine) bond strength, which can be extracted from the RR spectra, was shown to have a direct correlation with the redox potential of T1 copper sites (Solomon *et al.*, 1996; Blair *et al.*, 1985). The RR data qualitatively reproduce the experimental findings; an increase in the Cu–S(cysteine) bond length for the I494A mutant and a less pronounced lengthening in the case of the L386A mutant, accounting for lowering of the redox potential of both mutants, compared with wild-type. In order to understand the physical reasons behind the changes in the redox potential, simulations of redox behaviour of the wild-type and mutant proteins were performed, using the data of the solved X-ray structures. The calculations indicate lower redox potentials for the two mutants, when compared with the wild-type, 516 mV for I494A and 510 mV for L386A. This results from a higher exposure to the solvent of the T1 copper centre in the mutants, which stabilizes the oxidised state. In fact, given that the overall formal charge of the centre is +1, this is more likely to occur in a medium of higher dielectric constant such as water, than of a low dielectric constant, such as protein. The lowering of the redox potential of the mutants obtained from the calculations is not as pronounced as that observed experimentally (see above). The discrepancies may arise partially from the use of a somewhat 'unphysical' protein dielectric constant. A

dielectric constant of 10 may be adequate for protonatable groups, but does not always describe the redox centres sufficiently well, specifically if they are more buried in the protein (Teixeira *et al.*, 2005). A lower protein dielectric constant results in a larger difference, but the calculation would not be as accurate for protonatable groups which may have a strong effect on nearby redox centres. For instance, calculations with an internal dielectric constant of 4 (results not shown) result in larger differences between the mutants and the wild-type. Moreover, the calculations show a lower decrease of the redox potential for I494A than for L386A, when compared with the wild-type, in disagreement with the experiment. For the I494A mutant, the presence of the additional water molecule at the T1 copper site cannot be properly handled by the current methodologies due to its most likely quantum-mechanical nature, which goes beyond a simple solvation effect (as our calculations would model it). Nevertheless, and in a qualitative way, the water molecule, by orienting the negative oxygen atom towards the copper ion will probably stabilize the positive oxidised state, thereby decreasing the redox potential even more than shown by the calculations presented in the current study. Despite the fact that our calculations are not able to model this in full extent, they show, by comparison of the results obtained for the two mutants, that this effect is an important one, since it can change substantially what could be obtained by unspecific solvation effects.

Table 4 - Redox potential and kinetic constants of the wild-type CotA laccase and the L386A and I494A mutants.
The redox potentials were measured at pH 7.6. The kinetic constants were measured at the optimal pH for the different substrates for each variant enzyme (see Figure 17).

		ABTS			2,6-DMP			SGZ		
	E^{o} (mV)	K_m (μM)	k_{cat} (s^{-1})	k_{cat}/K_m ($s^{-1} \cdot \mu M^{-1}$)	K_m (μM)	k_{cat} (s^{-1})	k_{cat}/K_m ($s^{-1} \cdot \mu M^{-1}$)	K_m (μM)	k_{cat} (s^{-1})	k_{cat}/K_m ($s^{-1} \cdot \mu M^{-1}$)
CotA wild-type	525 ± 10	124 ± 17	322 ± 20	2.6	227 ± 41	36 ± 5	0.16	18 ± 3	80 ± 4	4.4
L386A	466 ± 6	145 ± 3	52 ± 1	0.36	576 ± 16	17.0 ± 0.3	0.03	33 ± 1	13 ± 0.2	0.39
I494A	429 ± 27	2027 ± 193	7.2 ± 0.5	0.0036	1295 ± 73	4.5 ± 0.2	0.0035	52 ± 1	9 ± 0.1	0.17

Catalytic properties of mutant enzymes

Three substrates, one non-phenolic (ABTS) and two phenolic (2,6-DMP and SGZ), were used to determine specific changes of the catalytic properties of the mutant enzymes. Table 4 shows that the I494A and L386A mutants have higher values for the K_m and lower k_{cat} values when compared with the wild-type enzyme. The L386A mutant exhibits an approximate 2-fold increase in the K_m for all tested substrates and a 2- to 6-fold decrease of k_{cat} values. The I494A mutant is more severely compromised in its catalytic activity. Major alterations in the enzyme affinity for different substrates were observed (up to 20-fold higher K_m values as compared with wild-type) indicating that this mutation must have caused a change in the substrate-binding pocket, as indicated by X-ray results. In addition, significant changes were found for the values of k_{cat}; a lowering by a factor of 10 to nearly 50 for the phenolic and non-phenolic substrates, respectively. The parameter k_{cat} depends on the rate-limiting step in the turnover of multi-copper oxidases, which was shown to be the reduction of the T1 copper site (Solomon *et al.*, 1996). According to the Marcus theory k_{ET}, a major component of the parameter k_{cat}, is dependent on three factors: the donor–acceptor electronic coupling, the reorganization energy and the redox potentials (Moser and Dutton, 1996). The lower redox potential determined for both mutants leads to a decreased thermodynamic driving force and thus to a decreased electron transfer rate and hence to lower k_{cat} values. In the case of the Ile494 mutant, major alterations of the structure near the T1 copper site were observed including a higher solvent accessibility. The reduction of this site may therefore require an increase in the reorganization energy, which in turn could result in lower k_{ET} and thus lower k_{cat} (Palmer *et al.*, 1999; Machonkin *et al.*, 2001). The mutation I494A leads to a shift in the

optimal pH by approx. 2 units for 2,6-DMP and 1 unit for SGZ, towards higher values, but not for ABTS (Figure 17).

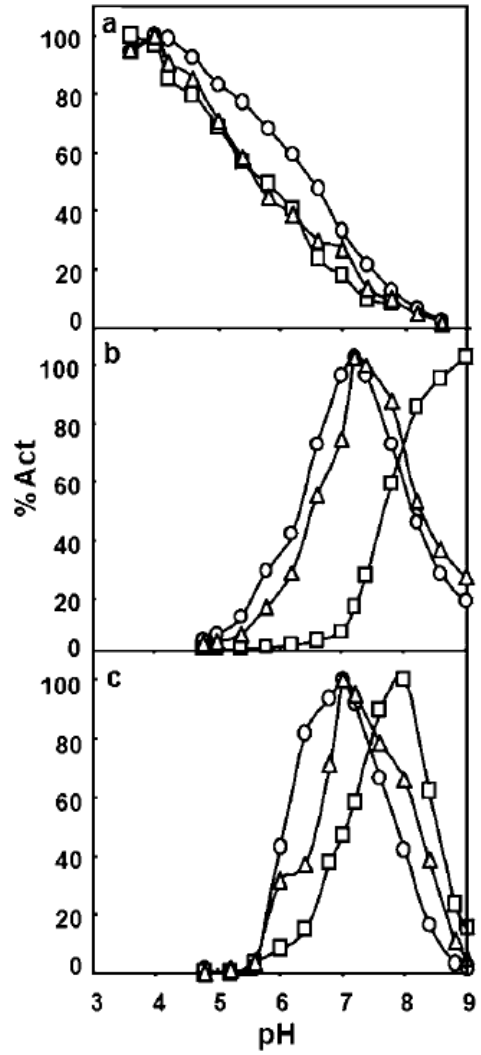

Figure 17 - pH profile for catalytic activities. ABTS **(a)**, 2,6-DMP **(b)** and SGZ **(c)** were used as substrates for wild-type CotA (○), the I494A mutant (□) and the L386A mutant (Δ).

It has been shown that oxidation of a phenolic substrate depends on its protonation state; the deprotonated phenol has a lower redox potential and, therefore, is more easily oxidised (Xu, 1997). A careful analysis of the

protonation behaviour of nearby groups of the substrate-binding pocket in the I494A mutant did not reveal any significant difference in their protonation behaviour compared with the wild-type enzyme. Therefore the altered pH dependence found for phenolic substrates might be attributable to altered protonation equilibrium of the phenolic substrates themselves in the T1 substrate-binding pocket of the I494A mutant, corroborating the changes at this pocket as revealed by increased K_m values. This effect would not be observed for ABTS because there is no protonation equilibrium for this substrate.

2.5 Concluding remarks

It is known that the redox potentials exhibited by the T1 copper sites of laccases span over a broad range of values, from 400 mV for plant laccases to 790 mV for some fungal laccases (Solomon *et al.*, 1996; Stoj and Kosman, 2005). The reasons for the wide potential range among laccases are not yet fully understood. Since a high redox potential increases the range of oxidisable substrates and improves the effectiveness and versatility of the enzyme, it is important to obtain a detailed description of the structure and reactivity of variants in the vicinity of the T1 copper site in order to be able to fine-tune its properties by protein engineering techniques. The redox potential of T1 copper sites can be influenced by a variety of factors, including the solvent accessibility of the metal centre and the electrostatic interactions between the metal centre and the protein (Solomon *et al.*, 1996). Most of the site-directed mutagenesis at the T1 copper site studies has been applied to simple blue copper proteins (possessing one T1 copper site) in an effort to elucidate their electron transfer mechanism (Solomon *et al.*, 1996) and the results of a similar approach for multi-copper oxidases are yet scarce (Durão *et al.*,

2006; Palmer *et al.*, 1999; Xu *et al.*, 1998 and 1999; Palmer *et al.*, 2003; Madzak *et al.*, 2006). In the present study the crystal structures of the I494A and L386A mutants show that replacement of hydrophobic residues with an alanine residue in the vicinity of the T1 copper site has increased the solvent accessibility, and consequently caused a decrease of the redox potential of the metal centre of both mutants. The larger cavity observed in the I494A mutant allowed for the specific binding of a water molecule to the T1 copper ion, leading to a change in the coordination geometry of this site, from distorted tetrahedral in the case of wild-type and the L386A mutant to a more trigonal bipyramidal in the I494A mutant. This resulted in a increased Cu–S(cysteine) bond length as observed by RR, and significant differences in the *g* values and the copper hyperfine coupling constant of the T1 copper in the EPR spectra. These geometrical and electronic changes further stabilized the oxidised state of the T1 copper site, resulting in a lower redox potential for the I494A enzyme as compared with the L386A mutant. As expected, the lower redox properties of the I494A and L386A mutants correlate well with their lower reactivity towards standard substrates. Therefore these results and our previous data (Durão *et al.*, 2006) show that changes in amino acid residues in direct contact with the metal centre (including ligands) significantly affect the properties of T1 copper sites of laccases and suggest that modulation of redox potential without compromising the overall reactivity may be performed through changes in residues away from this immediate contact shell.

2.6 Acknowledgements

This work was supported by POCI/BIO/57083/2004 and FP6-NMP2-CT-2006-026456 (BIORENEW) project grants. The provision of

synchrotron radiation facilities and the assistance of the staff at those facilities are sincerely acknowledged for help with X-ray data collection at the European Synchrotron Radiation Facility in Grenoble, France and the Swiss Light Source at the Paul Scherrer Institut, Villigen, Switzerland. Z. C. holds a FCT post-doctoral fellowship (SFRH/BPD/27104/2006).

2.7 Supplementary material

Table S1 – Refinement and quality of refined models. The G factor and Ramachandran analysis (Ramakrishnan and Ramachandran, 1965) were determined by PROCHECK (Laskowski *et al.*, 1993a).

Parameter	I494A	L386A: fully loaded	L386A: copper-depleted
Refinement			
No. of protein atoms	4211	4049	4074
No. of solvent atoms	628	44	386
No. of hetero atoms	5	5	5
Final R-factor	0.17	0.18	0.16
Final free R-factor (5.1 %)	0.19	0.24	0.20
Mean B values (Å^2)			
protein	21.736	34.435	31.119
solvent	36.227	34.447	37.568
overall	23.697	34.341	32.399
Estimated overall coordinate uncertainty (Å)†	0.066	0.329	0.182
Distances deviations*			
Bond distances (Å)	0.011	0.016	0.010
Bond angles (Å)	1.251	1.016	1.206
Planar groups (Å)	0.005	0.003	0.077
Chiral volume deviation (Å^3)	0.090	0.065	0.004
Quality of models			
Overall G factor	0.02	0.03	-0.01
Ramachandran analysis % (No.)			
Favourable	86.6	87.2	85.3
Additional	12.3	11.4	13.7
Generous	0.9	0.9	0.7
Disallowed	0.2	0.5	0.2
Copper occupancy			
Cu1	1.0	1.0	1.0
Cu2	1.0	1.0	0.6
Cu3	1.0	1.0	0.6
Cu4	1.0	1.0	0.5

*Root mean square deviations from standard values; †based on maximum likelihood.

CHAPTER 3

THE REMOVAL OF A DISULFIDE BRIDGE IN CotA LACCASE

This chapter was published in the following refereed paper:

A.T. Fernandes, M.M. Pereira, **C.S. Silva**, P.F. Lindley, I. Bento, E.P. Melo and L.O. Martins, "The removal of a disulfide bridge in CotA-laccase changes the slower motion dynamics involved in copper binding but has no effect on the thermodynamic stability", **J. Biol. Inorg. Chem.** (2011), **16**(4): 641-651.

The construction of the plasmids, expression, purification, biochemical and stability studies were performed by A.T. Fernandes. The EPR measurements were performed by M.M. Pereira. Catarina S. Silva performed the crystallisation experiments and has been involved in the X-ray structural characterization.

3.1 Summary

The contribution of the disulfide bridge in CotA laccase from *Bacillus subtilis* is assessed with respect to the enzyme's functional and structural properties. The removal of the disulfide bond by site-directed mutagenesis, creating the C322A mutant, does not affect the spectroscopic or catalytic properties and, surprisingly, neither the long-term nor the thermodynamic stability parameters of the enzyme. Furthermore, the crystal structure of the C322A mutant indicates that the overall structure is essentially the same as that of the wild-type, with only slight alterations evident in the immediate proximity of the mutation. In the mutant enzyme, the loop containing the C322 residue becomes less ordered, suggesting perturbations to the substrate binding pocket. Despite the wild-type and the C322A mutant showing similar thermodynamic stability in equilibrium, the holo or apo forms of the mutant unfold at faster rates than the wild-type enzyme. The picosecond to nanosecond time range dynamics of the mutant enzyme was not affected as shown by acrylamide collisional fluorescence quenching analysis. Interestingly, copper uptake or copper release as measured by the stopped-flow technique also occurs more rapidly in the C322A mutant than in the wild-type enzyme. Overall the structural and kinetic data presented here suggest that the disulfide bridge in CotA laccase contributes to the conformational dynamics of the protein on the microsecond to millisecond timescale, with implications for the rates of copper incorporation into and release from the catalytic centres.

3.2 Introduction

The family of multi-copper oxidases (MCOs), which includes the functional classes of metallo-oxidases and laccases, is mostly constituted

by proteins that contain approximately 500 amino acid residues and are composed of three Greek key β-barrel cupredoxin domains (domains 1, 2 and 3) that come together to form three spectroscopically distinct types of copper sites, i.e. type 1 (T1), type 2 (T2), and type 3 (T3) (Lindley, 2001; Messerschmidt, 1997). The T1 copper centre is the site of substrate oxidation and a wide range of compounds, such as polyphenols, diamines and even some inorganic metals, are electron donor substrates. The trinuclear centre comprises two T3 copper ions and one T2 copper ion that functionally cooperate in the reduction of dioxygen to water. Laccases have a high potential for biotechnological applications, mainly owing to their wide range of oxidisable substrates, the use of readily available oxygen as the final electron acceptor and the lack of requirement for expensive cofactors. In the past few years many studies have enabled the elucidation of a significant number of structural and functional aspects of these enzymes, but many questions still remain. One of these involves the understanding of the molecular determinants of enzyme long-term and conformational stability. However, using an enzyme in an industrial environment requires high stability, since most industrial activities are carried out at high temperatures, extreme pH values and high pressures, among other adverse physicochemical conditions. Therefore, understanding the molecular mechanisms involved in the stability properties of laccases is of utmost importance and may lead to the generation of improved biocatalysts by protein engineering techniques.

In recent years our attention has focused on the study of thermostable and hyperthermostable prokaryotic MCOs, the CotA laccase from *Bacillus subtilis* and the metallo-oxidases McoA from *Aquifex aeolicus* and McoP from *Pyrobaculum aerophilum* (Martins *et al.*, 2002; Fernandes *et al.*, 2010 and 2007). These enzymes are all thermoactive (T_{opt}>75 ºC) and remarkably

thermostable, with melting temperatures between 80 and 114 ºC (Fernandes *et al.*, 2009 and 2010; Martins *et al.*, 2002; Durão *et al.*, 2008a). Copper was identified as a major determinant of the longterm and thermodynamic stability of CotA laccase and McoA (Durão *et al.*, 2008a; Fernandes *et al.*, 2009), in agreement with previous studies performed with the eukaryotic MCOs ascorbate oxidase, human ceruloplasmin, yeast Fet3p and the laccases from *Rhus vernicifera* and *Coriolus hirsutus* (Agostinelli *et al.*, 1995; Savini *et al.*, 1990; Sedlak and Wittung-Stafshede, 2007; Sedlak *et al.*, 2008; Koroleva *et al.*, 2001). Unfolding kinetics measured by the stopped-flow technique revealed that McoA aggregates under unfolding conditions, an uncommon feature among proteins, and this was further confirmed by light scattering, gel filtration and ANS binding (Fernandes *et al.*, 2009). The kinetic partitioning between aggregation and unfolding should be the main factor behind the low chemical stability of McoA at room temperature (2.8 kcal mol^{-1}) and its low heat capacity change (ΔC_p = 0.27 kcal mol^{-1} $ºC^{-1}$) (Fernandes *et al.*, 2009). This leads to a flat dependence of stability on temperature and explains the hyperthermostable nature of this enzyme. On the other hand, CotA laccase, despite the narrower dependence of stability on temperature, shows remarkable chemical stability towards chemical denaturation (an energy gap of approximately 10 kcal mol^{-1} at room temperature) (Durão *et al.*, 2002) and therefore is more thermodynamically stable in the thermophilic temperature range (unpublished data). Furthermore, point mutations close to the T1 copper centre of CotA laccase have a profound impact on the thermodynamic stability of the enzyme without causing major structural changes in the tertiary structure (Durão *et al.*, 2006 and 2008a).

In the present study the long-standing topic of the role of disulfide bonds in protein stability is revisited for CotA laccase. Disulfide bridges, according to the classical theories, confer stability by reducing the conformational entropy of the unfolded state relative to the native state, thereby decreasing the entropy gain upon unfolding (Brockwell, 2007; Pace *et al.*, 1998; Radestock, 2008; Zhou *et al.*, 2008). The single intra-domain disulfide bridge of the enzyme CotA laccase from *B. subtilis* was disrupted, and the mutant C322A was characterized by using spectroscopic methods and fast kinetics of unfolding and of copper binding or release. Most of the studies on copper proteins using stopped-flow kinetics were confined to the simplest T1 copper proteins azurin and rusticyanin (Alcanaz *et al.*, 2005; Pozdnyakova and Wittung-Stafshede, 2001; Wittung-Stafshede, 2004). Overall, the data presented show that the disulfide bridge has no significant effect on the three-dimensional structure, catalytic properties and thermodynamic stability of CotA but contributes to its conformational dynamics on the microsecond to millisecond timescale, with implications for the rates of copper incorporation into and release from the catalytic centres. This study contributes to our understanding of the mechanisms of copper incorporation in MCOs.

3.3 Materials and Methods

Construction of the C322A mutant

Single amino acid substitution in one of the cysteines (C322A) involved in the disulfide bridge of CotA laccase was created using the QuikChange site-directed mutagenesis kit (Stratagene). Plasmid pLOM10 (containing the wild-type cotA sequence) was used as a template and the forward

primer 5'-GCAAACAGCGCGGGCAACGGCGGTGACGTCAATC-3' and the reverse primer 5'-GATTGACGTCACCGCCGTTGCCCGCGC TGTTTGC-3' were used to generate the C322A mutant. The presence of the desired mutation in the resulting plasmid and the absence of unwanted mutations in other regions of the insert were confirmed by DNA sequence analysis. The recombinant plasmid was transformed into *Escherichia coli* Tuner (DE3) strain (Novagen) to obtain strain AH3551.

Overproduction and purification

Strains AH3551 (containing the gene cotA with the point mutation C322A) and AH3517 (containing the wild-type cotA gene (Martins *et al.*, 2002)) were grown in Luria–Bertani medium supplemented with ampicillin (100 mg/mL) at 30 ºC. Growth was monitored until the optical density at 600 nm was 0.6, at which time 0.1 mM isopropyl-β-D-thiogalactopyranoside and 0.25 mM $CuCl_2$ were added to the culture medium and the temperature was lowered to 25 ºC. Incubation was continued for a further 4 h, when a change to microaerobic conditions was achieved (Durão *et al.*, 2008a). Cells were harvested by centrifugation (8000g, 10 min, 4 ºC) after a further 20 h. For the overproduction of the apo-CotA forms, no copper was added to the culture medium (Durão *et al.*, 2008a). Proteins were purified by using a two-step purification procedure as previously described (Martins *et al.*, 2002; Bento *et al.*, 2005).

UV/visible, EPR and circular dichroism spectra

Protein samples were routinely oxidised using potassium iridate followed by dialysis. UV/visible spectra were recorded using a Nicolet Evolution 300 spectrophotometer from Thermo Industries. The EPR spectra were measured with a Bruker EMX spectrometer equipped with

an Oxford Instruments ESR-900 continuous-flow helium cryostat. The spectrum obtained under non-saturating conditions was theoretically simulated using the Aasa and Vänngard approach (Aasa and Vänngard, 1975). A circular dichroism spectrum in the far-UV region was measured with a JASCO (Tokyo, Japan) 720 spectropolarimeter using a circular quartz cuvette with a 0.01 cm optical path length in the range from 190 to 250 nm.

Enzymatic assays

The oxidation reactions of 2,2'-azinobis(3-ethylbenzo-6-thiazolinesulfonic acid) (ABTS) and syringaldazine were photometrically monitored with either a Nicolet Evolution 300 spectrophotometer from Thermo Industries or a Molecular Devices Spectra Max 340 microplate reader with a 96-well plate. All procedures were carried out as previously described (Durão *et al.*, 2006).

Crystallisation and structure solution

Crystals of the C322A mutant protein were obtained from a crystallisation solution containing 12% PEG MME5k, 0.1 M sodium citrate at pH 5.5 and 16% 2-propanol, using the vapour diffusion method. Crystals were harvested after 6 days and cryoprotected in a solution containing the crystallisation solution plus 22% ethylene glycol. Data collection, from a flash-cooled crystal, was undertaken on beam line ID23-EH1 at the European Synchrotron Radiation Facility in Grenoble, France, and a data set with 2.25Å resolution was obtained. Diffraction data were processed and scaled using MOSFLM (Leslie, 1992 and 2006) and SCALA, from the CCP4 suite (CCP4, 1994), respectively (data collection statistics are listed in Table 5). The three-dimensional structure

of the mutant protein was solved by the molecular replacement method using the program MOLREP (Vagin and Teplyakov, 1997) and as a search model, the structure of the native CotA (1W6L) (Bento *et al.*, 2005), from which the solvent molecules as well as the copper ions had been removed. Refinement of the structural model was undertaken with the program REFMAC (Murshudov *et al.*, 1999) and model building and improvement were performed with the program COOT (Emsley and Cowtan, 2004). Isotropic refinement of the atomic displacement parameters was performed for all atoms. The occupancies of the copper ions were adjusted so that their isotropic thermal vibration parameters refined approximately to those observed for the neighbouring atoms. Solvent molecules were positioned after a few cycles of refinement as were several molecules of ethylene glycol. To model the species observed between the T3 copper sites, careful analysis of the omit and standard difference Fourier syntheses as well as of thermal vibration coefficients was undertaken, and a diatomic species was identified at this site (Bento *et al.*, 2010). The model giving the best refinement corresponded to a dioxygen moiety with the O–O distances constrained to the target value of 1.204 Å. Such a moiety could be an O_2^{2-} species, a partially protonated version or a mixture of such states. Refinement statistics are listed in Table 5.

Table 5 - Data collection and refinement statistics for the C322A mutant protein.

Data collection statistics	
Beam line at ESRF	ID23-EH1
Wavelength (Å)	0.9537
Detector distance (mm)	331.6
Resolution (Å)	2.25
Space group	$P3_121$
Cell parameters (Å)	
a	101.6
c	136.8
Mosaicity (°)	0.4
Oscillation angle (°)	0.65
Oscillation range (°)	63.05
No. of unique *hkl* reflections	36,605 (5,265)
Completeness (%)	99.9 (100.0)
$I/\sigma(I)$	7.0 (2.1)
R_{sym}	0.075 (0.349)
Multiplicity	3.7 (3.8)
Refinement statistics	
No. of protein atoms	4,120
No. of solvent atoms	402
No. of heteroatoms	4Cu + 2O + 6EDO
Final *R* factor	0.162
Final free *R* factor	0.206
Mean *B* values (Å^2)	
Protein	35.4
Solvent	41.6
Overall	36.0
Estimated overall coordinate uncertainty (Å)[a]	0.104
Distance deviations[b]	
Bond distances (Å)	0.010
Bond angles (Å)	1.232
Planar groups (Å)	0.005
Chiral volume deviation (Å^3)	0.079
Quality of models	
Ramachandran analysis (%)	
Favourable	96.4
Generous	3.6
Disallowed	0.0

Values in parentheses refer to the highest-resolution shells as follows: C322A (2.37–2.25Å). Ramachandran analysis was determined by PROCHECK (Laskowski *et al.*, 1993b).
ESRF, European Synchrotron Radiation Facility; EDO ethylene glycol.
a Based on maximum likelihood
b Rms deviations from standard values

Stability

Long-term thermostability was determined at 80 ºC for an enzyme solution in 20 mM tris(hydroxymethyl)aminomethane (Tris)–HCl buffer, pH 7.6. At appropriated times, samples were withdrawn, cooled and immediately examined for residual activity following oxidation by ABTS as previously described (Martins *et al.*, 2002). The thermodynamic stability assessed by steady-state fluorescence was measured with a Cary Eclipse spectrofluorimeter using 296 nm as the excitation wavelength. All proteins were in 20 mM Tris–HCl buffer at pH 7.6 and increasing concentrations of guanidine thiocyanate (GuSCN) were used to induce unfolding at 25ºC. Unfolding was measured by a combination of fluorescence intensity and the emission maximum and was quantified using two-state equations (Durão *et al.*, 2006). The stability of the tertiary structure was assessed by differential scanning calorimetry as previously described (Durão *et al.*, 2008a).

Stopped-flow kinetics

Kinetic experiments were carried out with an Applied Photophysics Pi-Star 180 instrument with absorption and fluorescence intensity detection. A mixing ratio of 1:1 to give final protein concentrations of 2 and 20 μM for fluorescence and absorption detection, respectively, was used. The unfolding or refolding of proteins was followed by fluorescence with an excitation wavelength of 296nm, and emission was detected above 320nm using a glass filter. For the unfolding experiments the proteins in 20 mM Tris–HCl, pH 7.6, were mixed with 100 mM Britton-Robinson buffer, pH 1.6, to a final pH of 1.8. Copper release and binding was measured by absorption at 600 and 330 nm to probe the T1 and T3 copper ions, respectively. For copper binding experiments, the apo forms of proteins

in 20 mM Tris–HCl, pH 7.6, were mixed with solutions ranging from 20 to 240 μM $CuCl_2$ in the same buffer. All kinetic traces were analysed according to a multiexponential fit using Pro-Data Viewer provided by Applied Photophysics.

Other methods

The copper content of proteins was determined by the trichloroacetic acid/bicinchoninic acid method (Brenner and Harris, 1995). The protein concentration was measured using the CotA absorption band at 280 nm ($\varepsilon 280$ = 84,739 M^{-1} cm^{-1}). Redox titrations were performed at 25 ºC and pH 7.6, under an argon atmosphere, and were monitored by visible absorbance (300–900 nm) as described previously (Durão *et al.*, 2006).

3.4 Results and Discussion

Spectroscopic analysis

The recombinant C322A mutant shows the same chromatographic pattern during purification as wild-type CotA laccase. Protein samples were judged to be homogeneous by the observation of a single band on sodium dodecyl sulfate polyacrylamide gel stained with Coomassie Blue. Each holoprotein "as isolated" contained approximately 4 mol copper per mole of protein. The UV/visible spectra of the wild-type and the C322A mutant are very similar, having an intense absorption band at 600 nm (ε = 4,000 M^{-1} cm^{-1}) due to the charge transfer transition characteristic of the T1 copper centre (Figure 18A). The EPR spectrum of the C322A mutant resembles that of the wild-type protein (i.e. the spin Hamiltonian parameters for the wild-type and mutant proteins for both T1 and T2 copper are similar; Figure 18B). The circular dichroism spectrum of the

mutant in the far-UV region reveals minimal changes in the secondary structure as compared with that of the wild-type; the signal is dominated by β-sheets, turns and random coils and a small percentage of α-helix (Figure 18C). Overall, it seems that the C322A mutation results only in very subtle differences in the electronic structure of the copper centres.

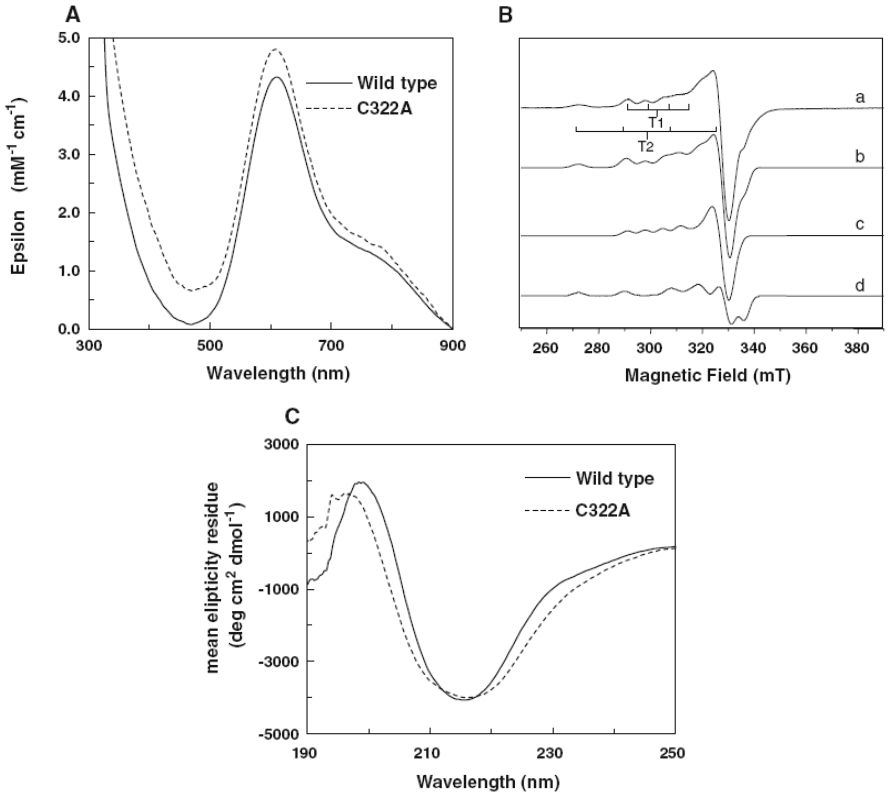

Figure 18 – A. UV/visible spectra of wild-type CotA and the C322A mutant in 20 mM Tris–HCl with 200 mM NaCl, pH 7.6. **B. EPR spectrum of the C322A mutant**. The spectrum obtained at -263 ºC with a microwave frequency of 9.39 GHz, microwave power of 2.4 mW and modulation amplitude of 0.9 mT (**a**); simulation of the total spectrum (**b**); and deconvolution of the different components (**c** and **d**). The parameters used were as follows: for type 1 (T1) copper g_{min} = 2.042, g_{med} = 2.046, g_{max} = 2.228 and A_{max} = 70 x 10^{-4} cm^{-1} and for type 2 copper (T2) g_{min} = 2.035, g_{med} = 2.094, g_{max} = 2.250 and A_{max} = 187 x 10^{-4} cm^{-1}. The contribution of the T1 and T2 components is 1:1 in the simulation of the total spectrum. The hyperfine splittings A_{max} of the T1 and T2 copper centres are indicated. **C) Circular dichroism spectra in the far-UV region**.

Redox and catalytic properties

The reduction of the T1 copper centre was monitored by the decrease of the $S(\pi)\rightarrow Cu(d_{x^2-y^2})$ charge transfer absorption band at around 600 nm. The replacement of C322 by an alanine resulted in a decrease of the redox potential of the T1 copper centre (E^0_{T1}) by approximately 70 mV (Table 6). The lower E^0_{T1} can reflect the variation of several factors, including the solvent accessibility and the electrostatic interactions between the metal centre and the protein (Solomon *et al.*, 1996). The enzymatic kinetic constants (k_{cat} and K_m) measured for the C322A mutant are similar to those exhibited by the wild-type enzyme (Table 6). The lower E^0_{T1} determined for the mutant enzyme would appear to favour a decreased reaction velocity as the rate of an electron transfer reaction (k_{ET}) is a major component of k_{cat}, and is directly dependent on E^0 (Moser and Dutton, 1996). However, according to the Marcus theory, two other factors affect the rate of an electron transfer reaction (k_{ET}): the electronic tunnelling, which depends on the exact geometry of the protein matrix, and the reorganization energy, which depends on the structure and dynamics of the protein (Solomon *et al.*, 1996; Moser and Dutton, 1996). Therefore, possible reasons for discrepancies in the reaction rate in relation to the redox potential of the C322A mutant must lie in the interplay among different and complex factors that are present in the catalytic mechanism of MCOs.

Table 6 - Activation energy ($\Delta G^{\pm}$), redox potential of the type 1 copper and steady-state kinetic constants for 2,2'-azinobis(3-ethylbenzo-6-thiazolinesulfonic acid) (ABTS) and syringaldazine (SGZ) for the wild-type and the C322A mutant. The activation energy was determined using ABTS as a substrate.

	$\Delta G^{\pm}$ (kcal mol^{-1})	E^{o} (mV)	ABTS		SGZ	
			K_m (μM)	k_{cat} (s^{-1})	K_m (μM)	k_{cat} (s^{-1})
Wild type	2.9 ± 0.1	525 ± 10	102 ± 1	264 ± 9	8 ± 2	79 ± 4
C322A	4.2 ± 0.9	457 ± 5	105 ± 9	238 ± 17	8 ± 0.3	73 ± 1

Thermodynamic stability characterization

The stability of CotA upon chemical-induced unfolding was evaluated by tryptophan fluorescence. The equilibrium curves at increasing concentrations of GuSCN show that the native state is more stable than the unfolded state by 5.5 and 5.4 kcal mol^{-1} for the wild-type and the C322A mutant, respectively, showing that the overall stability is maintained in the mutant despite the disruption of the disulfide bridge. Moreover, the other parameters that characterize the structural stability, namely the concentration of GuSCN at which 50% of the molecules are unfolded (midpoint) and the cooperativity of unfolding (m), are similar for the wild-type and mutant proteins (Figure 19A; Table 7).

The C322A mutant denatures irreversibly, according to a first-order process (Figure 19B), pointing to a simple pathway of unfolding and deactivation, as described previously for the wild-type enzyme (Martins *et al.*, 2002; Durão *et al.*, 2008a). At 80ºC the C322A mutant has a slightly higher long-term stability than the wild-type, with a half-life of inactivation of 207 ± 17 min as compared with 172 ± 19 min, but the error intervals overlap. The thermal stability was further probed by differential scanning calorimetry (Figure 19C). The transitions obtained

for the C322A mutant are as complex as those previously reported for the wild-type and other MCOs, because aggregation occurs after the first scan, leading to 100% irreversibility of the process (Fernandes *et al.*, 2009 and 2010; Durão *et al.*, 2008a). Moreover, the excess heat capacity could only be fitted using three calorimetric transitions, supporting sequential domain unfolding. The overall thermal stability of the C322A mutant is comparable to that of the wild-type, with midpoint temperatures (T_m) at each transition of 73, 78 and 81 ºC. Overall, these results show that the disulfide bridge does not have a major contribution to the thermodynamic or the thermal stability of CotA laccase.

Table 7 - Thermodynamic stability of the tertiary structure of wild-type CotA and the C322A mutant.

	Wild type	C322A
ΔG° (kcal mol^{-1})	5.5 ± 0.8	5.4 ± 1.3
m (kcal mol^{-1})	−3.4 ± 0.6	−3.4 ± 0.8
Midpoint (M)	1.6 ± 0.1	1.6 ± 0.1

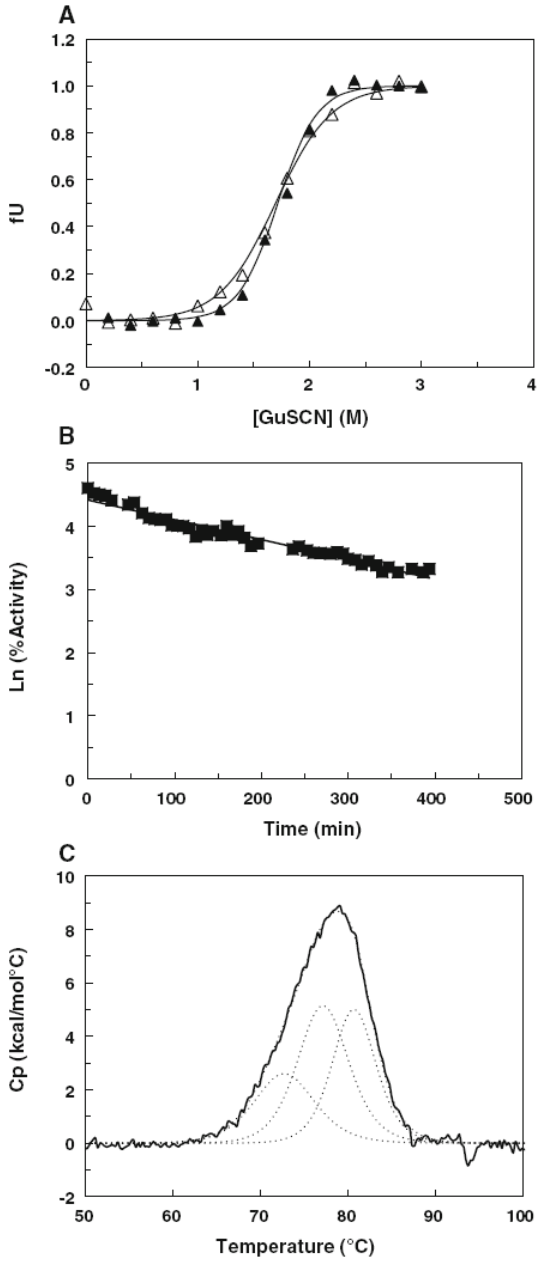

Figure 19 – A. Fraction of wild-type CotA (filled symbols) **and C322A mutant** (open symbols) **unfolded (*f*U) by guanidine thiocyanate (GuSCN) as measured by tryptophan fluorescence.** The solid lines are the fits using the equation $fU = \exp(-\Delta G^0/RT)/1 + \exp(-\Delta G^0/RT)$, which assumes the native ↔ unfolded equilibrium. **B. Long-term stability of the C322A mutant protein at 80ºC; C. Differential scanning thermogram of the C322A mutant protein** (solid line) **fitted by three thermal transitions** (dotted lines)**.**

Structural characterization

The three-dimensional structure of the C322A mutant was solved and the overall fold is very similar to that of the wild-type (the rms deviation of the Cα trace is 0.618 Å). Similarly to the wild-type holo structure, the copper centres in the C332A mutant show full occupancies and a diatomic oxygen species was modelled in the trinuclear centre (Figure 20A).

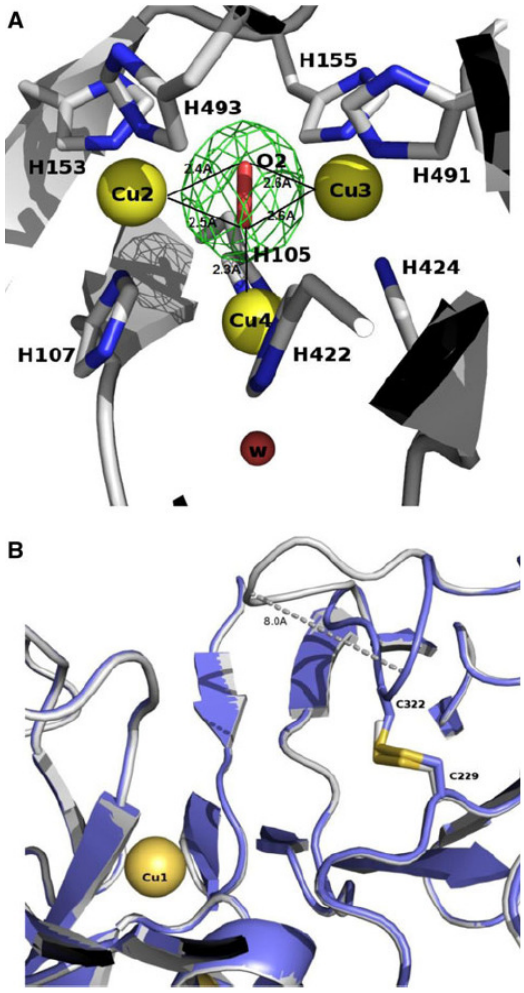

Figure 20 – A. Close-up view of the trinuclear centre in the C322A mutant structure. A difference Fourier synthesis contoured at the 4σ level. **B. Superposition of the Cα tracing of the C322A mutant protein and holo-CotA.** The loop that contains residue 322 is coloured blue for the wild-type and grey for the mutant. Residue 229 in the C322A mutant protein is coloured by atom type.

Interestingly, in the mutant enzyme the loop that comprises residues 90–97, which is usually very poorly defined in previous CotA structures (Bento *et al.*, 2005; Enguita *et al.*, 2003), became less disordered and it was possible to model into the electron density maps residues 90–92 and 95–97. In the structure of the C322A mutant, the Cys229 residue becomes exposed to the solvent and appears to be chemically modified, and a methyl thiocysteine moiety was modelled at this position. A similar modification of exposed cysteine residues into oxycysteines has been observed in other CotA structures where the protein was produced following the microaerobic expression protocol (Durão *et al.*, 2008a). In the wild-type, the loop where Cys322 is involved in the disulfide bridge with Cys229 is well ordered and defined. In contrast, the most significant difference in the mutant structure is observed at the position of this loop, which becomes less ordered and moves some 8Å away towards the solvent side (Figure 20B). As the disulfide bridge is located at one of the edges of the substrate binding pocket, the mutation induces a slight change in the configuration of the binding pocket and changes the substrate binding surface. This, in turn, may influence the incorporation of copper into the mononuclear T1 copper centre. This observation could contribute to the decreased E^0_{T1} determined for the C322A mutant (Karlin *et al.*, 1997). Indeed, substitutions of hydrophobic residues with an alanine residue near the T1 copper of CotA laccase in a previous study have been shown to increase the solvent accessibility and cause a decrease of the redox potential of the metal centre of the mutants (Durão *et al.*, 2008b).

Collisional quenching by acrylamide

To address possible modifications in the mutant protein dynamics, the accessibility of the tryptophan fluorophores was studied by using acrylamide as a fluorescence quencher (Figure 21). The Stern–Volmer plots for the wild-type and the C322A mutant are very similar, showing that the accessibility of tryptophan residues to acrylamide is similar in both proteins. The quenching of a fluorophore depends upon its "exposure" to the quencher. Indeed, a buried residue may occasionally expose itself to collisions with the quencher as a result of local or large-scale conformational fluctuations in the protein. Quenching of tryptophan fluorescence has to occur during the lifetime of the excited state and therefore only protein dynamics within this picosecond to nanosecond time range may allow tryptophan residues to collide with acrylamide. Therefore, collisional quenching also probes motion dynamics within the picosecond to nanosecond timescale of fluorescence lifetimes (Eftink and Ghiron, 1977; Somogyi *et al.*, 1994) at least for tryptophan residues that are partially exposed at the protein surface (Calhoun *et al.*, 1986). The results obtained show that the disruption of the disulfide bridge in CotA laccase does not affect protein dynamics on the picosecond to nanosecond timescale, which is generally defined as a fast timescale of protein motions.

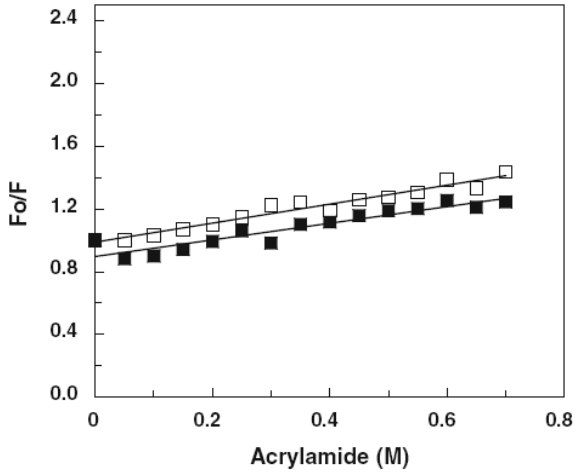

Figure 21 - Stern–Volmer plot. Collisional quenching of wild-type CotA (filled squares) and of the C322A mutant (open squares).

Kinetics of the acid-induced unfolding

Unfolding kinetics as assessed by tryptophan fluorescence, using the stopped-flow technique, were measured using the apo and holo forms of the enzymes under study. Acidification was used to promote protein unfolding and, interestingly, it was observed that unfolding of the apo forms is characterized by a decrease in fluorescence, whereas unfolding of the holo forms was characterized by an increase in fluorescence (Figure 22).

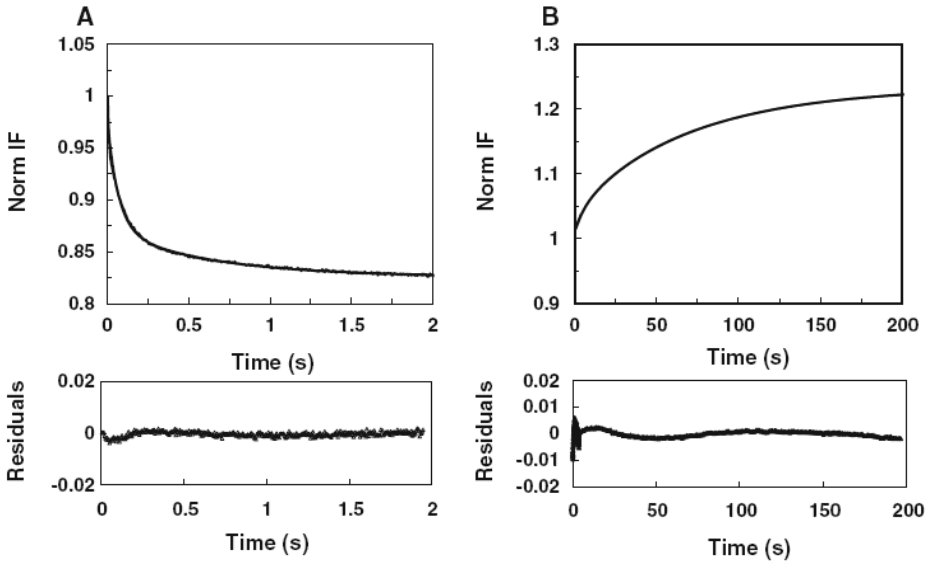

Figure 22 - Unfolding induced by acid and assessed by tryptophan fluorescence. A. Total fluorescence intensity variation of wild-type apo-CotA. B. Total fluorescence intensity variation of wild-type holo-CotA. Kinetic traces were fitted with a double exponential for the apo form and with a triple exponential for the holo form as shown in the residuals plots.

This inversion of the fluorescence signal is most probably due to the assigned role of copper as a quencher of fluorescence (Lakowicz, 1999). The conformational unfolding of apo forms was fitted with a second-order exponential, whereas the unfolding of the holo forms could only be accurately fitted by using a triple exponential (Table 8). This is most probably related to a higher complexity of the unfolding pathway in the holo forms, which certainly reflects the presence of copper ions at the catalytic centres.

Table 8 - Values for the k_1, k_2 and k_3 constants obtained from the fitting of kinetic traces reporting the variation in fluorescence intensity upon acid-induced unfolding.

	k_1 (s^{-1})	k_2 (s^{-1})	k_3 (s^{-1})
Apo-CotA	16.95 ± 1.09	1.81 ± 0.09	–
Apo-C322A	22.1 ± 0.07	1.59 ± 0.05	–
Holo-CotA	0.12 ± 0.01	0.02 ± 0.00	0.002 ± 0.001
Holo-C322A	0.38 ± 0.01	0.10 ± 0.01	0.03 ± 0.01

A lower number of unfolding phases, in apo forms, is also observed in other metalloproteins (Zhang and Matthews, 1998). In the blue copper azurin, an unfolding pathway of higher complexity caused by a redox-active copper ion that remains bound to the protein in the unfolded state was observed (Leckner *et al.*, 1997). The unfolding rates of the apo forms are almost 100-fold higher than those of the holo forms (Table 8), highlighting the effect of copper in stabilizing the protein three-dimensional structure. This stabilizing effect of copper could not be quantified through most classic approaches, such as equilibrium unfolding studies using chemical denaturants, because the enzymes become copper-depleted at low concentrations of denaturant prior to the overall unfolding (Fernandes *et al.*, 2009; Durão *et al.*, 2006). In consequence, the stabilizing effect of copper ion was calculated by applying the Arrhenius law (which accounts for the unfolding rates of the apo and holo forms) to each unfolding phase, for the mutant and the wild-type enzyme (Table 8) (Pozdnyakova *et al.*, 2001). For these enzymes no major differences were observed as the stabilizing effect for phase 1 (k_1) is 1.6 and 1.8 kcal mol^{-1} and for phase 2 (k_2) is 0.2 and 0.3 kcal mol^{-1} for wild-type CotA and the C322A mutant, respectively. These values are in the lower limit for the stabilizing effect of copper in the native state, i.e. assuming the absence of copper affinity in the transition state during unfolding, and are also in

agreement with the spectroscopic and structural analysis, which revealed no major differences in the properties of the copper centres. Overall, the present results show that the C322A mutant globally unfolds faster than the wild-type enzyme. This suggests that the mutant most likely also refolds faster than the wild-type, given that at the equilibrium the stability is not affected by the mutation (see above). However, owing to the occurrence of protein aggregation, the folding kinetics of these proteins could not be investigated.

Kinetics of copper release and binding

The rates of copper release from the T1 copper site were monitored upon acid-induced unfolding of the wild-type and C322A mutant holo forms. The kinetic traces measured at 600 nm were accurately fitted according to a double exponential (not shown), pointing to a complex process which might be a consequence of the centre reorganization, preceding the copper release from the T1 copper site (Table 9). The two-fold higher decay rates at 600 nm in the C322A mutant as compared with the wild-type indicate faster removal of the T1 copper ion in the mutant enzyme.

Table 9 - Values for the k_1 and k_2 constants obtained from the fitting of kinetic traces reporting the decay of absorbance at 600 nm upon acid-induced unfolding.

	k_1 (s^{-1})	k_2 (s^{-1})
Holo-CotA	3.37 ± 0.71	0.38 ± 0.08
Holo-C322A	7.43 ± 0.97	2.71 ± 0.90

The kinetic traces describing copper binding to the T1 and T3 sites of the apo forms, measured at 600 and 330 nm, respectively, required a triple exponential to be accurately fitted, despite the attempt to use pseudo-first-

order conditions (i.e. copper and apoprotein in a 10:1 ratio; Figure 23; Table 10).

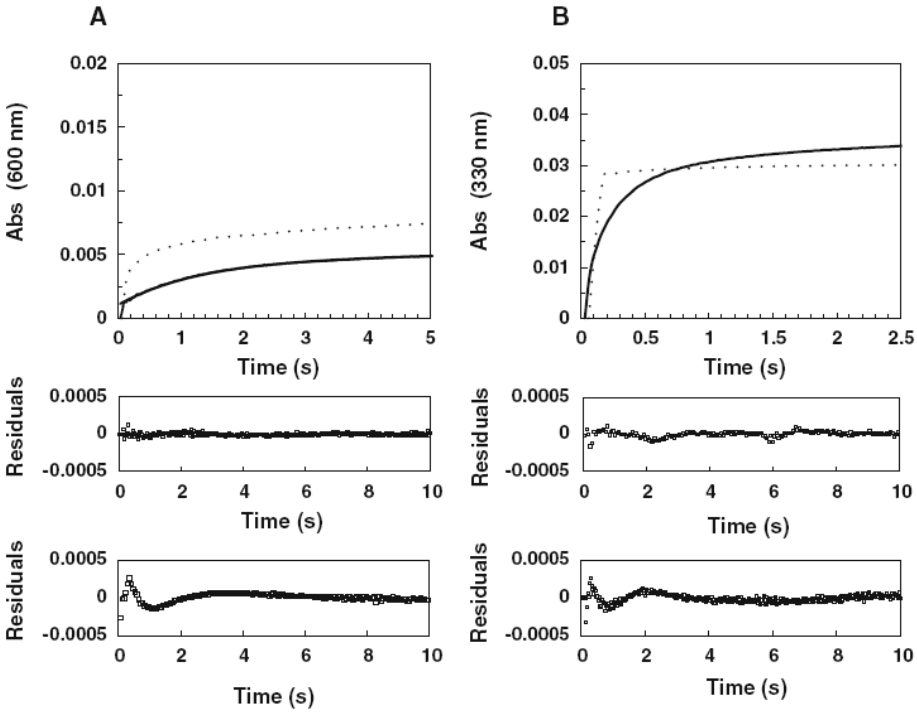

Figure 23 - Copper binding to apo forms of the wild-type (solid line) **and the C322A mutant** (dotted line)**. Kinetic traces measured by the absorbance at 600 nm (A) and at 330 nm (B).** Residuals are from triple exponential fits (upper plots for CotA and lower plots for the C322A mutant).

Table 10 - Values for the k_1, k_2 and k_3 constants obtained from the fitting of kinetic traces reporting copper binding to the T1 and T3 sites (absorbance at 600 nm and 330 nm, respectively).

	λ (nm)	k_1 (s^{-1})	k_2 (s^{-1})	k_3 (s^{-1})
Apo-CotA	600	20.1 ± 6.05	0.78 ± 0.02	0.09 ± 0.004
	330	4.93 ± 0.11	0.75 ± 0.04	0.06 ± 0.001
Apo-C322A	600	26.6 ± 6.2	1.7 ± 0.8	0.12 ± 0.02
	330	10.4 ± 0.15	1.4 ± 0.02	0.08 ± 0.008

These multiple rate constants might result from the presence of non-pseudo-first-order conditions or from binding followed by protein reorganization. Indeed, it has been recognized that metal binding to proteins may involve complex pathways with at least one intermediate during the binding process (Bah *et al.*, 2006; Cawthorn *et al.*, 2009; Choi *et al.*, 2006; Taniguchi *et al.*, 1990). For example, in human ceruloplasmin it has been proposed that copper binding *in vitro* is a cooperative process presumably mediated by conformational changes transmitted within the protein upon copper binding (Hellman *et al.*, 2002). On the other hand, copper binding to Sco from *B. subtilis*, a protein involved in the assembly of the Cu_A centre in cytochrome c oxidase, is described by a two-step binding mechanism where the first step is a bimolecular process producing an intermediate that undergoes an isomerization step to yield the final holo form (Cawthorn *et al.*, 2009). The fast rate constant k_1 measured in the wild-type and mutant enzymes was assigned to the first bimolecular step of copper binding (Table 10). This rate was shown to be dependent on the copper concentration (data not shown). The C322A mutant has slightly faster rates of copper binding followed at both 600 and 330 nm (Table 10). Interestingly, the rates of copper binding to the T1 centre are faster than the rates measured for copper binding to the T3 centre. This is in accordance with our previous results that pointed to a sequential process of copper incorporation into CotA laccase, with the T1 copper centre being the first to be reconstituted, followed by the T2 and T3 copper centres (Durão *et al.*, 2008a), similarly to what occurs in CueO from *E. coli*, yeast Fet3P and human ceruloplasmin (Blackburn *et al.*, 2000; Galli *et al.*, 2004; Kataoka *et al.*, 2005). The differences observed in the rates of copper incorporation and release in the mutant enzymes as compared with the wild-type should reflect subtle alterations in the

protein dynamics, with consequences in structural unfolding rates and in the rates of copper release and incorporation. Only this slower motion regime and not the picosecond to nanosecond time range dynamics was affected as shown by acrylamide collisional fluorescence quenching analysis. The faster dynamics observed does not seem to affect copper coordination in the catalytic centres. In fact, and as shown above, the stabilizing effect of copper is similar for both enzymes as are the spectroscopic and catalytic properties of the enzymes. Binding sites in proteins have a dual-stability character, and are often characterized by the presence of regions with low and with high structural stability, in an overall arrangement that contributes for an optimized binding affinity (Luque *et al.*, 2002). In most cases the low-stability regions are loops that become stabilized upon ligand binding and cover a significant portion of the ligand after binding, whereas catalytic residues of enzymes are usually located in regions with higher structural stability. Copper has a pivotal role in CotA laccase stability as well as in other MCOs (Durão *et al.*, 2008a; Agostinelli *et al.*, 1995; Savini *et al.*, 1990; Sedlak and Wittung-Stafshede, 2007; Sedlak *et al.*, 2008; Koroleva *et al.*, 2001) as shown here by the 100-fold faster unfolding rates of apo forms relative to the holo forms, as measured by fluorescence intensity. Copper incorporation in MCOs is, however, a poorly understood process at the molecular level (Sedlak and Wittung-Stafshede, 2007; Sedlak *et al.*, 2008; Blackburn *et al.*, 2000; Galli *et al.*, 2004; Kataoka *et al.*, 2005; Davis-Kaplan *et al.*, 1998; Kwok *et al.*, 2006; Shi *et al.*, 2003). The results presented in this study indicate that the disulfide bridge in CotA laccase should contribute to the stabilization of the loop near the T1 copper centre, highlighted in Figure 20, providing the necessary frame for the incorporation of the copper ions at the catalytic sites.

2.5 Acknowledgements

Instituto de Biotecnologia e Química Fina and J.S. Cabral are acknowledged for the use of the Pi-Star 180 instrument for stopped-flow kinetic measurements. The European Synchrotron Radiation Facility in Grenoble, France, and the Macromolecular Crystallography staff are sincerely acknowledged for provision of synchrotron radiation facilities and support. This work was supported by project grants from Fundação para a Ciência e Tecnologia (FCT), Portugal (POCI/BIO/57083/2004 and PTDC/QUI/73027/2006), and the European Comission (BIORENEW-FP6-2004-NMP-NI-4/026456). A.T.F and C.S.S. hold Ph.D. fellowships (SFRH/BD/31444/2006 and SFRH/BD/40586/2007, respectively) from FCT, Portugal.

CHAPTER 4

DIOXYGEN REDUCTION MECHANISM IN CotA LACCASE

CHAPTER 4.1

MECHANISMS UNDERLYING DIOXYGEN REDUCTION IN LACCASES:
STRUCTURAL AND MODELLING STUDIES FOCUSING ON PROTON TRANSFER

This chapter was published in the following refereed paper:

I. Bento, **C.S. Silva**, Z. Chen, L.O. Martins, P.F. Lindley and C.M. Soares, "Mechanisms underlying dioxygen reduction in laccases. Structural and modelling studies focusing on proton transfer.", **BMC Structural Biology** (2010) **10**(28): 1-14.

The proteins were provided by the Microbial & Enzyme Technology laboratory at ITQB. Catarina S. Silva performed the crystallisation experiments, spectral studies and analysis, and data collection. I. Bento carried out phase determination and structure solution. Simulation studies were performed by C.M. Soares.

4.1.1 Summary

Laccases are enzymes that couple the oxidation of substrates with the reduction of dioxygen to water. They are the simplest members of the multi-copper oxidases and contain at least two types of copper centres; a mononuclear T1 and a trinuclear that includes two T3 and one T2 copper ions. Substrate oxidation takes place at the mononuclear centre whereas reduction of oxygen to water occurs at the trinuclear centre.

In this study, the CotA laccase from *Bacillus subtilis* was used as a model to understand the mechanisms taking place at the molecular level, with a focus in the trinuclear centre. The structures of the holo-protein and of the oxidised form of the apo-protein, which has previously been reconstituted *in vitro* with Cu(I), have been determined. The former has a dioxygen moiety between the T3 coppers, while the latter has a monoatomic oxygen, here interpreted as a hydroxyl ion. The UV/visible spectra of these two forms have been analysed in the crystals and compared with the data obtained in solution. Theoretical calculations on these and other structures of CotA were used to identify groups that may be responsible for channelling the protons that are needed for reduction of dioxygen to water. These results present evidence that Glu498 is the only proton-active group in the vicinity of the trinuclear centre. This strongly suggests that this residue may be responsible for channelling the protons needed for the reduction. These results are compared with other data available for these enzymes, highlighting similarities and differences within laccases and multi-copper oxidases.

4.1.2 Introduction

Multi-copper oxidases (MCOs) are a group of enzymes that are able to couple the oxidation of a variety of different substrates concomitantly

with dioxygen reduction to water (Messerschmidt, 1997; Lindley, 2001; Bento *et al.*, 2006). This protein family comprises laccases, (p-diphenol: dioxygen oxidoreductase, EC 1.10.3.2), metallo-oxidases, ascorbate oxidase and ceruloplasmin (Lindley, 2001; Stoj and Kosman, 2005; Hoegger *et al.*, 2006). They are found in prokaryotes, eukaryotes as well as in archea. In plants, they have been associated with lignin formation; in fungi, with pigment formation, lignin degradation and detoxification processes; in yeast and mammals with iron metabolism; in bacteria with copper homeostasis and manganese oxidation (Nakamura and Go, 2005; Giardina *et al.*, 2010; and references therein). Overall, they are capable to oxidise substrates that vary from organic compounds, such as ascorbic acid, phenolate siderophores and organic amines, to inorganic ones, such as metal ions like Fe(II), Cu(I) and Mn(II) (Nakamura and Go, 2005; Giardina *et al.*, 2010; Kosman, 2010; and references therein). In addition, they are able to transfer their electrons to molecular oxygen with the concomitant production of water, a mechanism that can also constitute a key factor in the management of oxygen in aerobic organisms (Giardina *et al.*, 2010). These characteristics made them important targets for structure-function studies. Furthermore, laccases have been shown to have diverse biotechnological applications constituting a model for this type of studies (Giardina *et al.*, 2010).

Laccases, which are the simplest members of the MCOs family, show a characteristic fold that comprises three cupredoxin domains, with a mononuclear copper centre localised in the third domain, and a trinuclear copper centre located in between the first and the third domains (Figure 24a)). The four copper atoms can be classified in three different classes, based on their spectroscopic features (Malmström, 1982). The type 1 (T1) mononuclear copper centre (Figure 24b)) shows an intense absorption

band at ca. 600 nm, which is responsible for the blue colour of the protein, and is due to the ligand-to-metal charge transfer between the cysteine sulphur and the copper atom. This site also shows a characteristic EPR signal that is due to the high covalency at the copper site. The type 2 (T2) copper site, located in the trinuclear centre (Figures 24b) and 24c)), also exhibits a characteristic EPR signal, but no observable bands in the absorption spectra. The pair of type 3 (T3) copper ions are also localised in the trinuclear centre and are EPR silent, a fact attributed to their antiferromagnetic coupling in the presence of a bridging ligand, normally assumed to be hydroxyl. The T3 site also shows an absorption band at ca. 330 nm that has been attributed to the charge transfer between an hydroxyl bridging group and the copper atoms ($OH^- \rightarrow Cu2^+$) (Solomon *et al.*, 1996).

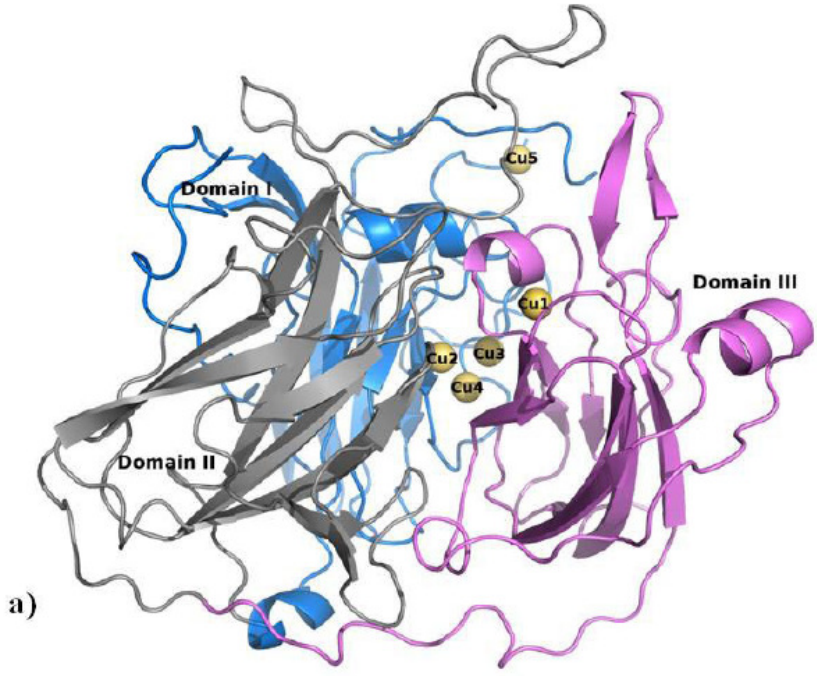

(Figure 24 –** to be continued**)

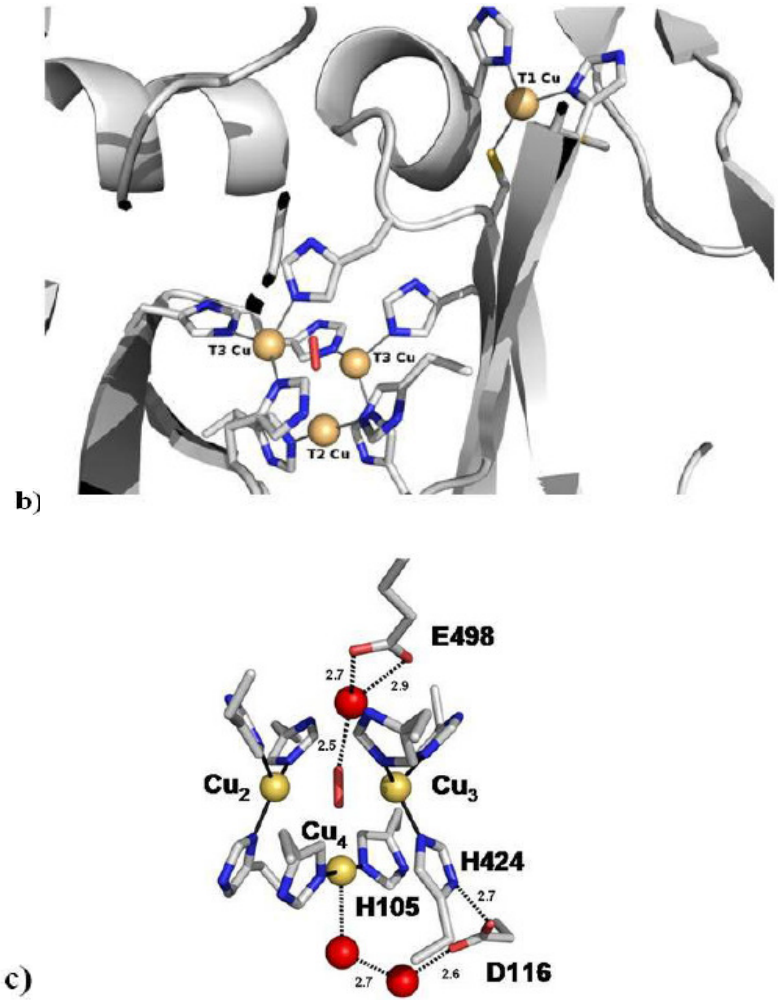

Figure 24 - Three-dimensional structure of CotA. a) Three-dimensional structure of CotA with each cupredoxin domain coloured in a different colour; domain I coloured in blue, domain II coloured in gray and domain III coloured in violet. Copper atoms are represented by spheres coloured in yellow. These correspond to the mononuclear coppers 1 and 5, and the trinuclear centre, comprising coppers 2, 3 and 4. **b)** Structural detail of the catalytic copper centres, the mononuclear type 1 copper centre (T1) where the copper atom is coordinated by a cysteine and two histidines, and the trinuclear centre which comprises a type 2 copper atom (T2) and two type 3 (T3) copper atoms. The cysteine residue (C492) that coordinates the T1 copper atom is bound to two of the histidine residues (H491 and H493) that coordinate the two T3 coppers in the trinuclear centre. This motif has been proposed to constitute the path for transfer of electrons from the T1 copper centre to the trinuclear centre. **c)** Close view of the CotA trinuclear centre - Important acidic groups are labelled (E498 and D116) as well as the histidine ligands to the copper that establish hydrogen bonds with D116.

MCOs catalyze one-electron oxidation processes, and four molecules of substrate are oxidised in order to reduce a dioxygen molecule to two waters molecules. Substrate oxidation occurs at the mononuclear T1 centre and then the electrons are shuttled, along a T1 coordinating cysteine, to the two histidines that are coordinating the T3 coppers of the trinuclear centre (Figure 24b)), where reduction of dioxygen occurs (Lindley, 2001; Stoj and Kosman, 2005; Solomon *et al.*, 2001). This constitutes a HCH conserved motif characteristically found in MCOs. Four electrons, as well as four protons, are used to reduce a molecule of dioxygen with the concomitant formation of two water molecules (Messerschmidt, 1997; Lindley, 2001; Sakurai and Kataoka; 2007). Electrons needed for this process are obtained through the oxidation of a variety of substrates, but not much is known about the mechanism of proton transfer during this process. Recently, site directed mutagenesis studies suggested that Asp112 of CueO (Asp116 in CotA; Figure 24c)) (Ueki *et al.*, 2006; Kataoka *et al.*, 2009), a conserved residue that is located in the exit channel in close proximity to the T2 copper ion, plays an important role in the protonation process. A similar role has been suggested for Asp94 in Fet3p (Quintanar *et al.*, 2005; Augustine *et al.*, 2007; Solomon *et al.*, 2008), which is also the equivalent residue of CotA Asp116. This internalised acidic group participates in a network of hydrogen bonds involving ligands of the trinuclear centre (see Figure 24c)), being connected with Cu4 through a chain of water molecules. Site directed mutagenesis studies, on the prokaryotic multi-copper oxidase CueO (Kataoka *et al.*, 2009) and on the eukaryotic multi-copper oxidase Fet3p (Augustine *et al.*, 2007; Solomon *et al.*, 2008), provided evidence for the importance of acidic residues located in the entrance channel in the reduction of dioxygen by these enzymes. These are Glu506 in CueO

(Kataoka *et al.*, 2009) (equivalent to Glu498 in CotA (see Figure 24c)), and Glu487 in Fet3p (Augustine *et al.*, 2007; Solomon *et al.*, 2008) (located in the other side of the channel). Despite the fact that these two residues are not conserved in sequence in all MCOs, the authors provide evidence for their participation in proton transfer to the reduction of dioxygen. In many structures, this acidic group can form a hydrogen bond with a water molecule that interacts with the oxygen species between the T3 coppers (see Figure 24c)).

In order to study the mechanism of dioxygen reduction to water by MCOs, CotA, a thermostable and thermoactive laccase, from *Bacillus subtilis*, was used as a model system (Martins *et al.*, 2002). The X-ray structure determination of CotA laccase, in different redox states and in complex with hydrogen peroxide and azide, together with the crystal structures from other MCOs already deposited in the PDB http://www.pdb.org (Berman *et al.*, 2000), allowed the proposal of a mechanism for such an enzymatic process (Bento *et al.*, 2005). However, many questions remain to be addressed, including the mechanism of protonation, the nature of the resting state of these enzymes and the identification of key residues that are involved in the reduction of dioxygen. The first MCO X-ray crystal structure to be reported was that of ascorbate oxidase (Messerschmidt *et al.*, 1992), in which a hydroxyl moiety bridged the two T3 copper ions; this structure has frequently been taken as the template for the native state. Most spectroscopic measurements have also indicated that MCOs, in their resting state, have a hydroxyl group as a bridging ligand. However, nearly all crystal structures of CotA that have been determined (Bento *et al.*, 2005; Durão *et al.*, 2006 and 2008b), and in particular the one where full copper content was achieved by soaking the crystals with $CuCl_2$ (from now on defined as

holoCu(II) (Bento *et al.*, 2005), PDB code: 1W6L), indicate that the structure of the oxidised state of this enzyme has a dioxygen moiety bridging the two T3 copper ions (Bento *et al.*, 2005) (Figures 24b) and 24c)). It is therefore pertinent to ask whether the CotA laccase has the same resting state as others MCOs. In order to try to answer this question the X-ray structures of two new preparations of CotA laccase (Durão *et al.*, 2008a) were determined. The first one corresponds to an *in vivo* fully copper loaded CotA protein (from now on called holoCotA), isolated from cells grown in copper supplemented media under microaerobic conditions. The second one corresponds to an *in vitro* reconstituted (with Cu(I)) fully copper loaded protein (from now on called apoCu(I)) (Durão *et al.*, 2008a). This apo protein was obtained from cells grown aerobically in unsupplemented copper media, and despite having been soaked with Cu(I), its spectra shows that it contains Cu(II) (Durão *et al.*, 2008a), meaning that the protein became oxidised when exposed to the oxygen. The structural comparison between these structures and the previous determined holoCu(II) (Bento *et al.*, 2005) will be performed in order to study the conformational effects of the different ways for incorporating copper in CotA. Moreover, the new structures determined here, together with the structures of other states, obtained for the same protein, were used in equilibrium protonation simulations in order to locate the groups likely to be involved in proton transfer. This combined structural biology approach, where X-ray structures of a system are obtained in controlled conditions by the same team (crystallisation conditions kept as similar as possible, as well as refinement procedures), and their conformational differences clearly identified in the electron density maps, is fundamental for the success of this type of calculations and mechanistic analysis, which are sensitive to small details. The application of careful procedures (see

below in Methods) was tested before with success in the analysis of multihaem cytochromes (Louro *et al.*, 2001; Bento *et al.*, 2004) as well as in CotA mutants (Durão *et al.*, 2008b). This type of proton transfer studies on laccases may also be helpful for understanding other dioxygen processing enzymes, where proton transfer plays a key role. The best known examples are the haem-copper oxidases (Pereira *et al.*, 2008), where electron transfer and dioxygen reduction, at the core of the protein, are associated with proton transfer of "chemical" protons, necessary for the reaction, as well as with vectorial proton pumping across the membrane. Similar types of approaches as the ones applied here for CotA laccase, based on Continuum electrostatics/Monte Carlo calculations (CE/MC) done on structural data, were used in haem-copper oxidases in order to understand their proton transfer determinants (Fadda *et al.*, 2008; Kannt *et al.*, 1998; Popovic and Stuchebrukhov, 2004 and 2005; Soares *et al.*, 2004). Despite different molecular architectures, the physical principles behind proton transfer mechanisms in multi-copper oxidases should be similar, at least in part, with the ones present in haem-copper, especially with what concerns "chemical" protons.

4.1.3 Materials and Methods

Crystallisation and Structure Solution

HoloCotA protein and the reconstituted apo-CotA soaked with Cu^{1+} (apoCu(I)) were obtained as described in Durão *et al.* 2008 (Durão *et al.*, 2008a). Crystallisation experiments were performed with both proteins samples and well diffracting crystals of holoCotA and apoCu(I) were obtained from crystallisation solutions containing 40% of methyl pentanodiol, 0.1 M of Hepes pH 7.5, and 22% PEG 4K, 0.1 M Sodium

Citrate pH 5.5 and 12% isopropanol, respectively. Crystals of the apoCu(I) were then harvested and cryo protected with a cryo solution containing the crystallisation solution with 22% of ethylene glycol. X-ray data collection was performed at the ID23-EH1 and ID23-EH2 beamlines at the ESRF, Grenoble, France. HoloCotA and apoCu(I) crystals diffracted to 1.7Å and 2.0 Å resolution, respectively. X-ray data sets were processed and scaled with MOSFLM (Leslie, 1992 and 2006) and SCALA from the CCP4 program suite (CCP4, 1994); the data collection statistics are listed in Table 11.

Table 11 – Data Collection statistics.

Protein	HoloCotA	apoCu(I)
Beam line at ESRF	ID23-2	ID23-1
Wavelength (Å)	0.87260	0.97625
Detector Distance (mm)	196.4	288.17
Resolution (Å)	1.8	2.0
Space group	$P3_121$	$P3_121$
Cell parameters (Å), a	101.4	101.3
c	137.3	136.1
Mosaicity (°)	0.43	0.32
Oscillation range (°)	0.8	0.45
Oscillation angle (°)	80°	81°
No. of unique *hkl*	76099 (10995)	54422 (7901)
Completeness (%)	99.9 (100.0)	99.0 (99.7)
$I/\sigma(I)$	6.4 (2.4)	6.6 (2.0)
R_{symm}	0.071 (0.311)	0.073 (0.384)
Multiplicity	5.0 (5.0)	4.9 (4.9)

† Values in parentheses refer to the highest resolution shells as follows: holoCotA (1.9 Å - 1.80 Å), ApoCu(I) (2.11 Å - 2.0 Å).

Both structures were solved by the molecular replacement method with the program MOLREP (Vagin and Teplyakov, 1997) and using, as a search model, the structure of the native CotA soaked with $CuCl_2$ (1W6L)

(Bento *et al.*, 2005), from which the solvent molecules, as well as the copper atoms, have been removed. Refinement of the structural models was undertaken using the maximum likelihood functions in the REFMAC program (Murshudov *et al.*, 1999) and model building and improvement was achieved with COOT (Emsley and Cowtan, 2004). Solvent molecules were positioned after a few cycles of refinement, as well as a few molecules of ethylene glycol. Isotropic refinement of the atomic displacement parameters was performed for all atoms. The occupancies of the copper ions were adjusted so that their isotropic thermal vibration parameters refined approximately to those observed for the neighbouring atoms. The careful use of omit and standard difference Fourier syntheses, as well as monitoring of thermal vibration coefficients during refinement, enabled the identification of a diatomic species between the T3 copper sites in the holoCotA structure. It could be argued that a more intense electron density peak could be also associated with a monoatomic species of another type of atom, having more electrons, as observed by Colloc'h *et al.* (Colloc'h *et al.*, 2008). Therefore, a chlorine ion was also modelled, instead of a dioxygen, but the difference map showed an extra positive density and, moreover, the B factor did not refine to a reasonable value (see Table S2). This procedure has been tried before, when refining other mutants structures of CotA laccase, and a similar result was observed (Durão *et al.*, 2006 and 2008b). At this resolution, it is not possible to distinguish between O_2, NO, and CO, but the enzyme has high affinity for dioxygen, and in an aerobic environment the availability of the other two species, when compared with dioxygen, is much lower; therefore the probability of the enzyme to bind them would be unlikely. Another possibility for the diatomic species would be peroxide, as present in the peroxide soaked structure of CotA (Bento *et al.*, 2005). This was also tried,

and the bond distance between the two oxygen atoms was set to 1.45 Å. However, the electron density difference map shows negative density and a higher B factor in one of the oxygen atoms, indicating that it was incorrectly positioned (Table S2). The careful analysis of these extensive tests showed that the entity that refines better in this case and in other published structures of CotA (Bento *et al.*, 2005; Durão *et al.*, 2006 and 2008b) is molecular oxygen, and refinement proceeded constraining the O-O distances to target values of 1.2 Å. Of course this cannot be considered the end of this story, but at the present resolution, the procedure applied here is the only possible one. Following the same procedure, a monoatomic oxygen species was modelled in the reconstituted apoCu(I). Refinement statistics are listed in Table 12.

Table 12 - Refinement and Quality of Refined Models.

Protein	HoloCotA	apoCu(I)
No. of protein atoms	4131	4119
No. of solvent atoms	527	518
No. of hetero atoms	4	4
Final R-factor	0.189	0.177
Final free R-factor	0.206	0.215
Mean B values (Å^2)		
: protein	22.6	24.3
: solvent	33.5	32.9
: overall	22.3	25.3
Estimated overall coordinate uncertainty (Å) ‡	0.092	0.089
Distance deviations †		
Bond distances (Å)	0.006	0.009
Bond angles (°)	0.993	1.145
Planar groups (Å)	0.004	0.004
Chiral volume deviation (Å^3)	0.067	0.077
Ramachandran analysis %		
Favourable	97.2	97.8
Allowed	2.8	2.2
Disallowed	0.0	0.0

‡based on maximum likelihood. † rms deviations from standard values
The Ramachandran analysis (Ramakrishnan and Ramachandran, 1965) was determined by Rampage (Lovell *et al.*, 2003).

CE/MC calculations (described below) require special care concerning the consistency of the structural models to be compared (different redox situations and different liganted states of active site are examples). The main reason for this is the fact that CE/MC calculations use rigid structures (or semi-rigid, if one considers the inclusion of tautomers), making the simulation of the titration of protonatable groups quite susceptible to conformational changes occurring in polar and charged groups in their vicinity. This effect is especially significant in protein interiors. The inclusion of flexibility in the methodology would alleviate this susceptibility, but this is quite difficult nowadays. Therefore, to overcome these limitations of the methodology, besides using protein crystals obtained in conditions as similar as possible for the different situations, a special crystallographic refinement procedure was applied here; when electron density was not enough to clearly identify the conformation of residue side-chains (evidencing natural flexibility), these were placed in a conformation as close as possible to the previously determined holoCu(II) structure (Bento *et al.*, 2005). This is very important, especially for charged side-chains, given that they can substantially influence the proton and electron binding calculations described next. Using this methodology, which we developed and used before in the analysis of multihaem cytochromes (Louro *et al.*, 2001; Bento *et al.*, 2004) and CotA mutants (Durão *et al.*, 2008b), we can distinguish clear effects from noise coming from undetermined structural details.

The atomic coordinates of both crystals structures have been deposited in Protein Data Bank http://www.pdb.org (Berman *et al.*, 2000): PDB ID code 2X87 and 2X88 for the apoCu(I) and HoloCotA, respectively.

Absorption Spectrophotometry

UV/Visible absorption spectra for holoCotA and on apoCu(I) crystals were collected under cryo conditions (110 K) using an offline microspectrophotometer at the Cryobench Laboratory, ESRF, Grenoble, France (Bourgeois *et al.*, 2002).

Theoretical calculations

Simulated pH and redox titrations were performed using methodologies, developed in our laboratory, for studying the binding equilibrium of protons and electrons (Baptista *et al.*, 1999; Teixeira *et al.*, 2002; Baptista and Soares, 2001). These methodologies are based on Continuum electrostatic (CE) methods and Monte-Carlo (MC) sampling of binding states. The CE methods (see Bashford, 2004 for a review), can be considered semi-microscopic and treat a protein like a low dielectric model, immersed in a high dielectric corresponding to the solvent (normally water), with charges placed at atomic positions. Electrostatic desolvation of charges and interactions between them are, therefore, treated by these methods, which normally solve the linear form of the Poisson-Boltzmann equation. The CE methods are used to compute the individual (pK_{int}) and interaction terms of the binding free energy of the protons and electrons. These free energy terms are then used in a MC method (see details in Baptista *et al.*, 1999; Teixeira *et al.*, 2002; Baptista and Soares, 2001) that samples the binding states of protons and electrons. Additionally, and given that the protein is considered rigid in CE methods, this MC method treats protonatable groups in a multiconfigurational way that considers alternative positions for the protons (tautomers) (Baptista and Soares, 2001). By the same limitation, the method also considers alternative configurations of the proton of

alcohol groups (Ser and Thr), considering these configurations (three) as tautomers. However, given the high pK_a of alcohol groups, here these are not considerable titrable. The procedure used allows us to deal with protonation-deprotonation and tautomeric exchange in a physically sound manner. The CE calculations were made using the package MEAD (version 2.2.0) (Bashford and Gerwert, 1992; Bashford, 1997). The sets of atomic radii and partial charges were taken from the GROMOS96 43A1 force field (van Gunsteren *et al.*, 1996; Scott *et al.*, 1999), except for the metal centres, where quantum chemical calculations (see below) were used to derive charges. The dielectric constants used were 80 for the solvent and 10 for the protein, which are values within the range where pK_a prediction is optimised (Teixeira *et al.*, 2005). The solvent probe radius was 1.4 Å, the ion exclusion layer 2.0 Å, the ionic strength 0.1 M and the temperature 27°C. The program PETIT (Teixeira *et al.*, 2002; Baptista and Soares, 2001) was used for the MC sampling of proton and electron binding states. Site pairs were selected for double moves when at least one pairwise term was greater than 2 pK units. Averages were computed using 10^5 MC steps. In all simulations, only the T1 centre was considered titrable, while the trinuclear centre was considered fixed in each state considered. Contrary to simulated pH titrations, which are done against a model compound reference (reflected in the $pK_{a\ mod}$) and can be directly compared with experimental values, simulated redox titrations are usually made against an unknown reference, due to the unavailability of a corresponding E_{mod}, i.e. the redox potential of an adequate model compound in water. This is due to the difficulty in finding such a model compound for protein metal co-factors, as it is the case for the T1 copper centre. The only option is to fit the value of E_{mod} to experimental data on redox titrations of the same group in different proteins, but this is only

usually exact if these proteins have only one type of redox centre (see for instance Teixeira *et al.*, 2002, for the case of bis-histidinyl coordinated tetrahaem cytochromes). However, in the case of multi-copper oxidases, more than one redox centre is present, and further approximations need to be used. Here, and in a similar manner to previous work (Durão *et al.*, 2008b), the experimental value obtained for the holoCotA enzyme was used to fit the calculations of the enzyme structure with a dioxygen species in the trinuclear centre. This is a crude approximation, since the trinuclear centres are not allowed to titrate in the simulations, and, in the real system, the titrations of all redox centres of the protein may be coupled (and therefore exert an influence on the experimentally observed redox potential of the T1 copper centre). Nevertheless, in this work, we are interested, not on the exact redox potential, but on the relative behaviour of the T1 centre, and on the effects that other alterations of the protein (for instance, the redox state of the trinuclear centre) may bring to its redox affinity. For consistency, we have used the conformational state found in holoCu(II) (Bento *et al.*, 2005) to model the holoCotA protein form. Since the present holoCotA structure contains an extra copper centre that has not been observed before, and we want to make comparisons with other CotA structures that do not contain it, we decided to use the equivalent holoCu(II) structure.

Partial charges for the T1 copper and the trinuclear centre were calculated considering model compounds for the different redox and liganted states analysed. These model compounds were created using coordinates of the centres as present in the structures with dioxygen, peroxide and in the fully reduced state as obtained previously (Bento *et al.*, 2005) and the new structure of CotA containing hydroxyl obtained here. The ligands of the metals were included down to the C-β carbon (C-α in

the case of the cysteine residue of the T1 copper). A water molecule bound to the T2 copper was also included. Single point calculations were performed using Gaussian 98 (Frisch *et al.*, 1998), using B3LYP and the 6-31G(d) basis set for all atoms, with the exception of copper atoms where the 6-31G(2df) basis set was used. These calculations were used to derive electrostatic potentials, which were then fitted using RESP (Bayly *et al.*, 1993) to calculate the partial charges. These charges were used directly with no scaling applied. While the GROMOS 43A1 charges are not derived using the RESP procedure, we believe that, from a physical standpoint, this is the most convenient way of deriving partial charges for metal centres. For the T1 copper, partial charges were calculated for the oxidised and reduced states, since these two situations are needed to simulate the redox titration of this group.

4.1.4 Results and Discussion

Structural characterization of holoCotA and of apoCu(I)

The overall comparison with holoCu(II) (Bento *et al.*, 2005) of the three-dimensional structures obtained for both holo-CotA and apoCu(I), showed no significant differences. The proteins comprise three cupredoxin domains with a mononuclear copper centre localized in domain 3 and a trinuclear centre in between domains 1 and 3. The rms deviation of the Cα trace of the holoCotA and apoCu(I) structures from the structure of holoCu(II) is about 0.1 Å. The most significant differences found between the structures were localized at the trinuclear centre and in the copper content. The holoCotA structure, in a similar manner as holoCu(II), shows full occupancy for all copper atoms in both

copper centres and has a dioxygen moiety modelled almost symmetrically between the two T3 coppers (Table 13 and Figure 25a)).

Table 13 - Occupancies of copper sites.

Mutant/ Copper Site	HoloCotA		apoCu(I)	
	occupancies	B_{factor} (Å^2)	occupancies	B_{factor} (Å^2)
T1	1.0	17.1	1.0	24.9
T2	1.0	18.0	0.3	29.4
T3 (x2)	1.0/1.0	15.0/16.1	0.7/0.4	26.1/25.2
Cu5	0.5	28.9		

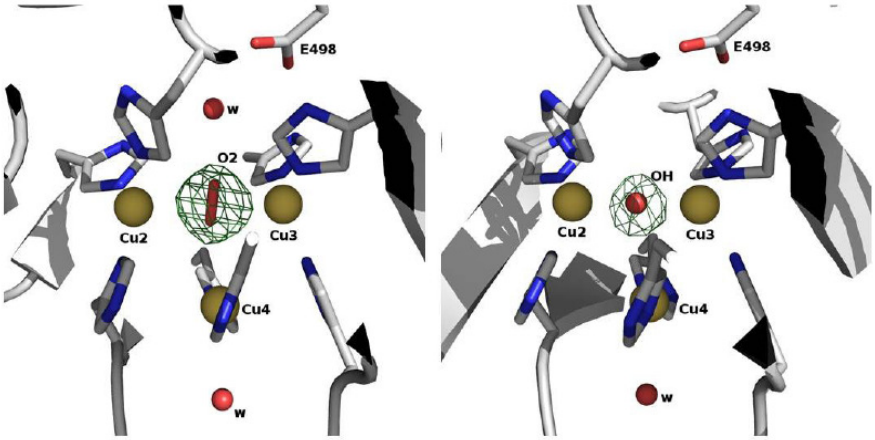

a) b)

Figure 25 - Structural detail of the trinuclear copper centre. In each picture the electron density for the moiety is derived from omit Fourier syntheses computed with SigmaA weighted coefficients |Fo| - |Fc|; the moieties were not included in the structure factor calculations and five cycles of maximum likelihood refinement were computed using REFMAC prior to Fourier synthesis to minimise phase bias. Contour levels are 5 rms for both electron density maps. **a)** In the holoCotA structure a dioxygen molecule is bound into the trinuclear centre. **b)** In the apoCu(I) a hydroxyl group is bound to the trinuclear centre. Both pictures were made with PyMol (DeLano, 2002).

However, in the holoCotA structure, a fifth copper atom was modelled with half occupancy at the surface of the molecule, located ca. 20Å away

from the other two copper centres (Figure 24a)). This copper atom, coordinated by two histidine residues and by two water molecules, is localised close to a disordered coil region that has been poorly defined in the calculated electron density maps for all other CotA structures determined until now. As the crystallisation conditions are different from the ones used previously, we cannot rule out the possibility that this may be an artefact of the crystallisation procedure. However, we did not add any extra copper to the crystallisation solutions. Therefore, this extra copper may be a consequence of the new protocol used to produce the protein. The overall structure of holoCotA determined here, with the exception of this extra copper, which has never been observed before, is basically the same as holoCu(II) determined previously (Bento *et al.*, 2005), and should correspond to the same chemical species.

The apoCu(I) structure shows full occupancy for the T1 copper centre but depletion for all copper atoms in the trinuclear centre (Table 13). As previously observed, the most depleted copper atom is the T2 copper. Interestingly, in the trinuclear centre a hydroxyl group was modelled in between the T3 coppers, with the same occupancy as the copper atoms (Figure 25b)). In this case, the distance between the two T3 coppers is slightly shorter (4.1 Å) than the observed for the structures where a dioxygen moiety was modelled at this position (4.9 Å). In addition, the water molecule that is localized at H-bond distance of the oxygen moiety in holoCotA was not observed in the electron density maps (Figure 25b)). In the apoCu(I) structure an oxycysteine residue was modelled at position 35, according to the electron density maps.

UV/Visible absorption spectra of holoCotA and apoCu(I) crystals (Figures 26a) and 26b)) were acquired as described above.

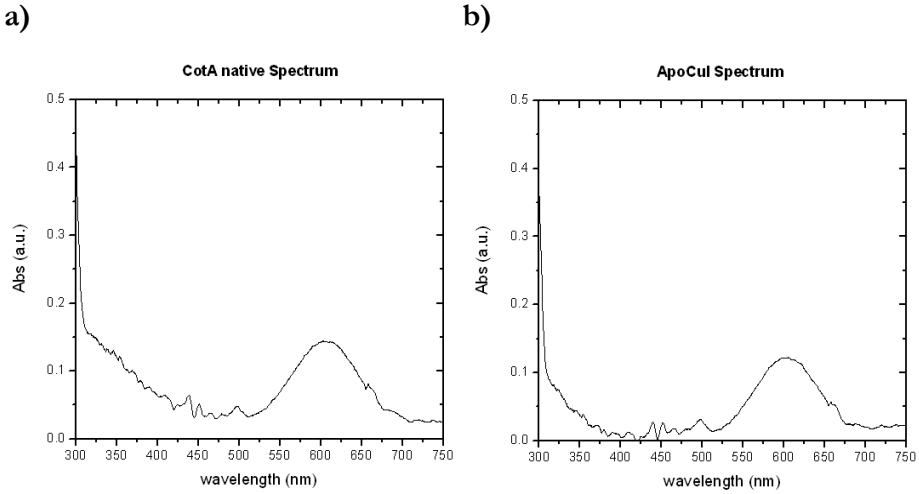

Figure 26 - UV/Visible absorption spectra of a) holoCotA crystal and of b) apoCu(I) crystal.

Both spectra show the characteristics observed for the holoCotA solution (Durão *et al.*, 2008a), namely an intense peak at 610 nm, which is due to the charge transfer between the copper atom (in the +2 state) and the cysteine residue at the mononuclear T1 copper centre, and a shoulder at around 330 nm. This shoulder is usually attributed to coupling of the T3 copper ions through a hydroxyl moiety in between them. The biochemical and spectroscopic characterization of holo-CotA and apoCu(I) showed that they have different catalytic and biophysical properties (Durão *et al.*, 2008a). Indeed, the reconstituted apoCu(I) is less efficient towards the oxidation of non-phenolic substrates, shows a lower redox potential and is less thermostable than the holoCotA enzyme (Durão *et al.*, 2008a). Since there are no significant changes in their overall three-dimensional structures, such differences can be attributed to changes at the copper centres, namely the copper content and the nature of the bridging ligand in between the two T3 coppers. An enzyme that

does not contain its full copper content, such as observed in the crystal structure of apoCu(I), will behave differently. The question as to why the enzyme was able to incorporate all the copper content *in vivo* and did not succeed in doing the same when incorporation was done *in vitro*, remains to be solved. One hypothesis is that, *in vivo*, the incorporation of copper occurs during the folding process, in a transition state that facilitates the incorporation of four positive charges (considering that the copper is incorporated in the Cu(I) state), whereas *in vitro*, when the final fold is already acquired, this incorporation process becomes less favourable and, therefore, less efficient. Work in our laboratories is currently being pursuit to address this question.

Mechanism of dioxygen reduction to water: insights into the characterization of the resting state of MCOs

The mechanism of dioxygen reduction to water includes a state where a dioxygen moiety is located between the two T3 coppers and another state where a hydroxyl group is at this position (Figure 27). The latter is formed after the oxidation of four substrate molecules and the transfer of four electrons to the trinuclear centre (Bento *et al.*, 2005).

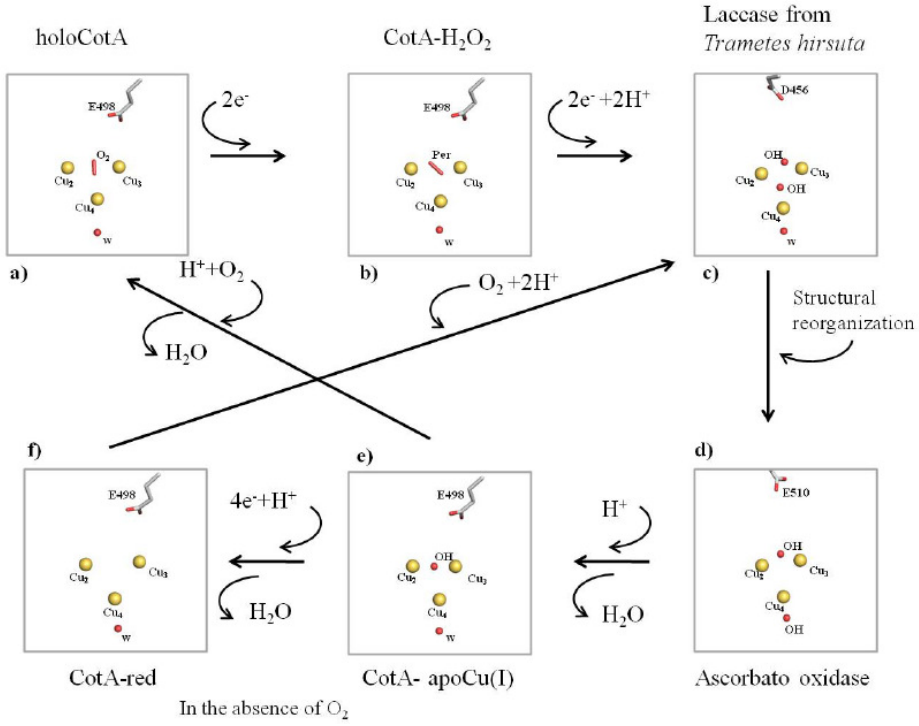

Figure 27 - Dioxygen reduction to water by multi-copper oxidases: crystal structures of several potential intermediates in the dioxygen reduction to water by multi-copper oxidases: a) HoloCotA. **b)** CotA-H_2O_2 (1W8E) (Bento *et al.*, 2005). **c)** Laccase from *Trametes hirsuta* (Polyakov *et al.*, 2009) (3FPX). **d)** Ascorbate oxidase from Zucchini (1ASO) (Messerschmidt *et al.*, 1992). **e)** ApoCu(I). **f)** reduced CotA (2BHF) (Bento *et al.*, 2005).

For the majority of studies on the multi-copper oxidases, this state has been assumed to be the resting state. However, in CotA this state has only been observed in the structure of a semi-reduced crystal (1GSK) (Enguita *et al.*, 2003) and, in the present study, in the structure of the reconstituted apoCu(I). The apo protein was incubated with Cu(I) in anaerobic conditions (Durão *et al.*, 2008a), implying that when oxygen became available the enzyme was ready to reduce it to water (Figure 27). Indeed, in many studies where such a moiety is observed, the experimental starting point is the reduced state of the enzyme. Moreover, studies on the effect of the X-ray radiation on laccase crystals reported by Hakulinen *et*

al. (Hakulinen *et al.*, 2006) showed that crystals exposed to high radiation doses present a hydroxyl moiety in the trinuclear site. This shows that reduction of the copper centres may occur during data collection, leading to an end-product that can be different from the starting state. Altogether, these data highlight that the observable state of the enzyme depends critically on the experimental conditions. Indeed, this has been clearly shown for bilirubin oxidase by Sakurai *et al.* (Sakurai and Kataoka, 2007). On the other hand, laccases usually show a characteristic absorption spectrum with a shoulder around 330 nm that has been attributed to the presence of the bridging hydroxyl in between the T3 coppers. The spectrum obtained for the holoCotA (Figure 26a) also shows this shoulder, but the crystal structure has a dioxygen moiety at the trinuclear cluster. Moreover, the same shoulder was observed in the spectrum acquired from crystals of the laccase from *M. albomyces*, before being exposed to the X-ray radiation (Hakulinen *et al.*, 2006), and this laccase has also a dioxygen moiety in the trinuclear centre. It could be argued that the dioxygen moiety was the well characterised peroxide intermediate (PI) (Solomon *et al.*, 2001; Augustine *et al.*, 2007; Solomon *et al.*, 2008; Shin *et al.*, 1996; Palmer *et al.*, 2001). However, in both cases, the enzymes were in the oxidised state and no electrons were available to reduce the dioxygen molecule. It is therefore clear that a shoulder around 330 nm in the absorption spectrum can also be attributed to a dioxygen moiety. What is the resting state of multi-copper oxidases is a question that still remains to be answered. It is possible that MCOs have more than one resting state depending on the residues that surround the trinuclear centre. In fact, the current work clearly shows that the final results are dependent on the process of obtaining the protein; therefore, it is still not possible to give a clear unbiased answer.

Mechanism of dioxygen reduction to water: groups involved in the proton transfer mechanism

The availability of three-dimensional structures for several states of the trinuclear centre, with different oxygen species bound, allows the investigation of the protonation of ionisable groups involved in the enzymatic mechanism. A working hypothesis for the mechanism in this type of enzymes is presented on Figure 27, only considering the water molecules that are consistently observed in all deposited three-dimensional structures (this is a revised version of the one presented on Bento *et al.*, 2005). CE/MC calculations were done on these structures, not taking into account any other water molecules in an explicit way. However, mobile water molecules that should exist inside protein structures are modelled implicitly by this procedure, since it considers empty cavities inside the protein as high dielectric zones containing solvent. Despite the fact that several studies (see for instance Young *et al.*, 2007; Qvist *et al.*, 2008; Berne *et al.*, 2009; Young *et al.*, 2010) document the existence of hydrophobic cavities inside proteins, which are devoid of water and are, therefore, not correctly treated by this procedure, no such cavities exist inside CotA near the two active sites. The closest cavity in CotA, which can potentially display such characteristics, is almost 20Å away from the dioxygen binding site and more than 22Å from the T1 copper. Not considering water molecules here, and in other proton transfer processes, is a simplification, and clearly we cannot describe the whole proton transfer process. However, this is a necessary limitation of the present methodology, given the high energetic cost of deprotonating water molecules. For this reason, their deprotonation is transient in nature, and they may act through a Grotthuss like mechanism (for a review, see Cukierman, 2006), being present in "proton wires".

Nevertheless, in long distance proton transfer, one usually finds protonatable groups that can form protonation intermediates in the "proton wire", allowing protons to be transferred in smaller steps. The aim here is to identify these protonatable groups that were likely to be involved in the process of proton transfer, necessary for the reduction of molecular oxygen to water. These groups are probably located close to the trinuclear centre in order to transfer protons to the intermediate oxygen species formed along the mechanism (see Figure 27). Analysis of the protonation equilibrium simulations evidenced that the only group actively titrating around pH 7, near the zone of interest, is Glu498, an acidic group present in the dioxygen entrance channel in CotA laccase. The pH titration of Glu498 obtained for all the available structurally characterised states of the trinuclear centre of CotA is presented in Figure 28 and will be discussed in the following paragraph. In view of the limitations of this type of simulations (which can have root mean square deviations below 1 pK units (Teixeira *et al.*, 2005)), the rationalisation of the results should consider pH ranges, rather than exact values of pH. Additionally, what we aim at analysing is the difference between the different redox and ligand binding states of the protein, which should be less prone to the errors described above; therefore we will concentrate on analysing differential behaviour mostly.

Starting from the fully functional enzyme with dioxygen between the T3 copper ions (see Figure 27a); holo-CotA), the simulations show that the protonation of Glu498 is negligible around pH 7. This situation changes dramatically for the peroxide adduct, which corresponds to a 2 electron reduced species of the previous state (Figure 27b); CotA-H_2O_2 (Bento *et al.*, 2005)): Glu498 increases its protonation by a large degree, showing a considerable protonated fraction around pH 7. The next two states in the

mechanism in Figure 27 (27c) and 27d)) have not been structurally characterised in CotA, and therefore we could not perform calculations on them. The state in Figure 27c) is observed if more electrons and protons (possibly coming from Glu498) are delivered to the trinuclear centre, resulting in the native intermediate that contains two hydroxyl groups; this is observed in the laccase structure from *T. hirsuta* (Figure 27c)) (Polyakov *et al.*, 2009). Upon further structural rearrangements another configuration for these two hydroxyl groups is reached; this is the state observed in the ascorbate oxidase structure (Figure 27d)) (Messerschmidt *et al.*, 1992). The next state in the mechanism could be structurally characterised in CotA and it is a state that results from a release, upon protonation, of one of the hydroxyl groups as water; this is the structure of apoCu(I) (Figure 27e)) determined in this work. Calculations using this structure show that the pH titration curve of Glu498 does not evidence a very marked protonation around pH 7, but a higher affinity for protons is observed instead, when compared with the dioxygen bound structure. Upon further protonation of this hydroxyl moiety (hypothetically by protons coming from Glu498), its release as a water molecule, and the entrance of another dioxygen molecule, the holoCotA structure is restored, closing the cycle. The fully reduced structure (Figure 27f); CotA-red) (Bento *et al.*, 2005), has Glu498 predominantly protonated.

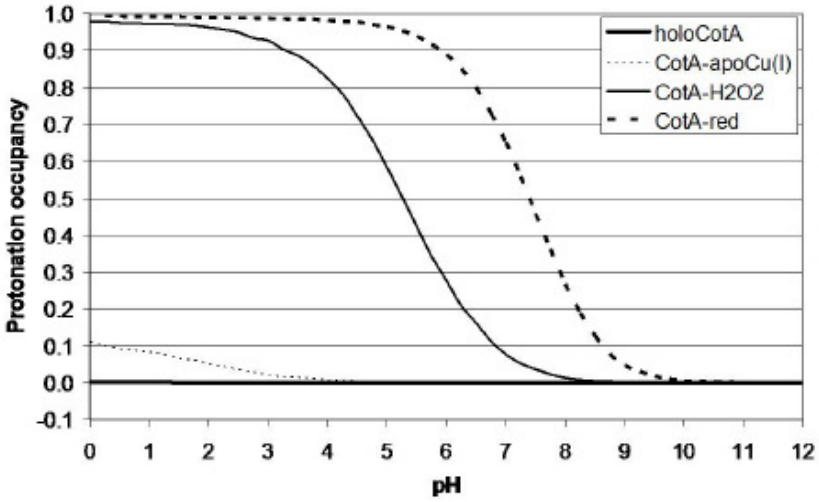

Figure 28 - Simulated pH titrations of Glu498 for the different CotA trinuclear centre states described in Figure 27. The state of T1 is set to oxidised for the dioxygen, hydroxyl and peroxide structures, and set to reduced for the reduced structure.

The simulation results reported above, and shown in Figure 28, clearly suggest that, irrespectively of details, the protonation of Glu498 is sensitive to the redox and liganted state of the trinuclear centre. Thus, being the only group in the vicinity of this centre to exhibit these characteristics, it is likely to play a proton transfer role for the reduction of oxygen to water. Additionally, its long redox titration curves, spanning almost 4 pH units in the cases of CotA-H_2O_2 and CotA-red (Figure 28), clearly show that its binding fluctuations (that are maximum in the zone of active titration (Baptista *et al.*, 1999) can be used for the deliverance of protons to the reaction, in a rather flexible way. Several reports describing mutants of other negatively charged residues in the oxygen access channel, namely in Fet3p (Glu487) (Augustine *et al.*, 2007) and CueO (Glu506, homologous to Glu498 in CotA) (Kataoka *et al.*, 2009), point to a role of these residues in the catalysis of oxygen reduction, a fact interpreted by the authors as their involvement in proton donation. DFT calculations

(Yoon *et al.*, 2007) have also been used in trinuclear centre models to highlight the potential effect of this residue in proton transfer along the mechanism. Therefore, the data that is presented here further corroborates these findings.

In laccases, the exit channel for water molecules also contains, at least, one acidic residue, Asp116 in CotA (Figure 24c)), in close proximity to the T2 copper centre. The equivalent residue in Fet3p (Asp94) (Augustine *et al.*, 2007) and in CueO (Asp112) (Ueki *et al.*, 2006; Kataoka *et al.*, 2009) has undergone mutation studies and been subject to DFT calculations (Yoon *et al.*, 2007). These studies have demonstrated the importance of such a residue for the mechanism of oxygen reduction in multi-copper oxidases. In some of these reports (Ueki *et al.*, 2006; Augustine *et al.*, 2007; Yoon *et al.*, 2007), it is suggested that this residue is involved in proton transfer. However, the present calculations on CotA shows that this group is not proton active around pH 7 in any of the states analysed; in fact, it is mostly charged in all the pH range considered (see Figure 29).

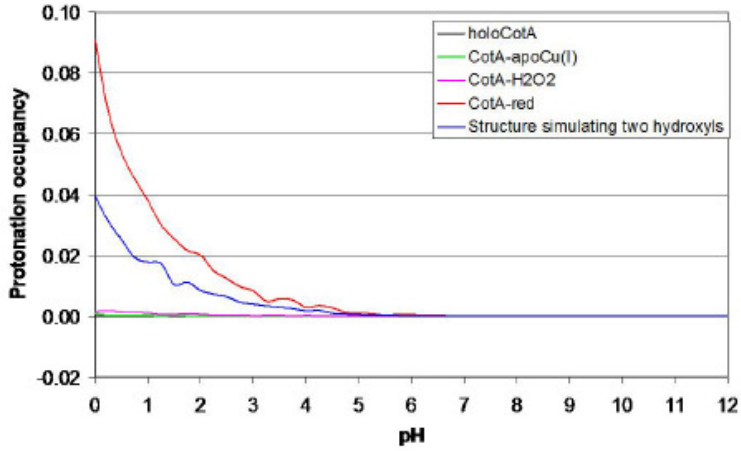

Figure 29 - Simulated pH titrations of Asp116 for the different CotA trinuclear centre states described in Figure 27. The state of T1 is set to oxidised for the dioxygen, hydroxyl, double hydroxyl and peroxide structures, and set to reduced for the reduced structure. Note that the maximum of the scale is one tenth of the maximum used for the other plots.

Given its proximity, this residue could become protonated when a hydroxyl group is bound to the T2 copper ion (the situation evidenced in ascorbate oxidase, Figure 27). We have not yet characterised this state in CotA, but we did perform test calculations on the apoCu(I) conformation by decreasing the overall charge of the T2 Cu bound water molecule by one charge unit (an exaggerated situation to simulate a hydroxyl group). These calculations (Figure 29, blue line), despite showing an increased protonation pattern of this acid, did not show an increase in the protonation of Asp116 to values that would make it proton-active around pH 7, further suggesting that this group is unlikely to be involved in proton transfer mechanisms. A possible explanation for its reported relevance in the activity of laccases, may be related with the role of this aspartate in maintaining a proper structural arrangement of the trinuclear centre, by being hydrogen bonded to His424 and His105, which coordinate one of the T3 and the T2 coppers, respectively (see Figure 24c)). The requirement for a charged residue at this position is suggested by the mutants made on Fet3p (Augustine *et al.*, 2007) and CueO (Ueki *et al.*, 2006; Kataoka *et al.*, 2009), which show that its mutation to glutamate results in the smaller perturbation in activity, whereas its mutation to alanine or to asparagine results in a drastic decrease of the enzyme activity.

One could argue that the results presented here, by having been done with one particular enzyme of the bacterial multi-copper oxidase family - CotA laccase - may be specific for this particular enzyme. Namely, one could raise the possibility that the residues equivalent to Glu498 and Asp116 in other multi-copper oxidases, which have been subjected to site-directed mutagenesis, may behave differently. In order to investigate this, we set up test calculations using the structure of the multi-copper oxidase CueO from *E. coli* (Roberts *et al.*, 2002). Given that the only structurally

characterised state in this multi-copper oxidase is the oxidised, hydroxyl bridged T3 state (corresponding to apoCu(I) state of CotA), we had to setup mimics for the two hydroxyl state (another hydroxyl bound to T2) and for the fully reduced state. These studies evidence (results not shown) that Glu506, similar to its equivalent Glu498 in CotA, is very sensitive to the redox and liganted states of the trinuclear centre, being mostly deprotonated in the oxidised, hydroxyl bridged T3 state (at around pH 7), but becoming mostly protonated in the fully reduced state (similar to the behaviour of Glu498 in Figure 28). On the other hand, the behaviour of Asp112 is also similar to its equivalent Asp116 in CotA, being mostly deprotonated in the whole of the pH range investigated, in all three states studied (results not shown). Therefore, these studies strongly suggest that the reported behaviour that we found in CotA laccase is probably general for other bacterial multi-copper oxidases.

Electron-proton coupling is at the core of many redox enzyme mechanisms, and it is possible that multi-copper oxidases are no exception. The methodology applied here was early developed to consider these effects in a complete way (Baptista *et al.*, 1999; Teixeira *et al.*, 2002). Despite the fact that the complete interplay between the two redox centres and protonatable groups cannot be studied, at this time, in an exact way, the coupling between the redox state of T1 and the protonation of any protonatable group is amenable to be analysed by our simulations. These clearly show that the titration of Glu498 depends on the redox state of T1. As an example, Figure 30 shows the effect of the reduction of this centre alone on the titration of Glu498 in the peroxide adduct structure (CotA-H_2O_2). The pK_a of this group increases by 1.4 pH units, from 5.3 to 6.7, evidencing the influence of the redox state of T1 on its protonation. On the other hand, the different redox and bridging

moieties of the trinuclear centre (which can include protonation changes of Glu498) also show an influence on the redox affinity of the T1 centre, as shown in the redox titrations (at pH 7) of the T1 centre performed in the different structurally characterised states of the trinuclear centre (Figure 31).

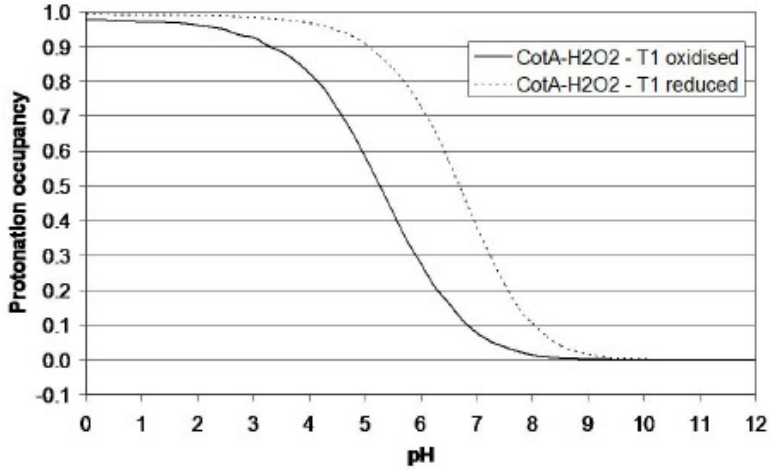

Figure 30 - Simulated pH titrations of Glu 498 for the CotA-H_2O_2 state upon changes on the redox state of centre T1.

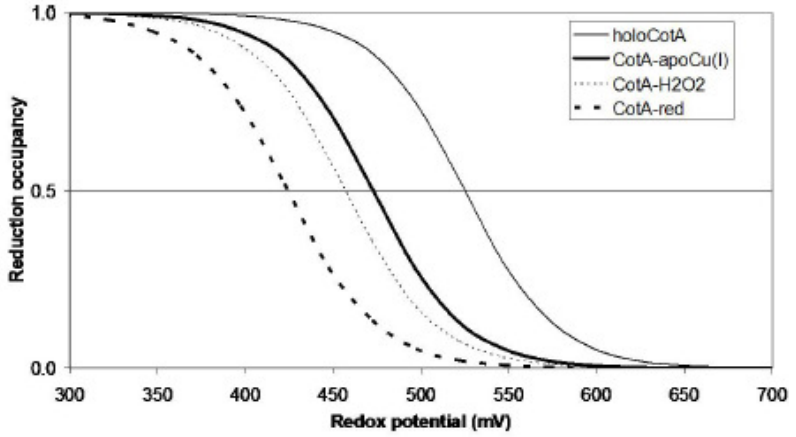

Figure 31 - Simulated redox titrations at pH 7 of the T1 site for the different CotA trinuclear centre states described in Figure 27. The redox potentials for each of the situations are 525 mV for the structure with dioxygen (which was set, see text), 473 mV for the structure with hydroxyl, 457 mV for the structure with peroxide, and 424 mV for the reduced structure.

Although the simulated situations correspond to "pure" states, that may not have direct experimental counterparts (given that the reduction of the protein may occur in the two copper centres at the same time), these results are illustrative of the interplay between the redox states of the two centres. The redox potential of T1 has a span of 100 mV in the situations analysed, and it decreases with higher reduction of the trinuclear centre and bound entities. This data can be compared to experimental data obtained previously for CotA (comparing the holo-CotA and apoCu(I)). Experimentally it was found (Durão *et al.*, 2008a) that the redox potential of apoCu(I) (found here with a hydroxyl ion at the trinuclear centre) was 498 mV versus 525 mV for the holoCotA (found here with a dioxygen moiety in the trinuclear centre). The present simulations also show a decrease, from 525 mV for holoCotA (value set) to 473 mV for apoCu(I), even if this decrease is larger than that experimentally observed. However, it must be stressed again that the experimental and simulated situations may not correspond to the same exact process. Nevertheless, and irrespectively of the actual value of the calculated redox potential, which is prone to considerable error in the present simulations (for instance, it is highly dependent on the value of the internal dielectric constant used (Teixeira *et al.*, 2005)), the present simulations show the same trend, and this is the important conclusion to be retained here. These observations show how the coupling between the T1 and trinuclear centres is important in the mechanism of laccases.

The present work suggests the importance of Glu498 in the proton transfer mechanisms operating at the trinuclear centre and its vicinity. However, it should be remembered that this acidic group is not conserved in all laccases, although it is found, to our knowledge, in the same position in all the prokaryotic laccases that have been structurally characterised. In

structurally characterised eukaryotic laccases, no acidic residue is found in this exact position, but an acid is always observed in the oxygen access channel (some examples can be found in the Figure 27 containing the mechanism), suggesting a similar role for this group. As stated before, mutations were made (Augustine *et al.*, 2007) on one of these acidic groups on the eukaryotic multi-copper oxidase Fet3p (Glu487, equivalent to Glu510 in ascorbate oxidase; Figure 27d)), showing its importance in the mechanism; additionally, the authors suggested its role in proton transfer. It is foreseeable that equivalent acidic groups, or other acidic groups in the oxygen access channel of other multi-copper oxidases, play a similar role. Nevertheless, the available structural characterisation of multi-copper oxidases evidences (results not shown) that the distance between these acidic groups and the trinuclear centre is larger in eukaryotic than in prokaryotic enzymes. This difference may have some consequences in the details of the proton transfer mechanism, but the overall reported importance of these acid groups corroborates the hypothesis that they are responsible for the proton transfer mechanisms in multi-copper oxidases.

The identification of Glu498 as involved in proton transfer, should not rule out other residues in the vicinity of the trinuclear centre that may be important. One should not forget that our calculations address the thermodynamics of proton transfer, and their redox coupling, not considering the other component of this process, which is proton transfer kinetics that is much more complex to model (see for example, Olsson *et al.*, 2007; Olsson and Warshel, 2006). Therefore, there may be other important groups in this kinetic process that have not been identified yet, despite the fact that no clear-cut experimental evidence has been provided so far. Nevertheless, the influence on the mechanism evidenced by

mutational and other studies of Asp116 (CotA numbering) in Fet3p (Augustine *et al.*, 2007; Yoon *et al.*, 2007) and in CueO (Ueki *et al.*, 2006; Kataoka *et al.*, 2009) may suggest such a role.

The differences in structurally characterised resting states observed for different laccases may result from the molecular details in the vicinity of trinuclear site. In addition to being observed in the CotA laccase (Bento *et al.*, 2005), the dioxygen entity is only observed in the eukaryotic laccase from *Melanocarpus albomyces* (Hakulinen *et al.*, 2002). However, in this latter case, the structure has a Cl^- anion bound to the T2 copper ion, instead of a water or hydroxyl group, as observed in other laccases. It is tempting to speculate that the proximity of Glu498, or equivalent groups, to the trinuclear centre in prokaryotic laccases (and to the dioxygen molecule itself) can be a factor for the stability of the dioxygen state, but other factors may exist. One example of the sensitivity of the trinuclear centre to the effects of its surroundings is the influence of the acidic group equivalent to Asp116 in CotA (Figure 29) on the calculated differential stability of different conformations of the peroxyl intermediate (Yoon *et al.*, 2007). In fact, the trinuclear centre in multi-copper oxidases seems to be fine tuned to achieve proper catalysis, as evidenced by a recent study focused on T3 copper sites (Yoon *et al.*, 2009). Further studies are clearly needed to further characterise this phenomenon.

4.1.5 Conclusions

In summary, these studies clearly indicate that in the CotA laccase, Glu498 in the entrance channel for the dioxygen moiety plays a role in channelling protons during the reduction process. They also show that the observation of a shoulder at 330 nm in the absorption spectrum, due to the antiferromagnetic coupling of the T3 copper ions, is present when the

bridging species is either a hydroxyl or a dioxygen moiety. The results also strongly support the mechanism of dioxygen reduction as indicated in Figure 27. However, one key stage that requires further study is the mechanism by which the hydroxyl or water molecules produced by the reaction migrate past the T2 copper ion, before leaving the enzyme through the exit channel.

Recently, after the submission of this work, we made mutants of Glu498 in CotA, which show severe catalytic impairment when this group is substituted by threonine or leucine (Chen *et al.*, 2010). Substitution by an aspartate renders an enzyme with 10% catalytic activity. These results are totally consistent with the results presented here, evidencing the need for an acidic residue at this structural position.

4.1.6 Acknowledgements

António M. Baptista and Miguel Teixeira are gratefully acknowledged for helpful discussions. Maria Arménia Carrondo is gratefully acknowledged for support. This work was supported by project grants from Fundação para a Ciência e Tecnologia, Portugal (POCI/BIO/57083/2004) and from European Union (BIORENEW - FP6-2004-NMP-NI-4/026456). C.S. Silva holds a Ph.D (SFRH/BD/40586/2007) fellowship and Z. Chen holds a Post-doc fellowship (SFRH/BBD/27104/2006) from Fundação para a Ciência e a Tecnologia, Portugal. The provision of synchrotron radiation facilities and the assistance of the macromolecular crystallography staff are sincerely acknowledged at the European Synchrotron Radiation Facility in Grenoble, France.

4.1.7 Supplementary material

Table S2 - $B_{factors}$ values (Å^2) for the different atoms in the trinuclear centre when different moieties were refined in between the two T3 coppers

HoloCotA/ Trinuclear Cu centre	Dioxygen refinement	Chloride refinement		Peroxide Refinement		Hydroxyl refinement	
	B_{factor} (Å^2)		B_{factor} (Å^2)		B_{factor} (Å^2)		B_{factor} (Å^2)
T1	17.1		16.7		16.9		16.7
T2	18.0		17.4		18.0		17.4
T3 (Cu2/Cu3)	15.0/16.1		14.6/16.0		14.8/16.4		14.6/16.1
O2 (O1/O2)	16.9/16.6	Cl	25.1	PER (O1/O2)	16.7/20.0	OH	11.4

CHAPTER 4.2

THE ROLE OF GLU498 IN THE DIOXYGEN REACTIVITY OF CoTA LACCASE FROM *BACILLUS SUBTILIS*

This chapter was published in the following refereed paper:

Z. Chen, P. Durão, **C.S. Silva**, M.M. Pereira, S. Todorovic, P. Hildebrandt, I. Bento, P.F. Lindley and L.O. Martins, "The role of Glu^{498} in the dioxygen reactivity of CotA-laccase from *Bacillus subtilis*", **Dalton Trans.** (2010) **39**(11): 2875-2882.

The construction of the plasmids, expression, purification and biochemical studies were performed by Z. Chen and P. Durão. The EPR and RR measurements were performed by M.M. Pereira and S. Todorovic, respectively. Catarina S. Silva performed the crystallisation experiments and has been involved in the X-ray structural characterization.

4.2.1 Summary

The multi-copper oxidases couple the one-electron oxidation of four substrate molecules to the four electron reductive cleavage of the O–O bond of dioxygen. This reduction takes place at the trinuclear copper centre of the enzyme and the dioxygen approaches this centre through an entrance channel. In this channel, an acidic residue plays a key role in steering the dioxygen to the trinuclear copper site, providing protons for the catalytic reaction and giving overall stability to this site. In this study, the role of the Glu498 residue, located within the entrance channel to the trinuclear copper centre, has been investigated in the binding and reduction of dioxygen by the CotA laccase from *Bacillus subtilis*. The absence of an acidic group at the 498 residue, as in the E498T and E498L mutants, results in a severe catalytic impairment, higher than 99%, for the phenolic and non-phenolic substrates tested. The replacement of this glutamate by aspartate leads to an activity that is around 10% relative to that of the wild-type. Furthermore, while this latter mutant shows a similar K_m value for dioxygen, the E498T and E498L mutants show a decreased affinity, when compared to the wild-type. X-ray structural and spectroscopic analysis (UV/visible, electron paramagnetic resonance and resonance Raman) reveal perturbations of the structural properties of the catalytic centres in the Glu498 mutants when compared to the wild-type protein. Overall, the results strongly suggest that Glu498 plays a key role in the protonation events that occur at the trinuclear centre and in its stabilization, controlling therefore the binding of dioxygen and its further reduction.

4.2.2 Introduction

CotA laccase is a structural component of the outer layer of the spore coat from *Bacillus subtilis*, (Martins *et al.*, 2002) and is thought to be involved in the synthesis of the brown pigment that protects the spore against UV light. Similarly to all the members of the multi-copper oxidase (MCO) family, it is able to couple one-electron oxidation of four substrate equivalents with the four-electron reduction of dioxygen to water (Lindley, 2001; Messerschmidt, 1997; Solomon *et al.*, 1996; Stoj and Kosman, 2005). The catalytic motif in these enzymes includes three distinct copper centres (Malmstrom, 1982). Type 1 (T1) Cu is characterized by an intense $S(\pi)\rightarrow Cu(d_{x^2-y^2})$ charge transfer (CT) absorption band at around 600 nm, responsible for the intense blue colour of these enzymes, and a narrow parallel hyperfine splitting [$A_{\parallel}$ = (43–90) x 10^{-4} cm^{-1}] in the electron paramagnetic resonance (EPR) spectra. This is the site of substrate oxidation and in this respect the MCO family can be separated into two classes; enzymes that oxidise small organic substrates with high efficiency and those that oxidise metal ion substrates (Stoj and Kosman, 2005). The trinuclear centre, where dioxygen is reduced to water, comprises two type 3 (T3) and one type 2 (T2) copper ions. The two T3 Cu ions, which are usually antiferromagnetically coupled through a bridging ligand and therefore EPR silent, show a characteristic absorption band at 330 nm. The T2 Cu site lacks strong absorption bands and exhibits a large parallel hyperfine splitting in the EPR spectra [$A_{\parallel}$ = (150–201) x 10^{-4} cm^{-1}].

CotA laccase has the dual advantage that it is both thermostable and thermoactive and is able to oxidise a variety of substrates including non-phenolic and phenolic compounds, and also a range of synthetic azo and anthraquinonic dyes, thus having a potential use for diverse

biotechnological applications (Pereira *et al.*, 2009a and 2009b; Xu, 1999). Several structure–function relationship studies have been performed with this enzyme (Bento *et al.*, 2005; Durão *et al.*, 2006 and 2008b; Enguita *et al.*, 2004). These revealed redox properties of the T1 copper site and gave structural insights into the principal stages of the mechanism of dioxygen reduction at the trinuclear centre. Studies on the reduced and oxidised forms of the enzyme and in the presence of peroxide and the inhibitor, azide, gave significant structural insights into the principal stages of the mechanism of dioxygen reduction (Bento *et al.*, 2005). Thus, after diffusing through the solvent channel leading to the trinuclear centre, the dioxygen binds to the centre so that it is sited approximately symmetrically between the two type 3 copper ions with one oxygen atom close to the type 2 copper ion. Further stages involve the formation of a peroxide intermediate in which the O–O axis is inclined by some 51º to the vector linking the two type 3 copper ions and following the splitting of this intermediate, the migration of the hydroxide moieties towards the solvent exit channel. The migration steps are likely to involve a significant movement of the type 2 copper ion and its environment. In order to convert dioxygen to two molecules of water, four protons are required in addition to the four electrons obtained from four individual substrate molecules. Careful comparison of crystal structures shows that MCOs have, with very rare exceptions, conserved negatively charged residues close to the trinuclear site, a glutamate or an aspartate within the entry channel for dioxygen, and an aspartate in the exit channels of the trinuclear centre (Bento *et al.*, 2005; Hakulinen *et al.*, 2008; Bento *et al.*, 2007; Ducros *et al.*, 1998; Ferraroni *et al.*, 2007; Garavaglia *et al.*, 2004; Li *et al.*, 2007; Lyashenko *et al.*, 2006a; Messerschmidt *et al.*, 1992; Piontek *et al.*, 2002; Taylor *et al.*, 2005). These residues may facilitate binding of

dioxygen and supply of protons to the reaction intermediate as suggested by mutagenesis studies performed with CueO from *Escherichia coli* and yeast Fet3p metallo-oxidases (Augustine *et al.*, 2007; Kataoka *et al.*, 2005 and 2009; Quintanar *et al.*, 2005). It has already been suggested that Glu498 (Figure 32) plays a crucial role in providing protons for the reduction of dioxygen in the bacterial laccase CotA (Bento *et al.*, 2005) and further studies involving both structural and modelling data (Bento *et al.*, 2010) have added strength to this proposition. In order to explore these putative roles in CotA laccase, site-directed mutagenesis has been employed to produce the mutants E498D, E498T and E498L. This is the first study that combines structural, spectroscopic and biochemical data in a (bacterial) laccase, and is complementary to what has been previously undertaken with the metallo-oxidases CueO and Fet3p.

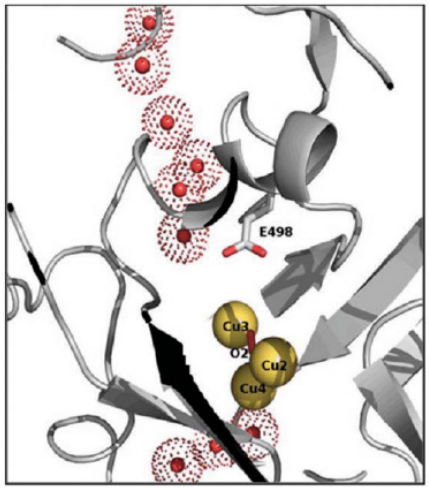

Figure 32 - Structural detail of the trinuclear Cu site in the native CotA laccase showing the Glu498 residue that forms a hydrogen bond with a water molecule in the access solvent channel to the trinuclear centre that in turn is hydrogen bonded to dioxygen.

4.2.3 Materials and Methods

Construction of CotA mutants

Single amino acid substitutions in the trinuclear centre were created using the QuikChange site-directed mutagenesis kit (Stratagene). Plasmid pLOM10 (containing the wild-type cotA sequence) was used as a template (Martins *et al.*, 2002) and the primers forward 5'-TGCCATATTCTAGAG CATTTAGACTATGACATG-3' and reverse 5'-CATGTCATAGTC TAAATGCTCTAGAATATGGCA-3' were used to generate the E498L mutant. The primers forward 5'-TGCCATATTCTAGAGCATACAGAC TATG-3' and reverse 5'-CATAGTCTGTATGCTCTAGAATATGGC A-3' were used to generate the E498T mutation. Finally, the primers forward 5'-TGCCATATTCTAGAGCATGATGACTATG-3' and reverse 5'-CATAGTCATCATGCTCTAGAATATGGCA-3' were used to generate the E498D mutant. The presence of the desired mutations in the resulting plasmids (pLOM53 (carrying the E498L point mutation), pLOM54 (bearing the E498T point mutation), and pLOM56 (with the E498D mutation) and the absence of unwanted mutations in other regions of the insert were confirmed by DNA sequence analysis. Plasmids pLOM53, pLOM54 and pLOM56 were transformed into *E. coli* Tuner (DE3) strains (Novagen) to obtain strains LOM408, LOM413 and LOM417, respectively.

Overproduction and purification

Strains AH3517 (containing pLOM10), LOM408, LOM413 and LOM417 were grown in Luria–Bertani medium supplemented with ampicillin (100 $\mu g\ mL^{-1}$) at 30 ºC. Growth was performed as described by Durão *et al.* (Durão *et al.*, 2008a), according to the optimized protocol to

yield a protein population fully loaded with copper. Cell harvesting and disruption and subsequent purification of proteins by using a two-step protocol procedure were performed as previously described (Martins *et al.*, 2002; Bento *et al.*, 2005). Purified enzymes were stored at -20 ºC until use.

UV/visible, EPR and RR spectroscopy

UV/visible spectra were acquired using a Nicolet Evolution 300 spectrophotometer from Thermo Industries. EPR spectra (100 to 160 μM protein contents) were measured with a Bruker EMX spectrometer equipped with an Oxford Instruments ESR-900 continuous-flow helium cryostat, with a microwave frequency of 9.39 GHz, power of 2.0 mW and modulation amplitude of 0.9mT. The spectra obtained under non-saturating conditions were theoretically simulated using the Aasa and Väangard approach (Aasa and Vaangard, 1975). RR spectra of 1 mM CotA wild-type, 2 mM E498T, 1.5 mM E498D and 0.8mM E498L mutants (in 20 mM Tris buffer, pH7.6) were measured as described before, (Durão *et al.*, 2008b) with 568 nm excitation, at -190 ºC.

Redox titrations and enzyme assays

Redox titrations were performed at 25 ºC in 20 mM Tris- HCl buffer pH 7.6 containing 0.2 mM NaCl under an argon atmosphere, and were monitored by visible spectroscopy (300-900 nm), using a Shimadzu Multispec-1501 spectrophotometer, as previously described by Durão *et al.* (Durão *et al.*, 2006). The laccase-catalysed oxidation of ABTS (pH 4) and 2,6-dimethoxyphenol (2,6-DMP, pH 7) were photometrically monitored at 37 ºC, in air saturated conditions by using the methods described by Durão *et al.* (Durão *et al.*, 2006). The optimum pH value for the oxidation of both substrates is in the case of E498L and E498D

similar to the wild-type, while the E498T mutant displays a 1.6 unit decrease in optimal pH for the oxidation of 2,6-DMP. Activities were also performed following the rate of oxygen consumption varying the concentrations of dioxygen at a fixed concentration of the reducing substrates (ABTS or 2,6-DMP) by using an oxygen electrode (Oxygraph; Hansatech, Cambridge UK). Stock solutions of 10 mM of ABTS (pH 4) and 50 mM 2,6-DMP (pH 7 or pH 5.6) were prepared in Britton-Robinson buffer. The oxygen electrode was calibrated at 37 ºC using buffer saturated with air and buffer deoxygenated with sodium dithionite. The initial concentration of dioxygen in solution was controlled by flushing the reaction vessel with a mixture of nitrogen and oxygen with the aid of two flow meters. All the reactions were corrected for background autoxidation. The kinetic constants K_m and k_{cat} were determined using the Michaelis–Menten model (Origin-Lab, Northampton, MA, USA). All enzymatic assays were performed at least in triplicate. The protein concentration was measured by using the absorption band at 280 nm (ε_{280} = 84,739 M^{-1} cm^{-1}) or the Bradford assay using bovine serum albumin as a standard (Bradford, 1976).

Azide inhibition

Enzymes were incubated with sodium azide (0 to 100 mM, final concentration) for different periods of time (0, 30, 60, 120 min) followed by activity measurements towards ABTS oxidation (1mM) with wild-type (0.0001 mg ml^{-1}) and mutant enzymes (0.02 to 2 mg ml^{-1}) in Britton-Robinson buffer at the optimum pH value.

Crystallisation

Crystals of the CotA mutant proteins were obtained by the vapour diffusion method, at room temperature, from crystallisation media containing 8–10% of PEG 4 K, 26–30% of isopropanol and 0.1M of sodium citrate pH 5.5. The crystals were harvested and cryofrozen with a solution that contained the crystallisation medium plus 22% of ethylene glycol.

X-ray data collection and refinement

X-ray diffraction data were collected at 100 K using the macromolecular crystallography beam lines as indicated in Table 14, at the European Synchrotron Radiation Facility at Grenoble, France.

Table 14 - X-ray data collection[a].

	E498D	E498T	E498L
Beam line at ESRF	ID23-2	ID14-1	ID14-1
Wavelength/Å	0.8726	0.934	0.934
Detector distance/mm	223.2	193.3	162.0
Resolution/Å	2.1	2.0	1.7
Space group	$P3_12_1$	$P3_12_1$	$P3_12_1$
Cell parameters/Å, *a*	101.83	101.90	101.57
c	136.57	136.93	136.29
Mosaicity (°)	0.85	0.66	0.50
Oscillation angle (°)	1.0	0.5	1.0
Oscillation range (°)	65	60	60
No. of unique *hkl*	48362 (7000)	55879 (8055)	89089 (12978)
Completeness (%)	99.9 (100.0)	99.6 (99.7)	99.5 (100.0)
$I/\sigma(I)$	6.6 (2.0)	9.2 (2.2)	10.4 (2.4)
R_{symm}	0.083 (0.37)	0.069 (0.348)	0.053 (0.321)
Multiplicity	4.0 (4.0)	5.1 (3.6)	5.5 (4.6)

[a] Values in parentheses refer to the highest resolution shells as follows; E498D (2.21–2.10 Å); E498T (2.11–2.00 Å); E498L (1.79–1.70 Å).

Data sets were processed and scaled using MOSFLM (Leslie, 2006) and SCALA from the CCP4 program suite (CCP4, 1994). The structure solution for each CotA mutant was found by the molecular replacement method, using the MOLREP program (Vagin and Teplyakov, 1997). The structure of CotA (PDB code: 1W6L) (Bento *et al.*, 2005) from which all the copper atoms and solvent molecules were removed served as a search model. For each mutant a unique solution was determined; typical *R*-factors and scores were 0.40 and 0.74 respectively. Refinement was performed using the maximum likelihood functions in the REFMAC program (Murshudov *et al.*, 1997), while model building and improvement were achieved with COOT (Emsley and Cowtan, 2004). Solvent molecules were positioned after a few cycles of refinement as well as several molecules of ethylene glycol. Isotropic refinement of the atomic displacement parameter was performed for all atoms. The occupancies of the copper ions were adjusted so that their isotropic thermal vibration parameters refined approximately to those observed for the neighbouring atoms. The careful use of omit and standard difference Fourier syntheses, as well as monitoring of thermal vibration coefficients during refinement, enabled the identification of a diatomic species placed in between the type 3 copper sites in all three mutants. These species were assumed to be a dioxygen type species and refinement proceeded constraining the O–O distances to target values of 1.207 Å . Similarly to what has been observed for the native fully loaded CotA, additional electron density was observed close to the Cys35 and this was modelled as an oxidised cysteine residue in two of the three mutants. In the E498T mutant two alternate conformations were modelled for the side chain of the Oxy-Cys35, whereas in the E498L mutant a mixture of Oxy-Cys and Cys was modelled according to the electron density map. In the E498D mutant no

alteration was observed and a cysteine side-chain was modelled in two alternate positions. As observed in the other crystal structures of CotA, the loop comprising residues 89 to 97 was poorly defined in the electron density maps in all three mutants and was not modelled. The final statistics of the refinement procedure are listed in Table S3.

4.2.4 Results

Kinetic characterization of mutant enzymes

Site-directed replacement of Glu498 by leucine, threonine or aspartate resulted in enzymes that show the same chromatographic pattern during purification when compared to the wild-type CotA laccase. Metal analysis indicated that all "as isolated" proteins contained around 4 moles of copper ions per mol of protein (with an associated 15% error, Table S4). Two reducing substrates, one non-phenolic (ABTS) and one phenolic (2,6-DMP), were used to identify specific changes in the catalytic properties of the studied mutant proteins. A comparison of the catalytic activities at the optimum pH shows that mutations in the Glu498 residue result in a lower catalytic efficiency when compared with the wild-type CotA (Table 15). Mutant E498L is the most affected in this respect showing virtually no enzymatic activity, with 3 to 4-orders of magnitude decreased efficiency (k_{cat}/K_m). The E498T mutant shows 2 to 3-orders of magnitude lower efficiency in relation to the wild-type. On the other hand, the E498D mutant shows catalytic efficiency closest to that of the wild-type strain, with a decrease between 10 and 45 times, depending on the substrate. Considering that only half of the E498D protein population has a fully loaded T1 site (see below), efficiency could be calculated as only 5 to 23 times lower than that of the wild-type.

Table 15 - Apparent steady-state kinetic constants for ABTS and 2,6-DMP by the CotA proteins measured at saturating concentrations of O^2.

	ABTS			2,6-DMP		
CotA	K_m/μM	k_{cat}/s^{-1}	k_{cat} /K_m/s^{-1}μM^{-1}	K_m/μM	k_{cat}/s^{-1}	k_{cat} /K_m/s^{-1}μM^{-1}
Wild type	110 ± 14	251 ± 30	2.3	227 ± 41	36 ± 5	0.16
E498D	61 ± 28	16 ± 2	2.6×10^{-1}	208 ± 46	1.3 ± 0.6	0.6×10^{-2}
E498T	120 ± 12	1.7 ± 0.6	1.4×10^{-2}	137 ± 28	0.05 ± 0.03	0.4×10^{-3}
E498L	106 ± 10	0.09 ± 0.03	0.6×10^{-3}	180 ± 4	0.006 ± 0.004	0.3×10^{-4}

Table 16 - $K_{m\ app}(O_2)$ of wild-type and mutants measured with 1 mM of ABTS and I_{50} after a 30 min incubation period with sodium azide (similar values were obtained after 60 and 120 min of incubation).

CotA	$K_{m\ app}(O_2)$/μM	Azide I_{50}/mM
Wild type	25 ± 13	2.3 ± 0.0
E498D	19 ± 13	2.3 ± 0.0
E498T	58 ± 15	4.7 ± 0.2
E498L	92 ± 10	9.8 ± 0.1

Neither of the mutations resulted in major and consistent alterations of K_m for the tested substrates and thus lower efficiency values are mainly due to a decrease of k_{cat} values.

The Michaelis–Menten constants for dioxygen reactivity (K_m (O_2)) of wild-type and mutants at the optimal pH are shown in Table 16. The $K_m(O_2)$ value measured for the wild-type and the E498D mutant was similar and, at the same time close to the values reported for other laccases (Xu, 2001). The mutants E498T and E498L exhibited around 2 to 4-fold lower values, respectively, suggesting a different binding interaction with O_2 in the steady state. The use of ABTS or 2,6-DMP as the reducing substrate did not significantly affect the K_m (O_2) (data not shown). The k_{cat} (O_2) values are similar to the k_{cat} (ABTS) or k_{cat} (2,6-DMP) (Table 15), as anticipated for a steady state with efficient coupling of the two redox halves of the catalysis. The ability of the trinuclear cluster to bind molecular oxygen, and to retain its partially reduced forms during the catalytic cycle is reflected in the relatively high affinity of this site for a number of anions (Solomon *et al.*, 1996). Azide is one of the most studied laccase inhibitors and, in the CotA laccase crystal structure soaked with azide, this molecule bridges the type 3 copper ions (Bento *et al.*, 2005). The inhibition of CotA and Glu498 mutants was followed in the presence of increasing concentrations of sodium azide. Total inhibition was observed at a concentration of 80 mM sodium azide, after a pre incubation period of 30 min. For the wild-type enzyme and E498D mutant similar I_{50} values (concentration of inhibitor required for achieving 50% reduction of the activity) were measured, while the E498T and E498L mutants show 2 and 4-fold higher I_{50} values as compared with CotA laccase (Table 16).

Spectroscopic characterization of Glu498 mutants

The UV/visible absorption spectrum of wild-type CotA is dominated by two charge transfer (CT) bands; a intense band centred at 609 nm originating from the T1 site and a shoulder at 330 nm associated with the T3 site, both with ε values around 4000 M^{-1} cm^{-1} (Figure 33 and Table S4).

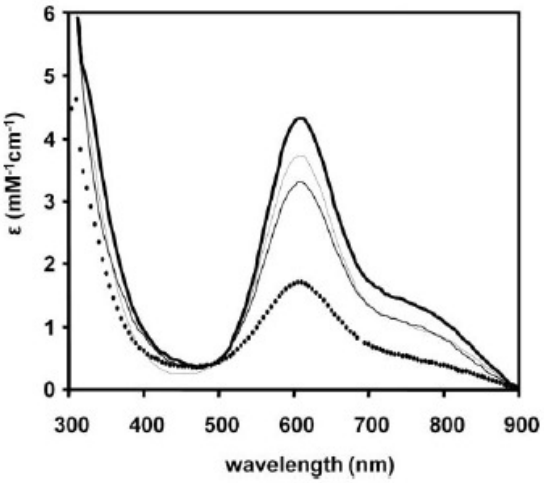

Figure 33 – UV/visible absorbance spectra of wild-type (thick line), **and CotA mutants: E498L** (semi-dotted line)**, E498T** (thin line) **and E498D** (dotted line). Proteins were treated with the oxidising agent potassium iridate.

All mutants in their as-isolated state appear to be partially reduced, as after treatment with potassium iridate an increase of intensity of both absorption bands was observed. Nevertheless, after the oxidation step, the maximal absorption intensity at 609 nm was lower than in the wild-type, by 55% for E498D, 27% for E498T and 10% for E498L, suggesting some T1 copper depletion in all mutant proteins. Mutants E498T and E498D seem to be fully reactive with dioxygen, since transition bands at 609 and 330 nm rapidly recover after exposure to air, from dithionite-reduced proteins, in a similar manner as observed for the wild-type enzyme. However, the mutant E498L remained in the reduced state even after

being exposed to the air for 24h, revealing highly impaired reactivity towards dioxygen.

The S(Cys)-Cu vibrational modes of the T1 site are selectively enhanced in RR spectra obtained by excitation into S(π)→Cu($d_{x^2-y^2}$) CT (Solomon *et al.*, 1996). The spectra of the wild-type, E498T and E498D mutants show several vibrational modes with stretching character centred at 400 cm^{-1}, with some subtle differences (Figure 34). The most intense band, which appears to have the greatest Cu–S(Cys) stretching character, is downshifted from 425 cm^{-1} to 417 cm^{-1} in the E498L mutant. However, the intensity weighted frequency of all stretching coordinates for all mutant proteins (409 cm^{-1}) is very similar to that of the wild-type (410 cm^{-1}), revealing an absence of substantial differences on the level of electronic configuration of the T1 site (Durão *et al.*, 2008b). Accordingly, all mutants present similar redox potentials of the T1 Cu site of the wild-type enzyme (around 525 mV, Table S4). Moreover, the signal to noise ratio is much lower in the spectrum of E498D, under the same experimental conditions and comparable protein concentration, indicating that this mutation decreased the stability of the T1 site.

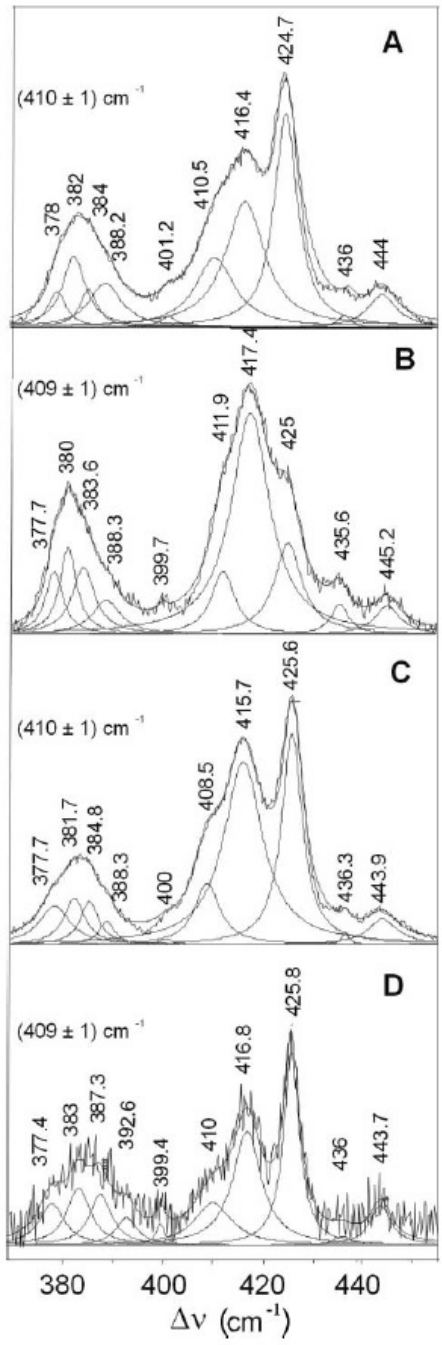

Figure 34 - Experimental and deconvoluted RR spectra of wild-type CotA (A), E498L (B), E498T (C) and E498D (D) mutants obtained with 568 nm excitation and 5 mW laser power at 77 K, accumulation time 40 s. The calculated intensity weighted frequencies are reported by the respective spectra.

The EPR spectra show strong similarities between wild-type CotA and E498L mutant, while the E498T and E498D mutants spectra show remarkable differences (Figure 35).

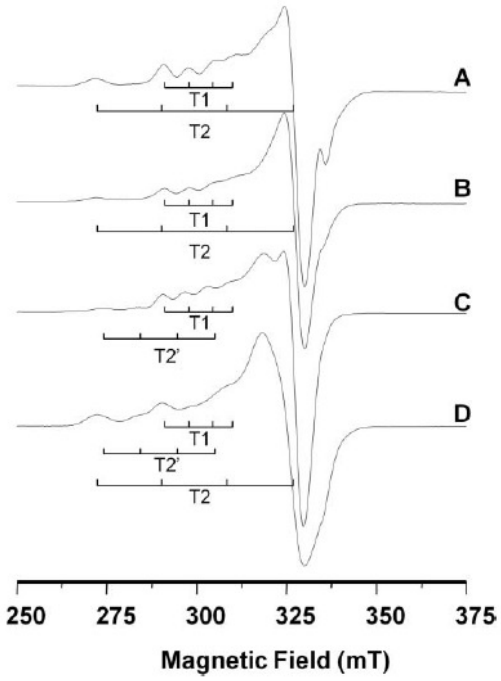

Figure 35 - EPR spectra of the wild-type (A), E498L (B), E498T (C) and E498D (D), obtained at 10 K and microwave frequency, 9.39 GHz; power, 2.0 mW; modulation amplitude: 0.9 mT. The spectra were simulated using the spin Hamiltonian parameters presented in Table 17.

Spectral deconvolution (data not shown) revealed that the copper T1 site in the latter mutants has the same conformation as in the wild-type protein, since it was simulated using the same spin Hamiltonian parameters (Table 17). However, for the E498D mutant, depletion in the T1 site has been observed as revealed by spectral integration, indicating that only half of the E498D population contains copper at this site. Nonetheless, the EPR spectra reveal the most striking differences between the mutants at the T2 copper site. In the case of E498T, the g_{max}

for this centre is higher than in the wild-type, while the hyperfine constant is lower, indicating that the copper T2 site in this mutant has a different conformation or experiences a different electronic vicinity (named the T2' form). Interestingly, both forms of the type 2 Cu, the one observed for the wild-type and E498L (T2) and that of E498T (T2'), are present in the E498D mutant. This protein spectrum can be simulated using the parameters of the T2 and T2' forms, integrated in a 1:1 ratio. A careful inspection of the EPR spectrum of the wild-type CotA reveals the presence of a very small signal identical to that assigned to the T2' form (Figure 35).

Table 17 - EPR parameters used in the simulation of wild-type and CotA mutants spectra.

CotA	Cu centres	Contribution	g_{min}	g_{med}	g_{max}	A_{max} (x 10^{-4} cm^{-1})
Wild type	T1	1	2.042	2.046	2.228	78
	T2	1	2.035	2.094	2.250	195
E498D	T1	0.5	2.042	2.047	2.230	78
	T2	1	2.035	2.094	2.245	210
	T2′	1	2.035	2.094	2.330	110
E498T	T1	1	2.042	2.046	2.235	75
	T2′	1	2.035	2.094	2.325	124
E498L	T1	1	2.042	2.046	2.225	78
	T2	1	2.035	2.090	2.250	190

Structural details of the mutant enzymes

The overall structure of the Glu498 mutant CotA proteins is essentially the same as the one obtained for the wild-type enzyme. Superposition of the backbones of each of the mutants onto the fully-copper loaded CotA structure (CCP4, 1994) gives root mean square deviations of only 0.131 Å, 0.124 Å and 0.131 Å for E498D, E498L and E498T mutants, respectively. The observed differences are located at the copper centres and in their neighbourhood. In the E498D mutant the orientation of the side chain of the mutated aspartate is different from the one observed for the native glutamate residue. In the native CotA laccase the glutamate is pointing towards the solvent channel, forming an H-bond with a water molecule that interacts with the dioxygen moiety found in between the two T3 copper ions (Figure 36A). In the E498D mutant, the aspartate points towards the interior of the protein having its $O^{\delta 1}$ atom at an H-bond distance from the $N^{\delta 1}$ atom of His491 (Figure 36B). In this mutant, the water molecule interacting with the dioxygen moiety in the native structure no longer exists. Moreover, all copper atoms in the trinuclear centre are fully occupied, as observed in the wild-type enzyme (Table S5). However, the occupancy of the T1 copper site in E498D is significantly less than one (0.7), corroborating the UV/Vis, RR and EPR data, although at first sight there appears to be no obvious structural reason for this finding. In the E498T mutant, containing a polar residue with a shorter side-chain than the native glutamate, no difference was found in copper occupancy in the type 1 copper centre, but a decrease of occupancy to 0.8 was observed for all the copper ions in the trinuclear centre (Figure 36D). The same was observed for the E498L mutant (Figure 36C). This effect was even more pronounced for the type 2 copper ion, which refined to an occupancy of only 0.3. In all three

mutants a dioxygen moiety was modelled in between the two type 3 copper ions and refined with the same occupancy that was observed for the type 3 copper ions (Figure 36).

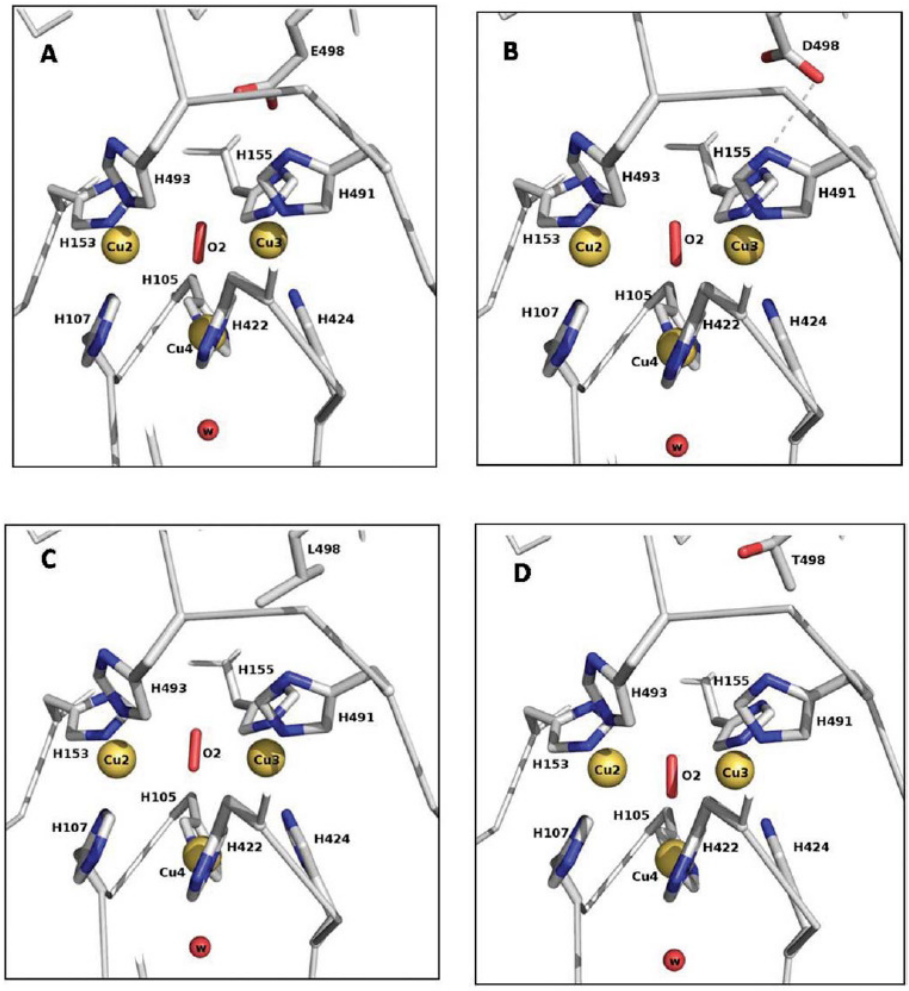

Figure 36 - Structural detail of the trinuclear centre and its neighbourhood in CotA (A), in E498D (B), in E498L (C) and in E498T (D) mutants.

4.2.5 Conclusions

This study aimed to address the role of residue Glu498 (Figure 32) present in the second coordination sphere of the trinuclear centre of CotA laccase. Three mutant enzymes were designed, expressed and purified.

Their catalytic properties were determined, and furthermore their structural differences were addressed by spectroscopic techniques and X-ray crystallography. All MCO appear to have at least one acidic residue (Glu498 in CotA) accessible to the entrance channel by which dioxygen reaches the trinuclear centre. Site-directed mutagenesis studies performed with CueO from *E. coli* and yeast Fet3p indicated that Glu506 and Glu487 (equivalent to Glu498 in CotA) participate in the proton assisted reductive cleavage of the O–O bond at the trinuclear site, respectively (Augustine *et al.*, 2007; Kataoka *et al.*, 2009). Other mutagenesis studies have indicated that an aspartate (corresponding to Asp116 in CotA laccase) located at the "outersphere" of the trinuclear centre, also plays a role in channelling protons in the O–O bond cleavage process (Augustine *et al.*, 2007; Kataoka *et al.*, 2005 and 2009; Quintanar *et al.*, 2005; Ueki *et al.*, 2006). The carboxylic moiety of this aspartate residue, is hydrogen bonded to a water molecule which, in turn, is hydrogen bonded to the water molecule that interacts with T2 copper. In the CotA laccase, Glu498 is hydrogen bonded to a water molecule that is located within the hydrogen bonded distance of the dioxygen moiety observed almost symmetrically positioned in between the type 3 copper ions (Bento *et al.*, 2005). Simulations of equilibrium protonation using structures of CotA indicated that Glu498 is involved in channelling protons for the reaction of reduction of dioxygen to water (Bento *et al.*, 2010). Therefore, mutation of this residue by aspartate, threonine and leucine has been undertaken to access its role in channelling protons to the trinuclear centre, in the stabilization and binding of dioxygen to this centre.

The E498D mutant is the only mutant that retains enzymatic activity, showing a similar dioxygen-binding affinity and azide inhibition when compared with the wild-type enzyme. The orientation of the side chain of

the mutated aspartate is different from that observed for the native glutamate residue and E498T and E498L mutants. However, kinetic data show that the shorter side chain carboxylate is still able, even with a lower efficiency, to assist the reductive cleavage of the O–O bond. On the other hand, when the glutamate is mutated to threonine or to leucine, residues without proton donating ability, a severe catalytic impairment, higher than 99%, is observed. These results indicate that protons from the bulk solvent, supplied through channels leading to the trinuclear centre (Bento *et al.*, 2005), without the final assistance of Glu498, are insufficient to provide the needed protons for the catalytic process. Moreover, they also suggest the absence of alternative pathways participating in the transfer of protons to the trinuclear centre of CotA laccase.

A perturbation of the T1 copper centre in the E498D mutant was observed by spectroscopic and crystallographic data. The different orientation of the aspartate residue, with its $O^{\delta 1}$ atom at a H-bond distance from the $N^{\delta 1}$ atom of His491, is likely to cause destabilisation of the type 1 copper site, by opening this centre and promoting its depletion, as observed experimentally. In fact, His491 is coordinated to one of the two T3 copper ions in the trinuclear centre (Cu3) while the targeted residue 498 is adjacent to His497 which coordinates directly to the type 1 copper atom. In the crystal structure of the E498D mutant no significant difference in the bond length between the His497 residue and the copper atom in the type 1 centre was observed. However, a 2 fold-lower K_m was measured in this mutant for the reducing substrate ABTS (Table 15). This finding could be indicative of subtle alterations near His497, a residue suggested to be involved in both ABTS binding and electron transfer to the T1 Cu site of CotA laccase (Enguita *et al.*, 2004).

The geometry of the trinuclear centre of Glu498 mutants is essentially the same as that found previously in the native structure (see for example Bento *et al.*, 2005) except for the lower occupancy at T3 and T2 centres in the E498T and E498L mutants (Table S5). However, the EPR spectra of the E498L mutant are similar to those of the wild-type in apparent contradiction with the X-ray results. It is possible that this discrepancy results from a destabilising effect of the mutation at the trinuclear centre making it more prone to losing copper during crystallisation. Some heterogeneity of the T2 species in E498D and E498T mutants are revealed in the EPR spectra. The nature of the "new" T2' form is not clear at this point. It can be due to direct structural (or conformational) alterations caused by the mutations or, alternatively, it could result from an intermediate state stabilized by the mutations, scarcely detected in the wild-type protein. The existence of different forms of type 2 copper was also observed in the case of bilirubin oxidase where an aspartate residue close to that site has been mutated (Kataoka *et al.*, 2005). The partial reduction of the dioxygen moiety and/or the simultaneous presence of a hydroxyl and a water molecule bound to the T2 centre, could give rise to two types of centre. The resolution of the X-ray crystal data does not, however, permit any significant structural insights in the geometry of the T2 copper centre that would confirm the spectroscopic data. Nevertheless, there has to be some flexibility at this centre to allow the water molecules, formed by the reduction of dioxygen, to access the exit channel. The concomitant movement of the T2 copper may be reflected in the EPR data.

The present study unequivocally indicates that the electrostatic environment of the trinuclear centre of CotA laccase is influenced by the presence of Glu498. The lack of reactivity of the E498L and E498T

mutants towards dioxygen confirms that Glu498 plays an important role in channelling the protons to the mechanism of dioxygen reduction and that no other alternative pathway is observed, as suggested previously (Bento *et al.*, 2010). Furthermore, the replacement of this residue by an aspartate, allowing the enzyme to retain part of the catalytic activity, also corroborates these findings. The kinetic data additionally suggest that Glu498 is involved not only in the dioxygen reduction catalytic step(s) but also in the binding of dioxygen and presumably, of peroxide. Further research is in progress to provide more insight into the dioxygen reduction mechanism in CotA laccase.

4.2.6 Acknowledgements

Cláudio M. Soares is gratefully acknowledged for helpful discussions. This work was supported by project grants from Fundação para a Ciência e Tecnologia, Portugal (POCI/BIO/57083/2004) and from the European Union (BIORENEW, FP6-2004-NMP-NI-4/026456). P. Durão and Catarina S. Silva hold a Ph.D. fellowship (SFRH/BD/40696/2007 and SFRH/BD/40586/2007, respectively) and Z. Chen a Post-doc fellowship (SFRH/BPD/27104/2006) from Fundação para a Ciência e Tecnologia, Portugal. The ESRF at Grenoble, France is gratefully acknowledged for the provision of synchrotron radiation facilities and efficient support.

4.2.7 Supplementary material

Table S3 - Refinement and quality of refined models. The Ramachandran analysis (Ramakrishnan and Ramachandran, 1965) was determined by Rampage (Lovel *et al.*, 2003).

	E498D	**E498T**	**E498L**
No. of protein atoms	4122	4119	4150
No. of solvent atoms	495	518	645
No. of hetero atoms	4	4	4
Final R-factor	0.177	0.177	0.175
Final free R-factor	0.206	0.215	0.194
Mean B values (Å^2)			
: protein	26.04	24.25	17.65
: solvent	36.91	32.94	30.69
: overall	27.25	25.26	19.47
Estimated overall coordinate uncertainty (Á) ‡	0.088	0.089	0.049
Distance deviations †			
Bond distances (Á)	0.007	0.009	0.007
Bond angles (°)	1.036	1.145	1.064
Planar groups (Á)	0.003	0.004	0.003
Chiral volume deviation (Á^3)	0.068	0.077	0.071
Quality of Models*			
Ramachandran analysis %			
Favourable	97.2	97.8	97.2
Allowed	2.8	2.2	2.8
Disallowed	0.0	0.0	0.0

‡ based on maximum likelihood.
† rms deviations from standard values

Table S4 - Copper content, molar absorptivity, and reduction potentials for CotA proteins

CotA	Copper content	E^o	$\varepsilon_{330\ nm}$	$\varepsilon_{330\ nm}$	$\varepsilon_{609\ nm}$	$\varepsilon_{609\ nm}$
			as-isolated	oxidized	as isolated	oxidized
	g atoms Cu/mol CotA	*mV*	$mM^{-1}.cm^{-1}$	$mM^{-1}.cm^{-1}$	$mM^{-1}.cm^{-1}$	$mM^{-1}.cm^{-1}$
Wild type	4.2 ± 0.1	525	3.4 ± 0.1	4.4 ± 0.8	3.8 ± 0.3	3.9 ± 0.4
E498D	3.7 ± 0.2	525	1.0 ± 0.02	3.1 ± 0.3	1.3 ± 0.02	1.6 ± 0.1
E498T	3.7 ± 0.1	521	1.8 ± 0.2	3.3 ± 0.9	3.2 ± 0.7	3.4 ± 0.7
E498L	3.7 ± 0.2	516	1.6 ± 0.1	3.7 ± 0.2	0.8 ± 0.1	3.4 ± 0.1

Table S5 - Occupancies of copper sites in the crystal structures

CotA / Copper Site	Wild type	E498T	E498L	E498D
Type 1	1.0	1.0	1.0	0.7
Type 2	1.0	0.8	0.3	1.0
Type 3 (x2)	1.0	0.8	0.8	1.0

CHAPTER 4.3

THE ROLE OF ASP116 IN THE REDUCTIVE CLEAVAGE OF DIOXYGEN TO WATER IN CotA LACCASE:

ASSISTANCE DURING THE PROTON-TRANSFER MECHANISM

This chapter was published in the following refereed paper:

C.S. Silva*, J.M. Damas*, Z. Chen, V. Brissos, L.O.Martins, C.M. Soares, P.F. Lindley, I. Bento, "The role of Asp116 in the reductive cleavage of dioxygen to water in CotA laccase: assistance during the proton-transfer mechanism", Acta Cryst. D (Biol Crystallogr.) (2012) 68(2), 186-193.

(* authors contributed equally to this work)

The proteins were provided by the Microbial & Enzyme Technology laboratory at ITQB. Crystallisation experiments were performed by Z. Chen. Catarina S. Silva performed the crystallisation experiments and has been involved in the X-ray structural characterization. J.M. Damas did the Equilibrium protonation simulations.

4.3.1 Summary

Multi-copper oxidases constitute a family of proteins that are capable of coupling the one-electron oxidation of four substrate equivalents to the four-electron reduction of dioxygen to two molecules of water. The main catalytic stages occurring during the process have already been identified, but several questions remain, including the nature of the protonation events that take place during the reductive cleavage of dioxygen to water. The presence of a structurally conserved acidic residue (Glu498 in CotA laccase from *Bacillus subtilis*) at the dioxygen entrance channel has been reported to play a decisive role in the protonation mechanisms, channelling protons during the reduction process and stabilizing the site as a whole. A second acidic residue that is sequentially conserved in multi-copper oxidases and sited within the exit channel (Asp116 in CotA) has also been identified as being important in the protonation process. In this study, CotA laccase has been used as a model system to assess the role of Asp116 in the reduction process of dioxygen to water. The crystal structures of three distinct mutants, D116E, D116N and D116A, produced by site-saturation mutagenesis have been determined. In addition, theoretical calculations have provided further support for a role of this residue in the protonation events.

4.3.2 Introduction

Laccases (p-diphenol: dioxygen oxidoreductases; EC 1.10.3.2) are the simplest members of the multi-copper oxidase (MCO) family of proteins and therefore constitute good model systems for examining structure-function relationships. Their overall three-dimensional fold comprises three cupredoxin-like domains with a type 1 (T1) copper centre located in domain 3 and a trinuclear copper centre, comprising a pair of type 3 (T3)

copper ions and a type 2 (T2) copper ion, located at the interface between domains 1 and 3 (Lindley, 2001; Solomon *et al.*, 1996; Nakamura and Go, 2005; Murphy *et al.*, 1997; Figure 37).

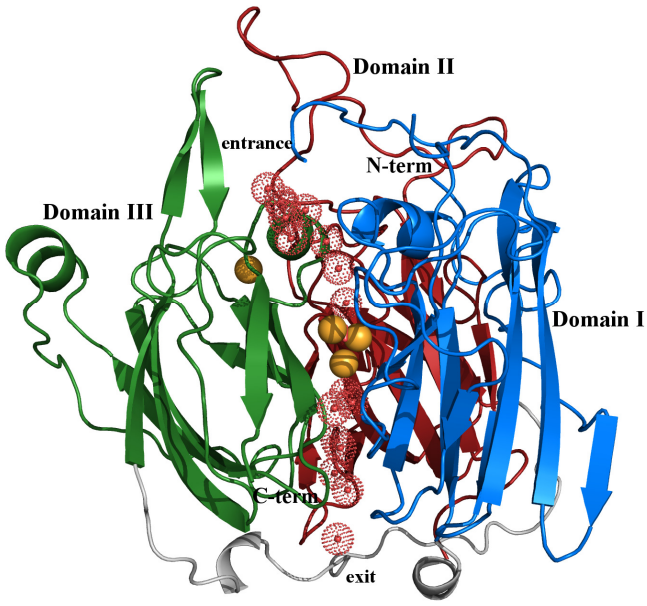

Figure 37 - Three-dimensional structure of CotA laccase: overall three-dimensional fold highlighting the entrance and exit channels, above and below the trinuclear cluster, for the dioxygen and water molecules, respectively. The three cupredoxin-like domains are coloured blue (domain 1), dark red (domain 2) and green (domain 3). Cu atoms are represented as spheres coloured yellow. Substrate oxidation occurs close to the mononuclear T1 Cu centre, shuttling electrons to the trinuclear Cu centre where dioxygen reduction occurs with the concomitant release of water molecules.

Widely distributed in the animal, plant, fungal and bacterial kingdoms, laccases have been reported to have many different functions and to play a central role in several processes (Solomon *et al.*, 1996; Nakamura and Go, 2005; Giardina *et al.*, 2010; Mayer and Staples, 2002). Their ability to oxidise a plethora of aromatic and inorganic compounds makes them interesting and useful targets from the biotechnological processing viewpoint (Mayer and Staples, 2002; Kosman, 2010; Rodríguez Couto and Toca Herrera, 2006; Riva, 2006). The present study involves the CotA

laccase from *Bacillus subtilis*, an enzyme isolated from the outer layer of the spore coat and known to be both thermostable and thermoactive (Martins *et al.*, 2002; Durão *et al.*, 2008a; Enguita *et al.*, 2003).

A putative mechanism for the reduction of dioxygen to water has been proposed based on the X-ray structures of CotA laccase in different redox states (Bento *et al.*, 2005) and with adducts (Bento *et al.*, 2005; Enguita *et al.*, 2004), and by comparison of these with other reported structures of different MCOs which correspond to potential structural intermediates in the mechanism (Bento *et al.*, 2005 and 2010). In addition to four electrons, the reduction process of dioxygen to water also requires four protons, which have been proposed to be facilitated by acidic residues placed within the entrance channel (Bento *et al.*, 2010; Chen *et al.*, 2010) and the exit channel (Kataoka *et al.*, 2009; Ueki *et al.*, 2006) of the enzyme (Figures 37 and 38a)).

The majority of MCOs have a carboxylate group from an acidic residue within the access channel to the trinuclear cluster; the exception appears to be that from *Melanocarpus albomyces*, in which the C-terminal carboxylate partially fills the channel mouth (Hakulinen *et al.*, 2002 and 2008). In the CotA laccase this residue is Glu498. X-ray structure determination and biochemical data analysis of three mutants of Glu498, in which this residue is replaced by site-directed mutagenesis to an aspartate (E498D), a threonine (E498T) and a leucine (E498L), clearly indicate its proton-facilitating role; it may also exert a role in the stabilization of the reduction site as a whole (Chen *et al.*, 2010). Other studies involving site-directed mutagenesis of Glu506 in prokaryotic CueO (Kataoka *et al.*, 2009) and Glu487 in eukaryotic Fet3p (Solomon *et al.*, 2008; Augustine *et al.*, 2007) (both of which are counterparts of Glu498 in CotA laccase, but in the latter case positioned on the opposite side of the channel) strongly

support the participation of a carboxylate residue as a proton donor in the dioxygen-reduction mechanism. Finally, equilibrium protonation simulations (CE/MC) of CotA laccase structures corresponding to different states of the mechanism have allowed the investigation of ionisable groups that are likely to be involved in proton-transfer mechanisms. These indicated that Glu498 is the only proton-active group in the surroundings of the trinuclear cluster in CotA (Bento *et al.*, 2010).

In the proposed mechanism, the addition of two electrons gives rise to a peroxide moiety bound to the trinuclear cluster. The addition of two further electrons and two protons results in this dioxygen species being split into two hydroxide ions and these in turn migrate through the cluster so that they bind to the T2 copper ion but oriented into the exit channel. This migration is a key stage in the overall mechanism and is not well understood or indeed studied. It must involve a spatial displacement of the T2 copper ion, which may be consistent with it being bound by only two histidine residues and being the most labile of the copper ions. The final stages of the mechanism involve the provision of two further protons to convert the hydroxide moieties into water molecules, which can then leave the enzyme through the exit channel from the trinuclear site. Biochemical studies on mutations in other MCOs, namely Asp94 in the eukaryotic Fet3p (Solomon *et al.*, 2008; Augustine *et al.*, 2007; Quintanar *et al.*, 2005), Asp112 in the prokaryotic CueO (Kataoka *et al.*, 2009; Ueki *et al.*, 2006) and Asp105 in the fungal bilirubin oxidase (Kataoka *et al.*, 2005) from *Myrothecium verrucaria*, have already indicated the importance of an acidic residue sited within the exit channel in the mechanism. This acidic residue is not coordinated to any of the copper ions in the trinuclear centre, but the carboxylate moiety points into the

channel and forms hydrogen bonds either directly or indirectly to a set of ligands belonging to or interacting with the trinuclear Cu centre.

In the present work, three distinct mutants of Asp116, the corresponding residue in CotA laccase, have been produced by site-saturation mutagenesis (Brissos *et al.*, 2012) and their crystal structures have been determined. These structures, D116E, D116N and D116A, were then used in equilibrium protonation simulations in order to further assess the role of Asp116 during the protonation process.

4.3.3 Materials and Methods

Crystallisation and Data collection

The CotA laccase mutants D116A, D116N and D116E were produced by site-saturation mutagenesis and batches were obtained as described elsewhere (Durão *et al.*, 2008a; Brissos *et al.*, 2012). Suitable well diffracting crystals were grown for each of the CotA laccase mutants using the vapour-diffusion method at 298 K. The crystals appeared from very diverse reservoir solutions: 35% ethylene glycol (D116A), 8% PEG 6000 with 25% 2-methyl-2,4-pentanediol (MPD) in 0.1 M HEPES buffer pH 7.5 (D116N) and 30% dioxane in 0.1 M HEPES buffer pH 7.5 (D116E). Drops were set up by the combination of 1.5 μl protein sample (at concentrations of 25 mg ml^{-1} for both D116A and D116N, and 50 mg ml^{-1} for D116E in 20 mM Tris–HCl pH 7.6) with the reservoir solution in a 1:1 ratio. Crystals were directly flash-cooled in liquid nitrogen prior to data collection, with no additional cryogenic agent added to the aforementioned crystallisation solutions as they themselves constitute cryogenic conditions.

Diffraction data were collected under a cold nitrogen stream at 100 K on the ID23-EH1 beamline, ESRF, Grenoble for the D116E mutant and using an in-house Bruker AXS MICROSTAR imaging-plate detector (X8 PROTEUM diffractometer) for the D116A and D116N mutants. The crystals of the D116A, D116N and D116E mutants diffracted to 1.95, 2.0 and 2.1 Å resolution, respectively, and belonged to the trigonal space group $P3_121$ with one single molecule per asymmetric unit.

Data sets were processed and the intensities were scaled using MOSFLM (Leslie, 2006) and SCALA from the CCP4 suite (Winn *et al.*, 2011) for the D116E mutant or using the programs SAINT and SADABS, respectively, as part of the Bruker AXS PROTEUM software suite with data statistics obtained using XPREP (Bruker AXS), for the D116A and D116N mutants. Data-collection details and processing statistics are presented in Table 18.

Table 18 - Data-collection statistics. Values in parentheses are for the highest resolution shell.

	CotA mutant		
	D116A	D116N	D116E
X-ray source	In-house Bruker AXS MICROSTAR	In-house Bruker AXS MICROSTAR	ESRF ID23-EH1
Wavelength (Å)	1.544	1.544	0.975
Detector	PLATINUM 135 CCD	PLATINUM 135 CCD	ADSC Quantum Q315r
Crystal-to-detector distance (mm)	85.0	85.0	305.4
Resolution (Å)	1.95 (2.0–1.95)	2.0 (2.05–2.00)	2.1 (2.21–2.10)
Space group	$P3_121$	$P3_121$	$P3_121$
Unit-cell parameters (Å)	a = 101.7, c = 136.6	a = 101.6, c = 136.7	a = 101.7, c = 136.8
No. of unique *hkl*	60037 (8283)	55571 (7488)	46481 (15233)
Completeness (%)	100.0 (99.9)	99.8 (100.0)	96.3 (90.0)
Mean $I/\sigma(I)$	17.5 (3.4)	12.4 (2.7)	12.6 (2.9)
R_{merge}	0.047 (0.290)	0.059 (0.358)	0.049 (0.254)
Multiplicity	5.3 (4.0)	4.5 (3.3)	3.0 (2.4)

Structure determination and refinement

For all three CotA laccase mutants, the structure was solved by the molecular replacement method using the coordinates of the native CotA laccase (PDB entry 1w6l; Bento *et al.*, 2005) as the initial search model,

from which all solvent atoms and heteroatoms had previously been removed. Molecular replacement was carried out using MOLREP (Vagin and Teplyakov, 2010) from the CCP4 program suite (Winn *et al.*, 2011), yielding single solutions with typical correlation coefficients and R factors of approximately 71% and 42%, respectively, for all three mutants. The positions of all four Cu atoms became evident in the electron density synthesis maps after a few refinement cycles. Refinement was then pursued using the maximum-likelihood functions in REFMAC (Murshudov *et al.*, 2011) from the CCP4 program suite (Winn *et al.*, 2011). Careful observation of the σ_A-weighted 2|Fo|-|Fc| and |Fo|-|Fc| maps throughout cycles of model building and manual fitting in Coot (Emsley and Cowtan, 2004) allowed improvement of the models. After a few rounds of refinement, solvent molecules were placed in the model obeying geometrical and stereochemical restraints. Molecules of ethylene glycol were also located in the D116A mutant, and molecules of HEPES buffer and MPD were modelled for the D116N mutant. Isotropic refinement of the atomic displacement parameters was also performed for all of the atoms present in the model. Full occupancy was assigned to all four copper ions on the basis that their isotropic thermal vibration parameters refined approximately to those of the ligand atoms to which they were bound. Determination of the species located between the two T3 Cu atoms was achieved by a combination of cautious use of omit and standard difference Fourier synthesis and inspection of thermal vibration coefficients throughout refinement, as described previously (Bento *et al.*, 2010). Modelling of monoatomic (chlorine ion and monoatomic oxygen species such as hydroxide) and diatomic (peroxide and a dioxygen molecule) species into the positive ovoid-like electron-density peak indicated that a peroxide moiety is the entity that best refines for all three

mutants (Figure S1). This species constitutes the peroxide intermediate, which is considered to be an O_2^{2-} moiety throughout the paper, in accordance with the proposed mechanism (Bento *et al.*, 2005 and 2010). The separation distance between Cu2 and Cu3 is 4.58, 4.63 and 4.74 Å in the D116A, D116N and D116E mutants, respectively, resembling that in the peroxide soaked structure of CotA laccase (Bento *et al.*, 2005).

Similarly to other reported structures of CotA, the loop region comprising residues 89–97 is very poorly defined and therefore not entirely modelled in the three mutants. Likewise, additional electron density was observed in the area surrounding Cys35 (Chen *et al.*, 2010); this was modelled as an oxidised cysteine residue for the D116E mutant, while for the remaining mutants, D116N and D116A, the cysteine side chain was modelled, with two alternate conformations in the latter case. Model validation was monitored using RAMPAGE from the CCP4 suite (Winn *et al.*, 2011). The coordinates and structure factors have been deposited in the PDB as entries 4a66, 4a67 and 4a68 for the D116A, D116E and D116N mutants, respectively.

Refinement statistics and details of the final quality of the models are listed in Table 19. Figures 37 and 38 and Figure S1 were drawn with PyMOL (DeLano, 2002).

Table 19 - Refinement statistics and quality of the refined models.

	CotA mutant		
	D116A	D116N	D116E
No. of protein atoms	4098	4058	4084
No. of solvent atoms	494 (11 EDO)	478 (1 HEPES + 2 MPD)	435
No. of heteroatoms	4 Cu + 2 O	4 Cu + 3 O	4 Cu + 2 O
Final *R* factor	0.174	0.169	0.183
Final free *R* factor (reflections used)	0.203 (5.0%)	0.200 (5.1%)	0.220 (5.1%)
Mean *B* values (Å^2)			
Protein	19.86	18.99	31.34
Solvent	28.77	28.29	38.60
Overall	20.82	19.96	32.03
Estimated overall coordinate uncertainty† (Å)	0.086	0.087	0.124
Distance deviations‡			
Bond distances (Å)	0.017	0.015	0.021
Bond angles (Å)	1.428	1.453	1.501
Planar groups (Å)	0.008	0.008	0.008
Chiral volume deviation (Å^3)	0.107	0.105	0.109
Model quality			
Ramachandran analysis§ (%)			
Favourable	96.6 (478)	97.2 (484)	97.20 (484)
Generous	3.0 (15)	2.8 (14)	2.8 (14)
Disallowed	0.4 (2)	0.0 (0)	0.0 (0)

† Based on maximum likelihood. ‡ R.m.s. deviations from standard values. § Determined using RAMPAGE (Winn *et al.*, 2011). Values in parentheses are the numbers of residues.

Theoretical calculations

Using the X-ray structures of the Asp116 mutants, simulated pH titrations have been made using Continuum electrostatic/Monte Carlo (CE/MC) methods. These calculations use semi-rigid structures owing to the employment of tautomers (see below); consequently, poorly defined regions of the structure were treated in an identical manner for all three mutants. This procedure is carefully explained in Bento *et al.* (Bento *et al.*, 2010). Additionally, and since the bound peroxides occupy slightly different positions (although contained within the estimated error of the coordinates), which can generate substantial electrostatic differences owing to the point-charge nature of the parameterization, it was decided to use the peroxide species of the CotA–H_2O_2 structure (Bento *et al.*, 2005). These choices for the mutant models help to minimize the bias that different positions of the ligand may have on the comparisons between the titration curves calculated for the mutants and for the native enzyme.

Additionally, the trinuclear centre was considered to be in the same state, which means that the hydroxyl bound to the T2 copper centre in the D116N mutant was considered to be a water molecule in the calculations. This decision was also aimed at reducing the bias by maintaining the consistency of the trinuclear centre.

The CE/MC methodology which we have developed considers different tautomeric positions for the ionisable groups and also alternative positions for the protons of the OH moieties of Ser and Thr residues. This is a necessity in order to improve the rigid nature of CE calculations. In CE methods the protein can be treated as a low-dielectric model immersed in a high dielectric corresponding to the solvent, with charges placed at atomic positions with a given atomic radii. The dielectric constants used were 80 for the solvent and 10 for the protein, which are values that reproduce experimental data well within the realm of the parameterization used (Teixeira *et al.*, 2005). Sets of partial charges and atomic radii were taken from the 43A1 GROMOS96 force field (van Gunsteren *et al.*, 1996; Scott *et al.*, 1999), except for the T1 copper and the trinuclear metal centres, for which partial charges were derived using quantum-chemical calculations as described previously (Bento *et al.*, 2010). The package MEAD v.2.2.0 (Bashford and Gerwert, 1992) was used for the CE calculations, with a solvent-probe radius of 1.4 Å, an ion-exclusion layer of 2.0 Å, an ionic strength of 0.1 M and a temperature of 300 K. The obtained individual and interaction terms of the binding free energy of the protons were then used in sampling of the binding states of the protons. The program PETIT v.1.3 (Baptista and Soares, 2001; Teixeira *et al.*, 2002) was used for the MC sampling of the protonation states, with averages computed using 105 MC steps. Site pairs were selected for double moves when at least one pairwise term was greater than 2 pK units.

4.3.4 Results

Structural characterization of the mutants

Crystal structure comparison of the three Asp116 mutant enzymes with the native CotA laccase structure shows no significant differences in terms of the overall three-dimensional fold. Superposition of the Cα traces of each mutant onto the fully loaded native CotA structure (PDB entry 1w6l; Bento *et al.*, 2005) yielded r.m.s. deviation values of 0.24, 0.17 and 0.16 Å for the D116A, D116N and D116E mutants, respectively. A few minor changes were observed in some of the external loop regions such as that composed of residues 212–219, for which the D116A mutant showed the most pronounced shift relative to the backbone chain. Additionally, the loop comprising residues 357–364 was found to have very poorly defined electron density in this mutant, which did not allow complete modelling. Within this loop is Tyr358, which was found to have a modification at position CD2 that was not modelled in this structure as no satisfactory fit to the electron density was achieved.

With respect to the copper centres, no significant changes were observed at the T1 copper centre, which shows full occupancy in all three mutants. At the trinuclear centre, full occupancy was observed for the copper ions and for the diatomic species in between the T3 copper ions. This moiety was modelled as a peroxide species in all of the mutants. In a similar manner to the native enzyme, this species interacts with a solvent molecule, which in turn hydrogen bonds to the side chain of Glu498, although this water is only weakly defined in the D116E mutant (and hence was not modelled). The reasons for the absence of such a solvent molecule in the latter mutant are not clear, with such an absence only being reported for the reduced state of native CotA (Bento *et al.*, 2005).

In the native enzyme, Asp116 is sited within the exit channel in close proximity to the T2 Cu ion in the trinuclear centre (Figure 38a)).

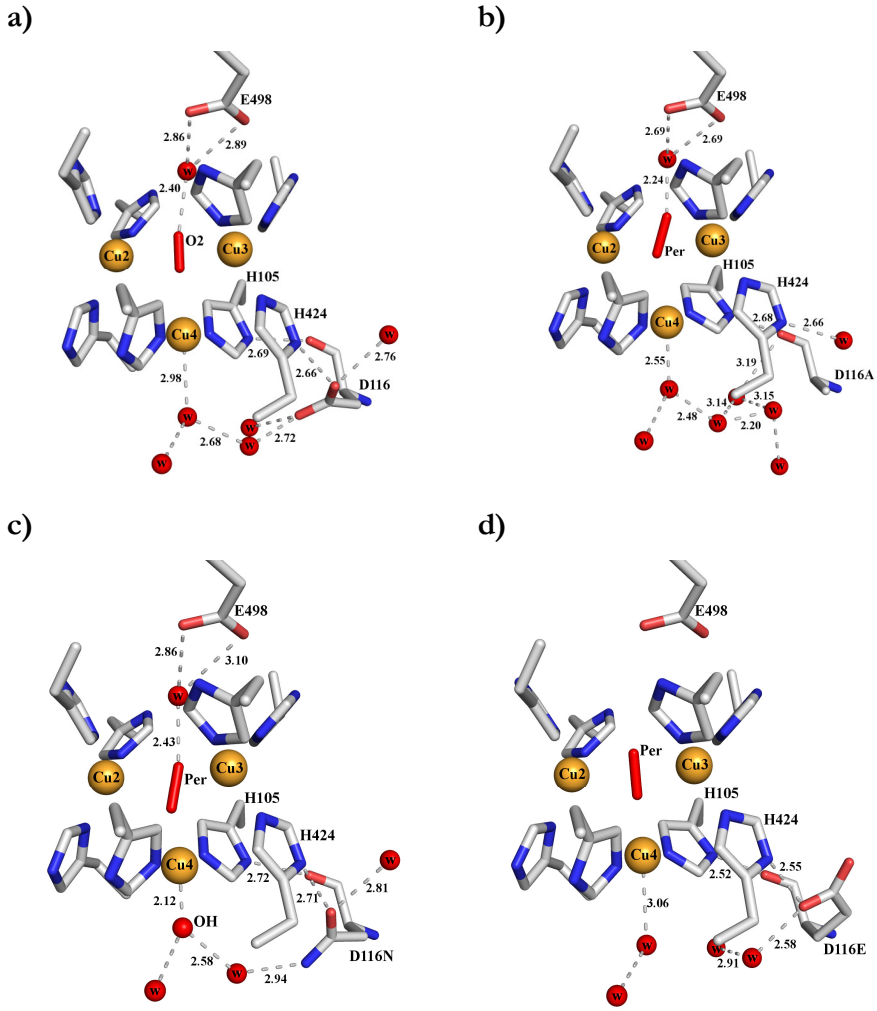

Figure 38 - Structural detail of the CotA trinuclear centre and its neighbourhood. The acidic residues Glu498 and Asp116 are highlighted. **(a)** Native CotA, **(b)** D116A, **(c)** D116N and **(d)** D116E. Cu ions are represented as yellow spheres.

Its backbone carbonyl O atom forms a hydrogen bond to the ND1 atom of His105 (2.69 Å), a ligand bound to the T2 site. On the other hand, its carboxylate side chain forms hydrogen bonds to both the ND1 atom of His424 (2.66 Å), a ligand bound to one of the T3 Cu ions, and a solvent

molecule (2.72 Å) which is part of a chain of waters oriented between the T2 Cu and the surface of the CotA molecule. In the case of the D116A (Figure 38b)) and D116N (Figure 38c)) mutants, in which the negatively charged aspartate has been mutated to an apolar alanine and a polar uncharged asparagine, respectively, the residue side chains remain oriented into the exit channel and the water network that interacts with the T2 Cu is maintained. In the D116A mutant two water molecules occupy the vacant side chain site, essentially mimicking the carboxylate O atoms with respect to hydrogen bonding and extending the water network. The mutated alanine is no longer able to establish hydrogen bonds through its side chain and hence does not interact with His424. In fact, a water molecule placed near the His424 ring in the native structure has adjusted its position in the D116A mutant, directly interacting with the ring. In the D116N mutant the side chain of the asparagine residue is slightly shifted with respect to the aspartate of the native protein, but still maintains hydrogen bonds to the histidines binding to the T3 and T2 Cu ions. It also interacts with Thr111, which has its side chain oriented towards the exit channel (ND2–OG1, 3.07 Å). Moreover, in this mutant the T2 Cu is directly bound to a hydroxyl species with a Cu4–OH distance of 2.12 Å.

On the other hand, in the D116E mutant (Figure 38d)), in which a negatively charged residue has been maintained at the aspartate position, the longer length of the side chain causes it to rotate towards the interior of the protein, with a concomitant change in the water network that interacts with the T2 Cu ion. The glutamate side chain still hydrogen bonds to water molecules, but these are some 4 Å away from the water molecule hydrogen-bonded to the T2 copper ion. This conformational movement of the side chain increases the distance of the carboxylate moiety from the T2 copper and it is therefore expected that its efficiency

in mediating or assisting protonation of hydroxyl groups bound to the T2 copper ion is decreased. As in D116N, this mutant remains hydrogen-bonded to both His424 and His105, the former through the OE2 atom and the latter through the main-chain carbonyl moiety. In all three mutants, the presence of a peroxide species between the T3 Cu ions indicates that a cycle of the reaction has been initiated.

Titration profiles of Glu498 in the Asp116 mutants

Previously reported protonation equilibrium simulations using CE/MC methods showed that Glu498 is the only proton active residue (i.e. that actively titrates in the physiological pH range; protonation between 0.05 and 0.95) in the surroundings of the trinuclear centre (Bento *et al.*, 2010). Furthermore, these simulations showed that Glu498 was deprotonated in native oxidised holo-CotA around pH 7, increasing its protonation in the peroxide intermediate and reduced state. In contrast, Asp116 was found to be essentially deprotonated in the active pH range of the enzyme in all of the states analysed (Bento *et al.*, 2010).

In the present study, with the aim of evaluating the role of Asp116 in the CotA laccase protonation process, the pH titration has again been simulated for all titratable groups using the determined structures of the D116A, D116E and D116N mutants. The previous conclusions remain valid (Bento *et al.*, 2010) and in all cases Glu498 remains the only proton-active residue in the surroundings of the trinuclear centre. However, changes in its protonation are observed, with a pK_a shift of ~1 unit in the titration profile of Glu498 when comparing the D116A and D116N mutants with the native enzyme (Figure 39). In contrast, the titration profile of Glu498 in the D116E mutant shifted only very slightly, suggesting that Glu498 retains its protonating capabilities in this mutant.

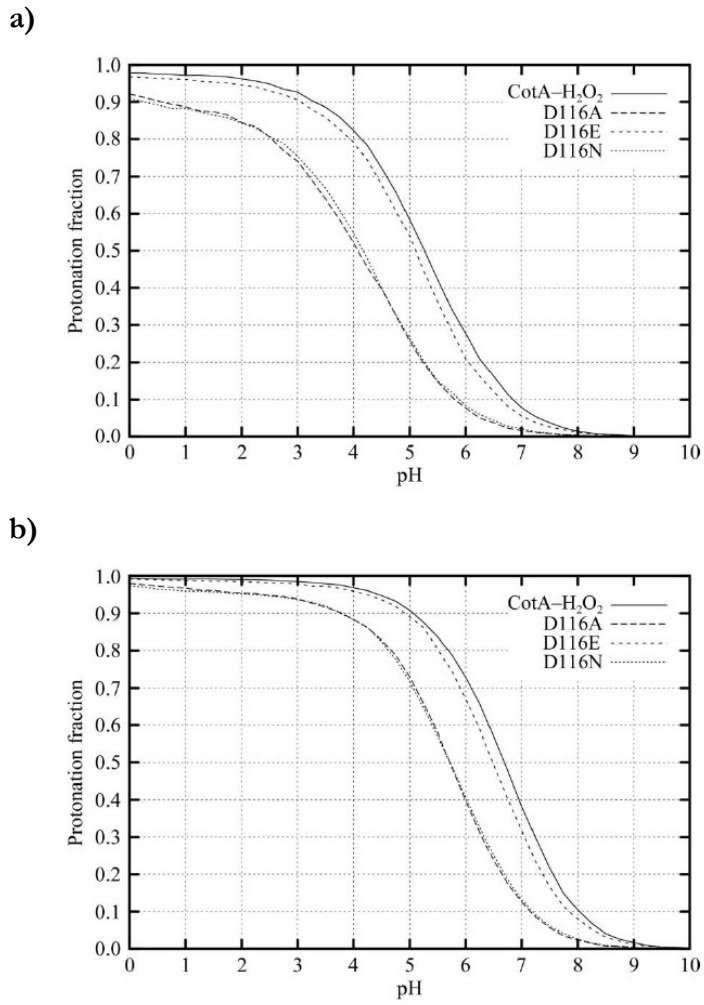

Figure 39 - Simulated pH titrations of Glu498 for the CotA–H_2O_2 state (Bento *et al.*, 2005) **and the three D116 mutants (a) with T1 copper centre oxidised and (b) with T1 copper centre reduced.**

Note that the titration properties of the glutamate residue in the D116E mutant are very similar to those of the aspartate in the native CotA (Bento *et al.*, 2010), indicating that the titration profile of this glutamate changes only very slightly and that the residue remains completely deprotonated at pH ranges around pH 7 (results not shown). These results are quite surprising and indicate that the presence of a negative charge in position

116 is a strong controlling factor in the protonation of Glu498; the physical basis relies on a long-range electrostatic effect between this negative charge and the protonation of Glu498, which is effectively stabilized and maintained ready for protonation of the initial dioxygen species. This electrostatic effect is stronger because it occurs in the protein interior. The elimination of this negative charge by mutation to Ala or to Asn has a substantial effect on the titration profile of Glu498 by lowering its protonation probability. Finally, these relative shifts in the titration profiles are independent of the T1 copper centre redox state (compare Figures 39a) and 39b)), which also has an effect on the titration of Glu498 but does not change the relative effect of the mutations.

4.3.5 Discussion

Previous studies on CotA (Bento *et al.*, 2010) indicated that Glu498 in the entrance channel is the only proton-active group in the neighbourhood of the trinuclear centre; indeed, mutations of this residue (Chen *et al.*, 2010) resulted in a catalytically compromised (E498D) or dead enzyme (E498T and E498L). In contrast, Asp116 in the exit channel has been suggested by these studies to be fully ionized in all physiological situations (Bento *et al.*, 2010). Recent kinetic studies by Brissos *et al.* (2012) on mutants of Asp116 (D116A, D116N and D116E) showed that their catalytic properties have been severely compromised, with the decrease in activity being mainly associated with the turnover of the enzymes. In enzymatic assays performed with 2,6-DMP (2,6-dimethoxyphenol) in the pH range 7–8 (Brissos *et al.*, 2012), a pH similar to our crystallisation conditions (pH 7.5), the Asp116 mutants showed turnover-number differences of 10^3 and 10^4 for D116A and D116N, respectively, and around 70-fold for D116E when compared with native CotA. Similar

assays performed in the pH range 3–4 with ABTS showed a decrease of only around one order of magnitude for all mutants.

Clearly, the presence of an aspartate at position 116 is important for catalysis and the present results suggest that a negative charge at this position may be critical for the protonation mechanisms of the dioxygen-reduction process. The absence of this negative charge in the D116A and D116N mutants causes no significant structural changes at the trinuclear site, with the water network that interacts with the T2 Cu being maintained (Figures 38b) and 38c)); however, it causes a pK_a downshift in the Glu498 simulated protonation profile (Figure 39a)) and a peroxide intermediate is observed in the crystal structures of both mutants (Figures 38b) and 38c)). On the other hand, in the D116E mutant, in which the negative charge is maintained, the water network connectivity near the T2 site is perturbed (Figure 38d)) and a peroxide intermediate is still observed in its crystal structure. However, in this case the protonation profiles for both Glu116 and Glu498 did not change, remaining similar to those observed for the native enzyme. As Glu498 is under comparable electrostatic influences in the D116E mutant and in the native enzyme, one could expect similar proton provision to the catalytic cycle in both situations. Yet, the D116E mutant is only capable of retaining residual activity. Together, these results seem to indicate that Asp116 not only has a role as a negative charge, controlling the protonation characteristics of Glu498, but may also be fundamental to maintain the connectivity of the water network in the vicinity of the T2 Cu (compare Figures 38a) and 38d)). Another important role may involve proton-transfer kinetics, which cannot be addressed using the current methodology.

Furthermore, in the light of the proposed mechanism (Bento *et al.*, 2005 and 2010), if the protonation of the dioxygen species bound between the

T3 Cu ions is incomplete it will affect the formation of hydroxide ions and consequently the rest of the catalytic mechanism. The resolved structures show that the Asp116 mutants are in a peroxide intermediate state, with the experimental starting point of the enzyme corresponding to the reduced state (owing to microaerophilic cell growth conditions; Durão *et al.*, 2008a; Brissos *et al.*, 2012), binding dioxygen as soon as it becomes available. This means that catalysis has been prevented from proceeding further, with the D116A and D116N mutants arrested in the peroxide intermediate state (Figures 38b) and 38c)), in agreement with the fact that these mutants are catalytically dead (Brissos *et al.*, 2012). In the structure of the D116E mutant the peroxide intermediate state was also captured (Figure 38d)), which is natural given that the activity of this mutant is almost nonexistent (Brissos *et al.*, 2012), increasing the probability of this state being found. This peroxide intermediate state has only been reported in T1-depleted or inactive enzymes (Kataoka *et al.*, 2005 and 2009; Augustine *et al.*, 2007; Palmer *et al.*, 2001), in peroxide-soaked structures (Bento *et al.*, 2005; Messerschmidt *et al.*, 1993), in the M502F mutant of CotA (Durão *et al.*, 2006) and in the blue laccase from *Lentinus tigrinus* (Ferraroni *et al.*, 2007), but in this latter case the crystals had been exposed to high X-ray radiation doses under aerobic conditions and high pH.

Similar studies on Asp116-counterpart mutants have been reported in other laccases. The mutations reported by Kataoka *et al.* (Kataoka *et al.*, 2005) of Asp105 of the fungal bilirubin oxidase (BO) from *M. verrucaria* showed comparable results at high pH values (pH 8.4), with a decreased catalytic activity for the D105E variant and a practically nonexistent or null activity for the D105A and D105N mutants, respectively. Furthermore, a structural role was also suggested for the aspartate residue, as the removal of the negatively charged moiety in D105A and D105N

resulted in some copper depletion and an inability to reincorporate it under anaerobic conditions (Kataoka *et al.*, 2005). Such a structural role in the integrity of the trinuclear cluster is not evident in the case of CotA laccase. Mutation of the equivalent Asp (Asp94) residue in yeast Fet3p (Quintanar *et al.*, 2005) to Ala (D94A) or Asn (D94N) resulted in significant electronic changes at the trinuclear site, and the enzyme became unreactive towards dioxygen. On the other hand, mutation to Glu (D94E) produced only minor electronic changes at the trinuclear site, rendering an enzyme that was still active (although with a slower decay of the peroxide intermediate). For the bacterial laccase CueO, mutations of the equivalent Asp112 residue yielded a significant catalytic impairment at pH 5.5 for all three variants D112E, D112A and D112N, although much more severe for the latter two, as reported by Ueki *et al.* (2006).

Altogether, it is evident that an aspartate at position 116 in CotA is important for catalysis, either by modulating the protonation events or by maintaining the local geometry and water connectivity at the trinuclear copper site. In fact, it appears that these sites are fine-tuned for proper catalysis (Yoon *et al.*, 2009), which further supports the concept that even subtle perturbations in its surroundings, such as that observed in the D116E mutant, may compromise the entire catalytic process. Finally, we propose that, unlike the effect of mutations of Glu498, which catalytically kill the enzyme activity (Chen *et al.*, 2010), the effect of mutating Asp116 tunes the catalytic properties of the enzyme, since at low pH values Glu498 may be in a protonation state of interest to the catalysis and the enzyme is still able to catalyse dioxygen reduction to some extent; hence, the differences between the catalysis with 2,6-DMP (at pH 7–8) and ABTS (at pH 3–4). This research has therefore clarified the respective roles of Asp116 and Glu498 in the mechanism of dioxygen reduction by

CotA, but one outstanding question remains to be addressed. This concerns the mechanism by which the hydroxyl species or water molecules produced during the catalytic process pass through the T2 Cu into the exit channel and clearly requires further study.

4.3.6 Acknowledgements

Maria Arménia Carrondo is gratefully acknowledged for support. The European Synchrotron Radiation Facility, Grenoble, France and the Macromolecular Crystallography staff are sincerely acknowledged for provision of synchrotron radiation facilities and support. This work was supported by a project grant from the European Union (BIORENEW, FP6- 2004-NMP-NI-4/026456) and by Fundação para a Ciência e Tecnologia through grant PEst-OE/EQB/LA0004/2011. CSS and JMD hold PhD fellowships (SFRH/BD/40586/2007 and SFRH/BD/41316/2007, respectively) and ZC and VB hold postdoctoral fellowships (SFRH/BPD/27104/2006 and SFRH/BPD/46808/2008, respectively) from Fundação para a Ciência e Tecnologia, Portugal.

4.3.7 Supplementary material

Table S6 - Copper-copper and copper-solvent ligand distances (Å) at the trinuclear site for the native CotA laccase and its mutants D116A, D116N and D116E.

	CotA laccase			
	Native	**D116A**	**D116N**	**D116E**
Cu2-Cu3	4.73	4.58	4.63	4.74
Cu2-Cu4	3.99	4.01	4.17	3.97
Cu3-Cu4	3.66	3.61	3.74	3.61
Cu2-O1	2.57	2.90	2.76	2.56
Cu2-O2	2.59	2.32	2.88	2.61
Cu3-O1	2.31	2.11	1.88	2.31
Cu3-O2	2.29	2.32	2.42	2.45
Cu4-O2	2.42	2.68	1.95	2.10
Cu4-O	2.98	2.55	2.12	3.06

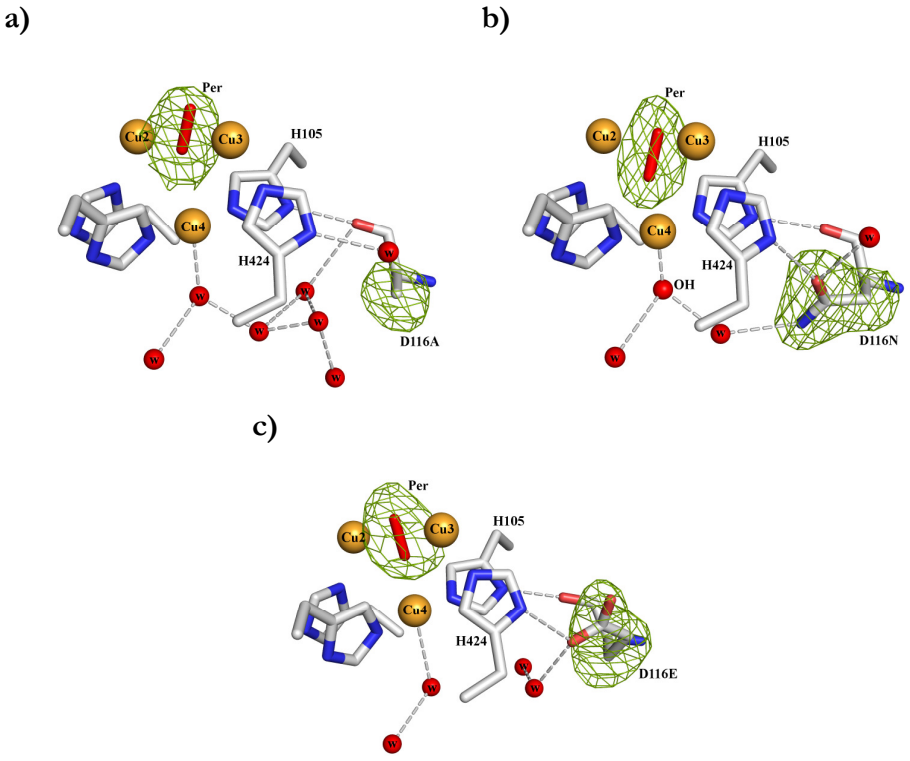

Figure S1 - Close view of the CotA trinuclear cluster at the dioxygen binding site. |Fo|-|Fc| difference-Fourier omit map for the peroxide species placed in between both type T3 Cu ions and for the D116 residue side chain in **(a)** D116A, **(b)** D116N and **(c)** D116E. Contour level is 4.0 . The peroxide species is shown as a red stick.

CHAPTER 5

CRYSTAL STRUCTURE OF THE MULTICOPPER OXIDASE FROM THE PATHOGENIC BACTERIUM *CAMPYLOBACTER JEJUNI* CGUG11284:

CHARACTERIZATION OF A METALLO-OXIDASE

This chapter was published in the following refereed paper:

C.S. Silva, P. Durão, A. Fillat, P.F. Lindley, L.O. Martins, I. Bento, "Crystal structure of the multicopper oxidase from the pathogenic bacterium *Campylobacter jejuni* CGUG11284: characterization of a metallo-oxidase", **Metallomics** (2012), **4**(1), 37-47 (Front cover).

Protein expression, purification and biochemical studies were performed by P. Durão. Catarina S. Silva performed the crystallisation experiments and X-ray structural characterization.

5.1 Summary

Multi-copper oxidases are a multi-domain family of enzymes that are able to couple oxidation of substrates with reduction of dioxygen to water. These enzymes are capable of oxidising a vast range of substrates, varying from aromatic to inorganic compounds such as metals. This metallo-oxidase activity observed in several members of this family has been linked to mechanisms of homeostasis in different organisms. Recently, a periplasmic multi-copper oxidase, encoded by *Campylobacter jejuni*, has been characterised and associated with copper homeostasis and with the protection against oxidative stress as it may scavenge metallic ions into their less toxic form and also inhibit the formation of radical oxygen species. In order to contribute to the understanding of its functional role, the crystal structure of the recombinant McoC (*Campylobacter jejuni* CGUG11284) has been determined at 1.95Å resolution and its structural and biochemical characterizations undertaken. The results obtained indicate that McoC has the characteristic fold of a laccase having, besides the catalytic centres, another putative binding site for metals. Indeed, its biochemical and enzymatic characterization shows that McoC is essentially a metallo-oxidase, showing low enzymatic efficiency towards phenolic substrates.

5.2 Introduction

Laccases (p-diphenol: dioxygen oxidoreductase, EC 1.10.3.2) are the simplest members of the Multi-copper oxidase (MCO) family of enzymes (Messerschmidt, 1997; Lindley, 2001; Hoegger *et al.*, 2006; Giardina *et al.*, 2010, and references therein) exerting a wide range of physiological functions. Overall, these enzymes are capable of coupling the oxidation of a vast range of substrates, from organic aromatic amines, non-phenols and

phenols to inorganic compounds (Nakamura and Go, 2005; Kosman, 2010 and references therein), with reduction of dioxygen to water. Such an asset makes these enzymes interesting targets for biotechnological purposes (Rodríguez Couto and Toca Herrera, 2006). To date, the vast majority of laccases whose structures have been reported are derived from fungi, whereas bacterial laccases remain far less well characterized (Sharma *et al.*, 2007 and references therein). Nevertheless, recent progress in whole genome analysis has provided evidence for novel bacterial laccases or laccase-like proteins, identified in many gram-negative and gram-positive bacteria (Giardina *et al.*, 2010; Sharma *et al.*, 2007; Claus, 2004). Even in thermophilic organisms, for which such proteins are rare, corresponding laccase-like proteins have been identified (Miyazaki, 2005; Fernandes *et al.*, 2010 and 2007).

The overall laccase structural fold comprises three cupredoxin-type domains, characterized by a Greek key β-barrel topology (Nakamura and Go, 2005 and references therein). In addition, two copper centres, a mononuclear type 1 blue copper centre (T1) and a trinuclear cluster, consisting of two type 3 (T3) and one type 2 (T2) copper atoms, mediate the oxidation of substrates and the concomitant reduction of dioxygen to water, respectively. The oxidation of four substrate molecules at the T1 copper centre (the primary electron acceptor site) leads to the reductive cleavage of dioxygen to two molecules of water at the trinuclear site (Messerschmidt, 1997; Lindley, 2001; Hoegger *et al.*, 2006; Solomon *et al.*, 2001). The first three-dimensional structure of a bacterial laccase was reported for the CotA laccase (Enguita *et al.*, 2003; Bento *et al.*, 2005 and 2010), a laccase with oxidase activity towards aromatic compounds, from the outer layer of the spore coat of *Bacillus subtilis* (Martins *et al.*, 2002). Another structure of a bacterial MCO is that of the *Escherichia coli* CueO

protein (Roberts *et al.*, 2002 and 2003). This enzyme, contrary to CotA laccase, is able to oxidise lower valency metal ions (Cu^{1+} and Fe^{2+}) more efficiently than aromatic substrates (Kataoka *et al.*, 2007). As such, this enzyme is more specifically a metallo-oxidase (Stoj and Kosman, 2005). The presence of a methionine-rich (Met-rich) region near the T1 Cu site has been suggested to provide additional binding sites for exogenous Cu, playing a role in Cu-dependent activity (Roberts *et al.*, 2003; Kataoka *et al.*, 2007). Just recently, Singh *et al.* have hypothesized that this region may in fact be used for copper binding during CueO's response to copper toxicity (Singh *et al.*, 2011). Such a region is also present in other proteins implicated in Cu homeostasis, additionally supporting its participation in Cu tolerance (Arsenano *et al.*, 2002; Huffman *et al.*, 2002; Outten *et al.*, 2001). Furthermore, CueO shows ferroxidase activity in a similar manner to its mammalian counterpart human ceruloplasmin (hCp), the major Cu-containing protein in plasma, which plays a vital role in iron homeostasis in vertebrates (Harris *et al.*, 1999). Similarly, the yeast MCO Fet3 protein (Fet3p) catalyses the conversion of ferrous to ferric iron, allowing its uptake across the yeast plasma membrane into the cytosol. Hence, a correlation between both copper and iron metabolism in these organisms has been suggested (Taylor *et al.*, 2005).

Campylobacter jejuni, a pathogenic, Gram-negative, microaerobic, flagellated, spiral bacterium, is one of the most significant causes of human enteric diseases worldwide (Parkhill *et al.*, 2000; Peterson, 1994). Included in *C. jejuni*'s virulence factors is its ability to acquire iron, a homeostasis system known in some detail (Palyada *et al.*, 2004; Holmes *et al.*, 2005). However, the way that other essential metals, such as copper, are acquired, processed and regulated in *C. jejuni* remains to be fully clarified. From its genome sequence (strain NCTC 11168) (Parkhill *et al.*,

2000), a gene (*Cj1516*) was identified as encoding for a periplasmic oxidoreductase, sharing 28% and 24% sequence identity with CueO and CotA laccase, respectively. Hall *et al.* (Hall *et al.*, 2008) confirmed that the *Cj1516* protein is a MCO as its spectroscopic properties matched those of typical MCOs. Moreover, and similar to its homologue CueO, *C. jejuni*'s MCO showed evidence of metallo-oxidase activity towards Cu^{1+} and Fe^{2+}. Further studies conducted by Hall *et al.* (Hall *et al.*, 2008) led these authors to propose that the major physiological role of the identified MCO seems to be copper detoxification in the periplasm.

In this paper the crystal structure of the recombinant Multi-copper oxidase from *Campylobacter jejuni* (McoC), obtained from the type strain CGUG11284, is reported as well as its biochemical characterization. The results clearly provide evidence for the enzyme's function as a metallo-oxidase. The presence of a Met-rich region (resembling its homologue CueO) and other secondary structure elements near the mononuclear T1 Cu site occludes a substantial portion of the highly exposed substrate binding cavity identified for CotA laccase, functioning as a barrier for the access of bulkier substrates to this site. McoC mainly shows specificity as a cuprous oxidase, possibly being involved in the detoxification of Cu^{1+} exported from the cytoplasm to the periplasm by converting it to the less toxic Cu^{2+} form. Moreover, it also exhibits slight ferroxidase activity.

5.3 Materials and Methods

Construction of a strain containing the mcoc gene

The *mcoC* gene was amplified from the genome of *C. jejuni* CGUG11284 by PCR using oligonucleotides *mcoC*-181D (5'-CTATAATACAAAAAAGCTAGCAAAAGG-3') and *mcoC*-1756R (5'-

CCTAAGAATTCCACTTTTACCATATTATTCC-3'). The primers were designed taking into account the *Cj1516* gene sequence of *C. jejuni* NCTC11168. The PCR product was digested with NheI and EcoRI and inserted between the same restriction sites of plasmid pET-21a(+) (Novagen) to yield pATF-5. A codon usage analysis of *mcoC* revealed that it contains codons rarely used by *E. coli* (25 arginine $tRNA^{Arg(AGG/AGA/CGG/CGA)}$, 18 lysine $tRNA^{Lys(CTC)}$ and 22 isoleucine $tRNA^{Iso(ATA)}$), a limiting expression factor by common *E. coli* strains. Therefore, the host-strain Rosetta (DE3) pLysS (Novagen), expressing rare tRNAs, was used. Introduction of pATF-5 into Rosetta *E. coli* created strain LOM 418, in which the protein was produced under the control of the T7*lac* promoter.

Overproduction and purification of McoC

Strain LOM 418 was grown in Luria-Bertani (LB) culture medium (10 g L^{-1} tryptone; 5 g L^{-1} yeast; 5 g L^{-1} NaCl) supplemented with ampicillin (100 μg mL^{-1}) and chloramphenicol (34 μg mL^{-1}). The cells were grown at 30ºC until reaching an OD600 of 0.6. At this time 0.1 mM isopropyl-β-D-thiogalactopyranoside (IPTG) and 0.25 mM $CuCl_2$ were added and the temperature reduced to 25ºC. Incubation was continued for further 4 h, when a change to microaerobic growth conditions was achieved (Durão *et al.*, 2008a). Cells were harvested by centrifugation (8000 x g, 10 min, 4ºC) and the cell sediment suspended in 20 mM Tris–HCl buffer, pH 7.6, with a mixture of protease inhibitors, DNase I and $MgCl_2$ (5 mM). Cells were disrupted in a French pressure cell (at 900 psi), followed by centrifugation (18 000 x g, 60 min, 4ºC) to remove cell debris. The cell lysate was then loaded onto a SP-Sepharose column equilibrated with 20mM Tris–HCl, pH 7.6, and the protein was eluted using a salt gradient up to 1 M NaCl.

The active fractions were pooled, concentrated and applied onto a Superdex 200 HR 10/300 column equilibrated with 20 mM Tris–HCl, pH 7.6, with 0.2 M NaCl. All purification steps were carried out at room temperature in AktaPurifier (GE Healthcare).

UV/visible, EPR and RR spectra and redox titration

UV/visible, electron paramagnetic resonance (EPR) and resonance Raman (RR) spectra were acquired, as described before (Fernandes *et al.*, 2010; Durão *et al.*, 2008a), using a Nicolet Evolution 300 spectrophotometer from Thermo Industries, a Bruker EMX spectrometer equipped with an Oxford Instruments ESR-900 continuous-flow helium cryostat and a confocal spectrograph (Jobin Yvon, XY) equipped with grating of 1800 lines per millimetre and a liquid nitrogen cooled back-illuminated CCD camera, respectively. Redox titrations were performed at 25ºC and pH 7.6, under an argon atmosphere, and were monitored by visible spectroscopy (300–900 nm) in a Shimadzu Multispec-1501 spectrophotometer as described by Durão *et al.* (Durão *et al.*, 2006).

Enzyme activities

The McoC oxidation reactions of ABTS (2,2'-azinobis-(3-ethylbenzothiazoline-6-sulfonic acid)), SGZ (syringaldazine), 2,6-DMP (2,6-dimethoxyphenol) and ferrous sulfate ($FeSO_4$) were monitored with either a Nicolet Evolution 300 spectrophotometer from Thermo Industries or a Molecular Devices Spectra Max 340 microplate reader with a 96-well plate. The oxidation reactions of ABTS, SGZ, 2,6-DMP and $FeSO_4$ were followed at 420 nm (ε = 36000 M^{-1} cm^{-1}), 530 nm (ε = 65 000 M^{-1} cm^{-1}), 468 nm (ε = 49600 M^{-1} cm^{-1}) and 315 nm (ε = 2200 M^{-1} cm^{-1}), respectively. Oxidations were determined by using Britton-Robinson (BR)

buffer (100 mM phosphoric acid, 100 mM boric acid and 100 mM acetic acid mixture with 0.5 M NaOH to the desired pH). Ferrous sulfate oxidation was performed in 100 mM Mes buffer, pH 5. The effect of pH on the enzyme activity was determined at 37 ºC for the different substrates, in BR buffer (pH 3–9). The reaction mixtures contained 1 mM of ABTS, 0.1 mM SGZ, 1 mM 2,6-DMP and 300 μM of $FeSO_4$. Kinetic parameters were determined at 37 ºC. Reaction mixtures contained ABTS (100–10 000 μM, pH 4), SGZ (1–100 μM, pH 8), 2,6-DMP (40–400 μM, pH 8) and $FeSO_4$ (10–300 μM, pH 5). The initial reaction rates were obtained from the linear portion of the progress curve. Kinetic constants K_m and k_{cat} were fitted directly to the Michaelis–Menten equation (OriginLab, Northampton, MA, USA). All enzymatic assays were performed at least in triplicate. Cuprous oxidase activity was measured in terms of rate of oxygen consumption by using an oxygen electrode (Oxygraph; Hansatech, Cambridge, UK) at 37 ºC, following the method described by Singh *et al.* (Singh *et al.*, 2004). Stock solutions of $[Cu(I)(MeCN)_4]PF_6$ (Sigma-Aldrich, St Louis, MO, USA) were freshly prepared in argon-purged acetonitrile and subsequently diluted anaerobically by using gas-tight syringes. Reactions were initiated by adding the enzyme to an air-saturated mixture containing substrate (1 mM), 100 mM MES buffer, pH 5 and 5% acetonitrile. The buffer was chosen to provide the best stability for the substrate used, and all reactions were corrected for background auto-oxidation rates of Cu(I). The protein concentration was measured by using the absorption band at 280 nm (ε_{280} = 40680 M^{-1} cm^{-1}) or the Bradford assay using bovine serum albumin as standard.

Crystallisation and data collection

Crystallisation experiments were carried out by the vapour diffusion method at 298 K. Sitting-drops were set in a 1 : 1 ratio, using 1.5 μL of protein sample (at concentrations of 7–8 mg mL^{-1}, in 20 mM Tris–HCl, pH 7.6 with 200 mM NaCl) and precipitant solutions. Suitable well diffracting crystals were grown after 4–10 days, within the following range of conditions: 25–32% PEG 3350 with 0.15/0.2 M $MgCl_2$ in 0.1 M Bis-Tris Propane, pH 5.5, containing 3% dioxane. The crystals used in X-ray analysis were grown in a drop containing 32% PEG 3350 with 0.2 M $MgCl_2$ in 0.1M Bis-Tris Propane, pH 5.5, with 3% dioxane. McoC crystals appeared as blue rectangular prisms of variable size (ca. 100–250 μm). Cryo conditions were provided by adding 22% ethylene glycol to the crystallisation condition, prior to data collection.

Diffraction data were collected under a cold nitrogen stream at 100 K, on ID14-EH4 at the European Synchrotron Radiation Facility (ESRF), Grenoble, France. Crystals diffracted to 1.95 Å resolution and belong to the monoclinic space group $P2_1$, containing one single molecule in the asymmetric unit and a solvent content of around 37% (as estimated by the Matthews coefficient) (Kantardjieff and Rupp, 2003). Data sets were processed with iMOSFLM v1.0.4 (Leslie, 1992 and 2006) and scaled using SCALA from the CCP4 programs suite (CCP4, 1994). Data collection details and processing statistics are listed in Table 20.

Structure determination and refinement

The three-dimensional structure of McoC was solved by the molecular replacement (MR) method. At a first stage, the molecular replacement software MrBUMP (Keegan and Winn, 2007) was used based on the protein sequence. The best search model found was the Met-rich region

deleted form of CueO (PDB id code 2YXW), which was identified only as a marginal solution (R_{free} ca. 48%) by both molecular replacement programs, MOLREP (Vagin and Teplyakov, 1997) and PHASER (McCoy *et al.*, 2007). At a second stage, the output model obtained from MrBUMP was used as a search model in PHENIX Auto-MR, (Adams *et al.*, 2010) using data up to 2.5Å resolution, and a correct structure solution was found with rotation and translation function Z-score values of RFZ = 18.1 and TFZ = 13.5. The structural model obtained was then submitted to 10 cycles of rigid body refinement using REFMAC (Murshudov *et al.*, 1997) and with all the data up to 1.95 Å, yielding the values for R and R_{free} factors of 42.4% and 48.0%, respectively. Before the initial model building and correction ARP/wARP (Lamzin and Wilson, 1993; Mooij *et al.*, 2009) was used to improve the quality of the electron density maps and minimise model bias. Subsequent iterative cycles of refinement and manual model building were performed using the maximum-likelihood functions enclosed in REFMAC and the program COOT (Emsley and Cowtan, 2004), respectively. Some 5% of the data was excluded for R_{free} calculation. Close to the end of the refinement procedure, BUSTER-TNT (Bricogne *et al.*, 2009) was additionally used for map improvement on the poorly defined region that comprises residues Met384 to Ser393. Based on the output maps, this region was manually built into the $2|Fo| - |Fc|$ electron density maps using COOT. For the very last stages of refinement REFMAC was run including translation/libration/screw (TLS) refinement (Winn *et al.*, 2001). The positions of the T1 Cu and T3 Cu2 ions became evident after the first cycles of refinement, based on electron density synthesis maps, but the positions of the remaining ions in the trinuclear cluster, Cu3 and Cu4, took longer to become apparent because of reduced occupancies. Solvent molecules were placed in the model after a few

rounds of refinement corresponding to standard geometrical and stereochemical restraints. Three molecules of ethylene glycol were also modelled in the structure. Isotropic refinement of the atomic displacement parameters was performed for all the atoms present in the model. Copper ion occupancy was assessed by adjusting their value so that their isotropic thermal vibration parameters refined approximately to those observed for their neighbouring atoms. The determination of the species located in between both T3 Cu atoms, Cu2 and Cu3, was achieved by combination of a cautious use of omit and standard difference Fourier synthesis, and inspection of thermal vibration coefficients throughout refinement, as previously described (Bento *et al.*, 2010). The positive ovoid electron density was best modelled as a dioxygen species rather than an hydroxide or chlorine ion. However, the resolution of the data does not permit a distinction between, for example, O_2^{2-} and H_2O_2. Model validation was monitored using RAMPAGE from the CCP4 programs suite (CCP4, 1994) and MOLPROBITY (Lovell *et al.*, 2003; Davis *et al.*, 2007). The coordinates and structure factors have been deposited in the PDB as entry 3ZX1. Refinement statistics and details of the final quality of the model are listed in Table 20. PyMOL (DeLano, 2002) was used to prepare the figures of the McoC and related molecules.

Other experimental methods

McoC peptides after tryptic digestion were analysed by MALDI-TOF-MS using a mass spectrophotometer Voyager STR (Applied Biosystems). Protein identification was performed using the peptide mass fingerprint as a query for the MASCOT-PMF software using the Swiss-Prot database. The N-terminal amino acid sequence was determined from protein transferred to PVDF using stepwise Edman degradation on an Applied

Biosystems Procise 491HT protein sequencer. The overall amount of copper was determined with the trichloroacetic acid/bicinchoninic acid (BCA) method of Brenner and Harris (Brenner and Harris, 1995).

Table 20 - Data collection and refinement statistics for McoC protein.

Data collection statistics	
Synchrotron beam line	ESRF ID14-EH4
Wavelength/Å	0.947
Detector distance/mm	301.8
Detector	ADSC Q315r
Resolution/Å	1.95
Space group	$P2_1$
Cell parameters *a*, *b*, *c*/Å	48.8, 94.7, 50.4
$\alpha = \gamma$, β/°	90, 100.6
Mosaicity/°	0.63
Oscillation angle/°	1.45
Oscillation range/°	217.5
No. of observed *hkl* reflections	141798 (19386)
No. of unique *hkl* reflections	32673 (4624)
Completeness (%)	99.4 (97.3)
Mn($I/\sigma(I)$)	14.9 (3.5)
$I/\sigma(I)$	6.6 (2.0)
R_{merge}	0.073 (0.369)
Multiplicity	4.3 (4.2)
Refinement statistics	
No. of protein atoms	3836
No. of solvent atoms	332
No. of hetero atoms	4Cu + 2O + 3EDO
Final *R*-factor	0.160
Final free *R*-factor	0.207
FOM	0.89
Mean *B* values/Å^2	
Protein	16.080
Solvent	21.475
Overall	16.514
Estimated overall coordinate uncertainty[a]/Å	0.097
Distance deviations[b]	
Bond distances/Å	0.015
Bond angles/°	1.534
Planar groups/Å	0.007
Chiral volume deviation/Å^3	0.110
Quality of models	
Ramachandran analysis (%)	
Favourable	98.1
Allowed	1.7
Disallowed	0.2

Values in parentheses refer to the highest-resolution shell (2.06–1.95 Å). Ramachandran analysis was determined by RAMPAGE.[39] ESRF, European Synchrotron Radiation Facility; EDO ethylene glycol. [a] Based on maximum likelihood. [b] Rms deviations from standard values.

5.4 Results and Discussion

Overproduction, purification and biochemical characterization of recombinant McoC

The *mcoC* gene was amplified by PCR and inserted into the pET-21a(+) expression vector resulting in pATF-5. Expression of the protein using *E. coli* Rosetta (DE3) pLysS (coding for rare tRNA's) revealed that upon induction with IPTG, a major band of around 59 kDa, that was absent in extracts prepared from non-induced LOM 418, appeared in the soluble and insoluble fraction of cell lysates, as visualised by SDS-PAGE gels (results not shown). Two chromatographic steps purified the protein close to homogeneity (Figure 40a)) and an enzyme solution with blue colour (typical of blue copper oxidases) with a copper per protein ratio close to four was obtained. The protein was identified by MALDI-TOF-MS with a score of 95 (31% coverage, 10 peptides identified). Interestingly, the N-terminal amino acid sequence determined was KNHSIN, eleven amino acids displaced from the most expected (theoretical) signal peptide incision (AYA-NP), as determined by SignalP (Bendtsen *et al.*, 2004).

The UV/visible, electron paramagnetic resonances (EPR) and Resonance Raman (RR) spectra obtained for McoC showed all the features that are characteristic of MCOs namely, a band at ~600 nm that corresponds to the Cu–Cys interaction at the T1 Cu centre, with a ε = 3.2 mM^{-1} cm^{-1} (Solomon *et al.*, 1996); resonances characteristic of the T1 and T2 copper centres; the intensity weighted frequency (ν_{Cu-S}=417 ± 1 cm^{-1}) obtained for the Cu–S bond length in the T1 site was within the range reported for other well-studied MCOs (Figure 40b) and data not shown) (Blair *et al.*, 1985). The T1 site redox potential was measured by monitoring the absorbance decrease at 600 nm in the visible spectra.

McoC displayed a redox potential of 422 ± 20 mV, a relatively low value within usual MCO range, from 340 to 790 mV for some fungal laccases (Solomon *et al.*, 1996).

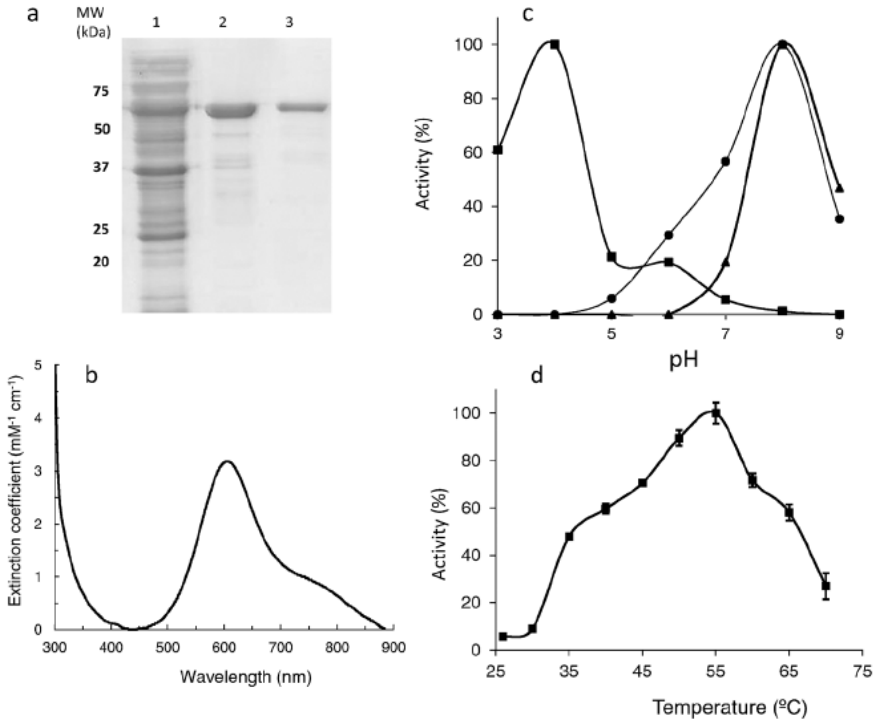

Figure 40 - (a) SDS-PAGE analysis of McoC purified from recombinant *E. coli* LOM418. Lane 1, protein mixture before purification, Lane 2, McoC after the first step of purification (SP-sepharose pH 7.6), Lane 3, McoC after the second purification step (Superdex 200 pH 7.6). **(b) UV/visible spectra of purified McoC. (c) pH profile for catalytic activities using as substrates ABTS** (full squares)**, 2,6-DMP** (full circles) **and SGZ** (full triangles) **of recombinant McoC. (d) Effect of temperature on the activity of recombinant purified McoC.** The enzyme activity was assayed at each temperature in 100 mM Briton-Robinson buffer (pH 4.0) in the presence of 2 mM ABTS. Activity was monitored at 420 nm.

Catalytic properties of recombinant McoC

Compared to CotA, McoC showed little activity towards aromatic substrates (Tables 21 and 22), but it has maximal activity at pH 4 for

ABTS and at pH 8 for SGZ and 2,6-DMP (Figure 40c)), pH values consistent with those exhibited by other bacterial MCOs such as CotA laccase. The temperature for this catalytic activity of McoC was found to be maximal at 55 ºC (Figure 40d)), identical to that observed for the CueO of *E. coli*, (Roberts *et al.*, 2002) but lower than CotA laccase or McoA that show an optimal temperature for activity around 75ºC (Martins *et al.*, 2002; Fernandes *et al.*, 2007). The steady state kinetic parameters of recombinant McoC were obtained from substrate saturation curves for the metal ion Cu(I), for ferrous sulfate Fe(II)SO_4 and also for the typical laccase substrates ABTS (non-phenolic), SGZ and 2,6-DMP (phenolics) in air saturated solutions, at 37 ºC. The dependence of the enzymatic rate on the substrate concentration followed Michaelis–Menten kinetics (Table 21).

Table 21 - Kinetic parameters for oxidation of the metal ions Cu(I), Fe(II) and the typical laccase substrates ABTS, SGZ and 2,6-DMP of the purified recombinant McoC from *C. jejuni*

Substrate	K_m/μM	k_{cat}/min^{-1}	k_{cat}/K_m/ min^{-1} μM^{-1}
Cu(I)	128 ± 25	1038 ± 89	8.1
Fe(II)	30 ± 4	34 ± 1.3	1.1
ABTS	791 ± 106	466 ± 22	0.59
SGZ	35 ± 2	10 ± 0.1	0.29
2,6-DMP	227 ± 36	0.70 ± 0.02	0.003
O_2 (ABTS)	31 ± 4	247 ± 10	8.0

These results showed that recombinant McoC is clearly a metallo-oxidase, exhibiting higher enzyme efficiency (k_{cat}/K_m) towards the oxidation of the metal ions than for the oxidation of aromatic substrates. The kinetic constants of McoC for Cu(I) are in the same range as those obtained for *E. coli* CueO, but quite different than the ones obtained for the yeast ferroxidase Fet3p, human ceruloplasmin (hCp) or McoA (Fernandes *et al.*, 2007; Singh *et al.*, 2004; Stoj and Kosman, 2003)

indicating that McoC is most likely a cuprous oxidase enzyme. Although the efficiency (k_{cat}/K_m) of McoC towards Fe(II) is 8 times lower than the one obtained for Cu(I), it is still higher than the efficiency observed towards all of the aromatic substrates tested, and in the same range as exhibited by CueO (Tables 21 and 22). The greatly diminished activity of McoC towards aromatic substrates compared to its bacterial homologue CotA laccase (Tables 21 and 22) strengthens the fact that McoC does not function as a phenoloxidase but instead as a metallo-oxidase.

Table 22 - Catalytic efficiency of McoC homologues; CotA laccase from *B. subtilis* (Durão *et al.*, 2008a), **CueO from *E. coli*** (Singh *et al.,* 2004), **McoA from *Aquifex aeolicus*** (Fernandes *et al.*, 2007), **Fetp3 from yeast and human ceruloplasmin (hCp)** (Stoj and Kosman, 2003).

	Substrate	k_{cat}/K_m/min^{-1} μM^{-1}
CotA laccase	ABTS	156.0
	SGZ	267.0
	2,6-DMP	8.1
CueO	Cu(I)	5.5
	Fe(II)	1.7[a]
McoA	Cu(I)	1.6
	Fe(II)	3.4
Fet3p	Cu(I)	2.1[b]
	Fe(II)	11.8[b]
hCp	Cu(I)	0.6[b]
	Fe(II)	3.6[b]

[a] Only measurable when in the presence of endogenous Cu(II).
[b] Values calculated based in the referred references.

The dioxygen-binding affinity, determined by measuring the initial rate of oxygen consumption, has also been investigated as a function of varying concentrations of dioxygen. The result obtained for the recombinant McoC (K_m (O_2) of 31 ± 4 mM) is within the same range of values reported for other MCOs (Chen *et al.*, 2010; Ueki *et al.*, 2006; Xu, 2001).

The overall structure of McoC

McoC has a typical laccase fold with three cupredoxin-like domains. However, there are some slight differences from the customary conformation (Figure 41a)) with domain 1 (residues 43–203) consisting of eight β-strands, while domains 2 (residues 212–353) and 3 (residues 373–513) comprise eleven β-strands each. Figure 41b) and c) enable a comparison of McoC with its bacterial homologues CotA laccase (36% sequence similarity, PDB:1W6L) (Bento *et al.*, 2005) and CueO (42% sequence similarity, PDB:1N68) (Kataoka *et al.*, 2007). Major differences were observed mainly at the protein surface in close proximity to the T1 copper centre, in the region of the substrate binding site (*vide infra*). Superposition of the McoC structure onto the CueO and CotA laccase structures, performed by Secondary Structure Matching (SSM) (CCP4, 1994), gave root mean square deviations of only 1.712Å and 1.670Å, respectively. Besides differing in β-strand lengths and disposition within the same β-barrel, in loop sizes and in the number of α-helices and 3_{10}-helices, all three MCOs retain a similar location for the C-terminus whereas the position of the N-terminus varies. In the McoC structure, in addition to the 22 amino acid residues corresponding to the putative signal peptide, 20 further residues in the protein N-terminus were not visible in the structure. Ten of these are not identifiable by MALDI-TOF-MS and the remaining 10 are apparently highly disordered in the structure. However, the McoC N-terminal domain still contains a long starting loop that spans over the top of the molecule and extends all the way towards domain 3; in CotA and CueO the equivalent loop is smaller starting on the proximity of the interface between domains 1 and 2, and not crossing the molecule over the top in either case (Figures 41a)–c)).

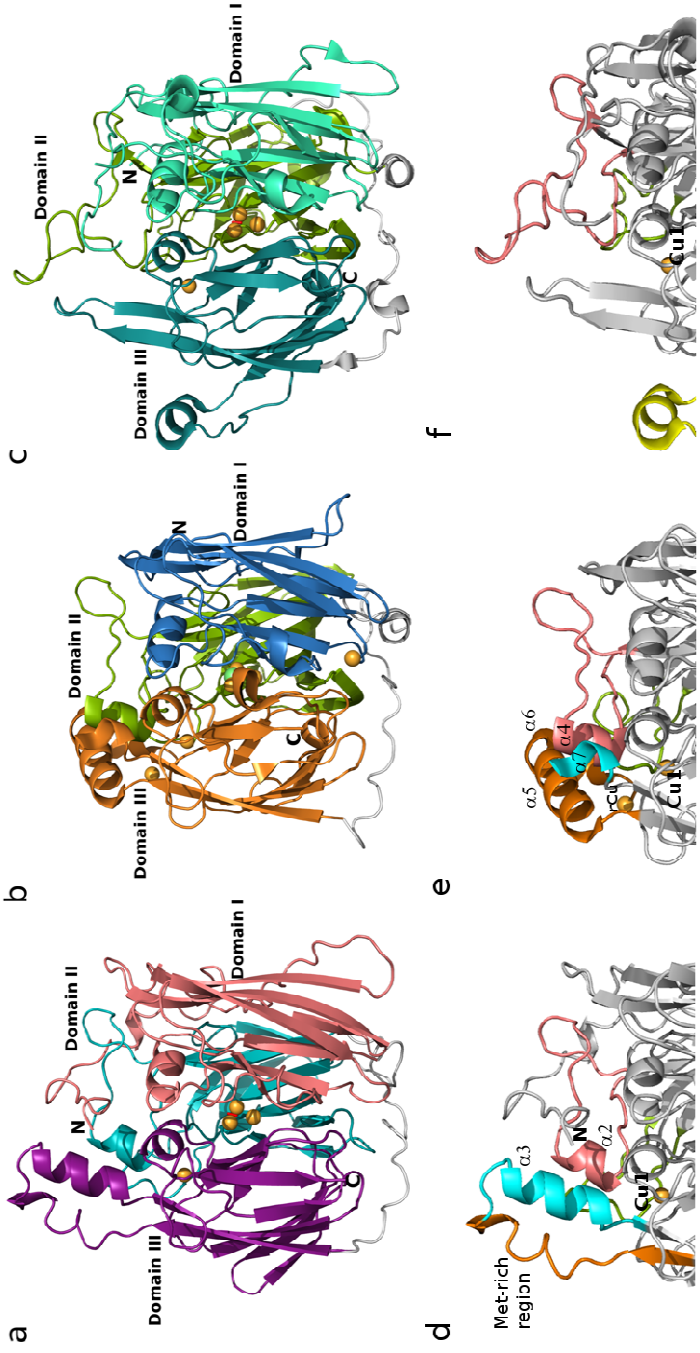

Figure 41 - Overall three-dimensional structure of McoC (a, d), CueO (PDB:1N68) (Roberts *et al.*, 2003) **(b, e) and CotA laccase (PDB:1W6L)** (Bento *et al.*, 2005) **(c, f).** Upper panel (a–c): Tripartite cupredoxin-domain organization with the mononuclear T1 Cu site located in domain 3 and the trinuclear cluster placed at the interface between domains 1 and 3. Lower panel (d–f): Major structural differences are observed at the protein surface, near the T1 Cu site. Highlighted are secondary structure elements interfering with the access to this site: N-terminal loop and other loops; α-helices; and Met-rich regions. The same colour code is used for corresponding regions between structures. Cu ions are represented as dark-yellow spheres, with a fifth regulatory Cu ion (rCu) identified in the CueO structure, near the T1 Cu site, and a sixth one near the exit channel with no apparent functional importance and only partially occupied (Roberts *et al.*, 2003).

In all three laccases, the linker peptides connecting the domains are placed at the bottom of the structure, constituting an external feature (Figures 41a)–c), in grey).

The copper binding sites

The crystal structure of McoC contains four copper atoms with the same spatial arrangement, relative to the polypeptide chains, as other members of the MCO family of enzymes (ascorbate oxidase, Fet3p and laccases in general). A mononuclear blue copper centre or T1 site is placed in domain 3 and a trinuclear cluster (T2/T3 site) is embedded in the interface between domains 1 and 3 (Figures 41a) and 42). The T1 Cu is coordinated by two histidines, a cysteine and a fourth axial "soft" ligand methionine, which confers distorted tetrahedral coordination geometry at this centre (Figure 42a) and b) and Table S7). The trinuclear site (Figure 42a) and c)), composed of two T3 and one T2 copper ions, is coordinated by four HXH structural motifs, 2 pairs coming from domain 1 and two other from domain 3. Each T3 Cu binds to three histidine residues whereas T2 Cu (Cu4) binds to two histidine residues (Figure 42 and Table S7). In a similar manner to other MCOs, the mononuclear Cu site interacts with the trinuclear cluster via the highly conserved HCH motif, where the cysteine binding to the T1 Cu shuttles electrons via the intramolecular pathway (13.0/12.3 Å for Cu2/Cu3), to each of the adjacent histidines binding to one of the T3 copper ions (His496 for Cu2 and His494 for Cu3) (Solomon *et al.*, 1996). Refinement of the occupancies of the copper ions in the McoC structure showed full occupancy for the T1 Cu centre, but substantial Cu depletion for the trinuclear centre. Occupancies of 60% and 30% were obtained for the T3

copper ions, Cu2 and Cu3, respectively, but only 20% for the T2 ion, Cu4 (Figure 42c) and Table S7).

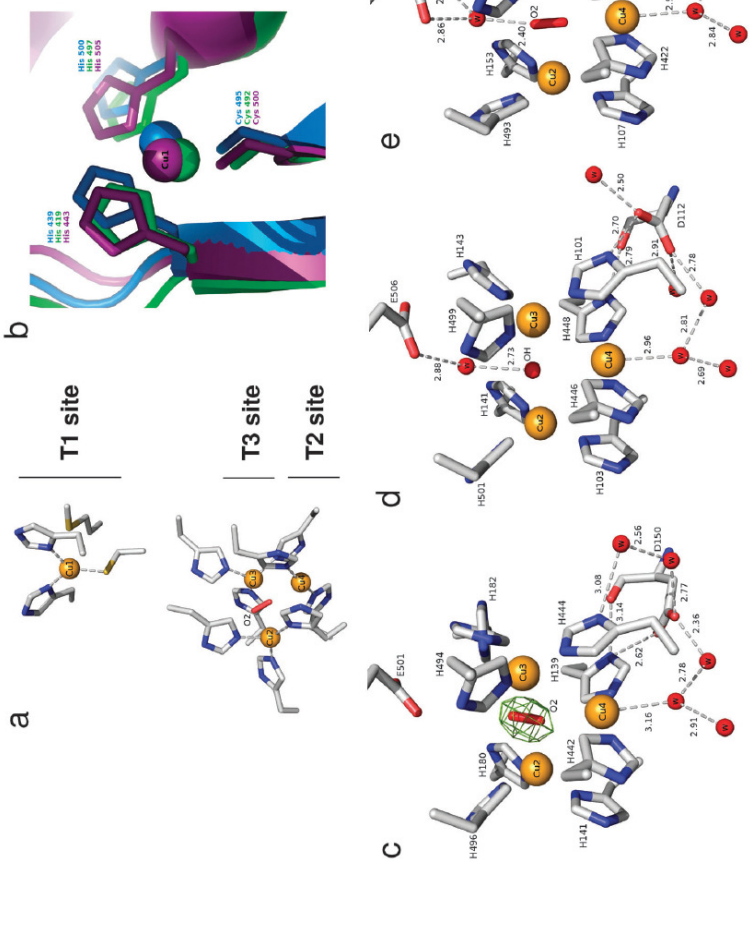

Figure 42 - (a) Overall organization of the catalytic motif in the MCO family of enzymes, comprising a mononuclear copper site and a trinuclear cluster. (b) Superposition of the mononuclear copper centres of McoC (blue), **CueO** (purple) **and CotA laccase** (green). **(c–e) Structural detail of the trinuclear centre and its neighbourhood in McoC (c), CueO (d, PDB:1KV7) and CotA laccase (e, PDB:1W6L).** Important acidic residues placed in the entrance and exit channels are identified (Glu and Asp residues, respectively). Cu ions are represented as spheres. In panel (c) the electron density for the molecular oxygen is derived from omit Fourier synthesis computed with Sigma A weighted coefficients $|Fo|-|Fc|$, where the dioxygen was not included in the structure factor calculations; the contour level is 5.0 rms.

As observed for other MCOs the T2 copper appears to be the most labile. A protein copper content of 6.4 atoms per polypeptide chain is reported by Hall *et al.* (Hall *et al.*, 2008) for *C. jejuni Cj1516* (strain NCTC 11168) and such a contrast with the present crystal structure presumably results from the different expression protocols and strains used and possibly the crystallisation conditions. In between the type 3 copper ions the dioxygen species was refined with occupancy of 60%, corresponding to the occupancy for Cu2 (Figure 42c)).

In a similar way to its bacterial homologues, McoC also has two well-defined solvent channels formed mainly by polar and neutral residues, giving clear access to the trinuclear cluster. McoC maintains a carboxylate moiety, Glu501 (equivalent residues in CotA (Bento *et al.*, 2005; Chen *et al.*, 2010), CueO (Roberts *et al.*, 2002; Kataoka *et al.*, 2009) and Fet3p (Kataoka *et al.*, 2009; Solomon *et al.*, 2008; Augustine *et al.*, 2007; Quintanar *et al.*, 2005) are Glu498, Glu506 and Glu487, respectively) strategically sited in the entrance channel to the trinuclear cluster (Sharma *et al.*, 2007; Chen *et al.*, 2010) and a second acidic residue, Asp150 (equivalent residues Asp116, Asp112 and Asp94 in CotA, CueO and Fet3p, respectively) placed within the exit channel (Figure 42c)). These acidic residues are believed to participate in the protonation processes required to convert dioxygen to two molecules of water (Bento *et al.*, 2005). However, unlike the CotA structure, no well-defined water molecule bridging Glu501 and the dioxygen moiety in the access channel appears to be present (Figure 42c)).

The substrate binding site

In general, MCOs are able to oxidise a wide range of aromatic compounds of different nature and size, as well as inorganic ones, such as

lower valency metal ions. Thus, these enzymes tend to lack a unique way of substrate binding, having broad binding pockets, often able to accommodate more than one type of substrate. Some, as is the case of human ceruloplasmin, appear to possess more than one binding site (Zaitsev *et al.*, 1999). For the reported structures of substrate complexed MCOs, the T1 Cu centre is sited at the bottom of the substrate binding region, relatively exposed to the solvent and interacting with the substrate molecule through the imidazole ring of one of its His ligands (His497 in CotA) (Enguita *et al.*, 2004). However, in McoC and CueO the equivalent residues, His500 and His505, are virtually buried and this constitutes a major difference between these two laccase-like MCOs and the remainder of the laccase family whose structures have been reported. Thus, in McoC, the T1 site becomes occluded by several secondary structure elements (Figure 41d)). Firstly, a Met-rich region (Figure 41d), in orange), comprising residues Met379–Gly391, blocks the site entrance and secondly two extra α-helixes, α2 and α3, placed not very far from the mononuclear Cu centre (Figure 41d), in salmon and cyan, respectively), partially hinder this substrate binding region. In this respect, the region containing the residues 383–396, and enclosing most of the Met-rich region, is somewhat disordered showing discontinuous electron density, except for His387 which is clearly defined. This is the only residue in the entire Met-rich region that establishes crystal contacts, whereas all the remaining residues are more loose and hence poorly defined in the structure. However, such crystal contacts were enough to provide some packing constraints to this loop, making it possible to be modelled. Within the Met-rich region it is likely that residues His387 to Gly391, shown as a random coil due to local disorder, comprise in fact a helix (as it resembles in Figure 41d)). Finally, the domain 2 loop (residues 327–344; Figure 41d),

in green) stretches over the substrate binding cavity, closely to the T1 Cu, and covers part of the access to this site (Figure 41d)). Thus, it is difficult to see how bulky aromatic substrates such as ABTS, which readily binds to CotA, can be easily accommodated by McoC (Figure 43d)). In CotA this region is mainly composed by apolar residues, in agreement with the enzymes' lack of specificity towards substrates (Enguita *et al.*, 2004). For CueO, the other bacterial MCO, whose structure has been reported (1N68) (Roberts *et al.*, 2003), the access to the T1 Cu site is also greatly reduced due to a large Met-rich helical region (Figure 41e), in orange). In CueO, this structural feature is shown to interfere with the access of organic substrates to the T1 Cu. Studies conducted by Kataoka *et al.* (Kataoka *et al.*, 2007), where the entire Met-rich helical region was deleted, together with α-helix 7 (Δα5–7 CueO) yield higher specificity of the truncated enzyme for bulky substrates (ABTS and p-phenylenediamine (p-PD)) than wt CueO. Nevertheless, these became comparable when in the presence of excess Cu^{2+}, and newly emerged activities are verified for some phenolic substrates (2,6-DMP, catechol, guaiacol and SGZ), with overall higher values for Δα5–7 CueO. A severe cuprous oxidase catalytic impairment is also attained for Δα5–7 CueO, while its ferroxidase activity is not affected by the truncation, becoming enhanced for both wt and truncated forms when in the presence of exogenous Cu^{2+}. For this enzyme, the presence of charged and polar residues in the active centre comes as a consequence of the higher substrate specificity (in Δα5–7 CueO a decrease of the negative potential area was observed) (Kataoka *et al.*, 2007). Similarly, in McoA when the equivalent Met-rich region (residues 321–363) was deleted, higher specificity for larger aromatic substrates is observed, while it remains unchanged for the metal substrates

tested, Cu(I) and Fe(II), suggesting that this region occludes the substrate binding site (Fernandes *et al.*, 2007). To identify possible substrate binding pockets in McoC and respective accessibility, calculations on the enzyme's solvent accessible surface near the T1 Cu were undertaken. A cavity analysis was performed on all three bacterial MCOs, using the CASTp server (Liang *et al.*, 1998) and Areamol from CCP4 programs suite (CCP4, 1994). As expected, CotA shows a higher accessible area in the proximity of the T1 Cu centre and hence higher solvent accessibility, favouring substrate binding (Figure 43a) and d)). At the other extreme, CueO shows a very limited access to the T1 Cu with a considerably low accessible area for substrates, in particular bulky ones (Figure 43c) and f)). For McoC (Figure 43b) and e)), half of the substrate binding region, identified for the binding of ABTS to CotA and located above the T1 copper site, is occluded. However, there is still some solvent accessibility suggesting substrates can bind, but less easily than for CotA. For both McoC and CueO the decrease in accessibility of the T1 Cu site becomes more evident when considering the accessibility of the histidine ligand (His500 and His505 in McoC and CueO, respectively) thought to be the initial electron acceptor (Table 23). This residue becomes non-accessible in these two MCOs. Identical results are observed for other residues placed at the bottom of CotA laccase binding pocket, in close proximity to the type 1 copper ion. This is also true for the counterparts of CotA laccase residues Ile494, His419 and even for Leu386 (in this latter case spatially equivalent to Phe405 in McoC and Asn408 in CueO), which again become non-accessible (Table 23). Other residues sited at the entrance site for ABTS, such as Pro384 in the CotA structure, also become highly concealed in McoC and CueO structures, as was seen from the accessibility of the spatially equivalent residues Met404 and Leu359, respectively (Table 23).

Therefore, in accordance with the measured kinetic parameters, McoC should be considered predominantly as a metallo-oxidase, able to accommodate and oxidise smaller compounds such as those containing the lower valency metal ions Cu^{1+} and Fe^{2+}, but showing radically reduced or non-existent affinity for aromatic substrates (Table 23).

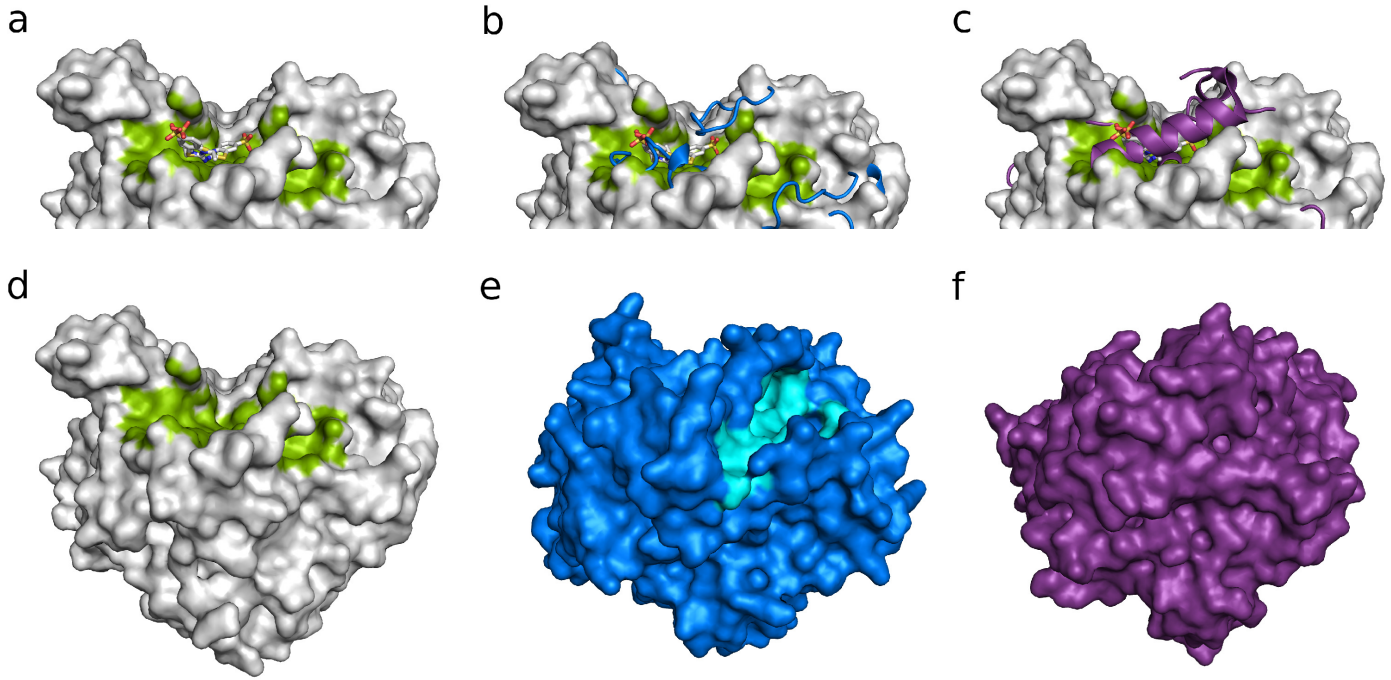

Figure 43 - Molecular surface representation and putative substrate binding sites identified for CotA laccase (PDB:1UVW), McoC and CueO (PDB:1KV7), near the T1 Cu. All molecular surface representations are in the same orientation. Cavity analysis was performed using the CASTp server. (Liang *et al.*, 1998) **(a)** CotA laccase shows a widely exposed substrate binding cavity (in green), where the bulky organic substrate ABTS has been shown to bind (Enguita *et al.*, 2004). **(b, c)** Superposition of the three-dimensional structures of McoC and CueO, respectively, onto the molecular surface and substrate binding pocket identified for CotA laccase. In both cases, secondary structure elements obstruct to some extent the binding cavity. **(d–f)** Overall molecular surface representation of CotA, McoC and CueO, with respective putative substrate binding cavities highlighted: green for CotA, cyan for McoC; for CueO the site is not visible in the orientation shown. For the latter two enzymes, a reduced access to the T1 Cu is observed, diminishing the accessibility of bulkier substrates to this site.

Table 23 - Accessible surface area (Å²) comparison of selected residues positioned at key spots on the substrate binding region of CotA laccase and their respective counterparts in McoC and CueO. Values were determined by Areamol from the CCP4 program suite (CCP4, 1994)

	Type 1 Cu ligands		Near T1 Cu (at the bottom of CotA substrate binding pocket)		ABTS entrance site
	H497/500/505	H419/H439/H443	I494/I497/L502	L386/F405/N408	P384/M404/L359
CotA	19.50	7.00	12.40	75.00	31.20
McoC	0.00	0.00	0.00	0.00	0.40
CueO	0.00	0.00	1.80	0.00	7.60

However, the possibility that McoC is able to oxidise smaller phenolic or non-phenolic substrates cannot be completely eliminated purely from structural considerations. For CueO a fifth Cu ion, buried just under the Met-rich region and close to the T1 copper site, is reported in the structure of CueO soaked with $CuCl_2$ (PDB:1N68) (Figure 44a)).

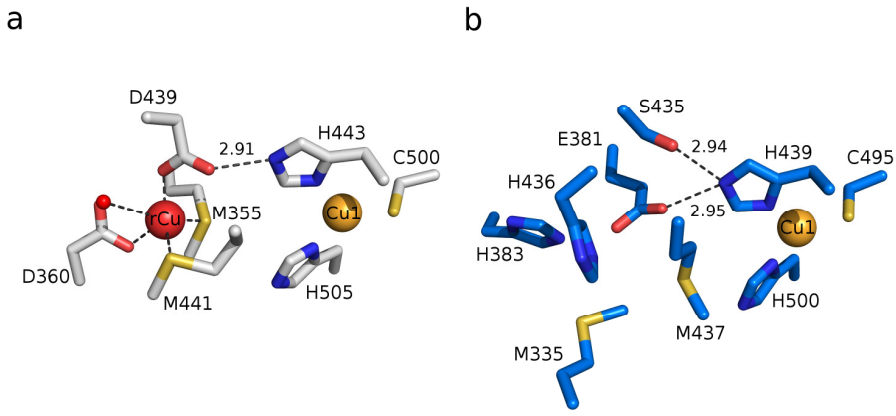

Figure 44 - (a) Representation of the regulatory copper ion site (rCu) region in the CueO structure (PDB:1N68). This site is directly linked to the T1 Cu site through a H-bond with one of its His ligands, assisting in the mediation of electrons from the substrates to the T1 Cu (Roberts *et al.*, 2003). **(b) Structurally equivalent region in McoC.** Cu ions are represented as spheres.

A regulatory role is proposed for this additional Cu ion (rCu) (Roberts *et al.*, 2003). Just recently Singh *et al.* have determined other CueO's structures, namely those of the C500S mutant bound to Cu(I) or Cu(II) (Singh *et al.*, 2011). In the former structure, besides the fifth Cu ion, two additional coppers are found binding along the Met-rich region (Singh *et al.*, 2011). Removal of those two coppers by mutation of the binding methionines into serines results in a four- and two-fold decrease of the Cu(I) and Fe(II) oxidation catalytic rates, respectively. Additionally, these sites appear to be specific for cuprous ions as neither of them was observed on the Cu(II) soaked structure of CueO. For this reason, Singh *et al.* have renamed this site from regulatory Cu site to substrate copper

site, and suggest that the Met-rich loop plays a role in the binding and oxidation of Cu(I) (Singh *et al.*, 2011). A structural comparison showed the presence of spatially equivalent residues at the rCu site in McoC (Glu381, His383, Ser435, Met437) (Figure 44b)). Furthermore, residues Met335 and His436 are also placed within very close proximity. Interestingly, in McoC, neither of the two methionines constituting this 'site' take part in the Met-rich region, whereas Glu381 and His383 do. However, in the McoC structure no additional Cu ions were observed. This is not too surprising, since copper depletion was observed in the structure even for the catalytic copper centres, as no additional copper was added either to the protein solution or to the protein crystals. Attempts are being made in order to obtain a full copper content of the McoC.

5.5 Concluding remarks

The structure of a multi-copper oxidase present in the pathogenic bacterium *Campylobacter jejuni* has been solved at 1.95Å resolution. Spectroscopic, biochemical and functional studies showed that McoC is a typical MCO, with higher efficiency (k_{cat}/K_m) towards metal ions, such as Cu(I) and Fe(II), than for the aromatic substrates ABTS, SGZ and 2,6-DMP. Similarly to its homologue CueO, McoC acts predominantly as a cuprous oxidase, although it also showed activity as a ferroxidase. The three-dimensional structure determined by X-ray studies showed that this enzyme is a three-domain laccase-like MCO, with a significantly smaller substrate binding pocket near the T1 copper site, when compared with its homologue CotA laccase. The presence of secondary structure elements partially occluding this site is likely to function as a barrier to the access of bulkier substrates. Such a site much resembles CueO from *E. coli*, for which the site cavity is even smaller. One of the secondary structure

elements hindering this site corresponds to a Met-rich region followed by an α-helix, also observed for CueO. For the latter enzyme, this region has been reported (Roberts *et al.*, 2003; Singh *et al.*, 2011) to bind additional Cu, constituting an extra Cu site proposed to have regulatory functions in electron transfer mediation during substrate oxidation, by facilitating Cu(I) binding and perhaps accelerating the oxidation rate. Such a binding site is not apparent in McoC, although residues seem to exist that could bind such copper ion. Examples of additional copper centres have also been reported for other MCOs of known structure, as is the case of human ceruloplasmin (Lindley *et al.*, 1997), phenoxazinone synthase laccase (Smith *et al.*, 2006) and holoCotA laccase (Bento *et al.*, 2010).

Altogether, these results indicate that McoC may act as a metallo-oxidase also *in vivo*, thus playing a protective role while converting Cu(I) and/or Fe(II) in *C. jejuni* towards the less toxic forms of copper and iron, Cu(II) and Fe(III). A role in copper homeostasis has also been proposed by Hall *et al.* for the recombinant MCO *Cj1516* obtained from a different strain of *C. jejuni* (NCTC11168) (Hall *et al.*, 2008).

5.6 Acknowledgements

André T. Fernandes is acknowledged for assistance with gene cloning, Manuela M. Pereira with the EPR spectrum and Smilja Todorovic with the RR spectrum of McoC. Maria Arménia Carrondo is gratefully acknowledged for support. The European Synchrotron Radiation Facility in Grenoble, France, and the Macromolecular Crystallography staff are sincerely acknowledged for provision of synchrotron radiation facilities and support. This work was supported by a project grant from the European Union (BIORENEW, FP6-2004- NMP-NI-4/026456). C.S.S.

and P.D. hold PhD fellowships from FCT, Portugal (SFRH/BD/40586/2007 and SFRH/BD/40696/2007, respectively).

Table S7 - Copper-copper and copper-ligand coordination distances and angles among bacterial laccases and other selected MCOs.

				Cu centres coordination distances (Å) and angles (°)				
Enzyme	**PDB**	**r.m.s.d. (Å)[a]**	**Sequence ID (%)**	**Type 1 Cu(1)** (occ: 1.00)[b]	**Type 2 Cu(4)** (occ: 0.20)[b]	**Type 3 Cu(2)** (occ: 0.60)[b]	**Type 3 Cu(3)** (occ: 0.30)[b]	**Cu2-Cu3**
McoC	-	-	-	His^{439} (2.03) Cys^{495} (2.29) His^{500} (2.00) Met^{505} (3.37)	His^{139} (1.94) His^{442} (1.93) O2(Oxy) (2.48) HOH (3.18)	His^{180} (1.99) His^{496} (2.17) His^{141} (1.98) O1(**Oxy**) (2.65) O2(**Oxy**) (2.19)	His^{182} (2.00) His^{494} (2.00) His^{444} (1.96) O1(**Oxy**) (2.06) O2(**Oxy**) (2.30)	Cu(2)-Cu(3) – 4.44 Cu(2)-Cu(4) – 3.60 Cu(3)-Cu(4) – 3.58 Cu(2)-O1-Cu(3) angle – 140.8° Cu(2)-O2-Cu(3) angle – 161.0°
CueO	**1KV7**	1.712	28.2	His^{443} (2.02) Cys^{500} (2.19) His^{505} (1.98) Met^{510} (3.23)	His^{101} (1.92) His^{446} (1.83) O1(OH) (3.12) HOH (2.96)	His^{141} (1.97) His^{501} (2.09) His^{103} (1.96) **OH** (2.43)	His^{143} (2.02) His^{499} (2.02) His^{448} (1.94) **OH** (2.29)	Cu(2)-Cu(3) – 4.70 Cu(2)-Cu(4) – 3.98 Cu(3)-Cu(4) – 3.54 Cu(2)-O-Cu(3) angle – 169.3°
CotA	**1W6L**	1.670	26.6	His^{419} (2.02) Cys^{492} (2.22) His^{497} (1.98) Met^{502} (3.26)	His^{105} (1.96) His^{422} (2.03) O2(Oxy) (2.42) HOH (2.98)	His^{153} (2.08) His^{493} (2.13) His^{107} (2.07) O1(**Oxy**) (2.57) O2(**Oxy**) (2.59)	His^{155} (2.11) His^{491}(2.07) His^{424} (2.04) O1(**Oxy**) (2.31) O2(**Oxy**) (2.29)	Cu(2)-Cu(3) – 4.73 Cu(2)-Cu(4) – 3.99 Cu(3)-Cu(4) – 3.66 Cu(2)-O1-Cu(3) angle – 151.4° Cu(2)-O2-Cu(3) angle – 151.8°
AO (chain A)	**1AOZ**	1.886	26.8	His^{445}(2.09) Cys^{507} (2.13) His^{512} (2.05) Met^{517} (2.90)	His^{60}(2.00) His^{448} (2.09) OH (2.02)	His^{104} (2.19) His^{508} (2.14) His^{62} (1.98) **OH** (2.06)	His^{106} (2.16) His^{506} (2.07) His^{450} (2.06) **OH** (1.99)	Cu(2)-Cu(3) – 3.69 Cu(2)-Cu(4) – 3.66 Cu(3)-Cu(4) - 3.79 Cu(2)-O-Cu(3) angle – 130.9°
MaLa (chain A)	**1GW0**	1.898	24.7	His^{431} (1.91) Cys^{503} (2.20) His^{508} (1.93) Leu^{513} (3.68)	His^{93}(1.89) His^{434} (1.92) O1(Oxy) (2.62) Cl (2.48)	His^{138} (1.94) His^{504} (1.95) His^{95} (1.90) O1(**Oxy**) (2.48) O2(**Oxy**) (2.66)	His^{140} (1.96) His^{502} (1.97) His^{436} (1.92) O1(**Oxy**) (2.59) O2(**Oxy**) (2.38)	Cu(2)-Cu(3) – 4.91 Cu(2)-Cu(4) – 4.16 Cu(3)-Cu(4) – 3.92 Cu(2)-O1-Cu(3) angle – 153.4° Cu(2)-O2-Cu(3) angle – 151.5°
TvLa	**1GYC**	2.114	23.0	His^{395} (2.02) Cys^{453} (2.19) His^{458} (2.04) Phe^{463} (---)	His^{64} (2.01) His^{398} (1.97) HOH (2.35)	His^{109} (2.12) His^{454} (2.17) His^{66} (2.15) **OH** (2.08)	His^{111} (2.23) His^{452} (2.16) His^{400} (2.12) **OH** (2.19)	Cu(2)-Cu(3) – 3.91 Cu(2)-Cu(4) – 3.81 Cu(3)-Cu(4) – 3.82 Cu(2)-O-Cu(3) angle – 132.9°

McoC *Campylobacter jejuni*; CueO *Escherichia coli* (Roberts *et al.*, 2002); CotA *Bacillus subtilis* (Bento *et al.*, 2005); Ascorbate oxidase (AO) *Cucurbita pepo* (Messerschmidt *et al.*, 1992); MaLa *Melanocarpus albomyces* (Hakulinen *et al.*, 2002); TvLa *Trametes versicolor* (Piontek *et al.*, 2002)
a Determined by structural superposition with McoC by Secondary Structure Matching (CCP4, 1994); b Copper occupancy in McoC copper centres.
CueO structure (PDB:1KV7) was considered as deposited, that is, with a monoatomic oxygen species in between both type 3 Cu ions, although later reports by Roberts *et al.* (Roberts *et al.*, 2003) have claimed to believe that this should in fact be considered a chlorine atom.

CHAPTER 6

GENERAL DISCUSSION

6.1 Modulation of the redox potential at the T1 Cu site of laccases

Multi-copper oxidases (MCOs) are responsible for coupling the one-electron oxidation of four substrate molecules with the four-electron reduction of dioxygen to two molecules of water. Included in this family of enzymes are the laccases, which make up their simplest representative members, therefore constituting good model systems for structure-function studies in MCOs. Laccases are capable of oxidising a wide range of substrate molecules, varying from aromatic to inorganic compounds. Such versatility and the use of readily available oxygen as the final electron acceptor makes these enzymes interesting biocatalysts for biotechnological purposes.

Oxidation of the reducing substrate at the T1 Cu centre is considered to be the catalytic rate-limiting step for these enzymes, being predominantly governed by the redox potential difference between the T1 Cu ($E°_{T1}$) and the substrate molecule ($E°_{S}$) (Solomon *et al.*, 1996; Xu, 1996; Garzillo *et al.*, 1998). Therefore, at a first stage, our studies aimed at gaining a better understanding on the modulation of the redox potential at this site, using CotA laccase as the model system.

Previous studies have investigated the effect of the non-coordinating hydrophobic residues, leucine and phenylalanine, natural variants at the T1 Cu site axial ligand position in fungal laccases, on their high redox potential at that site. With that purpose, Durão and co-workers (Durão *et al.*, 2006) replaced the weak axial Met502 ligand of the T1 Cu site of CotA laccase by Leu and Phe using site-directed mutagenesis. Comparison of the X-ray structures of these mutants with the wild-type CotA evidenced only a slight movement of the mutated residues towards the protein surface, no longer coordinating to the T1 Cu and slightly increasing the

exposure of this site to the solvent. Moreover, the produced mutations led to an increase in the redox potential of the site by approximately 100 and 60mV for the M502L and M502F mutants, respectively, relatively to the native enzyme, as well as a decrease in their turnover rates attributed to a possible change in the electronic tunnelling, as no direct correlation was observed between the redox potentials and the observed oxidation rates (Durão *et al.*, 2006). Similar site-directed mutagenesis studies at the T1 site have also been applied mostly to simple blue copper proteins (e.g. Marshall *et al.*, 2009) and a few other MCOs (Palmer *et al.*, 1999 and 2003; Xu *et al.*, 1999), showing that changes on the axial ligand of the T1 site is a key factor in the modulation of the site's redox potential, tuning it by around 100mV. Overall, these studies showed that subtle rearrangements in the direct coordination sphere of the T1 Cu site significantly affect the properties of the site.

With the present study we have taken a step further by investigating the role of the hydrophobic environment of the T1 Cu site, namely the hydrophobic patch framing its His497 ligand (thought to be the primary electron acceptor), in order to investigate the effect of solvent accessibility in the modulation of the redox potential at this site. To address this question, site-directed mutagenesis was used to replace the hydrophobic residues Ile494 and Leu386 placed at the vicinity of the T1 Cu site, by alanine residues. Comparison of the X-ray structures with the native CotA showed that for the L386A mutant the T1 Cu site is barely perturbed, whereas in the I494A mutant the shortening of the residue led to an increased accessibility of the site to the solvent allowing for a water molecule to interact with the T1 Cu, changing the site coordination geometry. This increased solvent accessibility led to a decrease of the T1 Cu site redox potential in both mutants, more pronounced for the I494A

mutant (60mV *vs* 100mV for L386A and I494A mutants, respectively), which correlates well with the decreased reactivity observed for both mutants compared with the wild-type CotA.

Based on structural studies performed on the fungal laccase from *Trametes trogii*, Matera and co-workers (Matera *et al.*, 2008) have suggested that several mutations would be needed near the T1 Cu site in order to tune the redox potential of the site by as much as 300mV. Matera and co-workers have identified a large number of hydrophobic residues in the near surroundings of the T1 Cu site: Phe460 and Ile452 (corresponding to Met502 and Ile494 in CotA laccase), as well as Phe336, Phe329, Phe396, Ala389 and Ile338 surrounding the Phe460 (and corresponding to Leu386, Leu374, Ile421, Thr415 and Leu388, respectively in CotA laccase), that could possibly be contributing to the high redox potential observed for this enzyme (760mV) (Matera *et al.*, 2008). Furthermore, studies performed by Marshall and co-workers (Marshall *et al.*, 2009) focused precisely on the effect of two important secondary coordination sphere interactions, hydrophobicity and hydrogen-bonding, on the T1 Cu site redox potential of the cupredoxin azurin (E^o=265mV at pH7.0). Through a rational approach, Marshall and co-workers were able to fine tune azurin's reduction potential over a 700mV range without perturbing the metal binding site beyond the typical for this family of proteins, also demonstrating that the effects from individual structural features are additive. Mutation of the Asn47 (N47) placed at ~5.5Å away from the T1 Cu into a serine (based on studies performed on rusticyanin) led to a redox potential increase of ~130mV, as a result of the strengthening of the hydrogen-bonding interactions between two ligand-containing loops, adding rigidity to these loops and influencing the direct hydrogen bonds between the backbone of the protein and the Cys ligand (Marshall *et al.*,

2009). Since the axial ligand Met121 (M121) influences differently the T1 Cu site, Marshall and co-workers set to investigate if the individual effects of each one of these two residues would be additive. Indeed, for both double mutants N47S/M121Q and N47S/M121L, a linear dependence of the redox potential on the hydrophobicity of the axial residue was observed, with N47S mutation exerting similar effects as before, resulting in a redox potential maximal increase of ~230mV for the N47S/M121L double mutant (Marshall *et al.*, 2009). Unlike other cupredoxins, azurin possesses a fifth ligand interacting with its T1 Cu ion, preferentially stabilizing the oxidised form of the Cu and therefore lowering its redox potential. For this reason, and because the carbonyl oxygen itself cannot be changed by site directed mutagenesis, Phe114 placed in proximity to Gly45 was found to be a good candidate to affect the carbonyl either by steric repulsion or hydrogen bonding. This residue was mutated into an asparagine (F114N) to observe the effect of introducing a hydrogen-bonding group at that position. Combination of N47S/F114N mutations resulted in a redox potential increase by ~230mV, whereas the triple mutant N47S/F114N/M121L yielded an increase of ~375mV, up to 640mV (Marshall *et al.*, 2009).

Identification and understanding of the molecular factors that dictate the fine-tuning of an enzyme's redox potential over a broad range, with little change on the redox-active site or electron-transfer steps, is of utmost importance, not only to advance our fundamental knowledge on the redox processes but also for design of redox-active proteins yielding tailor-made redox potentials.

Altogether, our results and those reported in the literature point to a concerted influence of different factors on the modulation of the redox potential of the T1 Cu site among laccases. Such factors include the

copper ligation pattern and charge dipole distribution around the copper, polarity of the protein environment, solvent accessibility and internal hydrogen-bonding to the T1 Cu ligands (Xu *et al.*, 1996; Marshall *et al.*, 2009). Furthermore, our results indicate that modulation of the T1 Cu centre redox potential may be accomplished without compromising the overall reactivity of the site through changes in residues located outside its immediate contact shell.

6.2 Role of the single disulfide bridge of CotA laccase

Originally from the outer layer of the spore coat from *Bacillus subtilis*, CotA laccase is an enzyme with acquainted thermostability and thermoactivity properties (Martins *et al.*, 2002). For this reason we proposed ourselves to assess the effect of the single disulfide bridge (Cys229-Cys322) present in this enzyme's structure as a possible molecular determinant of the enzyme's stability.

Disulfide bridges are established once a protein has acquired its three-dimensional structure, hence not being responsible for the acquisition of the proper fold itself but exerting an important role for the stabilization of the final protein structure (Price and Stevens, 2001). These can be established between cysteine residues contained within a same domain or subunit or between different subunits, in the latter case contributing to an augmented stability of the protein. Such stability results from the reduced conformational entropy of the unfolded protein state, thus decreasing the entropy gain upon unfolding (Vieille *et al.*, 2001).

In CotA laccase the single disulfide bridge is intra-domain, being located in domain II as part of a loop that flanks one of the edges of the enzyme's substrate binding site. Structurally, the disruption of this covalent bond by

site-directed mutation of Cys322 into an alanine conferred only a slightly altered configuration to the enzyme's binding pocket, as a result of the loop moving some 8Å away towards the solvent side. Consequently, the solvent accessibility to the T1 Cu site increased, with a concomitant decrease of the site's redox potential (in line with the studies reported in the previous section) and with an apparent influence over the incorporation of Cu at the T1 Cu site. Indeed, biochemical data showed that although the disulfide bridge does not affect the enzyme's catalytic, thermodynamic and thermostability properties, it is involved in its conformational dynamics with implications on the rates of copper uptake or loss from the copper centres. For the C322A mutant, Cu release from the holo form or binding to the apo form occurs faster than for the native CotA laccase, with the particularity of the binding rates being higher for the T1 Cu site as compared to the binuclear T3 centre, for both mutant and native forms. Such results point to the occurrence of a sequential process of copper incorporation, in agreement with the studies reported by Durão *et al.* (Durão *et al.*, 2008a). Using UV/visible and EPR spectroscopies, Durão *et al.* showed that in the presence of four Cu^{1+} equivalents, provided sequentially, the apoCotA incorporates copper first at the T1 and T2 sites, with a slight preference for the T1 Cu, followed by the T3 site (Durão *et al.*, 2008a). Similar studies performed by Galli and co-workers (Galli *et al.*, 2004), on the CotA homologue from *E. coli* (CueO), reported a similar sequential process for Cu reconstitution into this enzyme.

Additionally, structural unfolding studies revealed that not only the C322A mutant unfolds faster than the wild-type CotA (for both their holo and apo forms), but also suggests an important role of the copper in the stabilization of the proteins three-dimensional structure, as an

almost 100-fold faster unfolding rate was observed for the apo forms of the enzymes.

In sum, the single disulfide bridge present in CotA laccase seems to be relevant for the stabilization of the loop next to the T1 Cu centre, propitiating the right environment for Cu incorporation at this site.

Hence, in CotA laccase, other factors such as non-covalent interactions (e.g. hydrogen bonds, electrostatic interactions, ion pairs, van der Walls forces, hydrophobic interactions), amino acid composition, binding and coordination of the Cu cofactor (Price and Stevens, 2001; Creighton, 1996; Bushmarina *et al.*, 2006) must be in the basis of the enzyme's intrinsic stability when compared to other MCOs, although no dedicated studies exist that approach this matter.

Other examples of MCOs containing disulfide bridges are the human ceruloplasmin (hCp), which possesses five intra-domain disulfide bridges located in domains 1 to 5, where they serve to anchor the last strand of each domain (Zaitseva *et al.*, 1996); and the fungal laccase from *Melanocarpus albomyces* (MaLa), containing three disulfide bridges: the intra-domain bonds Cys4-Cys12 located at domain 1 and Cys298-Cys332 located in domain 2, near the substrate binding site, and the inter-domain bond, Cys114-Cys540, located between domains 1 and 3 (Hakulinen *et al.*, 2002). However, the influence of these structural elements, in all these examples, has not been investigated so far.

6.3 Mechanisms underlying dioxygen reduction in MCOs

Over the past decade the mechanism of dioxygen reduction to water in MCOs has been the object of intense studies by many groups, aiming to understand the molecular basis underlying this catalytic process (e.g. Messerschmidt *et al.*, 1993; Shin *et al.*, 1996; Solomon *et al.*, 2008; Bento *et al.*, 2005; Ferraroni *et al.*, 2012). Although a consensus has emerged over the way the electrons are captured from the reducing substrate and transferred from the T1 Cu to the trinuclear centre, various distinct mechanisms have been proposed for the dioxygen reduction process. Some of these are based predominantly on a structural and biochemical background (Messerschmidt *et al.*, 1993; Bento *et al.*, 2005; Ferraroni *et al.*, 2005), whereas others are mainly based on biochemical and spectroscopic information (Solomon *et al.*, 1996; Shin *et al.*, 1996). Overall, the proposed mechanisms have allowed the identification of the main catalytic stages of the dioxygen reduction process. A common feature between the proposed mechanisms is the number of electron transfer steps occurring per catalytic cycle (two electron steps); additionally, all mechanisms agree on the existence of a peroxide intermediate, as well as a state where a hydroxyl moiety bridges the two T3 Cu ions. Yet, considerable controversy exists in terms of the nature of the resting state of the enzymes and the mechanisms of protonation. In this perspective, the studies reported in this thesis have been aimed at gaining a better understanding of these questions, mainly through a structure-based (X-ray crystallography) approach and using CotA laccase as the model system.

6.3.1 The resting state of the enzyme

For the vast majority of studies on MCOs, the native state has been considered to be characterized by the presence of a hydroxyl species in between the two T3 Cu atoms (e.g. Solomon *et al.*, 1996 and 2008; Piontek *et al.*, 2002; Messerschmidt *et al.*, 1992 and 1993). Moreover, the spectral absorption shoulder detected at 330nm has also been associated to this state (Solomon *et al.*, 1996). However, for the CotA laccase, this hydroxyl moiety has only been reported for a semi-reduced form of the enzyme (Bento *et al.*, 2010), with all the other structures showing a dioxygen moiety at this position (Bento *et al.*, 2005, Durão *et al.*, 2008b; Chen *et al.*, 2010). In order to investigate the nature of the native state in CotA laccase, the structures of the holo-protein and of the oxidised form of the apo-protein, which had previously been reconstituted *in vitro* with Cu (I), have been determined. Analysis of such structures has unequivocally shown that holoCotA possesses a dioxygen moiety between the T3 Cu ions, while the apoCu(I) form has a monoatomic oxygen moiety, modelled as a hydroxyl ion. Furthermore, spectroscopic analysis of both, crystals (before and after data collection) and protein solutions, of the holoCotA and apoCu(I) forms, always showed the presence of the characteristic shoulder at around 330nm, in addition to the intense peak at 610nm due to the presence of an oxidised type 1 copper centre (Bento *et al.*, 2010). These results implicate that the shoulder observed at 330nm is not exclusive to a hydroxyl bridging moiety at the T3 Cu site, but may indicate effective coupling of the two T3 copper ions by other moieties including dioxygen species. As such, different resting states can exist for different MCOs.

6.3.2 Proton-transfer mechanisms in MCOs

In this thesis, the determination of the X-ray structure of two new forms of CotA laccase, the holoCotA and the apoCu(I) CotA, has provided support for the dioxygen reduction mechanism proposed by Bento and co-workers (Bento *et al.*, 2005). Moreover, a newly reported structure on the *Trametes hirsuta* laccase, where two hydroxyl moieties were observed bridging at the trinuclear cluster (Polyakov *et al.*, 2009), has provided experimental evidences for one of the intermediate stages of the mechanism, further strengthening its plausibility. In the proposed mechanism (Bento *et al.*, 2005 and 2010), the first stage involves the movement of dioxygen into the trinuclear cluster, so that it is symmetrically positioned between the two T3 copper ions ("resting state"). The provision of two electrons, one from each of the T3 Cu ions, results in a peroxide species (O_2^{2-}, "peroxide intermediate") that splits into two hydroxide ions, after two further electrons and two protons. Along with a site structural reorganization these then migrate sequentially across the cluster, remaining bound to the T2 Cu, and now oriented in the exit channel. Finally, after the sequential addition of two further protons, two water molecules are released and the enzyme is able to uptake another dioxygen molecule.

Through a combination of mutagenesis, structural, biochemical and simulation studies we identified the structurally conserved Glu498 and the sequentially conserved Asp116, two acidic residues placed within the entrance and exit channels of CotA laccase, respectively, as the residues responsible for the protonation events taking place during the enzyme's catalytic mechanism.

Indeed, Glu498 was identified as the only proton-active group present in the vicinity of the trinuclear centre; moreover, the E498D mutant is the

only one still able to retain some enzymatic activity, whereas the absence of the carboxylate group in the E498L and E498T mutants resulted in non-active enzymes. An overall destabilization of the Cu centres was also observed in all three mutants. As such, Glu498 is though to play a decisive role in the protonation mechanisms of CotA laccase, channelling protons during the reduction process and possibly stabilizing the site as a whole (Durão *et al.*, 2008b).

On the other hand, Asp116 was found to be fully ionized. Removal of the negative charge in the D116A and D116N mutants yielded no effect on the water network through which this residue interacts with the T2 Cu, whereas in the D116E mutant the connectivity of this water network was perturbed, as a result from the rotation of the residue's longer side chain towards the protein interior. Furthermore, a change in the protonation profile of Glu498 was observed for the D116A and D116N mutants, conversely to what was verified in the D116E mutant where both, Glu116 and Glu498 protonation profiles remained similar to those of native CotA. However, the D116E mutant shows only some residual activity with the catalytic properties of all three mutants being severely compromised (Brissos *et al.*, 2012). This suggests that Asp116 not only has a key role in the modulation of the protonation events occurring during catalysis, but is also fundamental for maintaining the local geometry and water connectivity at the trinuclear site.

Moreover, the three Asp116 mutants were shown to be in a peroxide intermediate state. For all the CotA forms/mutants studied in the present dissertation, the experimental starting point is equivalent to the reduced state of the enzyme (owing to microaerophilic cell growth conditions (Durão *et al.*, 2008a)), binding dioxygen as soon as it becomes available. This is then reduced by four electrons coming from the reduced coppers

(Cu^{+}) and split into two hydroxide moieties after the provision of two protons. However, for the Asp116 mutants the supply of protons at these initial steps is compromised. Therefore, such an intermediate state emerges from the lack of adequate protonation characteristics of the surrounding E498 in the case of the D116A and D116N mutants (arrested non-active enzymes); and from the much slower activity rate of the enzyme, in the case of the D116E mutant.

Mutagenesis studies performed in other MCOs have reported similar roles for these two acidic residues, with some variations verified for the Asp placed at the solvent exit channel. In fact, overall, Glu498-counterparts are recognized as an important proton-donor during the reductive cleavage of dioxygen to water also in CueO and Fet3p (Kataoka *et al.*, 2009; Augustine *et al.*, 2007; Solomon *et al.*, 2008). In its turn, additional roles have been attributed to the Asp116-counterparts in MCOs of different origins. Examples of these is the involvement of this residue in the binding of dioxygen at the trinuclear cluster of the prokaryotic CueO from *E. coli* (Ueki *et al.*, 2006); and the structural role suggested in the fungal bilirubin oxidase from *M. verrucaria*, as a result from copper depletion and inability to reincorporate it in the mutant enzymes (Kataoka *et al.*, 2005). Such a structural role was also suggested for the eukaryotic yeast Fet3p (Quintanar *et al.*, 2005; Augustine *et al.*, 2007). In CotA laccase no evidences exist for such roles.

With the reported studies we have therefore elucidated into more detail the protonation events occurring during the dioxygen reduction mechanism in CotA laccase (and MCOs in general). However, not everything related with catalysis is due to this proton transfer step; a bond needs to break and the resultant water molecules need to leave the active site. The exact mechanism by which the hydroxyl species or water

molecules produced during the catalytic process pass through the T2 Cu in the exit channel remains to be clarified and further studies are required to address this question. Nonetheless, it is likely that such migration involves a spatial displacement of the T2 Cu, as it is the most labile of the four Cu ions with only two His ligands.

6.4 The multi-copper oxidase McoC: functional role as a cuprous oxidase

Amongst all MCOs whose structures have been reported to date, the bacterial ones remain far less well characterized. However, in recent years, an increasing number of laccases or laccase-like proteins have been identified in many gram-negative and gram-positive bacteria, even in thermophilic organisms, with consequent increasing interest in their study.

In the present dissertation we solved the crystal structure of a new bacterial MCO, McoC, from the pathogenic bacterium *Campylobacter jejuni* CGUC11284. Our studies show that McoC presents the characteristic fold and spectroscopic properties of this family of enzymes; moreover, it provides evidence that McoC behaves essentially as a metallo-oxidase, exhibiting higher enzyme efficiency towards lower valency metal ions, and in particular for Cu(I) (specificity as a cuprous oxidase), than for bulky aromatic substrates. Contributing to this are a Met-rich region and other secondary structure elements (essentially helices and loops) placed near the T1 Cu site, that partially occlude the substrate binding site of the enzyme, possibly functioning as a barrier to the access of bulkier substrates. Such a Met-rich segment is also present in CueO and other proteins involved in copper homeostasis, therefore considered to be critical for Cu handling (binding and transport) (Roberts *et al.*, 2003;

Singh *et al.*, 2011). In CueO, this segment (residues 355-399, 14 Met), comprising an N-terminal Met-rich helical region and a C-terminal highly mobile segment rich in Met and His residues (Singh *et al.*, 2011), has been shown to block solvent access to the T1 site (buried in the protein interior) and to contribute ligands to an additional copper-binding site that must be occupied for full CueO activity (Roberts *et al.*, 2002 and 2003; Kataoka *et al.*, 2007). Indeed, in the structure of CueO soaked with $CuCl_2$ (PDB id:1N68) (Roberts *et al.*, 2003) a fifth Cu ion was found to be buried just under the Met-rich helical region and in close proximity to the T1 Cu site, at a distance of 7.5Å from the protein surface. This fifth Cu ion binds directly to the Met-rich helical region through Met355 and Asp360, being simultaneously coordinated by Asp439 and Met441, two residues placed in close proximity of the T1 Cu site, and a water molecule. In such a configuration, Asp439 is at the same time hydrogen-bonded to His443 (a T1 Cu ligand), producing a link between the T1 Cu centre and the fifth Cu ion, hypothesized to be involved in electron transfer mediation during substrate oxidation (Roberts *et al.*, 2003). In fact, disruption of this additional Cu site led to a reduced or lost copper oxidase activity *in vitro* and Cu tolerance *in vivo*, with a more pronounced effect on mutants integrating the Met-rich helix (Met355 or Asp360). As such, Roberts *et al.* (Roberts *et al.*, 2003) proposed a regulatory role for this labile Cu (rCu).

Although such a binding site is not apparent in the determined structure of McoC, spatially equivalent residues exist that could form such a site (Glu381, His383, Ser435 and Met 437), together with other residues placed in close proximity (Met335 and His436). Remarkably, in McoC structure both Ser435 and Glu381 are hydrogen-bonded to His439, the

equivalent T1 Cu ligand, further suggesting the formation of such a site when in the presence of excess exogenous copper.

Recently, Singh *et al.* set to investigate more thoroughly the functional role of the Met-rich sequence in CueO (Singh *et al.*, 2011). With that purpose, firstly, they investigated the role of the T1 Cu in the loading of substrate Cu at the regulatory site (rCu) and along the rest of the Met-rich segment, by mutating Cys500, one of the T1 Cu ligands. Mutation of Cys500 into a serine resulted in a T1 Cu depleted non-active protein. Soaking of this mutant's crystals with Cu(II) or Cu(I) resulted in the incorporation of a Cu atom at the regulatory site (rCu) only for the latter case, whereas in the Cu(II) complex the same site was unoccupied (Singh *et al.*, 2011). This is consistent with Cu(I) binding as a substrate and, for that reason, this additional Cu site was renamed from regulatory copper (rCu) to substrate copper site (sCu). However, the fact that a Cu ion was found previously at this position in the $CuCl_2$ soaked structure of wild-type CueO (Roberts *et al.*, 2003), suggests that binding of Cu(II) at the sCu site requires a functional T1 site (Singh *et al.*, 2011). Moreover, two additional Cu atoms were found to bind to the Met-rich helix, through juxtaposed Met residues, in the C500S Cu(I) structure, but not on the Cu(II) complex. To ensure the correct assignment of the oxidation states of the three additional coppers observed at the C500S Cu(I) structure, crystals of wild-type CueO were soaked with Ag(I), a Cu(I) mimic. Such a structure, demonstrated occupancy of the exact same three sites by Ag(I), without displacement of the catalytic coppers, with consequent strong inhibition of CueO oxidase activity *in vitro*. Such results allowed speculating on the role of the Met-rich region during response to copper toxicity, by binding the most toxic form of copper, Cu(I) (Singh *et al.*, 2011).

Furhermore, disruption of the two newly identified Cu sites, by mutation of all six Met comprised on the Met-rich helix, led to complete abolishment of Cu(I) at those sites, in spite of intact helical fold, with a consequent four-fold decrease of the Cu(I) oxidation catalytic rates (Singh *et al.*, 2011). Together with the fact that removal of the sCu site (Roberts *et al.*, 2003) yields a severely impaired enzyme, these results seem to support the role of the Met-rich region in facilitating Cu(I) oxidation. On this matter, Singh *et al.* propose that such mechanism is likely to involve either direct transfer of Cu(I) from the newly identified Cu sites into the sCu site, or provision of a electron transfer pathway from these to the sCu, and from there to the catalytic copper atoms (Singh *et al.*, 2011).

In the MCO from the hyperthermophilic bacterium *Aquifex aeolicus* (McoA) a Met-rich region (residues 321-363, 13 Met) reminiscent of that of CueO is also present. The gene encoding for this protein appears to be part of a putative copper-resistance determinant; moreover, the enzyme McoA was shown to present higher specificity for cuprous and ferrous ions than for aromatic substrates, with maximal catalytic efficiency when in the presence of exogenous copper (Fernandes *et al.*, 2007). Deletion of the Met-rich region in this enzyme resulted in higher specificity towards larger aromatic substrates, whereas specificity for the metal substrates Cu(I) and Fe(II) remained unchanged, thus suggesting that in McoA this region is likely to be occluding the substrate binding site (Fernandes *et al.*, 2007). Additionally, the lack of enzyme activation observed for the mutant, after addition of Cu(II), was correlated with the likely participation of exogenous Cu(II) in the modulation of the catalytic mechanism. Altogether, and although further studies would be needed, it is possible that McoA functions as a cytoprotrector *in vivo*, having a role in the suppression of copper and iron cytotoxicity (Fernandes *et al.*, 2007).

Recently, the crystal structure of the bacterial MCO from *Thermus thermophilus* HB27 was solved in its holo and apo forms (Serrano-Posada *et al.*, 2011; Martiniano *et al.*, 2012). Observation of its primary amino acid sequence denotes the presence of a small Met-rich region comparable to that of McoC (6 Met and 5 Met, respectively). In the solved structures, this region is part of a linker (residues 287-312) connecting β-strands 21 and 24 of the second domain, forming a flexible lid at the entrance of the substrate binding cavity of the enzyme, partially occluding its access. However, no evidences of additional Cu binding sites were reported in this region (Martiniano *et al.*, 2012).

Other examples of proteins containing Met-rich regions are the copper importer Ctr1 from *Saccharomyces cerevisiae,* where such motif is required for Cu(I) transport across the cytoplasmic membrane (Puig and Thiele, 2002), and PcoC from *E. coli*, where the Met-rich segment lies at the dimerization interface, suggesting a role in protein interactions (Wernimont *et al.*, 2003). Moreover, PcoC has also been suggested to transfer Cu(I) ions bound at its solvent-exposed Met-rich segments by docking with the Met-rich region of PcoA (both required for Cu resistance in *E. coli*), which then oxidises the transferred Cu(I) (Djoko *et al.*, 2010).

Altogether, and in line with that proposed by Hall *et al.* (Hall *et al.*, 2008), McoC may indeed act as a metallo-oxidase also *in vivo*, not only participating in copper and iron detoxification in the periplasm, by converting Cu(I) and/or Fe(II) to their less toxic forms Cu(II) and Fe(III), but also in the regulation of Cu homeostasis, by removing and detoxifying copper from the cytoplasm. Nevertheless, additional studies would be required to confirm such a role.

In summary the work reported in this thesis has given further insights into the nature of the T1 copper centre where electrons are initially captured at the start of the reduction mechanism. Evolution appears to have optimised the nature of this site and it is difficult to envisage how site-directed mutations in its immediate vicinity are going to improve significantly the functional efficiency. With respect to the trinuclear copper centre the research appears to favour the mechanism of dioxygen reduction proposed from biochemical and X-ray structural investigations rather than mechanisms that have been proposed based mainly on spectroscopic considerations. X-ray crystallography does have well characterised limitations (time and spatial averaging) but usually provides a very firm structural basis with which proposals for function and mechanism ought to concur. At last, the structure determination of a new bacterial MCO from *C. jejuni*, and likely to be involved in the Cu homeostasis system of this organism, has provided some light into the recently emerged link between periplasmic MCOs and metal metabolism in bacteria.

BIBLIOGRAPHIC REFERENCES

Aasa R, Väangard VT: **EPR signal intensity and powder shapes: a reexamination**. *Journal of Magnetic Resonance* 1975, **19**(3):8.

Adams PD, Afonine PV, Bunkóczi G, Chen VB, Davis IW, Echols N, Headd JJ, Hung LW, Kapral GJ, Grosse-Kunstleve RW *et al*: **PHENIX: a comprehensive Python-based system for macromolecular structure solution.** *Acta Crystallogr D Biol Crystallogr* 2010, **66**(Pt 2):213-221.

Agostinelli E, Cervoni L, Giartosio A, Morpurgo L: **Stability of Japanese-lacquer-tree (*Rhus vernicifera*) laccase to thermal and chemical denaturation: comparison with ascorbate oxidase**. *Biochem J* 1995, **306** (Pt3):697-702.

Alcaraz LA, Jiménez B, Moratal JM, Donaire A: **An NMR view of the unfolding process of rusticyanin: Structural elements that maintain the architecture of a beta-barrel metalloprotein**. *Protein Sci* 2005, **14**(7):1710-1722.

Alexandre G, Zhulin IB: **Laccases are widespread in bacteria**. *Trends Biotechnol* 2000, **18**(2):41-42.

Andrew CR, Yeom H, Valentine JS, Karlsson BG, Bonander N, Pouderoyen G, Canters GW, Loehr TM, Sanders-Loehr J: **Raman spectroscopy as an indicator of Cu-S bond-length in type-1 and type-2 copper cysteinate proteins**. *Journal of the American Chemical Society* 1994, **116**:10.

Arnesano F, Banci L, Bertini I, Thompsett AR: **Solution structure of CopC: a cupredoxin-like protein involved in copper homeostasis.** *Structure* 2002, **10**(10):1337-1347.

Augustine AJ, Quintanar L, Stoj CS, Kosman DJ, Solomon EI: **Spectroscopic and kinetic studies of perturbed trinuclear copper clusters: the role of protons in reductive cleavage of the O-O bond in the multicopper oxidase Fet3p**. *J Am Chem Soc* 2007, **129**(43):13118-13126.

Bah A, Garvey LC, Ge J, Di Cera E: **Rapid kinetics of Na^+ binding to thrombin**. *J Biol Chem* 2006, **281**(52):40049-40056.

Baptista AM, Martel PJ, Soares CM: **Simulation of electron-proton coupling with a Monte Carlo method: application to cytochrome c3 using continuum electrostatics**. *BiophysJ* 1999, **76**:2978-2998.

Baptista AM, Soares CM: **Some theoretical and computational aspects of the inclusion of proton isomerism in the protonation equilibrium of proteins**. *JPhysChem B* 2001, **105**:293-309.

Baptista AM, Teixeira VH, Soares CM: **Constant-pH molecular dynamics using stochastic titration**. *JChemPhys* 2002, **17**:4184-4200.

Bashford D: **An Object-Oriented Programming Suite for Electrostatic Effects in Biological Molecules**. In: *Scientific Computing in Object-Oriented Parallel Environments*. Edited by Ishikawa Y, Oldehoeft RR, Reynders JVW, Tholburn M, vol. 1343. Berlin: ISCOPE97, Springer; 1997: 233-240.

Bashford D: **Macroscopic electrostatic models for protonation states in proteins**. *Front Biosci* 2004, **9**:1082-1099.

Bashford D, Gerwert K: **Electrostatic calculations of the pKa values of ionizable groups in bacteriorhodopsin**. *JMolBiol* 1992, **224**:473-486.

Bayly CI, Cieplak P, Cornell WD, Kollman PA: **A well-behaved electrostatic potential based method using charge restraints for deriving atomic charges: the RESP model**. *JPhysChem* 1993, **97**:10269-10280.

Bello M, Valderrama B, Serrano-Posada H, Rudiño-Piñera E: **Molecular Dynamics of a Thermostable Multicopper Oxidase from *Thermus thermophilus* HB27: Structural Differences between the Apo and Holo Forms**. *PLoS One* 2012, **7**(7):e40700.

Bendtsen JD, Nielsen H, von Heijne G, Brunak S: **Improved prediction of signal peptides: SignalP 3.0.** *J Mol Biol* 2004, **340**(4):783-795.

Bento I, Carrondo MA, Lindley PF: **Reduction of dioxygen by enzymes containing copper**. *J Biol Inorg Chem* 2006, **11**(5):539-547.

Bento I, Martins LO, Gato Lopes G, Armenia Carrondo M, Lindley PF: **Dioxygen reduction by multi-copper oxidases; a structural perspective**. *Dalton Trans* 2005, **21**:3507-3513.

Bento I, Matias PM, Baptista AM, da Costa PN, van Dongen WM, Saraiva LM, Schneider TR, Soares CM, Carrondo MA: **Molecular basis for redox-Bohr and cooperative effects in cytochrome c3 from *Desulfovibrio desulfuricans* ATCC 27774: crystallographic and modeling studies of oxidized and reduced high-resolution structures at pH 7.6**. *Proteins* 2004, **54**(1):135-152.

Bento I, Peixoto C, Zaitsev VN, Lindley PF: **Ceruloplasmin revisited: structural and functional roles of various metal cation-binding sites**. *Acta Crystallogr D Biol Crystallogr* 2007, **63**(Pt 2):240-248.

Bento I, Silva CS, Chen Z, Martins LO, Lindley PF, Soares CM: **Mechanisms underlying dioxygen reduction in laccases. Structural and modelling studies focusing on proton transfer.** *BMC Struct Biol* 2010, **10**:28.

Berman HM, Westbrook J, Feng Z, Gilliland G, Bhat TN, Weissig H, Shindyalov IN, Bourne PE: **The Protein Data Bank**. *Nucleic Acids Res* 2000, **28**(1):235-242.

Berne BJ, Weeks JD, Zhou R: **Dewetting and hydrophobic interaction in physical and biological systems**. *Annu Rev Phys Chem* 2009, **60**:85-103.

Bertrand T, Jolivalt C, Briozzo P, Caminade E, Joly N, Madzak C, Mougin C: **Crystal structure of a four-copper laccase complexed with an arylamine: insights into substrate recognition and correlation with kinetics**. *Biochemistry* 2002, **41**(23):7325-7333.

Binkowski TA, Naghibzadeh S, Liang J: **CASTp: Computed Atlas of Surface Topography of proteins**. *Nucleic Acids Res* 2003, **31**(13):3352-3355.

Blackburn NJ, Ralle M, Hassett R, Kosman DJ: **Spectroscopic analysis of the trinuclear**

cluster in the Fet3 protein from yeast, a multinuclear copper oxidase. *Biochemistry* 2000, **39**(9):2316-2324.

Blair DF, Campbell GW, Cho WK, English AM, Fry HA, Lum V, Norton KA, Schoonover JR, Chan SI: **Resonance Raman studies of blue copper proteins: effects of temperature and isotopic substitutions. Structural and thermodynamic implications**. *J Am Chem Soc* 1985, **107**:5755-5766.

Bourgeois D, Vernède X, Adam V, Fioravanti E, Ursby T: **A microspectrophotometer for UV-visible and fluorescence studies of protein crystals**. *Journal of Applied Crystallography* 2002, **35**:319-326.

Bradford MM: **A rapid and sensitive method for the quantitation of microgram quantities of protein utilizing the principle of protein-dye binding**. *Anal Biochem* 1976, **72**:248-254.

Brenner AJ, Harris ED: **A quantitative test for copper using bicinchoninic acid.** *Anal Biochem* 1995, **226**(1):80-84.

Bricogne G, Blanc E, Brandl M, Flensburg C, Keller P, Paciorek W, Roversi P, Smart OS, Vonrhein C, Womack TO: **BUSTER-TNT**. In., **version 2.8.0** edn. Cambridge, United Kingdom: Global Phasing Ltd.; 2009.

Brissos V, Chen Z, Martins LO: **The kinetic role of carboxylate residues in the proximity of the trinuclear centre in the O2 reactivity of CotA-laccase**. *Dalton Trans* 2012, **41**(20):6247-6255.

Brockwell DJ: **Probing the mechanical stability of proteins using the atomic force microscope**. *Biochem Soc Trans* 2007, **35**(Pt 6):1564-1568.

Bushmarina NA, Blanchet CE, Vernier G, Forge V: **Cofactor effects on the protein folding reaction: acceleration of alpha-lactalbumin refolding by metal ions**. *Protein Sci* 2006, **15**(4):659-671.

Calhoun DB, Vanderkooi JM, Holtom GR, Englander SW: **Protein fluorescence quenching by small molecules: protein penetration versus solvent exposure**. *Proteins* 1986, **1**(2):109-115.

Cawthorn TR, Poulsen BE, Davidson DE, Andrews D, Hill BC: **Probing the kinetics and thermodynamics of copper(II) binding to *Bacillus subtilis* Sco, a protein involved in the assembly of the Cu(A) center of cytochrome c oxidase**. *Biochemistry* 2009, **48**(21):4448-4454.

CCP4 CCP, Number 4: **The CCP4 suite: programs for protein crystallography**. *Acta Cryst* 1994, **D50**:760-763.

Chen Z, Durao P, Silva CS, Pereira MM, Todorovic S, Hildebrandt P, Bento I, Lindley PF, Martins LO: **The role of Glu(498) in the dioxygen reactivity of CotA-laccase from *Bacillus subtilis***. *Dalton Trans* 2010, **39**(11):2875-2882.

Choi DW, Zea CJ, Do YS, Semrau JD, Antholine WE, Hargrove MS, Pohl NL, Boyd ES, Geesey GG, Hartsel SC *et al*: **Spectral, kinetic, and thermodynamic properties of Cu(I) and Cu(II) binding by methanobactin from *Methylosinus trichosporium***

OB3b. *Biochemistry* 2006, **45**(5):1442-1453.

Claus H: **Laccases and their occurrence in prokaryotes**. *Arch Microbiol* 2003, **179**(3):145-150.

Claus H: **Laccases: structure, reactions, distribution.** *Micron* 2004, **35**(1-2):93-96.

Colloc'h N, Gabison L, Monard G, Altarsha M, Chiadmi M, Marassio G, Sopkova-de Oliveira Santos J, El Hajji M, Castro B, Abraini JH *et al*: **Oxygen pressurized X-ray crystallography: probing the dioxygen binding site in cofactorless urate oxidase and implications for its catalytic mechanism**. *Biophys J* 2008, **95**(5):2415-2422.

Creighton TE: **Proteins: Structures and Molecular Properties**, 2nd edn; 1996.

Cukierman S: **Et tu, Grotthuss! and other unfinished stories**. *Biochim Biophys Acta* 2006, **1757**(8):876-885.

Dave BC, Germanas JP, Czernuszewicz RS: **The first direct evidence for copper(II)-cysteine vibrations in blue copper proteins: resonance Raman spectra of ^{34}S-Cys-labeled azurins reveal correlation of copper-sulfur stretching frequency with metal site geometry**. *Journal of the American Chemical Society* 1993, **115**(25):2.

Davis IW, Leaver-Fay A, Chen VB, Block JN, Kapral GJ, Wang X, Murray LW, Arendall WB, Snoeyink J, Richardson JS *et al*: **MolProbity: all-atom contacts and structure validation for proteins and nucleic acids.** *Nucleic Acids Res* 2007, **35**(Web Server issue):W375-383.

Davis-Kaplan SR, Askwith CC, Bengtzen AC, Radisky D, Kaplan J: **Chloride is an allosteric effector of copper assembly for the yeast multicopper oxidase Fet3p: an unexpected role for intracellular chloride channels**. *Proc Natl Acad Sci U S A* 1998, **95**(23):13641-13645.

DeLano WL: **The PyMOL Molecular Graphics System**. In. San Carlos, CA, USA: DeLano Scientific; 2002.

Diederix RE, Canters GW, Dennison C: **The Met99Gln mutant of amicyanin from *Paracoccus versutus***. *Biochemistry* 2000, **39**(31):9551-9560.

Djoko KY, Chong LX, Wedd AG, Xiao Z: **Reaction mechanisms of the multicopper oxidase CueO from *Escherichia coli* support its functional role as a cuprous oxidase**. *J Am Chem Soc* 2010, **132**(6):2005-2015.

Driks A: ***Bacillus subtilis* spore coat**. *Microbiol Mol Biol Rev* 1999, **63**(1):1-20.

Ducros V, Brzozowski AM, Wilson KS, Brown SH, Ostergaard P, Schneider P, Yaver DS, Pedersen AH, Davies GJ: **Crystal structure of the type-2 Cu depleted laccase from *Coprinus cinereus* at 2.2 A resolution**. *Nat Struct Biol* 1998, **5**(4):310-316.

Ducros V, Brzozowski AM, Wilson KS, Ostergaard P, Schneider P, Svendson A, Davies GJ: **Structure of the laccase from *Coprinus cinereus* at 1.68 A resolution: evidence for different 'type 2 Cu-depleted' isoforms**. *Acta Crystallogr D Biol Crystallogr* 2001, **57**(Pt 2):333-336.

Durao P, Bento I, Fernandes AT, Melo EP, Lindley PF, Martins LO: **Perturbations of the T1 copper site in the CotA laccase from *Bacillus subtilis*: structural, biochemical, enzymatic and stability studies**. *J Biol Inorg Chem* 2006, **11**(4):514-526.

Durao P, Chen Z, Fernandes AT, Hildebrandt P, Murgida DH, Todorovic S, Pereira MM, Melo EP, Martins LO: **Copper incorporation into recombinant CotA laccase from *Bacillus subtilis*: characterization of fully copper loaded enzymes**. *J Biol Inorg Chem* 2008a, **13**(2):183-193.

Durao P, Chen Z, Silva CS, Soares CM, Pereira MM, Todorovic S, Hildebrandt P, Bento I, Lindley PF, Martins LO: **Proximal mutations at the type 1 copper site of CotA laccase: spectroscopic, redox, kinetic and structural characterization of I494A and L386A mutants**. *Biochem J* 2008b, **412**(2):339-346.

Dwivedi UN, Singh P, Pandey VP, Kumar A: **Structure-function relationship among bacterial, fungal and plant laccases**. *Journal of Molecular Catalysis B: Enzymatic* 2011, **68**:12.

Eftink MR, Ghiron CA: **Exposure of tryptophanyl residues and protein dynamics**. *Biochemistry* 1977, **16**(25):5546-5551.

Emsley P, Cowtan K: **Coot: model-building tools for molecular graphics**. *Acta Crystallogr D Biol Crystallogr* 2004, **60**(Pt 12 Pt 1):2126-2132.

Enguita FJ, Marcal D, Martins LO, Grenha R, Henriques AO, Lindley PF, Carrondo MA: **Substrate and dioxygen binding to the endospore coat laccase from *Bacillus subtilis***. *J Biol Chem* 2004, **279**(22):23472-23476.

Enguita FJ, Martins LO, Henriques AO, Carrondo MA: **Crystal Structure of a Bacterial Endospore Coat Component: a laccase with enhanced thermostability properties**. *J Biol Chem* 2003, **278**(21):19416-19425.

Evans P: **Scaling and assessment of data quality**. *Acta Crystallogr D Biol Crystallogr* 2006, **62**(Pt 1):72-82.

Fadda E, Yu CH, Pomes R: **Electrostatic control of proton pumping in cytochrome c oxidase**. *Biochim Biophys Acta* 2008, **1777**(3):277-284.

Fernandes AT, Damas JM, Todorovic S, Huber R, Baratto MC, Pogni R, Soares CM, Martins LO: **The multicopper oxidase from the archaeon *Pyrobaculum aerophilum* shows nitrous oxide reductase activity.** *FEBS J* 2010, **277**(15):3176-3189.

Fernandes AT, Martins LO, Melo EP: **The hyperthermophilic nature of the metallo-oxidase from *Aquifex aeolicus***. *Biochim Biophys Acta* 2009, **1794**(1):75-83.

Fernandes AT, Soares CM, Pereira MM, Huber R, Grass G, Martins LO: **A robust metallo-oxidase from the hyperthermophilic bacterium *Aquifex aeolicus*.** *FEBS J* 2007, **274**(11):2683-2694.

Ferraroni M, Matera I, Chernykh A, Kolomytseva M, Golovleva LA, Scozzafava A, Briganti F: **Reaction intermediates and redox state changes in a blue laccase from *Steccherinum ochraceum* observed by crystallographic high/low X-ray dose experiments**. *J Inorg Biochem* 2012, **111**:203-209.

Ferraroni M, Myasoedova NM, Schmatchenko V, Leontievsky AA, Golovleva LA, Scozzafava A, Briganti F: **Crystal structure of a blue laccase from *Lentinus tigrinus*: evidences for intermediates in the molecular oxygen reductive splitting by multicopper oxidases**. *BMC Struct Biol* 2007, **7**:60.

Frisch MJ, Trucks GW, Schlegel HB, Scuseria GE, Robb MA, Cheeseman JR, Zakrzewski VG, Montgomery J, J. A., Stratmann RE, Burant JC *et al*: **Gaussian 98, Revision A.7**. In. Pittsburgh PA: Gaussian, Inc.; 1998.

Galli I, Musci G, Bonaccorsi di Patti MC: **Sequential reconstitution of copper sites in the multicopper oxidase CueO**. *J Biol Inorg Chem* 2004, **9**(1):90-95.

Garavaglia S, Cambria MT, Miglio M, Ragusa S, Iacobazzi V, Palmieri F, D'Ambrosio C, Scaloni A, Rizzi M: **The structure of *Rigidoporus lignosus* Laccase containing a full complement of copper ions, reveals an asymmetrical arrangement for the T3 copper pair**. *J Mol Biol* 2004, **342**(5):1519-1531.

Garzillo AM, Colao MC, Caruso C, Caporale C, Celletti D, Buonocore V: **Laccase from the white-rot fungus *Trametes trogii***. *Appl Microbiol Biotechnol* 1998, **49**(5):545-551.

Giardina P, Faraco V, Pezzella C, Piscitelli A, Vanhulle S, Sannia G: **Laccases: a never-ending story**. *Cell Mol Life Sci* 2010, **67**(3):369-385.

Green MT: **Application of Badger's rule to heme and non-heme iron-oxygen bonds: an examination of ferryl protonation states**. *J Am Chem Soc* 2006, **128**(6):1902-1906.

Hakulinen N, Andberg M, Kallio J, Koivula A, Kruus K, Rouvinen J: **A near atomic resolution structure of a *Melanocarpus albomyces* laccase**. *J Struct Biol* 2008, **162**(1):29-39.

Hakulinen N, Kiiskinen LL, Kruus K, Saloheimo M, Paananen A, Koivula A, Rouvinen J: **Crystal structure of a laccase from *Melanocarpus albomyces* with an intact trinuclear copper site**. *Nat Struct Biol* 2002, **9**(8):601-605.

Hakulinen N, Kruus K, Koivula A, Rouvinen J: **A crystallographic and spectroscopic study on the effect of X-ray radiation on the crystal structure of *Melanocarpus albomyces* laccase**. *Biochem Biophys Res Commun* 2006, **350**(4):929-934.

Hall SJ, Hitchcock A, Butler CS, Kelly DJ: **A Multicopper oxidase (Cj1516) and a CopA homologue (Cj1161) are major components of the copper homeostasis system of *Campylobacter jejuni*.** *J Bacteriol* 2008, **190**(24):8075-8085.

Harris ZL, Durley AP, Man TK, Gitlin JD: **Targeted gene disruption reveals an essential role for ceruloplasmin in cellular iron efflux.** *Proc Natl Acad Sci U S A* 1999, **96**(19):10812-10817.

Hellman NE, Kono S, Mancini GM, Hoogeboom AJ, De Jong GJ, Gitlin JD: **Mechanisms of copper incorporation into human ceruloplasmin**. *J Biol Chem* 2002, **277**(48):46632-46638.

Henriques AO, Moran CP: **Structure and assembly of the bacterial endospore coat**. *Methods* 2000, **20**(1):95-110.

Hoegger PJ, Kilaru S, James TY, Thacker JR, Kues U: **Phylogenetic comparison and classification of laccase and related multicopper oxidase protein sequences**. *FEBS J* 2006, **273**(10):2308-2326.

Holmes K, Mulholland F, Pearson BM, Pin C, McNicholl-Kennedy J, Ketley JM, Wells JM: ***Campylobacter jejuni*** **gene expression in response to iron limitation and the role of Fur.** *Microbiology* 2005, **151**(Pt 1):243-257.

Huffman DL, Huyett J, Outten FW, Doan PE, Finney LA, Hoffman BM, O'Halloran TV: **Spectroscopy of Cu(II)-PcoC and the multicopper oxidase function of PcoA, two essential components of *Escherichia coli* pco copper resistance operon.** *Biochemistry* 2002, **41**(31):10046-10055.

Hullo MF, Moszer I, Danchin A, Martin-Verstraete I: **CotA of *Bacillus subtilis* is a copper-dependent laccase**. *J Bacteriol* 2001, **183**(18):5426-5430.

Kallio JP, Auer S, Jänis J, Andberg M, Kruus K, Rouvinen J, Koivula A, Hakulinen N: **Structure-function studies of a *Melanocarpus albomyces* laccase suggest a pathway for oxidation of phenolic compounds**. *J Mol Biol* 2009, **392**(4):895-909.

Kannt A, Lancaster CR, Michel H: **The coupling of electron transfer and proton translocation: electrostatic calculations on *Paracoccus denitrificans* cytochrome c oxidase**. *Biophys J* 1998, **74**(2 Pt 1):708-721.

Kantardjieff KA, Rupp B: **Matthews coefficient probabilities: Improved estimates for unit cell contents of proteins, DNA, and protein-nucleic acid complex crystals.** *Protein Sci* 2003, **12**(9):1865-1871.

Karlin KD, Zhu ZY, Karlin S: **The extended environment of mononuclear metal centres in protein structures**. *Proc Natl Acad Sci* 1997, **94**(26):14225-14230.

Karlsson BG, Aasa R, Malmstrom BG, Lundberg LG: **Rack-induced bonding in blue copper proteins: spectroscopic properties and reduction potential of the azurin mutant M121L**. *FEBS Letters* 1989, **253**:4.

Kataoka K, Kitagawa R, Inoue M, Naruse D, Sakurai T, Huang HW: **Point mutations at the type I Cu ligands, Cys457 and Met467, and at the putative proton donor, Asp105, in *Myrothecium verrucaria* bilirubin oxidase and reactions with dioxygen.** *Biochemistry* 2005, **44**(18):7004-7012.

Kataoka K, Komori H, Ueki Y, Konno Y, Kamitaka Y, Kurose S, Tsujimura S, Higuchi Y, Kano K, Seo D *et al*: **Structure and function of the engineered multicopper oxidase CueO from *Escherichia coli* -deletion of the methionine-rich helical region covering the substrate-binding site.** *J Mol Biol* 2007, **373**(1):141-152.

Kataoka K, Sugiyama R, Hirota S, Inoue M, Urata K, Minagawa Y, Seo D, Sakurai T: **Four-electron reduction of dioxygen by a multicopper oxidase, CueO, and roles of Asp112 and Glu506 located adjacent to the trinuclear copper center**. *J Biol Chem* 2009, **284**(21):14405-14413.

Keegan RM, Winn MD: **Automated search-model discovery and preparation for structure solution by molecular replacement.** *Acta Crystallogr D Biol Crystallogr* 2007,

63(Pt 4):447-457.

Koroleva OV, Stepanova EV, Binukov VI, Timofeev VP, Pfeil W: **Temperature-induced changes in copper centers and protein conformation of two fungal laccases from *Coriolus hirsutus* and *Coriolus zonatus***. *Biochim Biophys Acta* 2001, **1547**(2):397-407.

Kosman DJ: **Multicopper oxidases: a workshop on copper coordination chemistry, electron transfer, and metallophysiology**. *J Biol Inorg Chem* 2010, **15**(1):15-28.

Kwok EY, Severance S, Kosman DJ: **Evidence for iron channelling in the Fet3p-Ftr1p high-affinity iron uptake complex in the yeast plasma membrane**. *Biochemistry* 2006, **45**(20):6317-6327.

Lakowicz JR: **Principles of fluorescence spectroscopy**. New York: Kluwer/Plenum; 1999.

Lamzin VS, Wilson KS: **Automated refinement of protein models.** *Acta Crystallogr D Biol Crystallogr* 1993, **49**(Pt 1):129-147.

Laskowski RA, MacArthur MW, Moss DS, Thornton JM: **PROCHECK: a program to check the stereochemical quality of protein structures**. *J Appl Crystallog* 1993b, **26**:283-291.

Laskowski RA, Moss DS, Thornton JM: **Main-chain bond lengths and bond angles in protein structures**. *J Mol Biol* 1993a, **231**(4):1049-1067.

Lawton TJ, Sayavedra-Soto LA, Arp DJ, Rosenzweig AC: **Crystal structure of a two-domain multicopper oxidase: implications for the evolution of multicopper blue proteins**. *J Biol Chem* 2009, **284**(15):10174-10180.

Leckner J, Bonander N, Wittung-Stafshede P, Malmström BG, Karlsson BG: **The effect of the metal ion on the folding energetics of azurin: a comparison of the native, zinc and apoprotein**. *Biochim Biophys Acta* 1997, **1342**(1):19-27.

Leslie A: **Joint CCP4, ESF-EAMCB**. *Newsletter on Protein Crystallography* 1992, **26**.

Leslie AG: **The integration of macromolecular diffraction data**. *Acta Crystallogr D* 2006, **62**(Pt 1):48-57.

Li X, Wei Z, Zhang M, Peng X, Yu G, Teng M, Gong W: **Crystal structures of *E. coli* laccase CueO at different copper concentrations**. *Biochem Biophys Res Commun* 2007, **354**(1):21-26.

Liang J, Edelsbrunner H, Woodward C: **Anatomy of protein pockets and cavities: measurement of binding site geometry and implications for ligand design.** *Protein Sci* 1998, **7**(9):1884-1897.

Lindley PF: **Multi-copper oxidases**. Basel, New York: Marcel Dekker, Inc.; 2001.

Lindley PF, Card G, Zaitseva I, Zaitsev V, Reinhammar B, Selin-Lindgren E, Yoshida K: **An X-ray structural study on human ceruloplasmin in relation to ferroxidase activity**. *J Biol Inorg Chem* 1997, **2**(4):454-463.

Louro RO, Bento I, Matias PM, Catarino T, Baptista AM, Soares CM, Carrondo MA, Turner DL, Xavier AV: **Conformational Component in the Coupled Transfer of Multiple Electrons and Protons in a Monomeric Tetraheme Cytochrome**. *JBiolChem* 2001, **276**:44044-44051.

Lovell SC, Davis IW, Arendall WB, 3rd, de Bakker PI, Word JM, Prisant MG, Richardson JS, Richardson DC: **Structure validation by Calpha geometry: phi, psi and Cbeta deviation**. *Proteins* 2003, **50**(3):437-450.

Luque I, Leavitt SA, Freire E: **The linkage between protein folding and functional cooperativity: two sides of the same coin?** *Annu Rev Biophys Biomol Struct* 2002, **31**:235-256.

Lyashenko AV, Bento I, Zaitsev VN, Zhukhlistova NE, Zhukova YN, Gabdoulkhakov AG, Morgunova EY, Voelter W, Kachalova GS, Stepanova EV *et al*: **X-ray structural studies of the fungal laccase from *Cerrena maxima***. *J Biol Inorg Chem* 2006a, **11**(8):963-973.

Lyashenko AV, Zhukova YN, Zhukhlistova NE, Zaitev VN, Stepanova EV, Kachalova GS, Koroleva OV, Voelter W, Betzel C, Tishkov VI *et al*: **Three-dimensional structure of laccase from *Coriolus zonatus* at 2.6Å resolution**. *Crystallography Reports* 2006b, **51**(5):7.

Machonkin TE, Quintanar L, Palmer AE, Hassett R, Severance S, Kosman DJ, Solomon EI: **Spectroscopy and reactivity of the type 1 copper site in Fet3p from *Saccharomyces cerevisiae*: correlation of structure with reactivity in the multicopper oxidases**. *J Am Chem Soc* 2001, **123**(23):5507-5517.

Madzak C, Mimmi MC, Caminade E, Brault A, Baumberger S, Briozzo P, Mougin C, Jolivalt C: **Shifting the optimal pH of activity for a laccase from the fungus *Trametes versicolor* by structure-based mutagenesis**. *Protein Eng Des Sel* 2006, **19**(2):77-84.

Malmström BG: **Enzymology of oxygen**. *Ann Rev Biochem* 1982, **51**:21-59.

Marshall NM, Garner DK, Wilson TD, Gao YG, Robinson H, Nilges MJ, Lu Y: **Rationally tuning the reduction potential of a single cupredoxin beyond the natural range**. *Nature* 2009, **462**(7269):113-116.

Martins LO, Soares CM, Pereira MM, Teixeira M, Costa T, Jones GH, Henriques AO: **Molecular and biochemical characterization of a highly stable bacterial laccase that occurs as a structural component of the *Bacillus subtilis* endospore coat**. *J Biol Chem* 2002, **277**(21):18849-18859.

Matera I, Gullotto A, Tilli S, Ferraroni M, Scozzafava A, Briganti F: **Crystal structure of the blue multicopper oxidase from the white-rot fungus *Trametes trogii* complexed with *p*-toluate**. *Inorganica Chimica Acta* 2008, **361**:9.

Mayer AM, Staples RC: **Laccase: new functions for an old enzyme.** *Phytochemistry* 2002, **60**(6):551-565.

McCoy AJ, Grosse-Kunstleve RW, Adams PD, Winn MD, Storoni LC, Read RJ: **Phaser**

crystallographic software. *J Appl Crystallogr* 2007, **40**(Pt 4):658-674.

Messerschmidt A: **Multi-copper Oxidases**. Singapore: World Science Press; 1997.

Messerschmidt A, Ladenstein R, Huber R, Bolognesi M, Avigliano L, Petruzzelli R, Rossi A, Finazzi-Agro A: **Refined crystal structure of ascorbate oxidase at 1.9 A resolution**. *J Mol Biol* 1992, **224**(1):179-205.

Messerschmidt A, Luecke H, Huber R: **X-ray structures and mechanistic implications of three functional derivatives of ascorbate oxidase from zucchini. Reduced, peroxide and azide forms**. *J Mol Biol* 1993, **230**(3):997-1014.

Messerschmidt A, Rossi A, Ladenstein R, Huber R, Bolognesi M, Gatti G, Marchesini A, Petruzzelli R, Finazzi-Agro A: **X-ray crystal structure of the blue oxidase ascorbate oxidase from zucchini. Analysis of the polypeptide fold and a model of the copper sites and ligands**. *J Mol Biol* 1989, **206**(3):513-529.

Miyazaki K: **A hyperthermophilic laccase from *Thermus thermophilus* HB27.** *Extremophiles* 2005, **9**(6):415-425.

Mooij WT, Cohen SX, Joosten K, Murshudov GN, Perrakis A: **"Conditional Restraints": Restraining the Free Atoms in ARP/wARP.** *Structure* 2009, **17**(2):183-189.

Moser CC, Dutton PL. In: ***Protein Electron Transfer***. Edited by Bendall DS: Bios Scientific Publishers Lda; 1996: 1-21.

Murphy ME, Lindley PF, Adman ET: **Structural comparison of cupredoxin domains: domain recycling to construct proteins with novel functions.** *Protein Sci* 1997, **6**(4):761-770.

Murshudov GN, Skubák P, Lebedev AA, Pannu NS, Steiner RA, Nicholls RA, Winn MD, Long F, Vagin AA: **REFMAC5 for the refinement of macromolecular crystal structures**. *Acta Crystallogr D Biol Crystallogr* 2011, **67**(Pt 4):355-367.

Murshudov GN, Vagin AA, Dodson EJ: **Refinement of macromolecular structures by the maximum-likelihood method.** *Acta Crystallogr D Biol Crystallogr* 1997, **53**(Pt 3):240-255.

Murshudov GN, Vagin AA, Lebedev A, Wilson KS, Dodson EJ: **Efficient anisotropic refinement of macromolecular structures using FFT**. *Acta Crystallogr D* 1999, **55 (Pt 1)**:247-255.

Nakamura K, Go N: **Function and molecular evolution of multicopper blue proteins**. *Cell Mol Life Sci* 2005, **62**(18):2050-2066.

Nakamura K, Kawabata T, Yura K, Go N: **Novel types of two-domain multi-copper oxidases: possible missing links in the evolution**. *FEBS Lett* 2003, **553**(3):239-244.

Nersissian AM, Shipp EL: **Blue copper-binding domains**. *Adv Protein Chem* 2002, **60**:271-340.

Olsson MH, Siegbahn PE, Blomberg MR, Warshel A: **Exploring pathways and barriers for coupled ET/PT in cytochrome c oxidase: a general framework for examining**

energetics and mechanistic alternatives. *Biochim Biophys Acta* 2007, **1767**(3):244-260.

Olsson MH, Warshel A: **Monte Carlo simulations of proton pumps: on the working principles of the biological valve that controls proton pumping in cytochrome c oxidase**. *Proc Natl Acad Sci U S A* 2006, **103**(17):6500-6505.

Outten FW, Huffman DL, Hale JA, O'Halloran TV: **The independent cue and cus systems confer copper tolerance during aerobic and anaerobic growth in *Escherichia coli*.** *J Biol Chem* 2001, **276**(33):30670-30677.

Pace CN, Hebert EJ, Shaw KL, Schell D, Both V, Krajcikova D, Sevcik J, Wilson KS, Dauter Z, Hartley RW *et al*: **Conformational stability and thermodynamics of folding of ribonucleases Sa, Sa2 and Sa3**. *J Mol Biol* 1998, **279**(1):271-286.

Palmer AE, Lee SK, Solomon EI: **Decay of the peroxide intermediate in laccase: reductive cleavage of the O-O bond**. *J Am Chem Soc* 2001, **123**(27):6591-6599.

Palmer AE, Szilagyi RK, Cherry JR, Jones A, Xu F, Solomon EI: **Spectroscopic characterization of the Leu513His variant of fungal laccase: effect of increased axial ligand interaction on the geometric and electronic structure of the type 1 Cu site**. *Inorg Chem* 2003, **42**(13):4006-4017.

Palmer AE, Randall DW, Xu F, Solomon EI: **Spectroscopic studies and electronic structure description of the high potential Type 1 copper site in fungal laccase: insight into the effect of the axial ligand**. *Journal of the American Chemical Society* 1999, **121**:12.

Palyada K, Threadgill D, Stintzi A: **Iron acquisition and regulation in *Campylobacter jejuni*.** *J Bacteriol* 2004, **186**(14):4714-4729.

Parkhill J, Wren BW, Mungall K, Ketley JM, Churcher C, Basham D, Chillingworth T, Davies RM, Feltwell T, Holroyd S *et al*: **The genome sequence of the food-borne pathogen *Campylobacter jejuni* reveals hypervariable sequences.** *Nature* 2000, **403**(6770):665-668.

Pereira L, Coelho AV, Viegas CA, Santos MM, Robalo MP, Martins LO: **Enzymatic biotransformation of the azo dye Sudan Orange G with bacterial CotA-laccase**. *J Biotechnol* 2009a, **139**(1):68-77.

Pereira L, Coelho AV, Viegas CA, Ganachaud C, Iacazio G, Tron T, Robalo MP, Martins LO: **On the mechanism of biotransformation of the anthraquinonic dye Acid Blue 62 by laccases**. *Advanced Synthesis & Catalysis* 2009b, **351**(11-12):9.

Pereira MM, Sousa FL, Verissimo AF, Teixeira M: **Looking for the minimum common denominator in haem-copper oxygen reductases: towards a unified catalytic mechanism**. *Biochim Biophys Acta* 2008, **1777**(7-8):929-934.

Peterson MC: **Clinical aspects of *Campylobacter jejuni* infections in adults.** *West J Med* 1994, **161**(2):148-152.

Piontek K, Antorini M, Choinowski T: **Crystal structure of a laccase from the fungus *Trametes versicolor* at 1.90-A resolution containing a full complement of coppers**. *J Biol Chem* 2002, **277**(40):37663-37669.

Polyakov KM, Fedorova TV, Stepanova EV, Cherkashin EA, Kurzeev SA, Strokopytov BV, Lamzin VS, Koroleva OV: **Structure of native laccase from *Trametes hirsuta* at 1.8 A resolution**. *Acta Cryst D* 2009, **65**:611-617.

Popovic DM, Stuchebrukhov AA: **Electrostatic study of the proton pumping mechanism in bovine heart cytochrome C oxidase**. *J Am Chem Soc* 2004, **126**(6):1858-1871.

Popovic DM, Stuchebrukhov AA: **Proton exit channels in bovine cytochrome c oxidase**. *J Phys Chem B* 2005, **109**(5):1999-2006.

Pozdnyakova I, Guidry J, Wittung-Stafshede P: **Copper stabilizes azurin by decreasing the unfolding rate**. *Arch Biochem Biophys* 2001, **390**(1):146-148.

Pozdnyakova I, Wittung-Stafshede P: **Copper binding before polypeptide folding speeds up formation of active (holo) *Pseudomonas aeruginosa* azurin**. *Biochemistry* 2001, **40**(45):13728-13733.

Price NC, Stevens L: **Fundamentals of Enzymology: the Cell and Molecular Biology of Catalytic Proteins**, 3rd edn. New York: Oxford University Press Inc; 2001.

Puig S, Thiele DJ: **Molecular mechanisms of copper uptake and distribution**. *Curr Opin Chem Biol* 2002, **6**(2):171-180.

Qiu D, Dong S, Ybe J, Hecht M, Spiro TM: **Variations in the Type I Copper Protein Coordination Group: Resonance Raman Spectrum of ^{34}S-, ^{65}Cu-, and ^{15}N-Labeled Plastocyanin**. *Journal of the American Chemical Society* 1995, **117**(24):4.

Quintanar L, Stoj C, Taylor AB, Hart PJ, Kosman DJ, Solomon EI: **Shall we dance? How a multicopper oxidase chooses its electron transfer partner**. *Acc Chem Res* 2007, **40**(6):445-452.

Quintanar L, Stoj C, Wang TP, Kosman DJ, Solomon EI: **Role of aspartate 94 in the decay of the peroxide intermediate in the multicopper oxidase Fet3p**. *Biochemistry* 2005, **44**(16):6081-6091.

Qvist J, Davidovic M, Hamelberg D, Halle B: **A dry ligand-binding cavity in a solvated protein**. *Proc Natl Acad Sci U S A* 2008, **105**(17):6296-6301.

Radestock S.G. H: **Exploiting the Link between Protein Rigidity and Thermostability for Data-Driven Protein Engineering**. *Engineering in Life Sciences* 2008, **8**(5):16.

Ramakrishnan C, Ramachandran GN: **Stereochemical criteria for polypeptide and protein chain conformations. II. Allowed conformations for a pair of peptide units**. *Biophys J* 1965, **5**(6):909-933.

Read RJ: **Improved Fourier coefficients for maps using phases from partial structures with errors**. *Acta Crystallogr A* 1986, **42**:140-149.

Riva S: **Laccases: blue enzymes for green chemistry.** *Trends Biotechnol* 2006, **24**(5):219-226.

Roberts SA, Weichsel A, Grass G, Thakali K, Hazzard JT, Tollin G, Rensing C, Montfort WR: **Crystal structure and electron transfer kinetics of CueO, a multicopper oxidase required for copper homeostasis in *Escherichia coli***. *Proc Natl Acad Sci U S A* 2002, **99**(5):2766-2771.

Roberts SA, Wildner GF, Grass G, Weichsel A, Ambrus A, Rensing C, Montfort WR: **A labile regulatory copper ion lies near the T1 copper site in the multicopper oxidase CueO.** *J Biol Chem* 2003, **278**(34):31958-31963.

Rodríguez Couto S, Toca Herrera JL: **Industrial and biotechnological applications of laccases: a review.** *Biotechnol Adv* 2006, **24**(5):500-513.

Rydén LG, Hunt LT: **Evolution of protein complexity: the blue copper-containing oxidases and related proteins**. *J Mol Evol* 1993, **36**(1):41-66.

Sakuraba H, Koga K, Yoneda K, Kashima Y, Ohshima T: **Structure of a multicopper oxidase from the hyperthermophilic archaeon *Pyrobaculum aerophilum***. *Acta Crystallogr Sect F Struct Biol Cryst Commun* 2011, **67**(Pt 7):753-757.

Sakurai T, Kataoka K: **Structure and function of type I copper in multicopper oxidases**. *Cell Mol Life Sci* 2007, **64**(19-20):2642-2656.

Savini I, D'Alessio S, Giartosio A, Morpurgo L, Avigliano L: **The role of copper in the stability of ascorbate oxidase towards denaturing agents**. *Eur J Biochem* 1990, **190**(3):491-495.

Scott WRP, Hünenberger PH, Tironi IG, Mark AE, Billeter SR, Fennen J, Torda AE, Huber T, Krüger P, van Gunsteren WF: **The GROMOS biomolecular simulation program package**. *JPhysChem* 1999, **103**:3596-3607.

Sedlak E, Wittung-Stafshede P: **Discrete roles of copper ions in chemical unfolding of human ceruloplasmin**. *Biochemistry* 2007, **46**(33):9638-9644.

Sedlák E, Ziegler L, Kosman DJ, Wittung-Stafshede P: ***In vitro* unfolding of yeast multicopper oxidase Fet3p variants reveals unique role of each metal site**. *Proc Natl Acad Sci U S A* 2008, **105**(49):19258-19263.

Serrano-Posada H, Valderrama B, Stojanoff V, Rudiño-Piñera E: **Thermostable multicopper oxidase from *Thermus thermophilus* HB27: crystallization and preliminary X-ray diffraction analysis of apo and holo forms**. *Acta Crystallogr Sect F Struct Biol Cryst Commun* 2011, **67**(Pt 12):1595-1598.

Sharma P, Goel R, Capalash N: **Bacterial Laccases**. *World J Microbiol Biotechnol* 2007, **23**(6):823-832.

Shi X, Stoj C, Romeo A, Kosman DJ, Zhu Z: **Fre1p Cu^{2+} reduction and Fet3p Cu^{1+} oxidation modulate copper toxicity in *Saccharomyces cerevisiae***. *J Biol Chem* 2003, **278**(50):50309-50315.

Shin W, Sundaram UM, Cole JL, Zhang HH, Hedman B, Hodgson KO, Solomon EI: **Chemical and Spectroscopic Definition of the Peroxide-Level Intermediate in the Multicopper Oxidases: Relevance to the Catalytic Mechanism of Dioxygen**

Reduction to Water. *J Am Chem Soc* 1996, **118**:3202-3215.

Shleev S, Jarosz-Wilkolazka A, Khalunina A, Morozova O, Yaropolov A, Ruzgas T, Gorton L: **Direct electron transfer reactions of laccases from different origins on carbon electrodes**. *Bioelectrochemistry* 2005, **67**(1):115-124.

Singh SK, Grass G, Rensing C, Montfort WR: **Cuprous oxidase activity of CueO from *Escherichia coli*.** *J Bacteriol* 2004, **186**(22):7815-7817.

Singh SK, Roberts SA, McDevitt SF, Weichsel A, Wildner GF, Grass GB, Rensing C, Montfort WR: **Crystal structures of multicopper oxidase CueO bound to copper(I) and silver(I): Functional role of a methionine-rich sequence.** *J Biol Chem* 2011.

Skálová T, Dohnálek J, Østergaard LH, Østergaard PR, Kolenko P, Dusková J, Stepánková A, Hasek J: **The structure of the small laccase from *Streptomyces coelicolor* reveals a link between laccases and nitrite reductases**. *J Mol Biol* 2009, **385**(4):1165-1178.

Smith AW, Camara-Artigas A, Wang M, Allen JP, Francisco WA: **Structure of phenoxazinone synthase from *Streptomyces antibioticus* reveals a new type 2 copper center.** *Biochemistry* 2006, **45**(14):4378-4387.

Soares CM, Baptista AM, Pereira MM, Teixeira M: **Investigation of protonatable residues in *Rhodothermus marinus* caa3 haem-copper oxygen reductase: comparison with *Paracoccus denitrificans* aa3 haem-copper oxygen reductase**. *J Biol Inorg Chem* 2004, **9**(2):124-134.

Solomon EI, Augustine AJ, Yoon J: **O2 reduction to H2O by the multicopper oxidases**. *Dalton Trans* 2008(30):3921-3932.

Solomon EI, Chen P, Metz M, Lee SK, Palmer AE: **Oxygen Binding, Activation, and Reduction to Water by Copper Proteins**. *Angew Chem Int Ed Engl* 2001, **40**(24):4570-4590.

Solomon EI, Sundaram UM, Machonkin TE: **Multicopper oxidases and oxygenases**. *Chem Rev* 1996, **96**:2563-2605.

Somogyi B, Punyiczki M, Hedstrom J, Norman JA, Prendergast FG, Rosenberg A: **Coupling between external viscosity and the intramolecular dynamics of ribonuclease T1: a two-phase model for the quenching of protein fluorescence**. *Biochim Biophys Acta* 1994, **1209**(1):61-68.

Stoj CS, Kosman DJ: **Copper proteins: Oxidases**, vol. II, 2nd edn. New York; 2005.

Stoj C, Kosman DJ: **Cuprous oxidase activity of yeast Fet3p and human ceruloplasmin: implication for function.** *FEBS Lett* 2003, **554**(3):422-426.

Taniguchi T, Ichimura K, Kawashima S, Yamamura T, Tachi'iri Y, Satake K, Kihara H: **Binding of Cu(II), Tb(III) and Fe(III) to chicken ovotransferrin. A kinetic study**. *Eur Biophys J* 1990, **18**(1):1-8.

Taylor AB, Stoj CS, Ziegler L, Kosman DJ, Hart PJ: **The copper-iron connection in biology: structure of the metallo-oxidase Fet3p.** *Proc Natl Acad Sci U S A* 2005,

102(43):15459-15464.

Teixeira VH, Cunha CA, Machuqueiro M, Oliveira AS, Victor BL, Soares CM, Baptista AM: **On the use of different dielectric constants for computing individual and pairwise terms in poisson-boltzmann studies of protein ionization equilibrium**. *J Phys Chem B* 2005, **109**(30):14691-14706.

Teixeira VH, Soares CM, Baptista AM: **Studies of the reduction and protonation behaviour of tetrahaem cytochromes using atomic detail**. *J BioI Inorg Chem* 2002, **7**:200-216.

Tronrud D: **The limits of interpretation, CCP4 Study Weekend Macromolecular Refinement**. In: *CCP4 Study Weekend Macromolecular Refinement: 1996; Dasbury*. Warrington: Dasbury Laboratory: 1-10.

Ueki Y, Inoue M, Kurose S, Kataoka K, Sakurai T: **Mutations at Asp112 adjacent to the trinuclear Cu center in CueO as the proton donor in the four-electron reduction of dioxygen**. *FEBS Lett* 2006, **580**(17):4069-4072.

Vagin A, Teplyakov A: **MOLREP: an Automated Program for Molecular Replacement**. *J Appl Cryst* 1997, **30**:1022-1025.

van Gunsteren WF, Billeter SR, Eising AA, Hunenberger PH, Kruger P, Mark AE, Scott WRP, Tironi IG: **Biomolecular simulation: The GROMOS96 manual and user guide**. Zurich, Groninger: BIOMOS b.v.; 1996.

Vieille C, Zeikus GJ: **Hyperthermophilic enzymes: sources, uses, and molecular mechanisms for thermostability**. *Microbiol Mol Biol Rev* 2001, **65**(1):1-43.

Wernimont AK, Huffman DL, Finney LA, Demeler B, O'Halloran TV, Rosenzweig AC: **Crystal structure and dimerization equilibria of PcoC, a methionine-rich copper resistance protein from *Escherichia coli***. *J Biol Inorg Chem* 2003, **8**(1-2):185-194.

Winn MD, Isupov MN, Murshudov GN: **Use of TLS parameters to model anisotropic displacements in macromolecular refinement.** *Acta Crystallogr D Biol Crystallogr* 2001, **57**(Pt 1):122-133.

Wittung-Stafshede P: **Role of cofactors in folding of the blue-copper protein azurin**. *Inorg Chem* 2004, **43**(25):7926-7933.

Xu F: **Oxidation of phenols, anilines, and benzenethiols by fungal laccases: correlation between activity and redox potentials as well as halide inhibition**. *Biochemistry* 1996, **35**(23):7608-7614.

Xu F: **Effects of redox potential and hydroxide inhibition on the pH activity profile of fungal laccases**. *J Biol Chem* 1997, **272**(2):924-928.

Xu F: **Laccase**. In: *The Encyclopedia of Bioprocess Technology:Fermentation, Biocatalysis and Bioseparation*. Edited by Flickinger MC, Drew SWe. New York: John Wiley & Sons Inc; 1999: 1545-1554.

Xu F: **Dioxygen reactivity of laccase: dependence on laccase source, pH, and anion inhibition.** *Appl Biochem Biotechnol* 2001, **95**(2):125-133.

Xu F, Berka RM, Wahleithner JA, Nelson BA, Shuster JR, Brown SH, Palmer AE, Solomon EI: **Site-directed mutations in fungal laccase: effect on redox potential, activity and pH profile**. *Biochem J* 1998, **334 (Pt 1)**:63-70.

Xu F, Palmer AE, Yaver DS, Berka RM, Gambetta GA, Brown SH, Solomon EI: **Targeted mutations in a *Trametes villosa* laccase. Axial perturbations of the T1 copper**. *J Biol Chem* 1999, **274**(18):12372-12375.

Xu F, Shin W, Brown SH, Wahleithner JA, Sundaram UM, Solomon EI: **A study of a series of recombinant fungal laccases and bilirubin oxidase that exhibit significant differences in redox potential, substrate specificity, and stability**. *Biochim Biophys Acta* 1996, **1292**(2):303-311.

Yoon J, Fujii S, Solomon EI: **Geometric and electronic structure differences between the type 3 copper sites of the multicopper oxidases and hemocyanin/tyrosinase**. *Proc Natl Acad Sci U S A* 2009, **106**(16):6585-6590.

Yoon J, Liboiron BD, Sarangi R, Hodgson KO, Hedman B, Solomon EI: **The two oxidized forms of the trinuclear Cu cluster in the multicopper oxidases and mechanism for the decay of the native intermediate**. *Proc Natl Acad Sci U S A* 2007, **104**(34):13609-13614.

Young T, Abel R, Kim B, Berne BJ, Friesner RA: **Motifs for molecular recognition exploiting hydrophobic enclosure in protein-ligand binding**. *Proc Natl Acad Sci U S A* 2007, **104**(3):808-813.

Young T, Hua L, Huang X, Abel R, Friesner R, Berne BJ: **Dewetting transitions in protein cavities**. *Proteins* 2010, **78**(8):1856-1869.

Zaitsev VN, Zaitseva I, Papiz M, Lindley PF: **An X-ray crystallographic study of the binding sites of the azide inhibitor and organic substrates to ceruloplasmin, a multi-copper oxidase in the plasma**. *J Biol Inorg Chem* 1999, **4**(5):579-587.

Zaitseva I, Zaitsev V, Card G, Moshkov K, Bax B, Ralph A, Lindley P: **The X-ray structure of human serum ceruloplasmin at 3.1 angstrom: Nature of the copper centres**. *J Biol Inorg Chem* 1996, **1**:15-23.

Zhang J, Matthews CR: **The role of ligand binding in the kinetic folding mechanism of human p21(H-ras) protein**. *Biochemistry* 1998, **37**(42):14891-14899.

Zhou XX, Wang YB, Pan YJ, Li WF: **Differences in amino acids composition and coupling patterns between mesophilic and thermophilic proteins**. *Amino Acids* 2008, **34**(1):25-33.

Zhukhlistova NE, Zhukova YN, Lyashenko AA, Zaitsev VN, Mikhailov AM: **Three-Dimensional Organization of the Three-Domain Copper oxidases: a Review**. *Crystallography Reports* 2008, **53**(1):18.